Three Essays in Sustainable Last-Mile Deliveries and Humanitarian Logistics

A DISSERTATION PRESENTED
BY
Minakshi Punam Mandal

IN PARTIAL FULFILLMENT OF THE REQUIREMENTS FOR THE DEGREE OF

Doctor of Philosophy in Business Administration
AND
Doctor en Sciences de Gestion
de l'Ecole Doctorale
«Economie, Management, Mathématiques, Physique et Sciences Informatiques»
ED 405
CY Cergy Paris Université

IN THE SUBJECT OF
Operations and Data Analytics

Presented and defended on the 3rd of December, 2024

Jury

Laurent Alfandari	Co-supervisor	Professor, ESSEC Business School
Claudia Archetti	Co-supervisor	Professor, University of Brescia
Teodor Gabriel Crainic	Referee	Professor, Université du Québec á Montréal
Ana Barbosa-Povoa	Referee	Professor, University of Lisbon
Ivana Ljubić	President	Professor, ESSEC Business School
Ahmadreza Marandi	Examiner	Assisstant Professor, Eindhoven University of Technology

Three Essays in Sustainable Last-Mile Deliveries and Humanitarian Logistics

Abstract

This thesis is motivated by challenges in two areas: last mile deliveries and humanitarian logistics. With a rising demand in e-commerce, it becomes imperative to work towards making it sustainable, economical, and efficient. The first part of the thesis contributes to this field. The last part deals with disaster management, focusing on earthquake preparedness. Earthquakes are one of the deadliest natural disasters that can cause catastrophic damages, leading to loss of life and property and displacing thousands of people. Thus, preparing for it becomes crucial. Mixed-integer linear programming (MILP) techniques have been used to study the problems, and both heuristic and exact methods are employed to solve them.

In Chapter 2, we explore the potential of using public transportation systems for freight delivery, where we intend to utilize the spare capacities of public vehicles like buses, trams, metros, and trains, particularly during off-peak hours, to transport packages within the city instead of using dedicated delivery vehicles. The study contributes to the growing literature on innovative strategies for performing sustainable last-mile deliveries. We study an operational level problem called the *Three-Tier Delivery Problem on Public Transportation*, where packages are first transported from the Consolidation and Distribution Center (CDC) to nearby public vehicle stations by delivery trucks. From there, public vehicles transport them into the city area. The last leg of the delivery is performed to deliver the packages to the customers using green vehicles or eco-friendly systems. We employ decomposition-based

matheuristics to solve our models. Our results on instances that mimic realistic cities show that this system has the potential to reduce the length of trips performed by traditional delivery trucks by 86%, thereby reducing the negative social and environmental impacts of existing last mile delivery systems. The paper based on this work is currently under revision in the journal Soft Computing. This work was also presented at the EURO 2021 conference, the Odysseus 2021 conference, the VeRoLog 2022 conference, and the 2nd EUROYoung workshop.

Chapter 3 tackles the problems of workforce sizing and shift scheduling of a logistic operator delivering parcels in the last mile segment of the supply chain. Our working hypothesis is that the relevant decisions are affected by two main trade-offs: workforce size and shift stability. A large workforce is able to deal with demand fluctuations but incurs higher fixed costs; by contrast, a small workforce might require excessive outsourcing to third-party logistic providers. Stable shifts, i.e., with predictable start times and lengths, improve worker satisfaction and reduce turnover; at the same time, they might be less able to adapt to an unsteady demand. Through an extensive computational campaign based on a novel mathematical formulation, we test these assumptions. We find that extreme shift stability is, indeed, unsuitable for last-mile operations. On the other hand, introducing a very limited amount of flexibility achieves similar effects as moving to a completely flexible system while ensuring a better work-life balance for the workers. Several recent studies in the social sciences have warned about the consequences of precarious working conditions for couriers and retail workers and have recommended—among other things—stable work schedules. Our work provides an actionable decision-support tool to achieve this objective without sacrificing the company's bottom line. The paper based on this work is currently under revision at the European Journal of Operational Research, and the work was presented at the TSL 2023 conference and the 3rd EUROYoung workshop.

In Chapter 4, we shift our focus to humanitarian logistics. We are all privy to the damage and destruction caused by earthquakes. Earthquakes are typically followed by major and minor aftershocks.

They also lead to other secondary disasters like tsunamis, floods, avalanches, building collapses, etc. We study an uncapacitated facility location problem for storing relief materials in the event of such a disaster. We adopt a two-stage budgeted-robustness approach. We consider a major earthquake in the first stage, followed by aftershocks in the second stage. We propose several MILP formulations for our problem and employ Branch-and-Cut methods to solve two of them. The performance of our models is analyzed on synthetically generated instances, followed by a case study on Turkey, which is highly prone to earthquakes. Managerial insights are finally provided regarding, in particular, the relevance of modeling the second-stage aftershocks and its impact on the optimal locations of the facilities. The paper based on the work in this chapter is in the final stages of completion, and the work was presented at the POMS 2023 conference and the ISMP 2024 conference.

Trois essais sur les livraisons durables du dernier kilomètre et logistique humanitaire

Résumé

Cette thèse est motivée par des enjeux dans deux domaines : l'optimisation des livraisons du dernier kilomètre et la logistique humanitaire. Avec une demande croissante en matière de commerce électronique, il devient impératif de travailler à le rendre durable, économique et efficace. La première partie de la thèse contribue à ce domaine. La dernière partie traite de la gestion de catastrophes humanitaires et plus particulièrement de la préparation aux tremblements de terre. Ceux-ci constituent l'une des catastrophes naturelles les plus meurtrières, entraînant des dommages gigantesques, des pertes de vies humaines et de biens et le déplacement de milliers de personnes. Il est donc crucial de s'y préparer. Des techniques de programmation linéaire en nombres entiers mixtes (MILP) ont été utilisées pour étudier les problèmes de la thèse et des méthodes heuristiques et exactes sont utilisées pour les résoudre.

Dans le chapitre 2, nous explorons le potentiel des réseaux de transport public pour la livraison de marchandises en ville, en utilisant les capacités inutilisées de véhicules publics comme les bus, tramways, métros et trains, en particulier pendant les heures creuses, pour transporter des colis dans une ville ou agglomération au lieu d'utiliser des véhicules de livraison dédiés. L'étude contribue à la littérature croissante sur les stratégies innovantes d'optimisation des livraisons durables du dernier kilomètre. Nous étudions un problème de niveau opérationnel appelé *Problème de livraison à trois niveaux dans les transports publics*, où les colis sont d'abord transportés en camion du centre de consolidation et de distribution (CDC) vers les stations de véhicules publics à proximité. De là, des véhicules publics les

transportent vers le centre-ville. La dernière étape de livraison est effectuée pour livrer les colis aux clients à l'aide de véhicules dits "verts", ou respectueux de l'environnement. Nous utilisons des méthodes mathématiques d'optimisation basées sur la décomposition pour résoudre nos modèles. Nos résultats sur des exemples imitant des villes réalistes montrent que ce système peut diminuer de 86 % la durée des trajets effectués par les camions de livraison traditionnels, réduisant ainsi les impacts sociaux et environnementaux négatifs des systèmes existants de livraison du dernier kilomètre. L'article basé sur ces travaux est actuellement en cours de révision dans la revue Soft Computing. Ce travail a également été présenté lors de la conférence EURO 2021, de la conférence Odysseus 2021, de la conférence VeRoLog 2022 et du 2e atelier EUROYoung.

Le chapitre 3 aborde les problèmes de dimensionnement de la main-d'œuvre et de planification des équipes d'un opérateur logistique livrant des colis dans le segment du dernier kilomètre de la chaîne d'approvisionnement. Notre hypothèse de travail est que les décisions pertinentes sont affectées par deux compromis principaux : le volume de main-d'œuvre et la stabilité des équipes. Une main-d'œuvre nombreuse est capable de faire face aux fluctuations de la demande mais supporte des coûts fixes plus élevés ; en revanche, une main-d'œuvre réduite peut nécessiter une sous-traitance excessive à des prestataires logistiques tiers. Des quarts de travail stables, avec des heures de début et des durées prévisibles, améliorent la satisfaction des travailleurs et réduisent le roulement du personnel ; dans le même temps, ils pourraient avoir une moindre capacité à s'adapter à une demande instable. Grâce à une vaste étude numérique basée sur une nouvelle formulation mathématique, nous testons ces hypothèses. Nous constatons qu'une stabilité extrême des changements de vitesse n'est pas adaptée aux opérations du dernier kilomètre. D'un autre côté, l'introduction d'un degré très limité de flexibilité produit des effets similaires à ceux d'un passage à un système totalement flexible, tout en garantissant un meilleur équilibre entre vie professionnelle et vie privée pour les travailleurs. Plusieurs études récentes en sciences sociales ont alerté sur les conséquences des conditions de travail précaires pour les coursiers et les travailleurs du commerce de détail et ont recommandé, entre autres, des horaires de travail stables. Notre travail fournit un outil d'aide à la décision exploitable pour atteindre cet objectif sans sacrifier les résultats financiers de l'entreprise. L'article basé sur ces travaux est actuellement en cours de révision au European Journal of Operational Research, et les travaux ont été présentés lors de la conférence TSL 2023 et du 3e atelier EUROYoung.

Au chapitre 4, nous nous concentrons sur la logistique humanitaire. Nous connaissons tous les dégâts et destructions causés par les tremblements de terre. Ceux-ci sont généralement suivis de répliques majeures et mineures. Ils conduisent également à d'autres catastrophes secondaires comme des tsunamis, des inondations, des avalanches, des effondrements de bâtiments, etc. Nous étudions un problème de localisation d'installations (sans capacité fixée a priori) pour stocker le matériel de secours en cas d'une telle catastrophe. Nous adoptons une approche de robustesse budgétisée en deux étapes. Nous considérons un séisme majeur dans un premier temps, suivi de répliques dans un deuxième temps. Nous proposons plusieurs formulations MILP pour notre problème et employons des méthodes de Branch-and-Cut pour résoudre deux d'entre elles. Les performances de nos modèles sont analysées sur des instances générées synthétiquement, suivies d'une étude de cas sur la Turquie, très sujette aux tremblements de terre. Des éclairages managériaux sont enfin apportés concernant notamment la pertinence et l'apport de la modélisation des répliques au-delà du seul séisme principal, et son impact sur les localisations optimales des installations. Le document basé sur les travaux de ce chapitre est en phase finale d'achèvement et les travaux ont été présentés à la conférence POMS 2023 et à la conférence ISMP 2024.

Contents

List of Figures

List of Tables

This thesis is dedicated to my parents, whose continuous support and inspiration brought me to where I am.

Acknowledgments

This thesis is a product of many amazing people I was fortunate to meet during my PhD. Though I am going to try, I am certain that I will not be able to express in words the depth of my gratitude for the people I encountered on this journey.

First and foremost, I am incredibly grateful to my supervisors, Prof Laurent Alfandari and Prof Claudia Archetti. Any amount of thanks will never be enough for the help, support, and kindness they extended to me. They encouraged me when I did not believe I would see an end to this journey. They played a significant role in helping me overcome all the hurdles that I faced during this time. They were patient with me when I didn't think I deserved patience anymore. They were available whenever I needed them, always kind, and always helped explain whenever I was stuck, even when I was hesitant. Working with them has been a privilege. I only hope that I can be to someone one day, even half of what they were to me during these years.

I am also extremely thankful to Prof Ivana Ljubić, with whom I had the opportunity to work on my last project. I am in awe of not only her depth of knowledge, but also her patience and kindness, and her taking the time to explain whenever I had any questions. My only regret is that I did not start working with her sooner.

I am grateful to Prof Diego Delle Donne, who I closely worked with during my first project, and Prof Alberto Santini, who I collaborated with on my second project. Apart from being brilliant researchers and wonderful people to work with, they are both fantastic coders. I greatly admire their skills and I learned a lot even by just observing their work.

I thank Prof Teodor Gabriel Crainic, who is always a joy to talk to, Prof Ana Barbosa-Povoa, and Prof Ahmadreza Marandi for agreeing to be a part of my PhD jury, and taking their time to review this work.

I would also like to thank Prof Fouad El Ouardighi, Prof Sara Rezaee Vessal, and Prof Felix Papier, for sharing their knowledge and experiences.

My PhD journey would have been incomplete without the best PhD office assistants ever– Lina, Christine, and Audrey. They went above and beyond to help everyone, and their door was always open if I ever needed to talk.

I feel fortunate to have been a part of the ODA department at ESSEC. The friendly work environment among colleagues and the respect and admiration everyone has for each other, both faculty members and students, set an example that I would take with me wherever I go.

Special thanks to all my friends in the PhD program, who carried me through days of insecurities and impostor syndrome, and nights of anxiety and depression. I would not have made it out on the other side without them. I adore them with all my heart.

Finally, thanks to the most incredible parents, Mamuni and Bapi, whose sacrifices made it possible for me to be here. They have been my biggest cheerleaders in every endeavor, and I could not be more grateful to them for everything. My brother, who has been my biggest support system in the last decade and my first phone call each time I mess up, thank you for being there. Finally, thank you to my amazing husband, whose constant encouragement got me through the last part of this journey.

1

Introduction

The last mile delivery (LMD) is the most expensive part of the whole freight delivery process, in addition to being the least sustainable one. 53% of the total shipping costs occurs in the last mile. It affects not only the shipping companies but urban life as well. LMD can have a multitude of negative impacts on the triple bottom line of sustainability– people, planet, and profit (Rai et al., 2017a; Viu-Roig & Alvarez-Palau, 2020). On the other hand, LMD grows to be more competitive everyday. Boom in e-commerce and evolving customer demands is leading to faster (same-day or few-hour) and cheaper deliveries starting to become the norm. Deloison et al. (2020) predicts a 78% growth in urban LMD by the year 2030. To satisfy e-commerce demand, remain relevant, and meet sustainability expectations, LMD companies have been adopting innovative strategies for the delivery process.

Verlinde (2015) provides a comprehensive list of the negative environmental, social, and economic impacts of LMD, which we briefly summarize here.

- Environmental impacts: Perhaps the greatest negative impact of LMD is faced by the environment. Emissions of harmful pollutants like CO_2, particulate matter (PM), and other greenhouse gases (GHGs) by delivery trucks deteriorate the air quality in urban areas. Moreover, high volume of demands and expectations of lower delivery times only worsen the situation putting more vehicles on roads and also causing congestion.

- Social impacts: Environmental impacts also lead to social impacts by hampering the living quality in urban areas. Traffic and congestion on roads increase accidents, health risks, and noise pollution. In the recent years, fast-paced LMDs have led to an increase in the gig economy, where freighters are usually independent workers and not employed with the company, and thus, do not have job security or access to health insurance. Furthermore, fast delivery schedules may lead to unsafe driving on roads and unreliable working hours for the freighters.

- Economic impacts: Traffic and congestion on roads lead to unreliable deliveries and thus promote mistrust among the customers. It also causes the delivery person to lose time. The cost of government regulations and planning also contribute to the costs of delivery.

However, not all is gloomy, as there has been a disruption in innovations in the last-mile sector in an effort to come up with sustainable solutions. Viu-Roig & Alvarez-Palau (2020) categorizes innovations in LMD into three types– organizational, technology-enabled, and data technique enabled. Organizational innovations include urban consolidation centers, local fulfillment centers, crowdsourcing, etc. Technology-enabled innovations consist of incorporating automated lockers, drones, and droids in the last phase of the delivery. Data-enabled innovations use big data and analytics to make the LMD process more sustainable and efficient.

The great news is that consumers are beginning to be flexible and prioritize sustainability over the speed of order fulfillment and the cost of their orders. For example, customers are more willing to sacrifice speed of delivery over cost (Caspersen & Navrud, 2021; Nogueira et al., 2021). Nogueira et al. (2021) find the type of product also plays a role. They are more flexible in delivery speed for fashion, accessories, sport, and leisure over products like health, cosmetics, and food and beverages. However, population demographics play a role in consumer preferences.

Yurchisin & Jaeger (2021) states that the LMD ecosystem stands at a tipping point. While it has the potential to be faster, greener, cheaper if all involved entities work together, it could also worsen horribly if we are not careful. Kiba-Janiak et al. (2021) identify several stakeholders in the last mile– receivers (e-customers), shippers (producers, online retailers and e-trade services), residents, government (local and national authorities), transport companies, and others. Any solution that seeks to curb the negative social and environmental impacts of LMD will not be viable in the long term if it is not economical at the same time. Thus, we need to develop solutions that are not only sustainable, but also provide economic benefits to all the stakeholders in LMD. To this end, we present two studies in this thesis. The first presents a solution whose goal is to reduce environmental emissions and congestion on roads caused by LMD vehicles. The second focuses on the social component by developing a LMD strategy which address stability of working schedules of couriers or freighters.

In the second chapter of the thesis, we propose to use the spare capacities of public vehicles like buses, trams, metros, and trains, particularly during off-peak hours, to deliver packages in the city instead of dedicated delivery vehicles. The integration of public transportation systems and last-mile deliveries is aimed at reducing the number of heavy combustion vehicles inside city premises, subsequently alleviating traffic congestion, enhancing environmental conditions, and fostering a better quality of life in urban regions. Moreover, the public transportation companies can be compensated accordingly, resulting in an additional source of income, which can be utilized to improve the quality of public service. Thus, the topic holds immense relevance and has significant social, economic, and environmental benefits.

One of the benefits of such an approach for the last-mile is that no new vehicles are added on the roads for delivery purposes. Our experiments showed that, on average, the length of trips using traditional large delivery trucks can be reduced by 86%. Moreover, the combined use of dedicated vehicles and personnel (trucks and freighters) can be reduced by 51% on average. These numbers can be even higher in large cities with an extensive public transit network because the majority of the delivery can be performed on public vehicles.

In the third chapter, we shift our gears to a tactical-level LMD problem of workforce sizing and shift scheduling. The decision maker wishes to hire couriers or freighters for a mid-term planning period (a few months) depending on the city's demand distribution. While a larger workforce can deal with a variety of demand patterns, it incurs higher fixed costs. On the other hand, a smaller workforce size leads to higher outsourcing costs. Thus, there needs to be a delicate balance between the two.

Another concept in our study is shift management. Shifts are consecutive units of time during which hired couriers would work. We study three kinds of shifts- completely fixed shifts with predetermined fixed start and end times, completely flexible shifts, and partially flexible shifts which lies between the two. Our idea of shifts is motivated by the desire to provide stable working hours for the freighters. Often, the freighters juggle multiple jobs, or they are students who look to work part-time for delivery companies. Thus, having stable working hours is critical for them. Our results show that having partially flexible shifts provides desired benefits without restricting the company's bottom line significantly.

The last part of this thesis deals with another critical topic in operations research– disaster management and planning. The United Nations Office for Disaster Risk Reduction (UNDRR) defines a disaster as "a serious disruption of the functioning of a community or society involving widespread human, material, economic or environmental losses and impacts, which exceeds the ability of the affected community or society to cope using its own resources" (Aydin & Cetinkale, 2023). Whether disasters are natural (earthquakes, floods, hurricanes, landslides, forest fires) or man-made (war, terrorism, industrial or nuclear accidents), they result in an unparalleled loss of lives and property and often cause a degradation in the environment.

Figure 1.1 shows the number of different types of natural disasters in the world between 1970 and 2023. On average, over the last few decades, disasters have claimed 40,000 to 50,000 lives per year (Ritchie & Rosado, 2022). Sometimes, they destroy a major part of a country, for example, the Gorkha earthquake of 2015 in Nepal. Disasters also displace thousands of people and cause severe economic losses. Some emergencies are so unpredictable that they cripple the whole world for a while– the COVID-19 pandemic. It took away millions of lives, affected more directly and indirectly, maimed economies, and brought the world to a standstill. It forced us to step back and reconsider how we prepare ourselves to face such adversaries.

Disaster management seeks to efficiently and systematically assess the risk associated with a disaster,

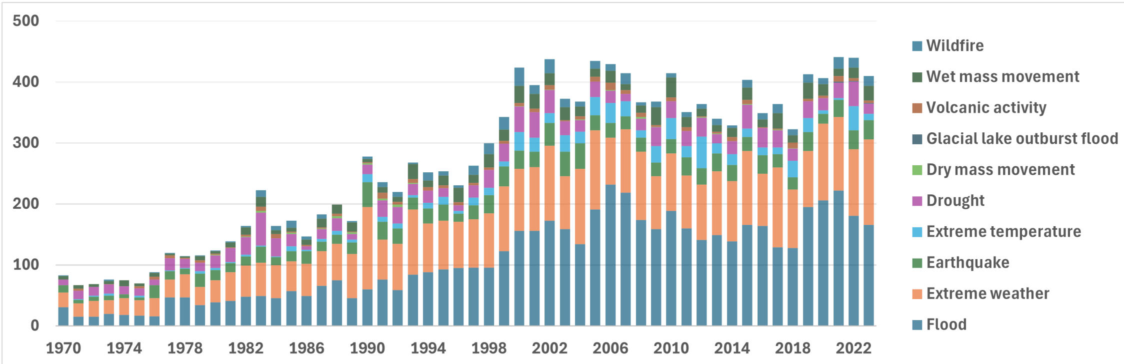

Figure 1.1: Global reported natural disasters by type, 1970 to 2023, Source: EM-DAT, CRED, Ritchie & Rosado (2022)

prepare an actionable plan for the community to fight back once a disaster strikes, and help rebuild the community and infrastructures back to their former self in the post-disaster phase. There are four primary phases in disaster management: mitigation, preparedness, response, and recovery (Altay & Green III, 2006). Mitigation and preparedness fall into the pre-disaster phase, while response and recovery fall into the post-disaster phase. The mitigation phase involves steps taken to prevent disasters or reduce their effect on the community, for example, constructing disaster-proof infrastructure by enforcing building codes, risk analysis to study the likelihood and strength of emergencies, insurance to reduce financial losses, etc. The preparedness phase builds the resilience of communities to combat an emergency. For example, maintaining inventories if a disaster occurs, recruiting and training volunteers, acquiring vehicles, and conducting disaster drills to train the community, among others. The response phase of disaster management occurs once a disaster has struck, and the community fights back. It includes putting into action the emergency operations plan, evacuation of people, opening and maintaining of shelter sites and emergency medical centers, and search and rescue operations. Finally, the recovery phase refers to the long-term actions that are taken after the immediate effects of a disaster have passed and to help the community rebuild and get back to their normal life. It includes, for example, debris clearance, rebuilding of roads and infrastructures, financial assistance and care for displaced people, and mental support to the community. The reader is referred to Altay & Green III

(2006) for a comprehensive discussion on the different phases of a disaster management system.

We direct our attention to a disaster preparedness model for earthquakes and aftershocks in the fourth chapter of this thesis. Aftershocks are earthquakes that follow the main earthquake and have magnitudes comparable to or smaller than that of the first earthquake. For example, the Turkey-Syria 2023 earthquake, which had a magnitude of 7.8 on the Richter scale, was succeeded by another of magnitude 7.5 about 9 hours later. Two more aftershocks of magnitude 6.4 and 5.6 hit the region a few days later. Not only that, the region has been hit by thousands of aftershocks of smaller magnitudes in the days that followed. While the impact of smaller aftershocks may not have been so severe earlier, they can trigger landslides and building collapses, in a region that is already vulnerable due to the earthquake. Another example is the 2015 earthquake in the Gorkha district of Nepal, which experienced a 7.8 magnitude earthquake. It was followed by several major aftershocks, which triggered landslides and avalanches further killing people.

Motivated by the above examples, we include aftershocks in our planning process. Our goal is to select a set of locations to establish facilities for the prepositioning of relief materials like canned food, bottled water, blankets and tents, medical supplies, and other non-perishable items that can be stored, to prepare for such catastrophic events of earthquakes followed by several aftershocks. We make a quick note here that though we explicitly consider aftershocks in the planning process, our model is not limited to aftershocks only. In fact, it can be used as a decision-making tool in anticipation of any simultaneous or compound hazards as well.

One of the most challenging tasks of dealing with disaster management is the intrinsic uncertainty associated with it. Nobody knows when and where a disaster will strike and to what scale it will impact social life, economies, and the environment. Incorporating uncertainty is crucial in the disaster management and planning process. Uncertainties can arise either on the supply side, on the demand side, or in the relief service network (Dönmez et al., 2021), or a combination of two or more of the above. Uncertainty in demand arises due to unknown time, scale, location, and time of a disaster. It manifests in people requiring relief, shelter, and support following a disaster. Uncertainty on the supply side may occur when facilities like warehouses with stocked relief items are damaged, either partially or completely. It could also occur in situations where the supply of materials is dependent on donations from various organizations. Finally, uncertainty in the relief network happens when the network is disrupted, for example, by disasters like floods and earthquakes.

Lack of data poses another challenge in disaster preparedness. Lack of data also hinders collaboration and coordination between organizations and stakeholders. Sometimes, the cost of poor-quality data is paid in lives and cannot be recovered (Jayawardene et al., 2021). Thus, data and information are pivotal for decision-makers (Starr & Van Wassenhove, 2014). In the preparedness phase, data on population, infrastructure, and road networks is required to set up facilities, preposition inventories, and making response plans. Access to reliable data in the response phase, including information on location and number of affected people, damaged infrastructure and disrupted road networks, is even more crucial to conduct search and rescue, providing relief to people, and timely treatment of the injured.

Thus, a decision-maker needs to consider such uncertainties and lack of data to build resilient disaster management plans. In the literature, robust optimization, stochastic optimization, fuzzy optimzation, or any combination from the above has been used to deal with uncertainties. In our study, we adapt a robust optimization approach, and hence this is where we focus our attention.

Robust optimization models seek to develop solutions that remain valid under a wide range of scenarios. A key concept in robust optimization is uncertainty sets. Any parameter whose value is not completely known is assumed to lie in an uncertainty set, which consists of a range of likely values for the parameter. Often, robust optimization is used to find solutions that remain feasible in the worst-case scenario (i.e., the parameters taking their worst possible in their uncertainty set), with the best possible objective function value. However, this might lead to solutions that are too conservative in nature. Thus, comes in the idea of "degree of conservatism", where a trade-off between robustness and objective function value is considered.

Bertsimas & Sim (2004) proposed a Γ-robustness approach which is based on the idea that the likelihood of all parameters taking their worst-case values at the same time is extremely low. In their approach, the solution remains feasible even if Γ_i number of coefficients deviate to their worst-case values for each constraint i. It is this idea that we were inspired by. Not every single possible aftershock would hit the affected region at the same time after an earthquake. We develop a solution that would minimize the worst-case allocation cost of the demand nodes to the facilities when the region is hit by at most Δ aftershocks.

We start by enumerating all possible combinations of an earthquakes and Δ aftershocks, and then formulating a model that finds the combination that generates the worst allocation cost. However, this becomes computationally challenging to solve, leading us to develop two solution approaches–one that utilizes a branch-and-cut algorithm, and another employing an extended formulation for the same. We also propose a two-stage approach to formulate the problem and use a branch-and-cut algorithm to solve it. An extensive case study on the Turkey based on data from the Turkey-Syria earthquake of 2023 shows the importance of incorporating earthquakes and aftershocks simultaneously in the decision-making process.

2

Decomposition Matheuristics for Last-Mile Delivery Using Public Transportation Systems

joint work with **Claudia Archetti**

2.1 Introduction

The boom in e-commerce over the last decade poses several challenges for last mile deliveries, particularly the need to make them more efficient, less expensive, and more sustainable. The negative impacts caused by delivery vehicles can be three-fold – economic, social, and environmental (Rai et al., 2017a). A study by the World Economic Forum (Deloison et al., 2020) states that there will be a 36% rise in the number of delivery vehicles on urban roads by 2030 due to the consistent and exponential growth of demands for e-commerce deliveries, leading to an additional emission of 6 million tonnes of CO_2. It can potentially increase the average commute time of each passenger by 21% (amounting to an additional 11 minutes) per day due to congestion. Thus, the need of the hour is solutions that are sustainable, competent, and economically viable.

To keep up with the growing demands, companies are looking towards innovative approaches that reduce the costs of social and environmental externalities. Several companies have tested the use of drones for the final leg of the delivery, including Google's Project Wing, Amazon's Amazon PrimeAir, DHL's PaketKopter, and GeoPoste's GeoDrone (Ranieri et al., 2018). Others propose using electric and other green vehicles as a viable option for delivery as well (Mucowska, 2021). The utilization of pickup points and lockers are effective, popular, and well-established alternatives (Cleophas et al., 2019). Crowdshipping has gained popularity over the last few years, where parcels are matched with couriers, see for example, (Rai et al., 2017b). Different shipping companies can also collaborate to reduce overall delivery costs (Cleophas et al., 2019).

In this paper, we propose to use public transportation systems to transport packages in urban areas. Over recent years, an increasing number of studies have identified and emphasized the opportunities and benefits of freight-on-transit (FOT), see for example, Galkina et al. (2019). One of the most significant advantages of using public vehicles is that it does not add any new vehicles on the road solely for package delivery, which means no extra congestion and no extra emissions caused by traditional delivery trucks. The reduced congestion due to the removal of delivery vehicles on roads would further ensure reliable running times of vehicles on the road. The transit companies would be compensated accordingly, and the revenue generated can be used to increase the services for passengers (Taniguchi et al., 2016). Thus, it could be a win-win solution for all parties involved. The idea is to use the spare capacities of public vehicles like buses, trams, trains, subways, and other public vehicles, particularly during off-peak hours, or to have dedicated spaces for freight in the vehicles.

We wish to explore the operational implementation of the system and optimize the delivery of packages on the network in a cost and time-effective manner. We consider a delivery company that wants to utilize the public transit network for its last mile deliveries. The problem can be divided into three tiers. In the first tier (also referred to as T1), delivery trucks belonging to the company carry the packages from the Consolidation and Distribution Center (CDC) to nearby stops, called *drop-in* stops, of the public transportation network. The second tier (T2) of the delivery is the one that occurs on board public vehicles, which have pre-determined schedules, itineraries, and stops. The vehicles pick up the packages from the drop-in stops and transport them to other stops on their route, which we call *drop-out* stops. These stops are within the city and typically close to customer locations. Finally, the city freighters pick up the packages from the drop-out stops and deliver them to the customers using sustainable modes of transport, like electric vehicles, drones, bikes, or even freighters simply walking for the delivery. These freighters could either belong to the company's fleet or be comprised of autonomous crowdsourced drivers. This constitutes the third and final tier (T3) of the system. We wish to find a delivery plan such that the delivery costs of the first and third tiers, and thereby distance traversed using dedicated delivery means, are minimized. We name this problem the *Three-Tier Delivery Problem on Public Transportation* (3T-DPPT hereafter). Figure 2.1 shows a small example of the

3T-DPPT. It consists of a CDC and three public vehicle lines– A, B, and C, and 15 customers.

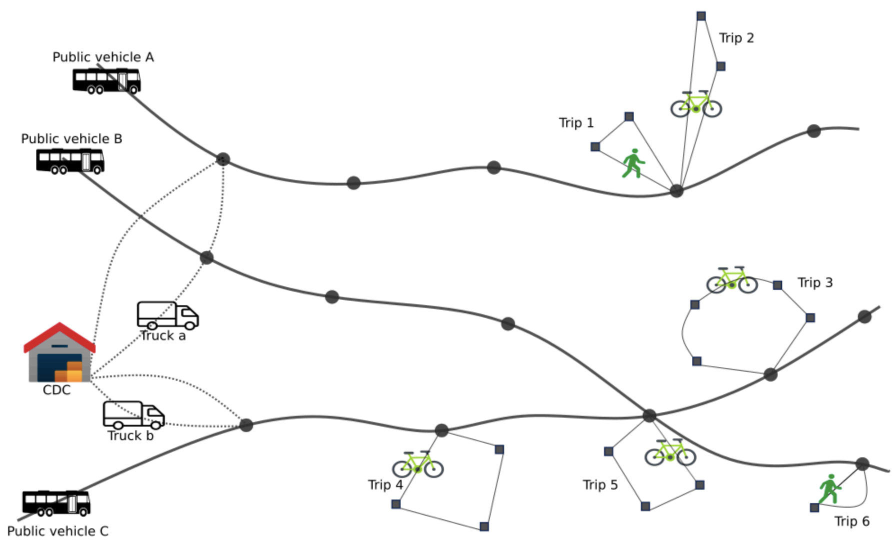

Figure 2.1: An example of the freight delivery structure

The effectiveness of such integrated delivery systems has already been demonstrated in several cities. Marinov et al. (2013) discuss the case of the French supermarket chain Monoprix, which uses urban trains and sustainable vehicles to transport non-perishable products in the city of Paris, resulting in 10,000 fewer trucks circulating in Paris (Onur, 2019). An article by Saito (2021) reports two companies, Nishi Tokyo Bus Co. and Yamato Transport Co., using buses to deliver packages from the city of Akiruno to the village of Hinohara in western Tokyo. This provided the bus company with a new revenue source on the unprofitable route and reduced the round-trip traveling distances for the delivery company by 50 kilometers a day. The village has also welcomed the collaboration and acknowledged its benefits. GB Railfreight, a freight delivery service based in the UK, has explored using old commuter trains to deliver parcels, using standard roll cages that can be easily loaded and offloaded (RailwayTechnology, 2020). Amazon is also looking to use public buses for its deliveries and has received a patent that would transform buses into parcel carriers, see for example, Baron (2019) and Reul (2019). This is aimed at customers who do not live near their pickup points or where carriers are scarce. The report mentions that Amazon was looking to invest $1.5 million in the public transportation system in Seattle. An article by Hermes (Zeitler, 2019) discusses several implementations of FOT in practice. For example, the TramFret project in the French city of Saint-Étienne used decommissioned trams to deliver goods inside the city. Moscow utilizes its metro network to deliver parcels from one end of the city to another. Hermes and the Frankfurt transport authority have partnered together to transport two boxes filled with packages from a hub outside the city to Europaviertel, a housing and business district in Frankfurt (Zeitler, 2019). Then, they use e-bikes to deliver the packages to their destinations. The researchers identify that such delivery projects have great potential to be impactful in the cities, particularly in pedestrian zones or areas around the transit stations. Galkina et al. (2019) analyze the effectiveness of FOT by conducting a study in the city of Bratislava and find that it has the potential to reduce overall transportation costs by 8-12 times. There has also been a recent case study by Bacher et al. (2024) to implement an integrated system in New York City. They provide estimates for reduced CO_2 emissions for different types of trucks. They also find a total of 16089.87 grams of reduced pollutants per 14.7 miles when trucks are replaced by subway trains. All these examples demonstrate the viability and advantages of shared transportation systems. Our problem is motivated by these examples, particularly the type of delivery systems proposed by Amazon and the one implemented by Hermes.

The FOT problem involves decision-making at several levels: strategic, tactical, and operational. Strategic level decisions are long-term and involve setting up the system in practice. For example, the public vehicle lines, drop-in stops, and drop-out stops of the system need to be selected based on the distribution of customers. Tactical level decisions are medium-term decisions and deal with setting up lockers and hiring personnel, among others. In this paper, we focus on the operational level decision-making involving the day-to-day implementation of the system. The delivery system and the contracts between parties like the government, the last-mile distributor, and the transportation companies need to be established beforehand. Necessary infrastructure like storage facilities for packages at the stops, or modifying public vehicles to have dedicated spaces for packages (if required), and equipment for transporting packages to and from the vehicles also need to be set up. These decisions vary by city and, thus, should be made by considering the existing public transportation infrastructure and the socio-economic factors of the city.

The contributions of the paper are the following. We introduce the 3T-DPPT and provide a mixed-integer linear programming formulation for it. Since the problem is extremely complex, involving decision-making at several levels, and given the nature of the problem, decomposition seemed like a natural choice to solve it. Based on the natural three tiers of the problem, and depending on which tier we start solving the problem from, we provide three different matheuristic approaches for decomposing and integrating the model. For the second tier of delivery on public vehicles, we formulate and analyze three objective functions that support the primary intent of the system, which is to minimize delivery distances using dedicated vehicles. We generate instances that mimic real-life public transportation networks and package demands, and we implement our models on them. Finally, we inspect our solutions and make recommendations for implementing such a delivery system.

The remainder of the paper is organized as follows. In Section 2.2, we provide a review of the literature with regard to our problem. Section 2.3 describes the setting of the problem and introduces a formulation for it. We dedicate Section 2.4 to describing different approaches for solving the problem. Section 2.5 provides numerical studies, and we conclude in Section 2.6 with some suggestions for future research avenues.

2.2 Literature review

In this section, we review the literature that studies deliveries using public transportation networks in some capacity, either together with passengers in the same vehicle or in isolation: only making use of the infrastructure. The works can broadly be classified into two categories from the perspective of our study. The first category is where the conceptual models of such a system are introduced, and the effectiveness of the integration is considered either theoretically or through small-scale implementations in practice. The second is the group of papers that study similar systems and propose mathematical models to optimize freight transport on public transit networks. We briefly discuss the first category and focus our attention primarily on reviewing the works in the second category.

Trentini & Mahléné (2010) and Trentini & Malhene (2012) conducted one of the earliest studies on the topic. Apart from providing a survey of existing examples of cities that have adapted strategies for shared passenger and goods flows, they provide a conceptual model for the same, which they then show how to implement using a case study in the French city of La Rochelle. Gatta et al. (2019a,b) combine crowdshipping with public transport, where the packages are dropped off or picked up by people traveling by these transit systems, specifically in or around public transit stations. On a survey in the city of Rome, Gatta et al. (2019a) estimate a reduction of 239kg of particulate matter each year. Villa & Monzón (2021) study the potential of using metro networks and their existing capacities and lockers in metro stations for parcel delivery. They investigate two kinds of scenarios: making use of the spare capacities of vehicles or utilizing dedicated runs of freight trains on the existing lines. They study the system from the perspective of costs and impacts and also provide a case study on the city of Madrid. They find that a shared system has 11.16% to 14.72% lower operating costs than current systems, and the average external delivery cost per parcel is 8.2 to 9.8 times lower. Cavallaro et al. (2023) conduct a Delphi study with international stakeholders to gather information for setting up an integrated system. They identify attributes like distance between stops, service frequency, availability of information (inclusion of personnel onboard), punctuality, ticket prices, that need to be considered when designing the service. They mention one of the greatest advantages to be cross-subsidization from freight services to the transit system, resulting in higher service frequency or reduced fares. While several other studies analyze the system's viability in real life, due to the scope of our study, we concentrate on works that employ mathematical programming models to optimize integrated delivery systems.

Crainic et al. (2009) provided one of the first modeling frameworks for tactical and operational strategies of two-tier city logistics systems, with the possibility of using public vehicles like trams in the first tier and electric vehicles in the second tier. They propose generalized two-tier models where the movement of urban vehicles and freight is integrated, and consider routing and scheduling decisions.

Cheng et al. (2018a,b) study the distribution of packages using Crowdsourced Public Transportation Systems. Cheng et al. (2018b) model the transport of packages using the idle capacities of public transportation systems, where the packages can be loaded at a starting node, unloaded and reloaded at intermediary nodes, and finally unloaded at their destination stop, using a multi-commodity flow model. They also propose a heuristic to solve the problem. In Cheng et al. (2018a), the authors explore the problem further. They divide the study into two parts – the first being a Passenger Transit Model that estimates the number of passengers at each station and, thereby, calculates the under-utilized capacity. In the second part, the decisions about the actual assignment and delivery of the packages are made. They propose two approaches for the second part – the Minimum Limitation Delivery Method, which uses only the minimum under-utilized capacity, and the Adaptive Limitation Delivery Method (ALD), which utilizes the entire under-utilized capacity at each trip. They find ALD to perform better, with only slightly higher risks of affecting the quality of passenger experience. The main focus of their study is on the transfer using public vehicles, which constitutes a part of the problem studied in our paper. Huang et al. (2020a,b) investigate the deliveries of parcels that use drones interacting with existing public transit vehicles like trains, trams, etc. They propose algorithms and simulations to demonstrate the performance of their models. Fatnassi et al. (2015) also explore the idea of transporting goods and passengers in a shared system, where they propose to use personal rapid transit and freight rapid transit (FRT) alternatively in a shared transportation network. They propose a dynamic or on-demand model that minimizes the waiting time of the passengers and goods, along with the movement of empty vehicles. These studies primarily deal with the delivery problems focused on the second tier of our study.

Ghilas et al. (2016a,b,c, 2018) utilize scheduled public transportation lines for freight delivery. They study the Pickup and Delivery Problem with Time Windows and Scheduled Lines (PDPTW-SL), where freight requests are transported via public vehicle lines from one end to another. The authors provide an arc-based mixed-integer programming formulation for the problem and perform computational studies to demonstrate the benefits of using such a system (Ghilas et al., 2016b). In this paper, we have considered one origin of packages – at the CDC, and the trucks deliver them to the drop-in stations, instead of considering a pickup and delivery problem at both ends. Our motivation is to use the scheduled lines to deliver packages from the outskirts of the city to the city center to reduce the usage of trucks inside the city. We also include multiple drop-in and drop-out stops on each line, which comprises another layer of decision-making while the authors consider end-to-end transport of packages on the lines. In Ghilas et al. (2016a), the authors use an Adaptive Large Neighborhood Search (ALNS) heuristic algorithm to solve the problem on several synthetic instances, and on an instance generated based on the metro system in Amsterdam. The results on instances of sizes up to 100 indicate significant benefits in terms of cost savings, which range from 0 to 30%, reduced driving times ranging from 0 to 31%, and, proportionally, reduced CO_2 emissions. The authors also study a stochastic version of the same problem in Ghilas et al. (2016c), called the Pickup and Delivery Problems with Time Windows, Scheduled Lines and Stochastic Demands, where the demands of the requests are considered uncertain. They solve the problem using ALNS embedded into a sample average approximation method. Their computational studies show up to 16% reduced costs compared to a traditional PDPTW on instances of sizes up to 40 requests (each request being a pickup and delivery destination pair). They also extend their study to propose an exact solution approach based on the branch-and-price algorithm in Ghilas et al. (2018). They are able to solve small and medium-sized instances with up to 50 requests optimally within the time limit. They also study the Pickup and Delivery Problem with Time Windows and Transfers (PDPTW-T) as a special case, which includes the transfer of packages between the pickup and delivery vehicles at predetermined nodes.

Mourad et al. (2021) also study a version of the PDPTW-SL, where the scheduled lines consist of shuttles that can transport passengers along with robots carrying packages. In their setting, robots replace the pickup and delivery vehicles, and these robots perform the task of transporting packages between the stations and their origins and destinations. They study a stochastic version of the problem where the capacity of the shuttles is unknown and use an ALNS algorithm to solve it. Their method solves instances with up to 60 requests and finds solutions within 0.6% of the optimal solutions. A fundamental difference between the studies by Ghilas et al. (2016a,b,c, 2018); Mourad et al. (2021) and ours is that they study pick-up and delivery problems with symmetric delivery modes and features at the two ends of the public transportation lines. We study three distinct delivery modes in the three tiers, and our focus is to utilize public transportation to bring packages into the city, thereby keeping heavy delivery trucks completely outside the urban living area.

Behiri et al. (2018) discuss strategic, tactical, and operational issues of integrating freight transport on the passenger rail network. Then, they study a problem called the Freight-Rail-Transport-Scheduling Problem, provide a mixed integer formulation for the same, and propose two heuristic methodologies for its solution that decompose the problem into single-train-related subproblems. Ozturk & Patrick (2018) study an operational level model for freight transport using urban rail networks with known demand and due dates with penalties. They first propose an approximation algorithm and a pseudo-polynomial dynamic programming algorithm for the case with one departure and one arrival station. Then they extend it to several stations and present a heuristic method, two mixed integer models– one which minimizes the total tardiness in the presence of a fixed schedule and the second does the same along with determining a schedule for trains dedicated to freight, and then integrate the second in an ε-constraint model. They find that while the first model is superior performance-wise, the second is valuable at generating insights into the problem.

Masson et al. (2017) introduce the Mixed Urban Transportation Problem. They consider the transportation of packages from the CDC to the city on a bus route and subsequent deliveries from the bus stations by city freighters simultaneously. They categorized the problem into two specific classes of Vehicle Routing Problems (VRP)– the Two-Echelon VRP (2E-VRP) and the Pickup and Delivery Problem with Transfers. To solve the problem, they also use an ALNS methodology. They evaluate their model in the city of La Rochelle. Our problem is an extension of the setting considered by Masson et al. (2017), as we consider a more generalized delivery system with multiple public vehicle routes. We also have the option of delivering packages by trucks to the drop-in stops, where they can be collected, instead of a bus passing through the CDC and collecting them there. Their primary focus is on the last leg of the delivery, where most of the decisions about package movement, particularly on public transportation, are already made beforehand. Azcuy et al. (2021) study a two-tier system with goods being moved on a public transit line to an intermediate transfer location, from where the packages can be delivered to the end customers. Their problem includes the location decision of the transfer station, apart from the routing decisions of the last mile vehicles. They consider line network and circular network configurations for the transit networks, and customers are assumed to be uniformly distributed around them. The problem is solved using an ALNS heuristic using a Greedy Randomized Adaptive Search Procedure, and they find savings of up to 7.1% for line networks and 5.4% for circular networks. Schmidt et al. (2022) introduce the last-mile delivery problem with scheduled lines (LMDPSL), which is a two-echelon problem with public lines in the first echelon and city freighters in the second echelon. They use branch-price-and-cut algorithms for exact and heuristic solutions.

They minimize hierarchically a combination of the following objective functions: minimizing the number of city freighters, minimizing the routing costs, and minimizing the trips. They provide extensive computational experiments and several managerial insights, like instances with higher lines and stops have the lowest routing costs and utilize fewer freighters. In contrast, lines operating in a circle around the city center always lead to the highest routing costs and freighters. They also find that limiting the capacity of the public lines results in a moderate increase in routing costs, and reducing the time windows leads to a noticeable increase in the routing costs and the number of city freighters.

In Delle Donne et al. (2023a), the authors study the FOT problem at the strategic level. They discuss decisions about the public vehicle lines and the drop-in and drop-out stops to be included in the delivery system to maximize the demand covered. They propose several formulations for the problem and employ column generation-based heuristic approaches to solve them. They find that the topology of the public transportation network, along with the demand distribution and density, play the most significant role in achieving their objective. Zhou et al. (2024) study collaborative route planning for buses and delivery trucks in rural areas, where buses carry both passenger and freight. They use hybrid heuristic algorithms to solve their problems. They also implement their study in three townships in the Hanzhong City, and find that integrated models could generate an additional revenue of 139,795 yuan per year for the bus routes of the three towns, and save fuel costs worth 8,161 yuan compared to the traditional setting.

Finally, a recent detailed survey has appeared on freight delivery on urban public transportation systems (Elbert & Rentschler, 2021). We refer the reader to this exhaustive review for a complete view of the literature on the topic. While there were several studies focusing on the operational aspect of FOT, to the best of our knowledge, we failed to find one having a comprehensive three-tier delivery problem, with three distinct delivery modes in the three stages. Our motivation was to keep heavy delivery vehicles outside the urban living area, leading to less congestion on roads and reduced noise and air pollution. Such a setting poses its own problem, which we tackle in our study. In Table 2.1, we summarize the setting of the problems in studies that are closely linked to ours, and the features that differentiate this research.

Table 2.1: Comparison of literature closely linked to this study

Paper	Pick-up (P) / Delivery (D) / Pick-up and Delivery (PD)	Number of tiers	Depots	Lines	Stops (End-to-End / Multiple)
Azcuy et al. (2021)	D	2	1	1	Multiple
Behiri et al. (2018)	D	1	-	1	Multiple
Cheng et al. (2018a)	D	1	-	1	Multiple
Cheng et al. (2018b)	D	1	-	Multiple	Multiple
Ghilas et al. (2016a)	PD	3	Multiple	Multiple	End-to-End
Ghilas et al. (2016b)	PD	3	Multiple	Multiple	End-to-End
Ghilas et al. (2016c)	PD	3	Multiple	Multiple	Multiple
Ghilas et al. (2013)	PD	3	Multiple	Multiple	Multiple
Masson et al. (2017)	D	2	1	1	Multiple
Mourad et al. (2021)	PD	3	Multiple	Multiple	Multiple
Ozturk & Patrick (2018)	PD	2	-	Multiple	Multiple
Schmidt et al. (2022)	D	2	-	Multiple	Multiple
This paper	D	3	1	Multiple	Multiple

2.3 Problem setting

Let $\mathcal{C}$ be the set of all the customers where a package has to be delivered. Let o denote the CDC or the parcel depot, and o' denote a copy of the CDC. Let the set of dedicated delivery trucks at the CDC be denoted by $\mathcal{D}$. Let $\mathcal{P}$ be the set of public vehicles that can be used for delivering packages. Let $\mathcal{S}$ be the set of all the stops that have been equipped for the delivery system. For each vehicle $p \in \mathcal{P}$, let $\mathcal{S}_p$ denote the set of its stops. In our notation, each public vehicle has a unique representation, and it can be identified by the route (or line) it serves and the time it starts from its depot. Furthermore, let $\mathcal{S}_{in}$ and $\mathcal{S}_{out}$ denote the drop-in and the drop-out stops on the public vehicle network, respectively, so we have $\mathcal{S} = \mathcal{S}_{in} \cup \mathcal{S}_{out}$. For each customer i, we pre-assign a set of drop-out stops that can potentially serve the customers based on the distance from the stop to them. This is denoted by the set $\mathcal{S}_i^{out}$. These drop-out stops lead to a set of drop-in stops from where customer i's package can be transported (the drop-in stops that are on the line of the public vehicles that serve the drop-out stops in $\mathcal{S}_i^{out}$) and is denoted by $\mathcal{S}_i^{in}$. On the other hand, the set of customers that can be served from each drop-out stop v and each drop-in stop u are denoted by C_v^{out} and C_u^{in}, respectively. Let $\mathcal{P}_s$ be the set of all public vehicles that visit stop s. Let $\mathcal{K}$ be the set of all city freighters, and for each stop, $s \in \mathcal{S}$, let $\mathcal{K}_s$ denote the set of freighters that serve stop s. In our setting, each freighter serves exactly one drop-out stop. $\mathcal{N}$ denotes the set of all nodes or locations in the delivery system – the customers, the stops, and the CDC. Finally, we introduce a hypothetical node $\tilde{o}$ that represents the depot for all public vehicles. For simplicity of modeling, we assume that all public vehicles start from the same imaginary depot $\tilde{o}$ before reaching their first drop-in stop. This is because we are not concerned about the route of a public vehicle before it reaches its first drop-in stop.

We consider a daily planning horizon here. Each customer i has to be delivered a package, which consumes a capacity q_i. The packages are delivered from the depot o by a delivery truck d, and dropped off at a stop $u \in \mathcal{S}_{in}$. The capacity of each delivery truck is given by Q_d^1. Then a public vehicle p collects the packages from the drop-in stop u and drops them off at the drop-out stop $v \in \mathcal{S}_{out}$. Let Q_p^2 be the capacity of each vehicle p. Let T_{sp} denote the time at which a public vehicle p visits a stop $s \in \mathcal{S}_p$ on its line. Each drop-out stop s is served by a group of freighters allotted to that stop ($\in \mathcal{K}_s$), who pick up the packages dropped off at the stop and deliver them to the respective customers. The capacities of the freighters are given by Q_k^3. Each customer i must be served within their time window $\left[\underline{T}_i, \overline{T}_i\right]$. Additionally, we consider that there is some service time, denoted by $T_s^{\prime}$, associated with the drop-in and drop-out stops in the first and the third tier. At the drop-in stops, this service time corresponds to the time it takes to unload the packages from the trucks, sort them according to the public vehicles that would transport them, etc. At the drop-out stops, the service time includes the time it takes to unload the packages from the public vehicles, hand them over to the assigned freighters, among others. In the third tier, each customer i also has a service time $\widehat{T}_i$, which refers to the time required to deliver a package at the customer location. It includes the time taken by freighters to find a parking spot and locate the exact apartment or building once they reach the customer, among others.

Let D_{ij} denote the distance between any two locations of the system, where $i, j \in \mathcal{N}$. Let T^1_{uvd} denote the time taken by delivery truck d to traverse arc (u, v), where $u \in \mathcal{S}_{in} \cup \{o\}$ and $v \in \mathcal{S}_{in} \cup \{o'\}$, and C^1_{uvd} be the cost of using a delivery truck to traverse the arc. Similarly, let T^3_{ijk} denote the travel time for traversing arc (i, j), where, $i, j \in \mathcal{C} \cup \mathcal{S}_{out}$, by freighter k, and C^3_{ijk} be the corresponding cost. We use the parameter α_{uvp} to identify the public vehicle routes. It takes the value 1 if the vehicle p goes from a stop u to a stop $v \in \mathcal{S}_p$, and 0 otherwise.

We study a deterministic version of the problem here, so the orders for the day are known. The residual capacities of public vehicles is assumed to have been estimated from observing previous occupancy data of the vehicles at the stops. We assume that there are enough delivery trucks and freighters, and enough capacity on the public vehicles to deliver all the packages. Finally, we assume that there is no transfer of packages within the same tier.

Table 2.2: List of sets and parameters used

Sets		**Parameters**	
o	the CDC or parcel depot	C^1_{uvd}	cost of traversing arc (u, v) using a delivery truck
o'	dummy CDC (a copy of the CDC)	C^3_{ijk}	cost of traversing arc (i, j) by a freighter
$\mathcal{C}$	set of customers	D_{ij}	distance between locations $i, j \in \mathcal{N}$
$\mathcal{P}$	set of public transportation vehicles	T_{sp}	time when public vehicle p is scheduled to reach stop s
$\mathcal{S}$	set of all stops for public transportation vehicles	Q^1_d	capacity of delivery truck d
$\mathcal{S}_{in}$	the set of *drop-in* stops	Q^2_p	capacity of public vehicle p
$\mathcal{S}_{out}$	the set of *drop-out* stops	Q^3_k	capacity of freighter k
$\mathcal{S}_p$	set of stops traversed by public transportation vehicle p	q_i	capacity consumed by the package of customer i
$\mathcal{P}_s$	set of public transportation vehicles that visit stop	T^1_{uvd}	time taken by delivery truck d to traverse arc (u, v)
$\mathcal{D}$	set of delivery trucks at the CDC	T^3_{ijk}	time taken by freighter k to traverse arc (i, j)
$\mathcal{K}$	set of all city freighters	$\underline{T}_i$	earliest time that customer i can be served
$\mathcal{K}_s$	set of freighters that serve drop-out stop s	$\overline{T}_i$	latest time that customer i can be served
$\mathcal{S}^{out}_i$	set of drop-out stops from where a customer i can be served	$\widehat{T}_i$	service time (delivery time) required at customer i
$\mathcal{S}^{in}_i$	set of drop-in stops where customer i's package can be loaded onto a public vehicle	T'_s	service time required at stop s
C^{in}_s	the set of customers that can be served via drop-in stop s	α_{uvp}	equals 1 if public vehicle p goes from stop u to stop v, 0 otherwise
C^{out}_s	the set of customers that can be served from drop-out stop s		
$\mathcal{N}$	the set of all nodes in the system, equals $\mathcal{C} \cup \mathcal{S} \cup \{o\} \cup \{o'\}$		
$\tilde{o}$	bus depot (dummy node)		

Next, we describe the decision variables for the problem. r_{isd} denotes binary variables that take the value 1 if delivery truck d transports the package i from the CDC to the drop-in stop s, and 0 otherwise.

Table 2.3: List of decision variables for the problem

Decision Variables	
Tier 1	
r_{isd}	equals 1 if the package for customer i is delivered by truck d to the drop-in stop s, 0 otherwise
w_{uvd}	equals 1 if a delivery truck d traverses arc (u, v), 0 otherwise
t^1_{ud}	time when delivery truck d starts from (or leaves) node $u \in \mathcal{S}_{in} \cup \{o\}$
Tier 2	
y^1_{isp}	equals 1 if the package for customer i is picked up by public vehicle p from drop-in stop s, 0 otherwise
y^2_{isp}	equals 1 if the package for customer i is dropped off by public vehicle p at drop-out stop s, 0 otherwise
l^2_{up}	load of a public vehicle p as it leaves stop $u \in \mathcal{S}_p$
Tier 3	
z_{ik}	equals 1 if freighter $k \in K_s$ picks up customer i's package, 0 otherwise
x_{ijk}	equals 1 if freighter k traverses arc (i, j), 0 otherwise
t^3_{ik}	time when freighter k starts from node $i \in \mathcal{C} \cup \mathcal{S}_{out}$

Binary variables w_{uvd} take the value 1 if delivery truck d traverses arc (u, v), where $u \in \mathcal{S}_{in} \cup \{o\}$ and $v \in \mathcal{S}_{in} \cup \{o'\}$, and 0 otherwise. t^1_{ud} is a continuous variable that notes the time as the truck d leaves the CDC (if $u = o$) or visits each drop-in stop $u \in \mathcal{S}_{in}$. These three sets of variables comprise the decisions of the first tier of the problem. Then, we have binary variables y^1_{isp} that take value 1 if the public vehicle p picks package i from the drop-in stop s, and 0 otherwise. Similarly, binary variables y^2_{isp} take value 1 if the public vehicle p drops package i at the drop-out stop s. Variables l^2_{up} are continuous variables that update the load of the public vehicle p as it visits each of its stops. This load is computed as the initial load of the vehicle p when visiting stop u, minus the volume of packages dropped off at u, plus the volume of packages picked up from stop u. These are the decision variables associated with the second tier of the problem. Finally, we have the variables that are related to the third tier. Binary variables z_{ik} take the value 1 if package i is assigned to freighter k, and 0 otherwise. Variables x_{ijk} are also binary and take the value 1 if freighter k traverses arc (i, j), where $i, j \in \mathcal{S}_{out} \cup \mathcal{C}$. Finally, we have continuous variables t^3_{ik} that update the time as each freighter k leaves a drop-out stop (if $i \in \mathcal{S}_{out}$) or visits the customers (if $i \in \mathcal{C}$). However, we must note that the drop-in stops lie at the intersection of Tiers 1 and 2, and the drop-out stops lie at the intersection of Tiers 2 and 3. Thus, whenever a variable is associated with a drop-in or a drop-out stop, it affects decisions corresponding to both the tiers it lies at the intersection of.

Our problem is to find a path for each package from the CDC via a delivery truck, followed by a public vehicle, and finally, a freighter to the customer, such that the total distance traveled by the delivery trucks and the freighters is minimized. Figure 2.2 shows the problem pictorially. While there are several other objective functions that pertain to the problem, we choose this because it aligns with the environmental goals of our study, which is to minimize the use of dedicated delivery vehicles and, thereby, additional emissions caused by them.

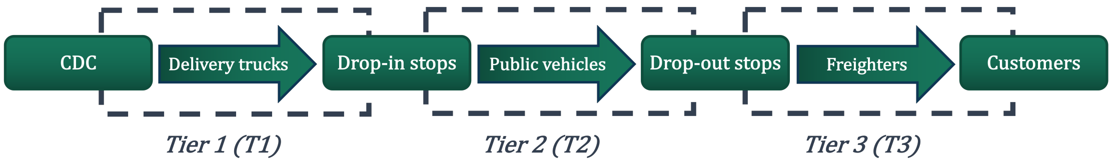

Figure 2.2: The path of a package

Tables 2.2 and 2.3 summarize the different notations and decision variables for the 3T-DPPT problem.

2.3.1 Model formulation

The formulation of the 3T-DPPV can be broken down into three parts based on the three tiers of the approach. Tiers 1 and 3 primarily constitute routing problems, while Tier 2 is an assignment problem with time restrictions. Along with these, we need to define constraints linking the three tiers.

The process starts with the delivery trucks transporting packages from the CDC to the drop-in stops in tier 1. Each package is assigned to precisely one delivery truck which delivers it to a drop-in stop. The assignment is done such that the truck's capacity is not exceeded. We model this using the following constraints:

$$\sum_{s \in \mathcal{S}_{in}} \sum_{d \in \mathcal{D}} r_{isd} = 1 \qquad \forall i \in \mathcal{C}, \tag{2.1}$$

$$\sum_{i \in C} \sum_{s \in \mathcal{S}_{in}} q_i r_{isd} \leq Q_d^1 \qquad \forall d \in \mathcal{D}. \tag{2.2}$$

The next set of constraints defines the route of the trucks. Each truck starts from the CDC, follows a route to deliver the packages to different drop-in stops, and returns to the CDC.

$$\sum_{v \in \mathcal{S}_{in} \cup \{o'\}} w_{ovd} = 1 \qquad \forall d \in \mathcal{D}, \tag{2.3}$$

$$\sum_{v \in \mathcal{S}_{in} \cup \{o\}} w_{vo'd} = 1 \qquad \forall d \in \mathcal{D}, \tag{2.4}$$

$$\sum_{\substack{v \in \mathcal{S}_{in} \cup \{o'\} \\ v \neq u}} w_{uvd} = \sum_{\substack{v \in \mathcal{S}_{in} \cup \{o\} \\ v \neq u}} w_{vud} \qquad \forall u \in \mathcal{S}_{in},\ d \in \mathcal{D}, \tag{2.5}$$

$$\sum_{\substack{u \in \mathcal{S}_{in} \cup \{o\} \\ v \neq u}} w_{uvd} \geq \frac{1}{M} \sum_{i \in \mathcal{C}} r_{ivd} \qquad \forall v \in \mathcal{S}_{in},\ d \in \mathcal{D}. \tag{2.6}$$

Constraints (2.3) and (2.4) ensure that the delivery trucks start and end at the CDC. Constraints (2.5) are the flow conservation constraints for the delivery trucks at each drop-in stop. Constraints (2.6) ensure that if a package is assigned to a drop-in stop via a delivery truck, that truck must visit the stop. M denotes a large number.

Then, we use constraints to link tier 1 to tier 2, i.e., if a delivery truck drops off a package at a drop-in stop, a public vehicle must pick it up from that stop, and the constraints are given by:

$$\sum_{d \in \mathcal{D}} r_{isd} = \sum_{p \in \mathcal{P}_s} y_{isp}^1 \qquad \forall i \in \mathcal{C},\ s \in \mathcal{S}_{in}. \tag{2.7}$$

Moreover, we have time constraints on when the packages can be dropped off and picked up at the drop-in stops.

$$t^1_{vd} \geq t^1_{ud} + T^1_{uvd} + T^{\prime}_v - M(1 - w_{uvd}) \qquad \forall u \in \mathcal{S}_{in} \cup \{o\},\ v \in \mathcal{S}_{in},\ u \neq v,\ d \in \mathcal{D}, \tag{2.8}$$

$$t^1_{sd} \leq \sum_{p \in \mathcal{P}_s} T_{sp} y^1_{isp} + M(1 - r_{isd}) \qquad \forall i \in \mathcal{C},\ s \in \mathcal{S}_{in},\ d \in \mathcal{D}. \tag{2.9}$$

Constraints (2.8) update the time for each delivery truck as it visits each drop-in stop, and constraints (2.9) ensure that a truck visits the drop-in stops before the packages that it carries are scheduled to be picked up by the public vehicles.

Next, we model the flow of the packages on the public vehicle network. We have the following constraints:

$$\sum_{p \in \mathcal{P}} \sum_{s \in \mathcal{S}_p \cap \mathcal{S}_{in}} y^1_{isp} = 1 \qquad \forall i \in \mathcal{C}, \tag{2.10}$$

$$\sum_{p \in \mathcal{P}} \sum_{s \in \mathcal{S}_p \cap \mathcal{S}^{out}_i} y^2_{isp} = 1 \qquad \forall i \in \mathcal{C}, \tag{2.11}$$

$$y^1_{isp} + y^2_{isp} \leq 1 \qquad \forall i \in \mathcal{C},\ s \in \mathcal{S}_{in} \cap \mathcal{S}_{out},\ p \in \mathcal{P}_s, \tag{2.12}$$

$$\sum_{s \in \mathcal{S}_p \cap \mathcal{S}_{in}} y^1_{isp} = \sum_{s \in \mathcal{S}_p \cap \mathcal{S}^{out}_i} y^2_{isp} \qquad \forall i \in \mathcal{C},\ p \in \mathcal{P}, \tag{2.13}$$

$$T_{up} y^1_{iup} \leq T_{vp} y^2_{ivp} + M\left(1 - y^2_{ivp}\right) \qquad \forall i \in \mathcal{C},\ p \in \mathcal{P},\ u \in \mathcal{S}_p \cap \mathcal{S}_{in},\ v \in \mathcal{S}_p \cap \mathcal{S}^{out}_i, \tag{2.14}$$

$$y^1_{iup} \leq \sum_{v \in \mathcal{S}_p \cap \mathcal{S}^{out}_i} \alpha_{uvp} y^2_{ivp} \qquad \forall i \in \mathcal{C},\ p \in \mathcal{P},\ u \in \mathcal{S}_p \cap \mathcal{S}_{in},$$

$$l^2_{\tilde{o}p} = 0 \qquad \forall p \in \mathcal{P}, \tag{2.15}$$

$$l^2_{vp} = l^2_{up} + \sum_{i \in \mathcal{C}^{in}_v} q_i y^1_{ivp} - \sum_{i \in \mathcal{C}^{out}_v} q_i y^2_{ivp}\ \forall p \in \mathcal{P},\ u \in \mathcal{S}_p \cup \{\tilde{o}\},\ v \in \mathcal{S}_p,\ u \neq v,\ \text{with } \alpha_{uvp} = 1, \tag{2.16}$$

$$l^2_{vp} \leq Q^2_p \qquad \forall p \in \mathcal{P},\ v \in \mathcal{S}_p. \tag{2.17}$$

Constraints (2.10) and (2.11) state that the package for each customer i is picked up by exactly one public vehicle p from a drop-in stop and dropped off at a drop-out stop. Constraints (2.12) ensure that the drop-in stop of a package is different from its drop-out stop. In practice, if there happens to be packages whose drop-in and drop-out stops are the same, then the customer can be directly serviced by trucks from the CDC. Constraints (2.13) make certain that the vehicle p that picks up a package for customer i from a drop-in stop is the same that drops off the package at a drop-out stop. Constraints (2.14) ensure that a package is picked up by a public vehicle before it is dropped off at one of the drop-out stops on its route. Constraints (2.15) set the load for each public vehicle to be zero initially, before it visits any drop-in stop. Constraints (2.16) update the load of each public vehicle at each stop, and (2.17) guarantee that the capacity of the public vehicles is respected.

Once the packages reach the drop-out stops, we have the third and final tier of the problem. We have some constraints that link T2 and T3, similar to what we had for T1 and T2. Specifically, the following constraints say that if a package is dropped off at a drop-out stop by a public vehicle, then a freighter serving that stop must pick it up:

$$\sum_{k \in \mathcal{K}_s} z_{ik} = \sum_{p \in \mathcal{P}_s} y^2_{isp} \qquad \forall i \in \mathcal{C},\ s \in \mathcal{S}^{out}_i. \tag{2.18}$$

Then, we have constraints that are exclusive to the third tier and that describe the routes of the freighters:

$$\sum_{k \in \mathcal{K}} \sum_{j \in \mathcal{C} \cup \mathcal{S}_{out}} x_{ijk} = 1 \qquad \forall i \in \mathcal{C}, \tag{2.19}$$

$$\sum_{\substack{j \in \mathcal{C} \cup \{s\} \\ j \neq i}} x_{jik} = z_{ik} \qquad \forall i \in \mathcal{C},\ s \in \mathcal{S}^{out}_i,\ k \in \mathcal{K}_s, \tag{2.20}$$

$$\sum_{i \in \mathcal{C}} q_i z_{ik} \leq Q^3_k \qquad \forall k \in \mathcal{K}, \tag{2.21}$$

$$\sum_{j \in \mathcal{C} \cup \mathcal{S}_{out}} x_{sjk} = 1 \qquad \forall s \in \mathcal{S}_{out},\ k \in \mathcal{K}_s, \tag{2.22}$$

$$\sum_{j \in \mathcal{C} \cup \mathcal{S}_{out}} x_{jsk} = 1 \qquad \forall s \in \mathcal{S}_{out},\ k \in \mathcal{K}_s, \tag{2.23}$$

$$\sum_{\substack{j \in \mathcal{C} \cup \mathcal{S}_{out} \\ j \neq i}} x_{ijk} = \sum_{\substack{j \in \mathcal{C} \cup \mathcal{S}_{out} \\ j \neq i}} x_{jik} \qquad \forall i \in \mathcal{C},\ k \in \mathcal{K}. \tag{2.24}$$

Constraints (2.19) ensure every customer is visited exactly once. Constraints (2.20) establish the link between variables x and z. Constraints (2.21) make sure that each freighter's capacity is respected. Constraints (2.22)-(2.23) state that the freighters start and end at their own pre-specified drop-out stop. Constraints (2.24) are flow conservation constraints for the freighters at each customer. The freighters start from a drop-out stop, follow a route to visit the customers, and come back to the same drop-out stop.

Finally, we have constraints that note the time that the freighters visit the customers and ensure that the packages reach the customers within their time windows:

$$t^3_{sk} \geq \sum_{p \in \mathcal{P}_s} T_{sp} y^2_{isp} + T'_s - M\left(1 - z_{ik}\right) \qquad \forall i \in \mathcal{C},\ s \in \mathcal{S}^{out}_i,\ k \in \mathcal{K}_s, \tag{2.25}$$

$$t^3_{jk} \geq t^3_{ik} + T^3_{ijk} + \widehat{T}_j - M\left(1 - x_{ijk}\right) \qquad \forall i \in \mathcal{C} \cup \mathcal{S}_{out},\ j \in \mathcal{C},\ i \neq j,\ k \in \mathcal{K}, \tag{2.26}$$

$$t^3_{ik} \geq \underline{T}_i \qquad \forall i \in \mathcal{C},\ k \in \mathcal{K}, \tag{2.27}$$

$$t^3_{ik} \leq \overline{T}_i \qquad \forall i \in \mathcal{C},\ k \in \mathcal{K}. \tag{2.28}$$

Constraints (2.25)-(2.26) update the time of the freighters as each customer is visited, and constraints (2.27) and (2.28) ensure that the time windows of the customers are satisfied. Constraints (2.8) and (2.26) also help prevent subtours for the trucks and the freighters, respectively.

Apart from the above constraints, we use the following standard symmetry-breaking constraints:

$$\sum_{v \in \mathcal{S}_{in}} w_{ovd} \geq \sum_{v \in \mathcal{S}_{in}} w_{ovd+1} \qquad \forall d \in |\mathcal{D}| - 1, \tag{2.29}$$

$$\sum_{u \in \mathcal{S}_{in} \cup \{o\}} \sum_{\substack{v \in \mathcal{S}_{in} \cup \{o'\} \\ u \neq v}} w_{uvd} \geq \sum_{u \in \mathcal{S}_{in} \cup \{o\}} \sum_{\substack{v \in \mathcal{S}_{in} \cup \{o'\} \\ u \neq v}} w_{uvd+1} \qquad \forall d \in |\mathcal{D}| - 1, \tag{2.30}$$

$$\sum_{j \in \mathcal{C}} x_{sjk} \geq \sum_{j \in \mathcal{C}} x_{sjk+1} \qquad \forall s \in \mathcal{S}_{out},\ k \in |\mathcal{K}_s| - 1, \tag{2.31}$$

$$\sum_{i \in \mathcal{C} \cup \{s\}} \sum_{j \in \mathcal{C}} x_{ijk} \geq \sum_{i \in \mathcal{C} \cup \{s\}} \sum_{j \in \mathcal{C}} x_{ijk+1} \qquad \forall s \in \mathcal{S}_{out},\ k \in |\mathcal{K}_s| - 1. \tag{2.32}$$

Constraints (2.29) say that delivery trucks with smaller indices have to be used first and (2.30) state that trucks with smaller indices have to be assigned larger routes. Constraints (2.31) and (2.32) establish the same, respectively, for the freighters.

The objective of our problem is to minimize the cost of using delivery trucks and freighters in the first and the third tier of the system, respectively, and is given by:

$$\mathit{Minimize} \quad \sum_{d \in \mathcal{D}} \sum_{u \in \mathcal{S}_{in} \cup \{o\}} \sum_{\substack{v \in \mathcal{S}_{in} \cup \{o'\} \\ u \neq v}} C^1_{uvd} w_{uvd} + \sum_{k \in \mathcal{K}} \sum_{i \in \mathcal{S}_{out} \cup \mathcal{C}} \sum_{\substack{j \in \mathcal{S}_{out} \cup \mathcal{C} \\ i \neq j}} C^3_{ijk} x_{ijk}. \tag{2.33}$$

We denote by *FULL* the complete mathematical formulation of the 3T-DPPT given by the objective function (2.33) subject to constraints (2.1)-(2.32).

Variables r_{isd}, w_{uvd}, y^1_{isp}, y^2_{isp}, z_{ik}, and x_{ijk} are binary, while t^1_{sd}, l^2_{up}, and t^3_{sk} are non-negative continuous variables.

The full model is huge and computationally challenging to solve. The commercial solver used in the computational experiments struggles to find a feasible solution for instances with as few as 40 customers within the time limit. In order to solve larger-sized instances, we employ a matheuristic methodology where the problem is decomposed into its natural three tiers and solved individually and sequentially. We describe this solution approach in detail in the next section.

2.4 The decomposition matheuristic

In order to solve the 3T-DPPT by decomposition matheuristics, we break down the decisions in the full formulation into the decisions for T1, T2, and T3. We obtain three decomposition approaches, each of which prioritizes one of the tiers–the one that is solved first. The solutions obtained then guide the solutions of the other tiers. We aim to analyze the three matheuristic approaches, and identify when one performs better than the others. We could start by solving T1 first, then solve T2, and finally T3; we call this approach *D1* (the *D* stands for decomposition, and the number represents which tier is solved first). Alternatively, we could do the reverse and solve T3 first, followed by T2 and T1 (called *D3*). Finally, we could start with T2 and then solve T1 and T3 simultaneously (called *D2*). Each of these methods has its own benefits and challenges, which we describe in detail in the following subsections.

2.4.1 Decomposition starting with Tier 2

We first discuss the case when the decomposition matheuristic solves T2 first. Since T2 is the tier that links the deliveries in T1 and T3, and our focus is on optimizing the use of public transport services, we first solve the T2 problem here. We use constraints from *FULL* primarily concerning this tier, along with some additional linking constraints. These additional constraints take into account the delivery time windows of the customers, which are addressed directly only in T3 of the problem. The idea is to assign a drop-in stop, a drop-out stop, and a public vehicle that traverses the two stops, to each package, along with the pickup and drop-off time. Then we feed these decisions to the problems in T1 and T3 to get the final complete solution.

Tier 2 problem

The first step of this decomposition technique is to model the flow of packages on public vehicles. For each package $i \in \mathcal{C}$, we consider the task of sending it from a drop-in stop u to a drop-out stop v via a public vehicle p. We use variables y^1_{isp}, y^2_{isp}, and l^2_{up} from the original formulation. The majority of the constraints used for this tier are also the same as in the *FULL* formulation and are given by (2.10)-(2.17).

Apart from the constraints mentioned above, we also need to make sure that the timing of the assignment of the packages to the public vehicles is such that there are no time inconsistencies for the deliveries in T1 and T3. In other words, firstly, the packages have to be assigned to the drop-in stops and the public vehicles so that the delivery trucks have enough time to deliver them from the CDC to the drop-in stop before a public vehicle is scheduled to pick them up. Secondly, we must also ensure that the freighters have enough time to make the deliveries in T3 to satisfy the customers' time windows. We achieve these by using the following constraints:

$$T_{sp} y^1_{isp} \geq \left[T^{1avg}_{os} + T^{'}_{s} \right] y^1_{isp} \qquad \forall i \in \mathcal{C},\ s \in \mathcal{S}_{in},\ p \in \mathcal{P}_s, \tag{2.34}$$

$$\sum_{p \in \mathcal{P}} \sum_{s \in \mathcal{S}_p \cap \mathcal{S}^{out}_i} \left[T_{sp} + T^{3avg}_{si} + T^{'}_{s} + \widehat{T}_i \right] y^2_{isp} \leq \overline{T}_i \qquad \forall i \in \mathcal{C}. \tag{2.35}$$

T^{1avg}_{os} denotes the average time taken by a delivery truck to go from the CDC to the drop-in stop s, and T^{3avg}_{si} denotes the average time that a freighter requires to travel from drop-out stop s to customer i. T^{1avg}_{os} and T^{3avg}_{si} are calculated based on the geographical locations of the drop-in and drop-out stops and the locations of the customers. The first set of constraints ensures that the time when the delivery trucks deliver a package to a drop-in station does not exceed the scheduled time when it is supposed to be picked up by a public vehicle. The second set of constraints ensures that the package can be delivered to its customer before their time window ends.

Next, we discuss the objective functions for the problem in T2. Recall that in the *FULL* formulation, we only had objectives corresponding to minimizing the travel distances in T1 and T3, and nothing specific to T2. We develop three objective functions for the T2 problem, keeping in mind our objective of the original formulation- to minimize the routing costs. The three objectives we propose are: 1) to minimize the number of drop-in stops or drop-out stops or both used, 2) to minimize the approximate routing distances in T1 and T3, and 3) to minimize the approximate number of freighters used in T3. For the third objective function, we focus only on T3 because the third tier is the most complicated one: the distance traveled for delivery in T3 is much higher than T1, firstly, due to a significantly larger number of customers than drop-in stops, and secondly, due to lower capacities of freighters. We describe the objectives in detail in the following paragraphs.

Minimizing the number of drop-in and drop-out stops (*Obj1*): The first objective is to minimize the number of drop-in and drop-out stops used. We develop this objective to encourage high consolidation of packages on the delivery trucks and freighters, thereby using fewer vehicles. This objective function is given by

$$Minimize \sum_{s\in\mathcal{S}_{in}} \min\left\{\sum_{i\in\mathcal{C}}\sum_{p\in\mathcal{P}} y^1_{isp}, 1\right\} + \sum_{s\in\mathcal{S}_{out}} \min\left\{\sum_{i\in\mathcal{C}}\sum_{p\in\mathcal{P}} y^2_{isp}, 1\right\}. \tag{2.36}$$

This objective function is non-linear. To linearize it, we use binary variables φ^1_s and φ^2_s, which represents if some package is picked up or dropped off at stop s, respectively. Then the objective function can be written linearly as

$$Minimize \sum_{s\in\mathcal{S}_{in}} \varphi^1_s + \sum_{s\in\mathcal{S}_{out}} \varphi^2_s, \tag{2.37}$$

with two additional constraints:

$$\varphi_s^1 \geq \frac{\sum_{i\in\mathcal{C}} \sum_{p\in\mathcal{P}} y_{isp}^1}{M} \qquad \forall s \in \mathcal{S}_{in}, \tag{2.38}$$

$$\varphi_s^2 \geq \frac{\sum_{i\in\mathcal{C}} \sum_{p\in\mathcal{P}} y_{isp}^2}{M} \qquad \forall s \in \mathcal{S}_{out}. \tag{2.39}$$

A drawback of this objective is that it might lead to the selection of very few drop-in and drop-out stations, and assign customers to drop-out stops that might not be the closest to them, resulting in an increase in the routing distances.

Minimizing the approximate routing cost (distance traveled) in T1 and T3 (*Obj2*): We construct the second objective function by taking into account the distances of the drop-in stops from the CDC and the drop-out stops from the customers. Though these distances will not be precisely equal to the routing distances obtained from T1 and T3, they serve as a proxy for the objectives of T1 and T3. The second objective function is given by:

$$Minimize \sum_{i\in\mathcal{C}} \sum_{s\in\mathcal{S}_{in}} D_{os} \sum_{p\in P} y_{isp}^1 + \sum_{i\in\mathcal{C}} \sum_{s\in\mathcal{S}_{out}} D_{is} \sum_{p\in P} y_{isp}^2. \tag{2.40}$$

Minimizing the approximate number of freighters used in T3 (*Obj3*): Finally, we introduce the objective of minimizing the number of freighters used in T3, taking into account the average capacity, denoted by $\overline{Q}_F$. This is aimed at reducing the overall routing cost of the third tier. The approximation is made in the following way. First, we divide the entire day into time periods over which the public vehicles operate, denoted by $\mathcal{T} = \{\tau_0, \tau_1, \ldots, \tau_n\}$. Let $\mathcal{P}_s^{\tau_j}$ denote the set of public vehicles that visit drop-out station s during period τ_j.

To estimate the number of freighters required, we introduce new decision variables $h_s^{\tau_j}$, which give the number of freighters required during any period to deliver the parcels dropped off in that period.

We determine the value of $h_s^{\tau_j}$ through the following constraints:

$$\sum_{i \in \mathcal{C}} \sum_{p \in \mathcal{P}_{\tau_j}^s} q_i y_{isp}^2 \leq \overline{Q}_F h_s^{\tau_j} \qquad \forall s \in \mathcal{S}_{out},\ \tau_j \in \mathcal{T}, \tag{2.41}$$

and the objective function is:

$$Minimize \sum_{\tau_j \in \mathcal{T}} \sum_{s \in \mathcal{S}_{out}} h_s^{\tau_j}. \tag{2.42}$$

We solve the tier 2 problem with each of the objectives discussed above. From the solution, we obtain a drop-in stop, a drop-in time, a drop-out stop, and a drop-out time associated with each package. Then, we use these as inputs for the T1 and T3 problems. In the following subsections, we describe the formulations of the problems in T1 and T3.

Tier 1 problem

For the tier 1 problem, the task is to assign packages to the delivery trucks and determine the routes of the delivery trucks from the CDC to the drop-in stops. Let B_{is}^{in} be a parameter that takes the value 1 if package i is picked up by a public vehicle from drop-in station s, and T_i^{in} be the corresponding time. We obtain these values from the solution of T2. Let r_{id} be a binary variable that takes the value 1 if package i is assigned to delivery truck d, and g_{dv} be a binary variable that denotes if a truck d visits drop-in stop v or not. Apart from these, we use the variables w_{uvd} and t_{vd}^1, denoting the arc traversal variables and the time variables, respectively, from the *FULL* model. The objective of the T1 model is

$$Minimize \sum_{d \in \mathcal{D}} \sum_{u \in \mathcal{S}_{in} \cup \{o\}} \sum_{v \in \mathcal{S}_{in} \cup \{o'\}} C_{uvd}^1 w_{uvd}, \tag{2.43}$$

and the constraints are:

$$\sum_{d \in \mathcal{D}} r_{id} = 1 \qquad \forall i \in \mathcal{C}, \tag{2.44}$$

$$\sum_{i \in \mathcal{C}} q_i r_{id} \leq Q_d^1 \qquad \forall d \in \mathcal{D}, \tag{2.45}$$

$$g_{dv} \geq B_{iv}^{in} r_{id} \qquad \forall i \in \mathcal{C}, d \in \mathcal{D}, v \in \mathcal{S}_{in}, \tag{2.46}$$

$$g_{dv} = \sum_{\substack{u \in \mathcal{S}_{in} \cup \{o\} \\ u \neq v}} w_{uvd} \qquad \forall d \in D,\ v \in \mathcal{S}_{in}, \tag{2.47}$$

$$t_{vd}^1 \leq T_i^{in} + M(1 - r_{id}) \qquad \forall i \in \mathcal{C},\ v \in \mathcal{S}_{in},\ s.t.\ B_{iv}^{in} = 1,\ d \in \mathcal{D}, \tag{2.48}$$

plus constraints (2.3)-(2.5), (2.8), and (2.29)-(2.30) from the *FULL* model. Constraints (2.44) and (2.45) are analogous to constraints (2.1) and (2.2), respectively. Constraints (2.46) say that if a delivery truck is assigned to a package, the truck must visit the corresponding drop-in station for the package. Constraints (2.47) link variables g_{dv} to the arc variables w_{uvd}. Finally, constraints (2.48) guarantee that a package is delivered to its respective drop-in station before a public vehicle is scheduled to pick it up.

Tier 3 problem

For the tier 3 problem, we need to determine the route of the freighters from the drop-out stops to their respective customers. Let B_{is}^{out} denote a parameter that takes the value 1 if package i is dropped off at station v by a public vehicle, and let T_i^{out} be the corresponding time. These parameters, once again, are determined from the output of T2. For writing this formulation, we use variables z_{ik}, x_{ijk}, and t_{jk}^3 from the *FULL* model.

An interesting fact about the T3 problem for the decomposition approach is that it completely separates into subproblems for each drop-out stop and can be solved individually. Once B_{is}^{out} is known, we know the customers that need to be delivered from a drop-out stop s precisely and can, thus, solve the routing problem for each stop. Let $\mathcal{C}_s$ be the set of customers scheduled to be served from drop-out stop s. The tier 3 model, for each drop-out stop s, is given by:

$$\textit{Minimize} \quad \sum_{k\in\mathcal{K}_s}\sum_{i\in\mathcal{C}_s\cup\{s\}}\sum_{\substack{j\in\mathcal{C}_s\cup\{s\}\\ j\neq i}} C^3_{ijk}x_{ijk}, \tag{2.49}$$

$$\textit{subject to:} \quad \sum_{k\in\mathcal{K}_s} z_{ik} = 1 \qquad \forall i \in \mathcal{C}_s, \tag{2.50}$$

$$\sum_{\substack{j\in\mathcal{C}_s\\ i\neq j}} x_{jik} = z_{ik} \qquad \forall i \in \mathcal{C}_s \cup \{s\},\ \forall k \in \mathcal{K}_s, \tag{2.51}$$

$$\sum_{i\in\mathcal{C}_s} q_i z_{ik} \leq Q^3_k \qquad \forall k \in \mathcal{K}_s, \tag{2.52}$$

$$\sum_{j\in\mathcal{C}_s\cup\{s\}} x_{sjk} = 1 \qquad \forall k \in \mathcal{K}_s, \tag{2.53}$$

$$\sum_{j\in\mathcal{C}_s\cup\{s\}} x_{jsk} = 1 \qquad \forall k \in \mathcal{K}_s, \tag{2.54}$$

$$\sum_{\substack{j\in\mathcal{C}_s\cup\{s\}\\ j\neq i}} x_{ijk} = \sum_{\substack{j\in\mathcal{C}_s\cup\{s\}\\ j\neq i}} x_{jik} \qquad \forall i \in \mathcal{C}_s,\ \forall k \in \mathcal{K}_s, \tag{2.55}$$

$$t^3_{sk} \geq B^{out}_{is} T^{out}_i z_{ik} + T^{'}_s,\ \forall k \in \mathcal{K}_s \qquad \forall i \in \mathcal{C}_s, \tag{2.56}$$

$$t^3_{jk} \geq t^3_{ik} + T^3_{ijk} + \widehat{T}_j - M(1 - x_{ijk}) \qquad \forall i \in \mathcal{C}_s \cup \{s\},\ j \in \mathcal{C}_s, i \neq j,\ \forall k \in \mathcal{K}_s, \tag{2.57}$$

$$t^3_{ik} \geq \underline{T}_i - M(1 - z_{ik}) \qquad \forall i \in \mathcal{C}_s,\ \forall k \in \mathcal{K}_s, \tag{2.58}$$

$$t^3_{ik} \leq \overline{T}_i + M(1 - z_{ik}) \qquad \forall i \in \mathcal{C}_s,\ \forall k \in \mathcal{K}_s, \tag{2.59}$$

$$\sum_{j\in\mathcal{C}_s} x_{sjk} \geq \sum_{j\in\mathcal{C}_s} x_{sjk+1} \qquad \forall k \in |\mathcal{K}_s| - 1, \tag{2.60}$$

$$\sum_{i \in \mathcal{C}_s \cup \{s\}} \sum_{\substack{j \in \mathcal{C}_s \\ j \neq i}} x_{ijk} \geq \sum_{i \in \mathcal{C}_s \cup \{s\}} \sum_{\substack{j \in \mathcal{C}_s \\ j \neq i}} x_{ijk+1} \qquad \forall k \in |\mathcal{K}_s| - 1. \tag{2.61}$$

The above formulation is very similar to the constraints of *FULL* that pertain to T3, decomposed stop-wise. Constraints (2.56) ensure that the freighters start their journey only after all the packages to be delivered by them have been dropped off.

We denote by *D2-Obj1* the decomposition approach that solves the T2 problem first, followed by T1 and T3, and uses *Obj1* for the problem in T2. When the objective functions used in T2 is *Obj2* or *Obj3*, we denote it by *D2-Obj2* and *D2-Obj3*, respectively.

2.4.2 Decomposition starting with Tier 1

Next, we discuss the decomposition matheuristic when we solve the 3T-DPPT starting from T1. Since we propose to use environmentally and economically sustainable transportation means in T3, whereas T1 uses dedicated delivery vehicles, most of the harmful emissions occur in the first tier. Thus, if our objective is to minimize the emissions caused, it would be more beneficial to prioritize the solution of T1. Here, we solve tier 1 first and make decisions about assigning the packages to drop-in stops and delivery trucks, and the routes of the trucks. The T1 solution also guides us about the arrival of the packages at the drop-in stops. We use this as an input to solve the T2 problem, where we assign the packages to public vehicles and drop-out stops. Finally, we solve T3 using the solution of T2. Here, we assign the packages to freighters, and develop their routes.

Tier 1 problem

For the tier 1 model, similar to *FULL*, we use variables pertaining to T1, viz. r_{isd}, w_{uvd}, and t^1_{sd}. Variables y^1_{isp} from *FULL* are replaced by variables γ^1_{is} which take the value 1 if a customer i is assigned to drop-in stop s, and 0 otherwise. The model is given by:

$$\textit{Minimize} \quad \sum_{d \in \mathcal{D}} \sum_{u \in \mathcal{S}_{in} \cup \{o\}} \sum_{\substack{v \in \mathcal{S}_{in} \cup \{o'\} \\ u \neq v}} C^1_{uvd} w_{uvd}, \tag{2.62}$$

$$\textit{subject to:} \quad \sum_{s \in \mathcal{S}_i^{in}} \sum_{d \in \mathcal{D}} r_{isd} = 1 \qquad \forall i \in \mathcal{C}, \tag{2.63}$$

$$\sum_{i \in C} \sum_{s \in \mathcal{S}_{in}^i} q_i r_{isd} \leq Q_d^1 \qquad \forall d \in \mathcal{D}, \tag{2.64}$$

$$\sum_{d \in \mathcal{D}} r_{isd} = \gamma^1_{is} \qquad \forall i \in \mathcal{C},\ s \in \mathcal{S}_i^{in}, \tag{2.65}$$

$$\sum_{s \in \mathcal{S}_i^{in}} \gamma^1_{is} = 1 \qquad \forall i \in \mathcal{C}, \tag{2.66}$$

plus constraints (2.3)-(2.6), (2.8), and (2.29)-(2.30) from the *FULL* model. Constraints (2.63) and (2.64) are analogous to constraints (2.1), and (2.2), restricted to specific drop-in stops based on the drop-out stops from where the customers can be served. Constraints (2.65) and (2.66) say that if a package is delivered to a drop-in stop, it must be picked up by a unique public vehicle.

Additionally, we need to ensure that the freighters have enough time to deliver the packages to the customers within their time windows. We do so by adding the following constraints:

$$t^1_{sd} \leq T_i^{avg} - 1.3 \cdot D_{is} + M(1 - r_{isd}) \qquad \forall i \in \mathcal{C},\ s \in \mathcal{S}_i^{in},\ d \in \mathcal{D}, \tag{2.67}$$

where, $T_i^{avg} = \frac{\underline{T}_i + \overline{T}_i}{2}$. To approximate the time, the idea is to assume that we go directly from the CDC to the customer and reach them in the middle of their delivery window. However, since, in practice, the package would be transported first by a public vehicle and then by a freighter, and could also potentially wait in between, the time taken would be greater. To account for the longer journey, we multiply the time taken by a factor greater than 1. From preliminary experiments, we find 1.3 to be a suitable multiplicative factor.

Tier 2 problem

From the solution of T1, we get the drop-in stop for each package i, and the time when the package is delivered to the drop-in stop s. We denote them by B^{in}_{is} and T^{in}_i, respectively. These parameters are used as inputs for the T2 problem. Let $\bar{s}_i$ denote the drop-in stop that serves customer i. In T2, we make decisions about allocating each package to a public vehicle and a drop-out stop, and consequently, the time when the package reaches a drop-out stop. For the problem described here, we replace variables y^1_{isp} from *FULL* with γ^1_{ip} to denote the assignment of packages to public vehicles. We also use variables y^2_{isp} and l^2_{up} from the original formulation. The constraints are:

$$\sum_{p\in\mathcal{P}_{\bar{s}_i}} \gamma^1_{ip} = 1 \qquad \forall i \in \mathcal{C}, \tag{2.68}$$

$$\sum_{\mathcal{P}\setminus\mathcal{P}_{\bar{s}_i}} \gamma^1_{ip} = 0 \qquad \forall i \in \mathcal{C}, \tag{2.69}$$

$$B^{in}_{is}\gamma^1_{ip} + y^2_{isp} \leq 1 \qquad \forall i \in \mathcal{C},\ s \in \mathcal{S}_{in} \cap \mathcal{S}_{out},\ p \in \mathcal{P}_s, \tag{2.70}$$

$$\gamma^1_{ip} = \sum_{v\in\mathcal{S}_p\cap\mathcal{S}^{out}_i} y^2_{ivp} \qquad \forall i \in \mathcal{C},\ p \in \mathcal{P}, \tag{2.71}$$

$$T_{up}B^{in}_{iu}\gamma^1_{ip} \leq T_{vp}y^2_{ivp} + M(1 - y^2_{ivp}) \qquad \forall i \in \mathcal{C},\ p \in \mathcal{P},\ u \in \mathcal{S}_p \cap \mathcal{S}_{in},\ v \in \mathcal{S}_p \cap \mathcal{S}^{out}_i, \tag{2.72}$$

$$l^2_{vp} = l^2_{up} + \sum_{i\in\mathcal{C}^{in}_v} B^{in}_{iv}q_i\gamma^1_{ip} - \sum_{i\in\mathcal{C}^{out}_v} q_i y^2_{ivp} \qquad \forall p \in \mathcal{P},\ u \in \mathcal{S}_p \cup \{\tilde{o}\},\ v \in \mathcal{S}_p,\ u \neq v,\ \text{with } \alpha_{uvp} = 1, \tag{2.73}$$

$$\sum_{p\in\mathcal{P}_s} T_{sp}B^{in}_{is}\gamma^1_{ip} \geq T^{in}_i B^{in}_{is} \qquad \forall i \in \mathcal{C},\ s \in \mathcal{S}^{in}_i, \tag{2.74}$$

plus constraints (2.11), (2.15), and (2.17). Constraints (2.68)-(2.73) are similar to that of *FULL*, with variables y^1_{isp} replaced by variables γ^1_{ip}. Constraints (2.74) ensure that the public vehicles pick up the packages only after the trucks have delivered them to the drop-in stops.

In addition, we need to ensure that there is enough time for the freighters to deliver the packages once the public vehicles have dropped them off at the drop-out stops so that the customers receive the packages before their closing time window. To do so, we add the following constraint:

$$\sum_{p\in\mathcal{P}}\sum_{s\in\mathcal{S}_p\cap\mathcal{S}_{out}}\left[T_{sp}+T_{si}^{3avg}+T_s^{\prime}+\widehat{T}_i\right]y_{isp}^2\leq\overline{T}_i\qquad\forall i\in\mathcal{C}.\tag{2.75}$$

The objective functions for T2, as described in section 2.4.1, could be to minimize the number of drop-out stops used in T3, or to minimize the approximate distance traveled by the freighters in T3, or to minimize the approximate number of freighters used. Since we have already solved T1 here, the objective functions only correspond to the decisions of tier 3.

Minimizing the number of drop-out stops (*Obj1*) : The objective function is:

$$Minimize\sum_{s\in\mathcal{S}_{in}}\sum_{s\in\mathcal{S}_{out}}\varphi_s^2,\tag{2.76}$$

along with the additional constraint (2.39).

Minimizing the approximate routing cost of T3 (*Obj2*) : The objective function in this case is given by:

$$Minimize\sum_{i\in\mathcal{C}}\sum_{s\in\mathcal{S}_{out}}D_{is}\sum_{p\in P}y_{isp}^2.\tag{2.77}$$

Minimizing the approximate number of freighters used in T3 (*Obj3*) : Here, the objective function is given by (2.42), along with constraints (2.41).

The tier 3 model takes as input B_{is}^{out} and T_{is}^{out}, which denote the drop-out stop and the drop-out time and come from the output of T2. The T3 model here is the same as in the approach described in Section 2.4.1. As done previously, we denote by *D1-Obj1*, *D1-Obj2*, and *D1-Obj3* the decomposition approaches where the objectives used in T2 are *Obj1*, *Obj2*, and *Obj3*, respectively.

2.4.3 Decomposition starting with Tier 3

The third and final decomposition technique first solves the T3 problem. Here, apart from making decisions about assigning packages to freighters and their routes, we also decide the drop-out station for each package. This guides the decisions of assigning the packages to the drop-in stops and public vehicles in T2. Finally, the output of tier 2 can be used to make the decisions in T1. This sequence of solving the problem is beneficial when most of the delivery distance (and hence delivery costs) arises in T3 due to significantly larger number of customers.

Tier 3 problem

For T3, we introduce additional variables γ^2_{is}, which take the value 1 if package i is to be dropped off at drop-out stop s by a public vehicle, analogous to variables y^2_{isp}. We also use variables x_{ijk}, z_{ik} and t^3_{ik}. The T3 model is given by:

$$\text{Minimize} \sum_{k\in\mathcal{K}} \sum_{i\in\mathcal{S}_{out}\cup\mathcal{C}} \sum_{\substack{j\in\mathcal{S}_{out}\cup\mathcal{C}\\ i\neq j}} C^3_{ijk} x_{ijk}, \tag{2.78}$$

$$\text{subject to:} \sum_{s\in\mathcal{S}_i^{out}} \gamma^2_{is} = 1 \qquad i\in\mathcal{C}, \tag{2.79}$$

$$\sum_{k\in\mathcal{K}_s} z_{ik} = \gamma^2_{is} \qquad \forall i\in\mathcal{C},\ s\in\mathcal{S}_i^{out}, \tag{2.80}$$

$$t^3_{sk} \geq T_s^{first} + T'_s - M(1-x_{sik}) \qquad \forall i\in\mathcal{C},\ s\in\mathcal{S}_i^{out},\ k\in\mathcal{K}_s, \tag{2.81}$$

plus constraints (2.19)-(2.24), (2.26)-(2.28), and (2.31)-(2.32) from *FULL*. Constraints (2.79) assign each customer to a drop-out station, constraints (2.80) ensure that if a package is dropped at a drop-out stop, then it is assigned to a freighter. Finally, constraints (2.81) update the time as the freighters leave the drop-out stops. T_s^{first} in constraint (2.81) is an estimated time when the freighters can start making deliveries. We introduce this parameter to make sure that the trucks and the public vehicles have enough time to deliver the packages before the freighters start their journey. We define T_s^{first} as the time when the first public vehicle visits stop s.

We obtain the drop-out stops and the time by which the packages must be available there from the solution of tier 3. These are then used as inputs for T2, which we describe below.

Tier 2 problem

For tier 2, we use as inputs the solutions from T3– B_{is}^{out} and T_i^{out}. B_{is}^{out} denotes the drop-out stop s for each package i. T_i^{out} is the time when package i is supposed to leave the drop-out stop for its delivery, or, in other words, the time by which the package must reach the drop-out stop. Let $\bar{s}_i$ denote the drop-out stop for package i. The model is similar to tier 2 of *FULL*, with variables y_{isp}^1 and l_{up}^2, along with variables y_{isp}^2 replaced by γ_{ip}^2. At this step, we decide the assignment of drop-in stops and public vehicles for each package. Variable γ_{ip}^2 is equal to 1 if vehicle p transports package i, and 0 otherwise. The constraints of the problem are the following:

$$\sum_{p \in \mathcal{P} \cap \mathcal{P}_{\bar{s}_i}} \gamma_{ip}^2 = 1 \qquad \forall i \in \mathcal{C}, \tag{2.82}$$

$$\sum_{p \in \mathcal{P} \setminus \mathcal{P}_{\bar{s}_i}} \gamma_{ip}^2 = 0 \qquad \forall i \in \mathcal{C}, \tag{2.83}$$

$$y_{isp}^1 + \gamma_{ip}^2 \leq 1 \qquad \forall i \in \mathcal{C},\ s \in \mathcal{S}_{in} \cap \mathcal{S}_{out},\ p \in \mathcal{P}_s,\ \text{if } B_{is}^{out} = 1, \tag{2.84}$$

$$\sum_{s\in\mathcal{S}_p\cap\mathcal{S}_{in}} y^1_{isp} = \left[\sum_{s\in\mathcal{S}_p\cap\mathcal{S}_{out}} B^{out}_{is}\right]\gamma^2_{ip} \qquad \forall i\in\mathcal{C},\ p\in\mathcal{P}, \tag{2.85}$$

$$T_{up}y^1_{iup} \leq T_{vp}B^{out}_{iv}\gamma^2_{ip} + M(1 - B^{out}_{iv}\gamma^2_{ip}) \qquad \forall i\in\mathcal{C},\ p\in\mathcal{P},\ u\in\mathcal{S}_p\cap\mathcal{S}_{in},\ v\in\mathcal{S}_p\cap\mathcal{S}^{out}_i, \tag{2.86}$$

$$\alpha_{uvp}\left[l^2_{vp} = l^2_{up} + \sum_{i\in\mathcal{C}^{in}_v} q_i y^1_{iup} - \sum_{i\in\mathcal{C}^{out}_v} q_i B^{out}_{iv}\gamma^2_{ip}\right] \qquad \forall p\in\mathcal{P},\ u\in\mathcal{S}_p\cup\{\tilde{o}\},\ v\in\mathcal{S}_p, \tag{2.87}$$

$$T_{sp}B^{out}_{is}\gamma^2_{ip} \leq T^{out}_i \qquad \forall i\in\mathcal{C},\ s\in\mathcal{S}_{out},\ p\in\mathcal{P}_s, \tag{2.88}$$

$$T_{sp}y^1_{isp} \geq \left[T^{1avg}_{os} + T^{'}_s\right]y^1_{isp} \qquad \forall i\in\mathcal{C},\ s\in\mathcal{S}_{in},\ p\in\mathcal{P}_s, \tag{2.89}$$

plus constraints (2.10), (2.15), and (2.17). Constraints (2.82)-(2.88) are quite similar to the constraints of *FULL*. Finally, (2.89) ensure that the trucks have enough time to deliver the packages to the drop-in stops before the public vehicles pick them up. T^{1avg}_{os} denotes the average time that a truck takes to travel from the origin to a drop-out stop s.

However, when we start the decomposition technique from T3, the freighters that deliver at least one package start from their respective drop-out stop at time T^{first}_s. Thus the parameter T^{out}_i takes the value T^{first}_s for each package. It is easy to see that this results in infeasibilities in T2 whenever the capacity of the first public vehicle to visit that stop is lower than the sum of the capacities consumed by all the packages to deliver. Merely changing the time T^{first}_s to a higher value is not sufficient to resolve the issue. This is because the problem would persist whenever the sum of the volumes of all the packages to be delivered from the stop exceeds the sum of the capacities of the public vehicles visiting the stop before the time mentioned above. Because of how we formulated the tier 3 model, the freighters always start their journey from the stop at whatever time we provide as T^{first}_s.

To find a way around this without complicating the problem further, we shift the starting time of the freighters' routes. The idea is to shift these routes as late as possible, keeping in mind the time window of the customers. This allows the public vehicles enough time to transport the packages to the drop-out stops. The shifting is done in the following way. For each freighter k, we take the list of customers it visits in order. Then, we start with the last customer visited by the freighter and set the time of delivery to their closing time window. For the other customers, say i, we consider the customer visited after i, say j, and denote the time when j is visited by t_j^*. Then, the time when the freighter k delivers the package to customer i is given by $\min\{\overline{T}_i, t_j^* - T_{ijk}^3\}$. Though this approximates the delivery time, the routing cost remains the same because we keep the order of visits intact and only play with the time.

Once again, we can have multiple objectives for T2 similar to the previous decomposition approaches. The first objective is to minimize the number of drop-in stops utilized in T1. The second is to minimize the approximate distance traversed in T1.

Minimizing the number of drop-in stops (*Obj1*): The objective function is:

$$Minimize \sum_{s \in \mathcal{S}_{in}} \varphi_s^1, \tag{2.90}$$

along with constraints (2.38).

Minimizing the approximate routing cost of T1 (*Obj2*): Finally, in this case, the objective function is given by:

$$Minimize \sum_{i \in C} \sum_{s \in \mathcal{S}_{in}} D_{os} \sum_{p \in P} y_{isp}^1. \tag{2.91}$$

We do not need the third objective function, minimizing the approximate number of freighters being used, here, like in the previous approaches, since *Obj3* corresponds exclusively to T3, which has already been solved.

The T1 problem here is the same as the T1 model in *D2* as described in Section 2.4.1. It takes as input the same parameters as described there and gives the same outputs: assigning the packages to the delivery trucks and their routes. Depending on the objective used for T2, we refer to the decomposition approaches as *D3-Obj1* and *D3-Obj2*, respectively.

While all the subproblems solved in the decomposition method are NP-hard, their complexity is much smaller than the full formulation as they consider a smaller set of variables and constraints. Figure 2.3 shows a visual representation of all the decomposition approaches. The order of solving the tiers is shown by the arrows. For tier 2, we also list the objective functions. The text accompanying the arrows give the output from the previous tier that is fed as input in the next tier. For D2, after solving tier 2, tiers 1 and 3 can be solved simultaneously since T2 is the linking tier. For D1 and D3, we solve the tiers sequentially.

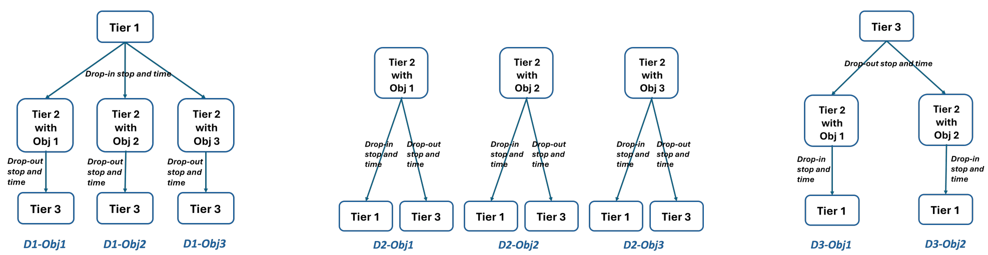

(a) Decomposition starting with Tier 1 (D1)

(b) Decomposition starting with Tier 2 (D2)

(c) Decomposition starting with Tier 3 (D3)

Figure 2.3: The decomposition matheuristic

Let us also fix a quick notation here to easily refer to the models of a specific tier for the different decomposition approaches. We call them as *decomposition approach number-tier number*. For example, the T3 model from *D2* would be referred to as *D2-T3*.

2.5 Numerical experiments

This section describes building a typical instance for the 3T-DPPT problem comprising the public vehicle network, the customers, and the CDC. We then solve our models on these instances, and provide computational results and analysis. We implemented the models on the Spyder IDE of Python 3.8.5 and solved them using the CPLEX 22.1.0 standard solver. The tests were conducted on an Intel(R) Xeon(R) W-2255 CPU with a clock speed of 3.70 GHz and 128 GB RAM.

2.5.1 Instance generation

We test our models on artificial instances, generated to mimic real-life transportation networks. We use networks similar to the ones described in the paper by Delle Donne et al. (2023a), with some modifications to suit our setting. In their paper, the authors handle a strategic problem associated with the one studied in this paper, so we adapt some of the features for the operational level problem. Figure 2.4 shows a typical example of an instance. The red square denoted by O0 denotes the CDC. The thick lines, along with the triangles, depict the public transit network. Each line refers to a single bus or metro line, which consists of several public vehicles throughout the day. We represent the stops on the public vehicle network with triangles: upward triangles denote drop-in stops, while inverted triangles represent drop-out stops. Finally, the circles represent the customers. The figure shows an instance with three public vehicle lines, five drop-in stops, nine drop-out stops, and twenty customers.

To generate the instances, we have set the ratio of the average distance between the CDC and the customers and the average distance between the CDC and the drop-out stops inspired by the article by Lopez (2017). The report mentions that the distance between customers and the distribution centers lies between 6 to 9 miles on average. Since our idea is to utilize sustainable delivery modes like freighters walking or biking, we aim to keep the average distance from the drop-out stops to the customers to be less than a mile, and we generate our instances accordingly. For each customer, we assign $\mathcal{S}_i^{out}$ to be

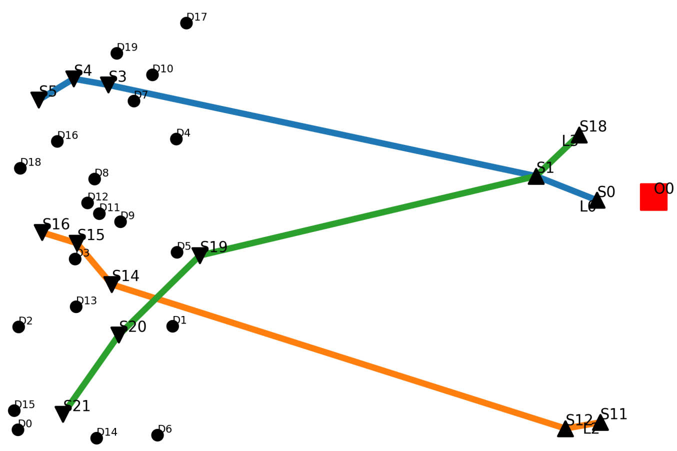

Figure 2.4: An example of an instance

the three closest drop-out stops from the customer. We also conducted some preliminary experiments with S_i^{out} comprising of the set of drop-out stops within a given radius of the customer and found similar results.

We divide the day into 30 periods, each 30 minutes long. Thus, the time horizon during which the delivery system is active is 15 hours in our implementations. We assume that the first period starts with the 0^{th} hour of the delivery system. We reserve the first two and a half hours of the system exclusively for the delivery trucks to start transporting packages from the CDC to the drop-in stops. Hence, we do not include buses or metros during this period. The public vehicles that are supposed to carry packages start operating from time point 150 (or after two and a half hours), and are assumed to run every 30 minutes. We require the definition of periods primarily for *Obj3*, where we estimate the number of freighters required per period.

We generate the customer time windows so that each window is at least 3 hours long and can potentially be as long as the entire delivery horizon. This ensures we have enough time and resources to deliver each customer's package. It is also realistic because, in practice, some customers have narrower time windows while others have wider time windows. Here, we have not restricted the delivery period to certain hours of the day. If we want to limit the delivery system to specific periods during the day, like early hours of the morning or late at night, we need to consider solely the public vehicles during those hours, without any change in the model. We have considered the service time at each stop to be 10 minutes. The service time at each of the customers is assumed to be 0. Adding a positive service time does not change our analyses; it only adds a fixed value to the delivery times.

For the numerical experiments, we use a homogeneous fleet of delivery vehicles. We consider the capacity of the delivery trucks to be 160 units and that of the freighter to be 20 units. The capacities of the delivery trucks are significantly higher than that of the freighters because typically delivery trucks are larger. We generate the capacity of public vehicles randomly between 70 and 150 units. We have a wide range of values for public vehicle capacities because, firstly, public vehicles vary in size. For example, metros and subways have a significantly higher capacity than buses. Moreover, some lines are busier and would have lesser spare capacities. All the public vehicles that run on the same line are assumed to have the same capacity. This is a very simplistic assumption, but it can be changed easily by manipulating the capacities as a percentage of the total available capacity of the vehicles. These numbers could be higher during the off-peak hours and very small or even zero during the busy hours. These numbers could also come from a distribution that models passenger traffic on public vehicles.

The demands of the customers lie between 5 and 20 units. Thus, on average, a truck carries 12.8 packages, a freighter carries 1.6 packages, and a public vehicle carries between 5.6 and 12 packages. While in realistic implementations of the system, the actual capacities, particularly of the trucks and the public vehicles, might be higher, we chose such values of demands and capacities to help us study the structure of the solutions and generate relevant insights about the system. This facilitates some level of consolidation of the packages on the vehicles while preventing all the packages from being assigned to the same vehicle at any tier.

We measure the distance between any two nodes (the CDC and the drop-in stops, any two stops, the drop-out stops and the customers, and any two customers) by the Euclidean distance between them. For our tests, we assume that the speed of each vehicle in the system is the same, or in other words, the time taken by any transportation mode is the same for traversing between any two locations. Even though this is a crude assumption, we can modify it by simply changing the data without any change in the formulations. The time taken for delivery and the corresponding cost is assumed to be proportional to the distance. To convert the distance into the time taken for traversal between any two points in the network, we multiply the distance by 0.2.

The cost of using the delivery trucks in tier 1 is assumed to be equal to the distance traversed, i.e., $C^1_{uvd} = D_{uv}, u, v \in \mathcal{S}_{in} \cup \{o\}, d \in \mathcal{D}$. For the third tier, we assume that the cost of using freighters is 50% of the costs of using trucks, i.e., $C^3_{ijk} = 0.5 * D_{ij}, i, j \in \mathcal{S}_{out} \cup \mathcal{C}, k \in \mathcal{K}$. We use these values because we intend to use vehicles of lower costs here, both economic and environmental.

We created 24 instances, each with a different number of customers, lines, drop-in stops, and drop-out stops. The number of customers in the instances ranges from 10 to 80. We have three instances per customer size, i.e., three instances with 10 customers each, three instances with 20 customers each, and so on, up to three instances with 80 customers each. We did not go beyond 80 customers because not all solution methods could solve the instances beyond this size. The number of public vehicle lines ranges between 1 and 5. The number of drop-in stops varies between 2 and 14, and the number of drop-out stops varies between 2 and 18. We do not define the size of an instance due to the different elements in it. An instance with 20 customers, 4 lines, 10 drop-in stops, and 12 drop-out stops would be very different from an instance with 20 customers, 3 lines, 8 drop-in stops, and 9 drop-out stops. We could consider the instance size to be the total number of nodes in the network. However, the number and function of the individual elements in the instances would cause them to behave differently owing to the structure of the network and the problem itself. Hence, we refrain from formally defining an instance size.

For solving the models, we provide a time limit to CPLEX. We set the time limit to 3 hours for *FULL*. For *D1*, the time limit for solving T1 was 2 hours, and 1 hour each for T2 and T3. Similarly, for *D3*, the time limit for solving T3 was 2 hours and 1 hour for the consecutive tiers. For *D2*, we had a time limit of 1 hour for solving each tier. Whenever T3 is not the first tier to be solved, since the problem decomposes for each drop-out stop, the 1-hour time limit is for solving the problem for each drop-out stop. Thus, the total time limit for solving the third tier is higher. However, we would like to make a note here that, often, particularly for larger instances, the solution time taken is greater than the time limit. This is because of the model building time taken by CPLEX before solving the problem.

Finally, we use 1000 as the value of M used to linearize our constraints, particularly those related to time. We chose such a value because 1000 is an upper bound on the time– the highest value of the customer time window does not exceed 1000. Moreover, the traveling time between any two nodes in the system is also less than 1000.

2.5.2 Computational results

We solve our instances using the formulations described by *FULL*, *D1-Obj1*, *D1-Obj2*, *D1-Obj3*, *D2-Obj1*, *D2-Obj2*, *D2-Obj3*, *D3-Obj1*, and *D3-Obj2*. An example of the solution of an instance is shown in figure 2.5. It shows the routes obtained in T1 and T3. The dotted lines show the routes of the delivery trucks, and the dashed lines show the routes of the freighters.

For each of the solution approaches, we report the best solution found. Table 2.4 provides the solution of the *FULL* formulation for the problem on the instances with up to 30 customers.

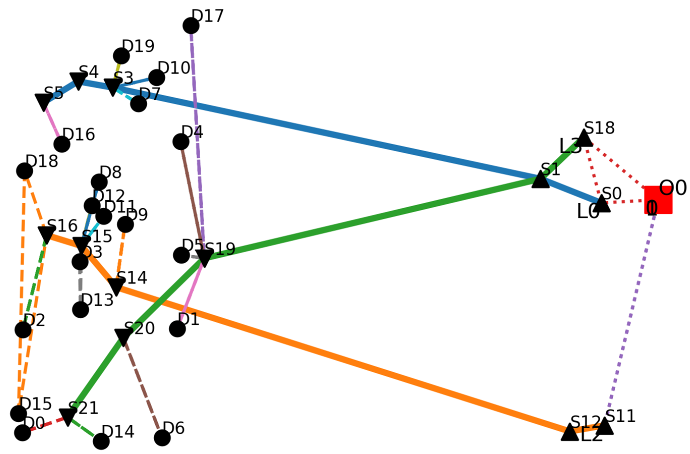

Figure 2.5: An example of the solution of an instance

FULL could not find a feasible solution for the other instances within a reasonable time. The total time increases dramatically when moving from 10 to 20 customers and blows up for instances beyond 30 customers.

In Tables 2.5 and 2.6, we provide a summary of the solutions obtained through each of the solution approaches. Table 2.5 reports the number of best solutions found using each decomposition method. Each row and column combination refers to a decomposition method. The numbers in the cells (outside brackets) give the number of instances for which the technique found the best solution, and the number in brackets provides the number of instances the method could solve. For *D1*, since tier 1 is the first tier to be solved, we have a unique T1 routing cost. The same happens for the routing costs of T3 for *D3*. For *FULL*, we have one value in each column reporting the routing costs of T1, T3, and the total routing cost. *D1* and *D2* could find a feasible solution for all 24 instances within the time limit, while *D3* could solve only up to instance 15. In Table 2.6, we report the average percentage de-

Table 2.4: Solution using formulation *FULL*

Instance number	Number of customers	Routing cost T1	Routing cost T3	Total routing cost	Running time
1	10	358.72	1026.43	1385.15	13.02
2	10	706.24	826.11	1532.35	9.44
3	10	448.33	871.98	1320.31	22.18
4	20	660.79	1259.65	1920.43	431.46
5	20	559.32	1199.82	1759.14	6776.01
6	20	708.92	1347.03	2055.95	11410.44
7	30	938.09	1363.82	2301.91	13038.68
8	30	1536.38	1980.14	3516.52	14269.30
9	30	659.85	1630.71	2290.56	14105.17

viation of the solutions found by each decomposition method from the best solution found for that instance, the average taken only over the instances that the approach could solve.

Table 2.5: Number of best solutions found by each solution method

Decomposition technique	Routing cost T1			Routing cost T3			Total routing cost		
with Objective function	*Obj1*	*Obj2*	*Obj3*	*Obj1*	*Obj2*	*Obj3*	*Obj1*	*Obj2*	*Obj3*
FULL		5 (9)			5 (9)			9 (9)	
D1		23 (24)		0 (24)	0 (24)	0 (24)	0 (24)	0 (24)	0 (24)
D2	2 (24)	1 (24)	2 (24)	0 (24)	10 (24)	0 (24)	0 (24)	10 (24)	0 (24)
D3	1 (15)	2 (15)	–		15 (15)		1 (15)	6 (15)	–

Table 2.6: Average percentage deviation of the solutions wrt the best solution found for each instance

Decomposition technique	Routing cost T1			Routing cost T3			Total routing cost		
with Objective function	*Obj1*	*Obj2*	*Obj3*	*Obj1*	*Obj2*	*Obj3*	*Obj1*	*Obj2*	*Obj3*
FULL		14.35%			1.21%			0.00%	
D1		1.20%		83.95%	46.90%	80.65%	52.38%	27.06%	49.89%
D2	121.42%	44.94%	113.54%	55.66%	18.63%	51.27%	60.56%	19.96%	55.73%
D3	74.31%	43.99%	–	0.00%		–	13.52%	6.29%	–

The average running time using each method is provided in Table 2.7, with the average, again, considered only over the instances for that the method could find a solution within the time limit. The running time reported is the sum of the running times of all the tiers for any approach.

The performance of the approaches is depicted in figures 2.6, 2.7, and 2.8. Each column in the graphs shows a solution approach– either the full formulation or a decomposition technique with one of the three objectives for T2. The x-axis represents the number of customers. The y-axis gives the

Table 2.7: Average computational time in seconds

Decomposition technique with Objective function	*Obj1*	*Obj2*	*Obj3*
FULL		6675.08	
D1	1928.98	2222.21	2495.69
D2	4272.69	1841.44	3065.04
D3	10464.83	10195.84	–

value of the solutions, i.e., the routing costs. For each customer size, we show the average of the three instances with the said number of customers. When we solve *D1*, we have only one set of solutions for tier 1, regardless of the objective function used in T2, since T1 is solved first. Similarly, for *D3*, we have one set of solutions for the routing costs of tier 3, irrespective of whether *Obj1* or *Obj2* is used later in T2. This is why we have only one line showing the routing costs of T1 (*D1*) and T3 (*D3*) in figures 2.7 and 2.8, respectively. Below, we discuss the performance of the approaches in detail.

Among all the approaches, the best-performing objective function for T2 is *Obj2*, i.e., to minimize the approximate routing costs of T1 and T3. This is related to the fact that our true objective is to minimize the routing costs. *Obj1* and *Obj3* are able to find the best solutions in only a handful of cases. The approaches that use *Obj1*, which is to minimize the number of drop-in and drop-out stops used, generally perform the worst within each decomposition method, especially as the instances grow larger. This is also reflected in Table 2.5, where we see that the average percentage deviations from the best solution found are the highest for *Obj1*.

The full formulation beats the decomposition approaches in terms of the total routing costs, but it can only solve very small instances, and even then, CPLEX takes a long time to build the models. Between the three decomposition approaches, *D3-Obj2* performs the best initially. However, compared to the other decomposition techniques, it can solve relatively smaller instances– only instances with up to 50 customers. Moreover, the running times of *D3* also escalate quickly after instances with 20 customers. For larger instances, almost all of the best total routing costs were found by *D2-Obj2*.

For the routing costs of T1, *D1* performs the best, however, *D2-Obj2* provides competitive solutions even as the size of the instances increases. For T3 routing costs, *D3* finds the best solutions for instances that it can solve. After that, *D2-Obj2* obtains the best T3 routing costs as well. Thus, overall, *D2-Obj2* dominates the other decomposition techniques as the instance size increases.

These findings pertain partially to the particularity of our setting and implementations. We have considered one CDC, up to 80 customers, equal delivery speeds for trucks and freighters, and the majority of the distance covered comes from T3. Moreover, the cost of covering a certain distance in T3 is assumed to be 50% of the cost in T1 using trucks. If we have multiple CDCs, and the cost of using delivery trucks is even higher, or our objective is to minimize emissions in particular, and low-cost green means are used in T3, it would be beneficial to use *D1*. If the cost of vehicles used in T3 is significantly higher and greatly depends on the individual trips performed, we might want to start the decomposition technique from T3. Finally, if the setting is such that the routing costs of T1 and T3 are comparable, we would be better off using *D2*. For the objective functions, we can conclusively say that *Obj2* is the best performing one because our actual goal is to minimize routing costs. Overall, we find the decomposition approach *D2-Obj2* to perform the best, taking into account the objective values, the size of instances solved, and the running times.

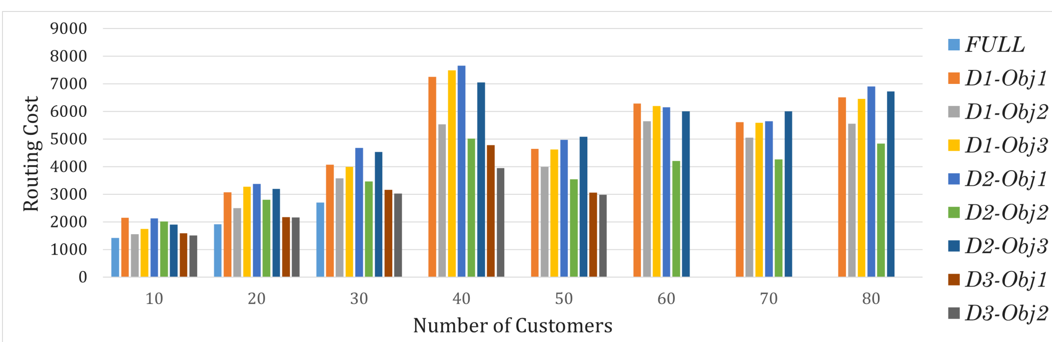

Figure 2.6: Comparison of the total routing cost obtained by each of the solution approaches

Figure 2.9 shows the average number of packages assigned to the delivery trucks and freighters for

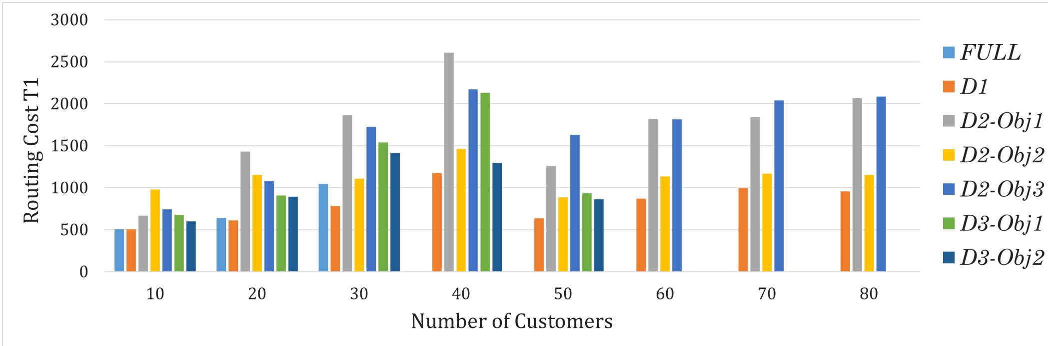

Figure 2.7: Comparison of the routing cost of T1 obtained by each of the solution approaches

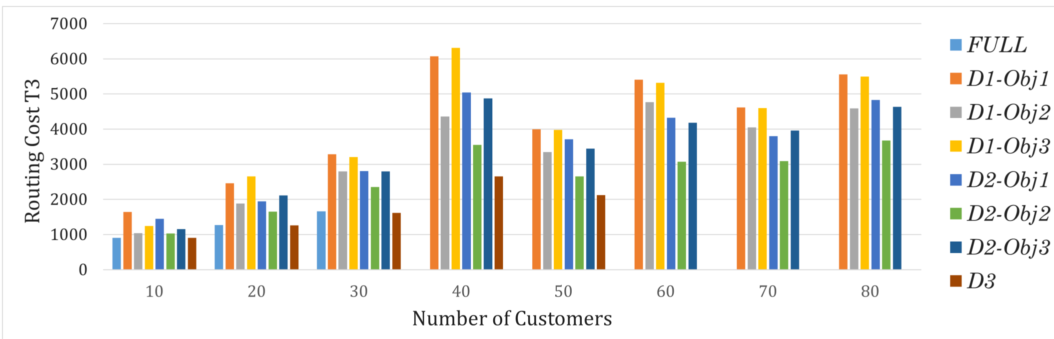

Figure 2.8: Comparison of the routing cost of T3 obtained by each of the solution approaches

each instance for each solution approach. There does not seem to be a significant difference between the different decomposition techniques in the utilization of delivery trucks (figure 2.9(a)). This is because we have one CDC, and the number of trucks used is far fewer than the number of freighters to demonstrate any significant difference.

Since *D1* uses a higher number of freighters than any other solution method, there is little to no consolidation of packages in *D1*, regardless of the objective function used in T2, with the ratio of packages to freighters rarely exceeding 1 (figure 2.9(b)). Though *D1* would be beneficial if our objective is to minimize the emissions caused by large delivery vehicles, it would not be ideal if the routing costs in T3 are also high. In that case, we would need to make more trips and recruit a higher number of

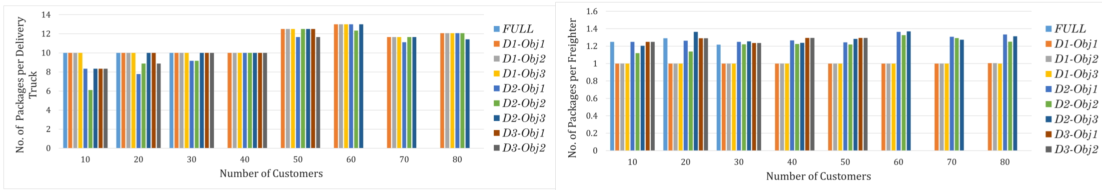

(a) Average number of packages per truck

(b) Average number of packages per freighter

Figure 2.9: Comparing the usage of delivery trucks and freighters by the different solution approaches

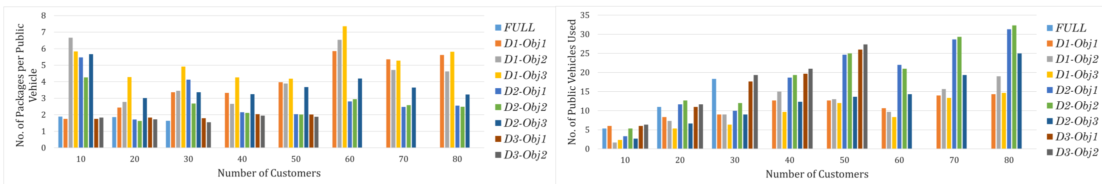

(a) Average number of packages per public vehicle

(b) Number of public vehicles used

Figure 2.10: Comparing the usage of public vehicles by the different solution approaches

freighters. However, we can use it in some cases, for example, if we use drones to make deliveries to the end customers, and our sole aim is to control the use of trucks.

Figure 2.10 shows the average number of customers per public vehicle and the number of public vehicles used by each solution technique. On average, *Obj2* utilizes the highest number of public vehicles, and *Obj3* the lowest. Thus, *Obj3* has a higher percentage of packages per vehicle, as the consolidation of packages in T3 is encouraged here. We also find from our solutions that decomposition approaches *D3* followed by *D2-Obj2* and *D2-Obj3* consistently use a higher number of drop-out stops and, thus, have a lower ratio of customers per drop-out stop. The highest usage of drop-in stops is shown by *D2-Obj3*, since *Obj3* focuses solely on minimizing the use of freighters in tier 3. *D2-Obj1* utilizes the lowest number of drop-in and drop-out stops among all the approaches.

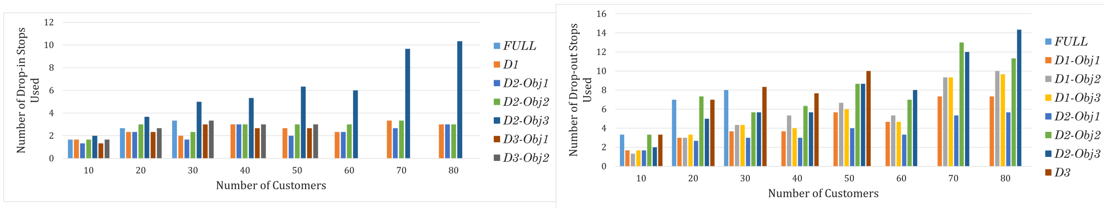

(a) Average number of drop-in stops utilized

(b) Average number of drop-out stops utilized

Figure 2.11: Comparing the usage of drop-in and drop-out stops used by the different solution approaches

2.5.3 Comparison with traditional methods

In order to compare the effectiveness of using public vehicles, we compare the system with a standard delivery method, where trucks are sent directly from the CDC to the customer locations. This corresponds to a Vehicle Routing Problem with Time Windows (VRPTW, henceforth). We use a standard 2-index formulation of the VRPTW and present the model in appendix A.

Figures 2.12-2.14 shows the comparison of the routing costs and distances obtained by the VRPTW compared to the different approaches for the 3T-DPPT. Figure 2.12 gives the total routing costs of T1 and T3, and Figure 2.13 shows the costs (and equivalently, distances covered) of using delivery trucks; thus, we consider only the cost associated with tier 1 for 3T-DPPT in this case. Finally, in Figure 2.14, we show the total distances covered using dedicated delivery vehicles, i.e., trucks and freighters. It is easy to see that for the VRPTW, the costs explode as the number of customers increases. In our approaches, since the majority of the distances are being covered on public vehicles or sustainable freight systems, we keep a check on the use of delivery trucks. The difference is even more pronounced in Figure 2.13. The total delivery distances covered using dedicated delivery vehicles in T1 and T3, however, remain comparable to the VRPTW, as illustrated in Figure 2.14. However, one must remember that the differences in costs and distances covered depend highly on the instances. The difference is higher when the longest part of the delivery occurs on board using public vehicles. If the CDC is located close to the drop-in stops, and the drop-in stops are also very few, compared to the number of customers and the distances between them and the drop-out stops, it would also be highly beneficial to use the public transportation system.

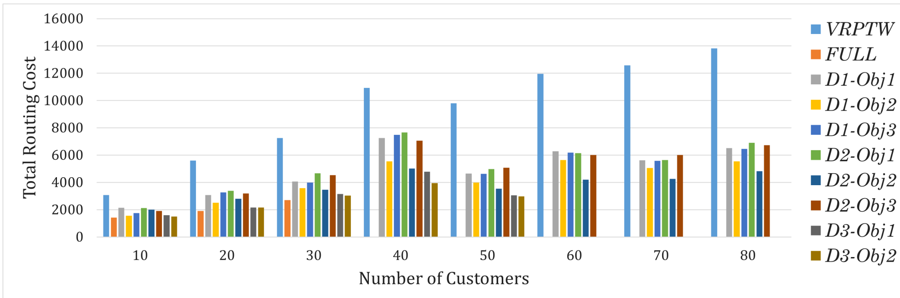

Figure 2.12: Total routing costs

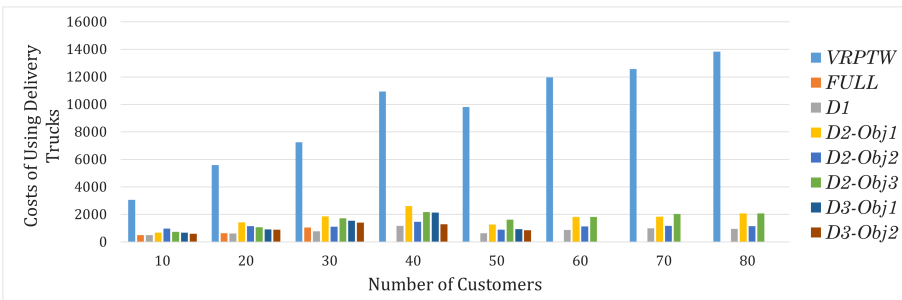

Figure 2.13: Distances covered by delivery trucks

Our results show that using public vehicles could lead to a 85.91% reduction in the distances traversed using heavy trucks on average, consequently reducing the emissions caused by these vehicles proportionally. Sometimes, even though the service does not seem profitable for a small number of customers, as the instance size increases, the cost reductions, particularly environmental costs, are significantly high. We find a 50.8% reduction in total costs on average. The higher the distances covered on the public transportation systems, the greater the benefits. Thus, in larger cities, we expect to see higher cost savings in the day-to-day implementation of the service.

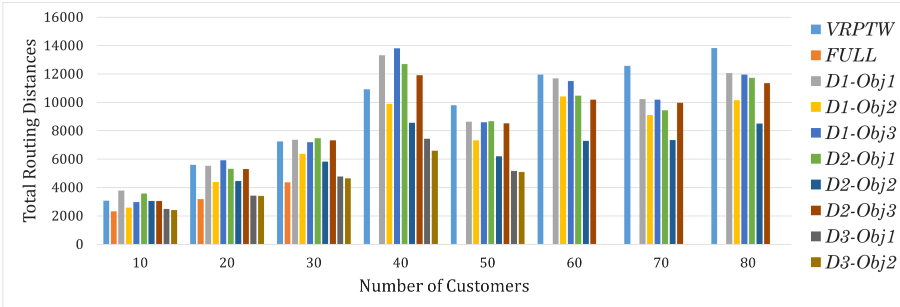

Figure 2.14: Total distances covered using dedicated delivery vehicles (trucks and freighters)

2.5.4 Managerial insights

Impact of heterogeneity in delivery costs

In this section, we analyze the behavior of the solutions on small-sized instances–instances with up to 30 customers, for different proportions of costs in T3 compared to costs in T1. We consider $C^1_{uvd} = D_{uv}, u, v \in \mathcal{S}_{in} \cup \{o\}, d \in \mathcal{D}$, and $C^3_{ijk} = \beta \cdot D_{ij}, i, j \in \mathcal{S}_{out} \cup \mathcal{C}$, where β is a parameter that determines the proportion of costs between T1 and T3. In our computations, we have $\beta = 0.1, 0.25, 0.5, 0.75$, and 1. We have solved the formulations *D1-Obj1*, *D1-Obj2*, *D1-Obj3*, *D2-Obj1*, *D2-Obj2*, *D2-Obj3*, *D3-Obj1*, and *D3-Obj2* on instances with up to 30 customers to study how the solutions, particularly the usage of delivery trucks, vary.

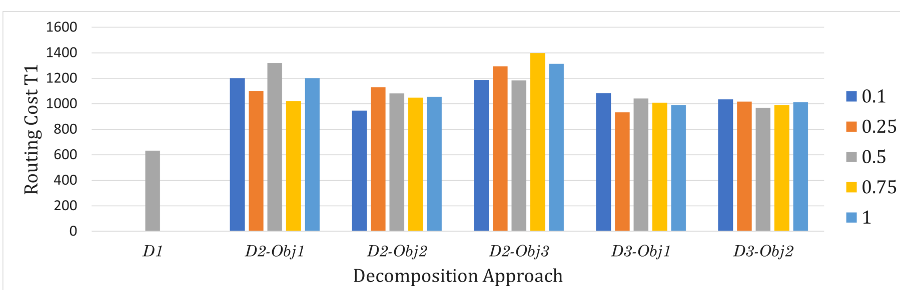

Figure 2.15: Comparison of T1 routing costs for different values of β

Figure 2.15 shows how the routing costs in T1 change when we use different values of β. For *D1*, we have only one column representing the cost because: firstly, T1 is the first tier to be solved here, and the routing costs obtained here do not depend on which objective function is used in T2; and secondly, the value of β does not change T1 routing costs in *D1*, they impact only the costs obtained in T3. Apart from *D1*, which is expected to perform well for tier 1, *D2-Obj2* provides quite competitive solutions.

In figures 2.16 and 2.17, we show how each decomposition method performs in terms of T3 routing costs and total routing costs, respectively, for different values of β. Once again, for T3 routing costs, we have a single column, named D3, for each value of β. This is because when T3 is solved first, we have not yet used the objective functions of T2, so we obtain the same solutions. For tier 3 routing costs, *D3* performs the best, and *D2-Obj2* follows closely behind.

D3 also performs well in terms of the total routing costs of the instances. However, we know that once the instance sizes increase further, *D3* is unable to find feasible solutions. In its absence, *D2-Obj2* performs the best and provides solutions comparable with the best solutions obtained, regardless of the values of β. This is because tier 2 is the linking tier, which balances the objectives of T1 and T3, even though we use approximations, thereby producing good-quality solutions. Other than the routing costs, there is no significant difference in the features of the solutions obtained compared to section 2.5.2.

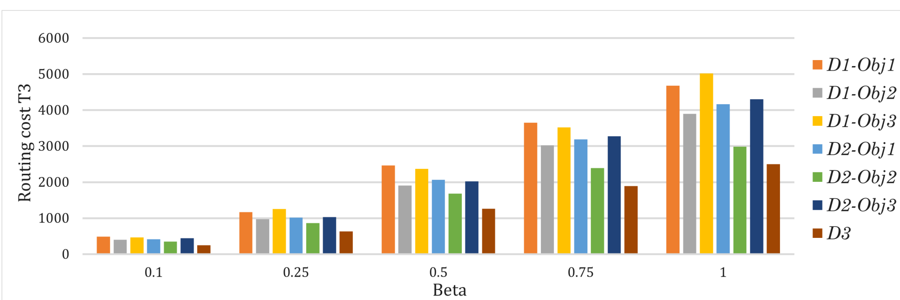

Figure 2.16: Comparison of T3 routing costs for different values of β

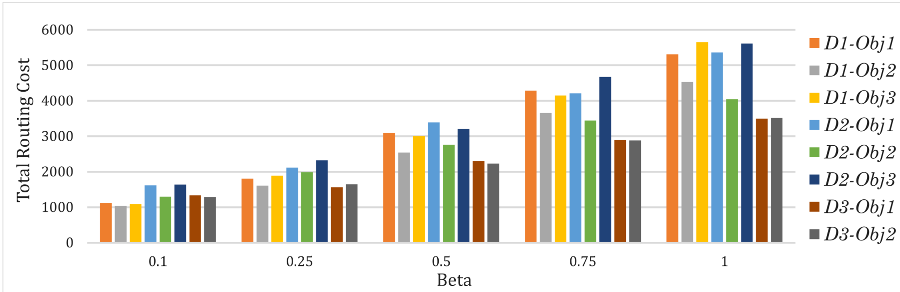

Figure 2.17: Comparison of total routing costs for different values of β

Service costs related to Tier 2

So far in our experiments, we have assumed zero delivery costs related to the second tier. In this section, we discuss the impact of adding service costs related to delivery using public transit lines and drop-in and drop-out stops. These costs arise from the cost of personnel recruited at the stops for loading and unloading packages, daily maintenance of the infrastructure, and the cost of space, among others. To address them, we assume that these costs can be incorporated at the drop-in and drop-out stops, i.e., every time a truck visits a drop-in stop or a freighter leaves a drop-out stop, we add a cost to our objective function.

$$\begin{aligned}
\textit{Minimize} \quad & \sum_{d\in\mathcal{D}} \sum_{u\in\mathcal{S}_{in}\cup\{o\}} \sum_{\substack{v\in\mathcal{S}_{in}\\ u\neq v}} \left(C^1_{uvd}+\lambda_1\right) w_{uvd} + \sum_{d\in\mathcal{D}} \sum_{u\in\mathcal{S}_{in}} \sum_{v=o'} C^1_{uvd} w_{uvd} \\
& + \sum_{k\in\mathcal{K}} \sum_{i\in\mathcal{S}_{out}} \sum_{\substack{j\in\mathcal{C}\\ i\neq j}} \left(C^3_{ijk}+\lambda_3\right) x_{ijk} + \sum_{k\in\mathcal{K}} \sum_{i\in\mathcal{C}} \sum_{\substack{j\in\mathcal{S}_{out}\cup\mathcal{C}\\ i\neq j}} C^3_{ijk} x_{ijk}. \qquad (2.92)
\end{aligned}$$

λ_1 and λ_3 are parameters that represent the service costs at tier 1 and tier 3, respectively. This does not imply that the costs are paid to the freighters or truck drivers exclusively; rather, it is a daily operating cost of delivery on the transit line. All the costs mentioned are integrated directly at the stops whenever there is an exchange of packages.

We made computational experiments with the value of $\lambda_1 = \mu * \textit{average routing cost of T1}$ and $\lambda_3 = \mu * \textit{average routing cost of T3}$, with $\mu = 0, 0.5, 1.0$, to see the impact of adding the service costs on the structure of the solutions. We solved *FULL* on instances with ten customers since only those instances could be solved up to optimality, to study if the solution structure changes on incorporating service costs. Over the instances described above, we did not find any significant change in the solution structure because the value of parameters already facilitates significant consolidation (we expected to see more consolidation as service costs increase). However, once the capacity of freighters was increased from 20 to 30 and 50, we observed some increase in consolidation.

Next, we analyzed its impact on the decomposition methods, with objective function 2, since it has been established as the dominant objective function, on instances with up to 30 customers. In Figure 2.18, we show the utilization of trucks and freighters for different values of service costs. Interestingly, we do not find a change in the number of trucks and freighters utilized for *D1-Obj2*. This is because trucks are utilized completely when tier 1 is solved first, and, in most cases, each package is assigned to one freighter. For *D2-Obj2* and *D3-Obj2*, we observe a higher consolidation of packages on the trucks and freighters as the service cost increases. The total cost, or the objective value described in (2.92), increases proportionally to the service cost parameter based on the number of trucks and freighters used, which, in turn, depends on the number of packages that need to be delivered. If the service costs associated with some lines or stops are relatively high, for example, for stops with extremely high traffic, it is advisable to avoid them, even though the routing costs might increase. From preliminary experiments, we also found that when a customer could potentially be served from a greater number of stops, i.e., $|S_i^{out}|$ is higher, there is a greater level of consolidation as the service costs increase, to the extent that sometimes only one line is used to deliver the packages.

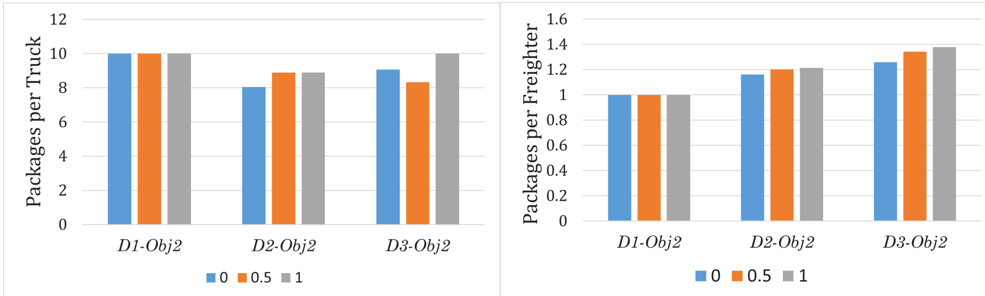

(a) Average number of packages per truck

(b) Average number of packages per freighter

Figure 2.18: Comparing the usage of trucks and freighters when service costs are introduced

Capacity of public vehicles

We also analyze the impact of changing the capacity of public vehicles for transporting packages. We solve the instances with up to 30 customers by increasing the public vehicle capacities by 25% and by decreasing their capacities by 25%, once again using objective function 2. In figure 2.19, we show the routing costs of T1 and T3 as the capacity changes. 1 represents the original capacity, 0.75 represents the capacity reduced by 25%, and 1.25 represents the capacity increased by 25%. We do not observe a significant change in the structure of the solutions as the capacities are changed. This is likely related to the fact that the capacities are not limiting in our case. In other words, the number and volume of packages are small compared to the carrying capacity of all the public vehicles over the day.

We also notice that if the capacity of the public vehicles is increased to 1.5 (or more) times the original capacities in our instances, the computational complexity of the model increases, and the instances become harder to solve.

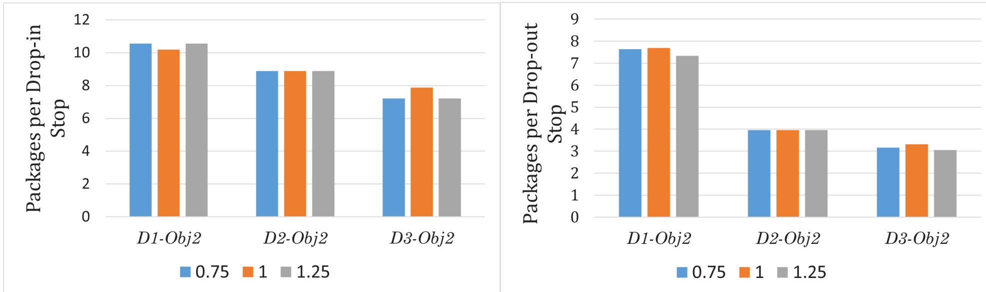

(a) Packages per drop-in stop

(b) Packages per drop-out stop

Figure 2.19: Impact of the change in capacities of public vehicles on the packages per stop

Public vehicle frequency

Next, we study the impact of changing the frequency of the public vehicles. For the base case, we had vehicles that run every 30 minutes. Here, we analyze the solution structures when the vehicles run every 15 minutes (increasing the frequency of service) and every hour (decreasing the frequency of service).

In figure 2.20, we show the T1 and T3 routing costs as the frequencies or the time between two public vehicles on the same line changes. We do not find a significant impact on the routing costs for the third tier. For T1, the routing costs decrease using *D2-Obj2*, as we both increase and decrease the frequency. As the frequency increases, we have more flexibility in assigning the packages to the trucks, and as it decreases, we have greater consolidation on the trucks, both leading to lowered routing costs. In Figure 2.21, we observe a higher number of packages per public vehicle as the frequency both increases and decreases. For the number of packages per freighter, once again, there is no significant change as the frequency of the public vehicles changes.

Thus, we can conclude that we do not need to use all public vehicles on a line for package deliveries, as long as there is enough capacity on the vehicles to carry the packages. A selected number of vehicles, for example, once every hour, could also be enough for the delivery system. Further analysing the schedules could lead us to select off-peak hours during which we can deliver the packages.

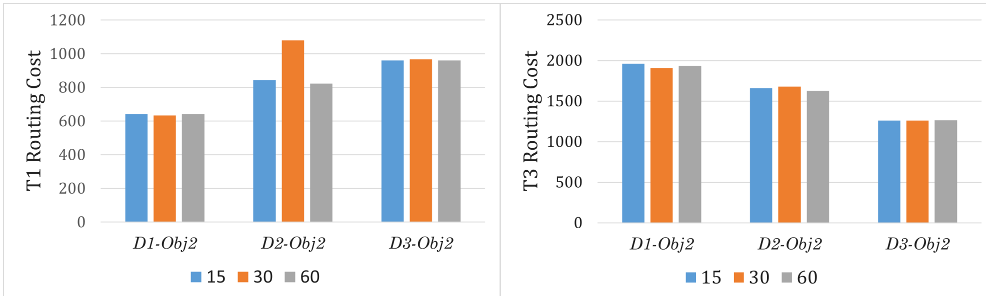

(a) Routing costs of Tier 1

(b) Routing costs of Tier 3

Figure 2.20: Impact of changing the frequency of public vehicles on the T1 and T3 routing costs

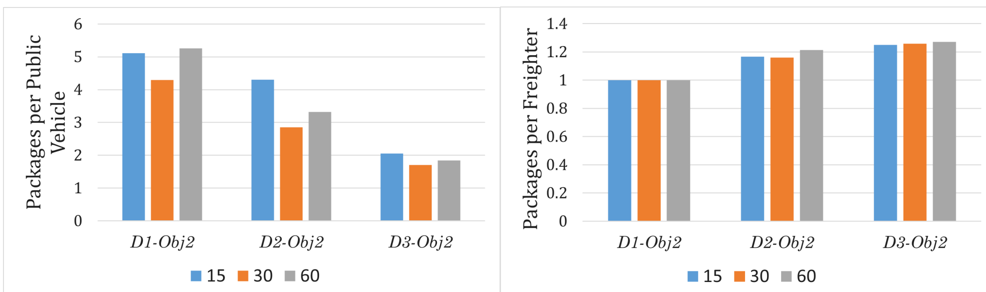

(a) Packages per public vehicle

(b) Packages per freighter

Figure 2.21: Impact of changing the frequency of public vehicles on the packages per public vehicle and freighter

2.6 Conclusion and directions for future work

In this paper, we advocate using public transportation systems for package delivery in cities to reduce emissions and traffic-related issues caused by large delivery vehicles, and show the feasibility and advantages of utilizing such a delivery network. We build on the existing literature to introduce a three-tier transportation problem using the public transit network, with three distinct modes of delivery in the tiers. We provide a comprehensive mixed-integer programming formulation for the entire problem. Since the complete model is computationally complex, we develop a decomposition matheuristic methodology to solve it. We have three decomposition algorithms based on the sequence of solving the tiers. For the delivery on public transit, or tier 2, we propose three objective functions aligning with our goal of minimizing the use of dedicated delivery vehicles and, thus, emissions. Among all the decomposition approaches, we find the performance of *D2-Obj2*, the algorithm that starts solving the problem from T2 and then solves T1 and T3, to be the best overall. The decomposition technique *D3* performs the best for instances with up to 50 customers but cannot find feasible solutions within the time limit beyond that. We find *Obj2*, minimizing the approximate routing distances in T1 and T3 to be the best-performing objective function among all. Extensive computational studies support the effectiveness of such an integrated system. On average, we find a reduction of 85.91% in the use of delivery trucks, and a reduction of 50.8% in the overall distances covered by dedicated vehicles (T1 and T3). Thus, the system proves to be more sustainable and provides economic opportunities for freight shipping companies as well as public transportation agencies. Extensive sensitivity analysis shows the robustness of the solution structure obtained with respect to service costs for using the transit network and the capacity available on the public vehicles.

Though our solution method is limited to handling small-sized instances, they can be used heuristically to design delivery plans. For example, cities are inherently divided into districts, and our approaches can be implemented in each district individually. The longest part of the delivery is intended to be performed on the public transit network, and the delivery routes in each district can be designed separately. Moreover, we might not have complete information about customers before the delivery plan is formulated, and thus, the decisions can be subject to uncertainties. However, the deterministic model studied here can still be beneficial. If we have dynamically arriving customer demands, or we only have an estimate of the customer demands each day instead of the actual demands, from previous implementations of our model, we would know the path that a package at a certain destination needs to follow– in particular, the drop-in stop, the public vehicle line, and the drop-out stop. Thus, as packages arrive during the day, the delivery company already has an idea of what route a package must follow depending on the hour and the customer's location. Sometimes public vehicles are subject to delays. Incorporating time intervals for package pick-up and drop-off times, instead of deterministic points in time, can help alleviate the uncertainty arising from the public transit system. Thus, our study can serve as a viable tool in guiding operational decisions even when uncertainty is involved.

While we achieved some promising results, a lot remains to be done on the 3T-DPPT for future work. It would be interesting to explore the change in the structure of the solutions as the setting of the problem evolves. Extensions to our problem include multiple CDCs, transshipment of packages within the public transit networks, bi-directional package flows on each line, considering uncertainties in the second tier that arise from travel time or capacities, incorporating storage facilities at the stops, among others. It is also worth investigating other objective functions for the full model, like minimizing the number of dedicated delivery vehicles in tiers 1 and 3, maximizing the distance covered on public vehicles, and minimizing emissions by quantifying them, among others. We have also assumed an infinite number of vehicles in the first and third tiers. It would be interesting to study the problem with a limited number of delivery vehicles that perform several trips per day. One of the limitations of our study is that we study a deterministic case of the problem. Uncertainties due to dynamic order arrival times, delays in the public transportation schedules, and unreliable capacities on the transit system play a crucial role in the successful implementation of the system. While our system is robust in terms of small delays in picking up the packages by the freighters or trucks, larger delays need a closer and more detailed inspection. There is a need to develop more efficient solution methodologies for the problem. Each of the tiers poses its own challenges, so they need to be studied in themselves. Heuristic approaches based on route generation schemes or standard local search techniques could provide competent solution methodologies, particularly for the first and the third tier and are worth exploring. Finally, implementing the theoretical models on real-world public transit and customer dataset would help study the system, and bring to light unanticipated challenges that would help in better implementation of the system across cities.

We have focused our study here on the operational level problem. The efficiency of our approach depends on successful decision-making at the tactical and strategic levels. Thus, the system needs to be set up after careful study and analysis. For example, establishing storage facilities at the stops, recruiting personnel, selecting lines and stops, and determining the schedules of the public transit during which the packages would be transported are all crucial decisions that would impact the system's efficiency. In particular, the strategic level decisions require a thorough cost-benefit analysis of the system and cooperation and coordination among all involved stakeholders– the public transit agency, the freight delivery company, and the municipal corporation of the city. This would ensure that initial investments and installation costs are minimized, all involved parties are satisfied, the delivery service reaches its full potential, and the primary objective of reducing emissions and congestion on roads is fulfilled.

A

Appendix Chapter 2

A.0.1 Two-index Formulation for Simple VRP with Time Windows (VRPTW)

We use similar notations and variables to formulate a simple VRP with time windows, with only minor changes. The set of customers is denoted by $\mathcal{C}$. o denotes the CDC, and o' denotes a copy of the CDC. Let variables $x_{ij}, i \in \mathcal{C} \cup \{o\}, j \in \mathcal{C} \cup \{o'\}$ denote the routes of delivery trucks. Continuous variables $t_i, i \in \mathcal{C} \cup \{o\} \cup \{o'\}$ update the time of the routes at each location i, and variables $h_i, i \in \mathcal{C} \cup \{o\} \cup \{o'\}$ update the corresponding capacities. Then, the two-index formulation for the VRPTW is given by:

$$\textit{Minimize} \quad \sum_{i \in \mathcal{C} \cup \{o\}} \sum_{\substack{j \in \mathcal{C} \cup \{o'\} \\ i \neq j}} C^1_{ij} x_{ij} \tag{A.1}$$

$$\textit{sub to:} \quad \sum_{\substack{j \in \mathcal{C} \cup \{o\} \\ i \neq j}} x_{ji} = 1, \ \forall i \in \mathcal{C} \tag{A.2}$$

$$\sum_{j \in \mathcal{C} \cup \{o'\}} x_{ij} = 1, \ \forall i \in \mathcal{C} \tag{A.3}$$

$$t_i - t_j + (\widehat{T}_i + T_{ij}) x_{ij} \leq (\overline{T}_i - \underline{T}_j)(1 - x_{ij}), \ \forall i \in \mathcal{C} \cup \{o\}, \ j \in \mathcal{C} \cup \{o'\} \tag{A.4}$$

$$h_i - h_j + q_j \leq (Q - q_j)(1 - x_{ij}), \ \forall i \in \mathcal{C} \cup \{o\}, \ j \in \mathcal{C} \cup \{o'\} \tag{A.5}$$

$$\underline{T}_i \leq t_i \leq \overline{T}_i, \ \forall i \in \mathcal{C} \tag{A.6}$$

$$h_i \leq Q, \ \forall i \in \mathcal{C} \tag{A.7}$$

$$x_{ij} \in \{0, 1\}, \ \forall i \in \mathcal{C} \cup \{o\}, \ j \in \mathcal{C} \cup \{o'\} \tag{A.8}$$

$$t_i, h_i \geq 0, \ \forall i \in \mathcal{C} \tag{A.9}$$

3

Tactical Workforce Sizing and Scheduling Decisions for Last-Mile Delivery

joint work with **Claudia Archetti** and **Alberto Santini**

3.1 Introduction

Last-mile delivery (LMD) is the final segment of the supply chain, starting at the last warehouse and ending when the goods reach the customer. With the boom of e-commerce, especially during and after the Covid-19 pandemic, LMD in large cities is dominated by home deliveries, i.e., by carriers delivering many small parcels up to the customers' doorsteps using a fleet of vehicles from legacy vans to more sustainable means such as cargo bikes (Alfonso et al., 2021). A fundamental tactical question arises for logistic operators involved in LMD in the urban environment: how many couriers should they employ? On the one hand, a more extensive workforce is associated with higher staffing costs; on the other hand, using fewer couriers degrades the quality of service or forces the operator to resort to expensive outsourcing options. Demand for home delivery is highly seasonal (throughout the year and at specific hours of the day), further complicating the challenge of choosing the correct workforce size. This paper introduces a decision support system for tactical hiring decisions, incorporating realistic constraints and demand uncertainty.

The importance of increasing the efficiency of LMD stems from its relevance in the global economy. For example, LMD is expected to grow at a compound annual rate of 6.12% from 2023 to 2030 (Contrive Datum Insights, 2023). Among the optimization problems linked with LMD, Boysen et al. (2021) identified staffing and fleet sizing as needing attention from the operational research community because of the "lack [of] scientific decision support".

We fill this gap by considering the problem of a logistics operator who must deliver parcels throughout the day and faces the tactical problem of sizing its workforce. The operator can decide to fulfill each delivery with either a fleet of owned vehicles driven by couriers or paying a fee to an outsourcing (or crowdsourcing) provider. Maintaining a large workforce would allow the operator to avoid paying such fees at the price of high fixed staffing costs. Conversely, hiring few couriers means the operator must extensively resort to outsourcing, leading to high variable costs. The logistic operator must then balance the tactical workforce sizing and operational outsourcing decisions. From this point of view, our work contributes to a recent research stream about workforce sizing in the logistics and service industries (see, e.g., Section 3.2.2 and (Dai & Liu, 2020a; Turan et al., 2022; Pandey et al., 2021)).

A central concept in our setting is that of *satellites* (Crainic et al., 2021). These are locations within the city where the couriers start and end their delivery trips. They are intermediate between large distribution centers (usually on the city's outskirts) and the customers. They are used for transhipments and have little or no temporary storage capabilities. Examples of satellites are small warehouses, parking lots, mobile vehicles (Gonzalez-Feliu, 2012), micro-consolidation centers (Arrieta-Prieto et al., 2022), or even public transit stops (Delle Donne et al., 2023b, 2024).

Each satellite is associated with a given portion of the city, called an *area*. All deliveries within a given area will occur with vehicles starting and ending their routes at the corresponding satellite. Areas are further grouped into *regions*. We assume that hiring decisions must be taken at the tactical and regional level, i.e., a courier is hired for a specific region and an extended period. Assignment of couriers to satellites (and, therefore, to areas) happens on the operational level according to the needs of the logistic operator. Figure 3.1 shows the example of a city in which three regions (delimited with thicker black lines) are further divided into several areas (delimited with white lines). Blue squares indicate the locations of the satellites.

The logistic operator must decide (i) how many couriers to hire in the mid-to-long term in each region (workforce sizing) and (ii) which area to assign them in the short term to minimize the combined labor costs and expected outsourcing costs (assignment and scheduling). To build a mathematical model to address this problem, we will first present intermediate models with simplifying assumptions. We consider these models not only because they simplify our exposition but also because they correspond to different levels of flexibility allowed to the decision-maker. For example, we will first

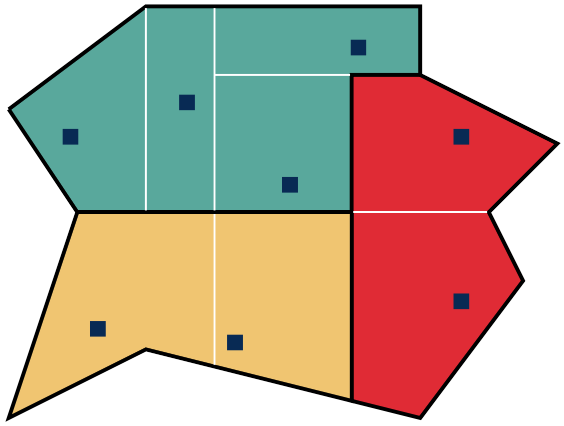

Figure 3.1: Example of a city with three regions (delimited with thicker black lines) subdivided into smaller areas. Blue squares indicate the position of the satellites.

assume that the logistics company can employ couriers to work shifts as short as desired. Potentially, the company could hire ten couriers to work from 19:00 to 21:00 and assign them to a different area every day. However, concerns about job quality and service level suggest that further conditions be imposed. We will then consider situations in which couriers must be hired for fixed shifts (e.g., 08:00–16:00 each day) or for flexible shifts (e.g., a period of 8 consecutive hours, but starting at any time during the day) and that couriers can move between areas, but only within the same region. Indeed, one of the contributions of our work is to initiate a discussion on the impact of shift flexibility on the company's bottom line, complementing research in the social sciences, which instead addresses the effect of shift instability on workers' wellbeing (see Section 3.2.3).

We emphasize that we are concerned with sizing and scheduling the workforce, assuming that the company already owns a fleet of vehicles. Therefore, we do not study the problem of purchasing or leasing vehicles and consider the corresponding costs sunk. For recent works in fleet sizing, we refer the reader to, e.g., (Franceschetti et al., 2017; Banerjee et al., 2022; Shehadeh et al., 2021; Ertogral et al., 2017; Kunz & Van Wassenhove, 2019; Goulart et al., 2021; Rahimi-Vahed et al., 2015; Castillo et al., 2022; Loxton & Lin, 2011). We review the contributions more closely related to the present paper in

Section 3.2.2.

Finally, we highlight the stochastic nature of our problem. The decision-maker can estimate the number of deliveries in each area but cannot know this number precisely on the timescale required to make tactical decisions. Therefore, we will introduce a subproblem to estimate the number of parcels delivered by the hired couriers in each area and the number of parcels that must instead be outsourced. To this end, we will evaluate several demand scenarios and adapt approximation formulas from the literature (Figliozzi, 2008).

The rest of the paper is organized as follows. In Section 3.2, we position our contribution in the literature on LMD scheduling and review related topics such as fleet sizing and districting. We also review current literature on the topic of stability in workforce scheduling from both operations research and the social sciences. In Section 3.3, we formalize our problem and introduce several mathematical formulations, which share the same base but differ in the amount of flexibility available to the decision-maker. Because the formulations are extremely quick to solve using commercial software, in Section 3.4, we present the results of an extensive computational campaign. We provide managerial insights and highlight the roles of stability and flexibility on the costs and operations of an LMD logistics company. Finally, we summarise the main findings and our recommendations in Section 3.5.

To the best of our knowledge, this work is the first to explore the impact of stability in the context of workforce sizing and scheduling problems. In particular, we propose a new mathematical formulation that estimates the hiring and outsourcing costs of a company performing parcel deliveries in an urban environment. By extending this formulation, we can model different levels of shift stability and—through a vast computational campaign—provide insights into how the company performs under different exogenous conditions such as the demand volume, outsourcing costs, or demand patterns.

3.2 Literature Review

This section presents related contributions and positions the current work in the literature. We focus on three main areas. The first is tactical workforce scheduling, focusing exclusively on LMD. Compared with classical scheduling, LMD presents additional challenges. Most notably, demand is stochastic and seasonal; when some couriers are crowdsourced, supply is also stochastic. The second research area is fleet sizing and districting. These decisions usually happen before workforce scheduling and are better classified as strategic rather than tactical. Still, there are several points of contact with our work, especially in the methodology used to approximate operational-level costs. Finally, we add an ethical dimension to our research by considering the stability of employee shifts. Research in social science associates stable work shifts with higher job satisfaction, better work-life balance, and reduced turnover. We briefly review this literature, motivating the investigation into the impact of shift stability vs. flexibility on the bottom line of logistic operators.

We remark that the above areas are by no means exhaustive. Indeed, recent literature on optimising LMD operations has focused on timely real-world problems at all decision-making levels. For example, at the operational level, on determining which deliveries to outsource to crowd couriers (Fatehi & Wagner, 2022); at the tactical level, on balancing driver workload over a week or a month (Wang et al., 2022); at the strategic level, on partitioning urban areas into regions (Carlsson et al., 2024). While these decisions are related to workforce sizing and scheduling, we include in the following review only the contributions that share either methodological or motivating characteristics with our work.

3.2.1 Workforce scheduling for last-mile delivery

Workforce scheduling concerns the assignment of couriers to perform deliveries in given areas during specific periods. It is a critical task in all parts of the supply chain, particularly in its most labor-intensive segment: the last mile. Yildiz & Savelsbergh (2019) have identified “the importance of having the right number of couriers at the right time" in last-mile meal delivery, and indeed, their observations can be generalized to other types of LMD.

A few works in the literature tackle workforce scheduling in the LMD setting. Restrepo et al. (2019) consider the combined problems of scheduling couriers (at the tactical level) and assigning them specific orders (at the operational level). Unlike our approach, the authors assume staffing is already decided and the workforce size is fixed. On the other hand, similarities with our setting include the possibility of outsourcing deliveries when over capacity and the fact that the territory is divided into areas. The authors propose an exact two-stage stochastic approach. The first-stage tactical problem assigns couriers to shifts and areas, while the second-stage operational problem allocates orders to couriers (or an outsourcing provider). Using an L-shaped method (Laporte & Louveaux, 1993), they achieve solutions with average gaps of 1.07% from the optimum in realistic instances with up to 150 orders, 42 couriers, 23 scenarios and a capacity of at most two orders for each courier in a given period.

Another stream of work deals with courier scheduling under supply uncertainty. Some delivery companies use a mixed workforce of scheduled couriers and occasional ones, e.g., because they partly rely on crowdsourcing (Santini et al., 2022). Depending on the number of occasional couriers available, they face the double challenge of uncertain customer demand and supply capacity. Behrendt et al. (2023) and Ulmer & Savelsbergh (2020) tackle the problem of a company relying on a mix of scheduled and crowdsourced couriers. This problem differs from ours because even scheduled couriers are hired and dismissed per shift. The company, in fact, can use the crowdsourcing platform to offer both shifts and single deliveries. If a person accepts a shift, they become available for the corresponding period, during which they can be assigned multiple deliveries. Otherwise, a person can accept to perform a single delivery without committing to be available for an extended period. The objective of the problem is to determine the ideal number of scheduled couriers to hire at each period to minimize labor costs and late-delivery penalties and thus decide the start time and duration of the shifts offered on the crowdsourcing platform. In (Behrendt et al., 2023), the authors use continuous approximations and value function approximation methods to estimate the number of couriers required to meet a given service level, assuming a homogeneous order arrival rate. To the same end, Ulmer & Savelsbergh (2020) use a neural network trained on an off-line dataset generated via sample average approximation (Kleywegt et al., 2002).

Finally, we mention the work of Dai & Liu (2020b), who tackle the problem of determining the correct workforce size and parcel allocation for a combined staff of in-house couriers and crowdsourced drivers. They remark that an over-reliance on crowdsourcing can provide short-term benefits but sacrifices long-term objectives such as workforce retention and system robustness to fluctuation.

3.2.2 Fleet sizing and districting for last-mile delivery

The problem of deciding the size and composition of a fleet of vehicles is known as fleet sizing. Because purchasing or leasing vehicles involves high capital costs or long-term contracts, fleet sizing often happens at the strategic level. Similar to our staff scheduling problem, operational decisions are usually approximated when performing fleet sizing.

Fleet sizing happens before staff scheduling because the number of available vehicles determines how many couriers can work simultaneously. It can also happen before, after or simultaneously with districting, i.e., the problem of partitioning a given geographical region into fixed areas and distributing the vehicles among the areas. While, in principle, an operator could skip districting and solve a large routing problem each day, real-life practice has shown that geographical partitions drastically simplify operations and increase service quality (see, e.g., Boysen et al., 2021; Liu et al., 2021; Monteiro Ferraz et al., 2022). In the following, we review two contributions closest to our approach.

Franceschetti et al. (2017) consider the problem of partitioning a rectangular city into rectangular areas. There are several differences between their approach and the problem we tackle in this paper.

(a) In Franceschetti et al. (2017)'s settings, there is only one central depot from where all vehicles are deployed. From this point of view, their work is tailored more towards classical delivery vans than zero-emission vehicles. (b) The authors also consider the problem of designing the areas. However, one vehicle operates in each area; therefore, the operational problem is a Travelling Salesman Problem, compared to a Vehicle Routing Problem (VRP) in our case. (c) The couriers fulfill all requests with no possibility of outsourcing. (d) Because they focus on classical delivery vehicles, the authors also consider the cost of owning or leasing such vehicles and the transportation costs. Similar to our work, they use continuous approximation formulas to estimate operational routing decisions. The authors consider the case of a heterogeneous fleet with some vehicle types subject to access restrictions (i.e., they cannot enter certain areas during some parts of the day). After analyzing optimal solutions obtained via Dynamic Programming and a Mixed-Integer model, they conclude that access restrictions can sometimes be counterproductive, increasing the total number of vehicles on the road. Their computational results also show that the advantage of having a heterogeneous fleet is minor compared with the corresponding increase in operational complexity.

Banerjee et al. (2022) tackle a similar problem of designing distribution areas and determining the correct fleet size to deploy in a same-day-delivery system. Similar to Franceschetti et al. (2017), all vehicles start and end their routes from the depot, each area is allocated one vehicle, and no outsourcing is possible. However, the city and its areas are not limited to being rectangular. The problem characteristics hint at a strong correspondence between minimizing the fleet size and maximizing the area covered by each vehicle. The authors exploit this link to develop area-maximizing policies and apply a fleet-size minimization algorithm.

3.2.3 Geographical and temporal stability in workforce scheduling

While, on paper, extremely flexible and volatile schedules might appear the most suited to meet a highly dynamic demand, real-world practice reveals the importance of stability and planning at the tactical level.

Regarding *geographical* stability, a stable assignment of couriers to areas or even to customers leads to shorter routing and service times. In classical supply chains where drivers visit a few large customers, consistency leads to quicker operations and increased customer satisfaction. In a seminal work, Groër et al. (2009) introduced the Consistent Vehicle Routing Problem (ConVRP), a multi-period routing problem rewarding stability in assigning drivers to customers and visiting the same customer at similar times. This problem has garnered considerable attention: we refer the reader to a survey by Kovacs et al. (2014) and to the work of Smilowitz et al. (2013) for links between the ConVRP and workforce management. Regarding recent contributions published after the survey, see, e.g., (Rodríguez-Martín et al., 2019; Schneider, 2016; Goeke et al., 2019). Stable assignment of drivers to areas is also beneficial in modern last-mile settings. For example, in a recent keynote presentation at the 12$^{\text{th}}$ DIMACS implementation challenge, Werneck (2022) has emphasized the importance of consistency and driver familiarity for last-mile delivery at Amazon.

The topic of *temporal* stability falls in the broader literature of workforce scheduling with workers' preferences (see, e.g., (Ruiz-Torres et al., 2015; Mohan, 2008; Yura, 1994) and the survey of Van den Bergh et al. (2013)).

The issues of shift instability and low wages have been identified among the most critical aspects of the modern logistics industry, especially in the last mile.

From the couriers' point of view, unstable or unreliable shifts cause a sensible decrease in happiness and worsen the work-life balance. In a survey of workers in Illinois, United States, Dickson et al.

(2018) showed that, in 2018, 35% knew their schedule at least one week before and 10% only knew it 24 hours in advance. Furthermore, the average gap between the minimum and maximum weekly hours during the six months before the survey was 14 hours, suggesting large fluctuations from one week to another. Part-time workers, who are largely represented in LMD, are particularly affected: Dickson et al. (2018) report that "the incidence of unpredictable or varying shift times [...] falls disproportionately on part-time workers—12 percent of part-timers experience irregular shift times". Furthermore, the downsides of erratic shifts affect some categories, such as single parents, more than others (Ananat & Gassman-Pines, 2021; Harknett et al., 2022). Carrillo et al. (2017) highlights that: "as dual-earner couples, single parent families, and irregular work schedules have risen in prevalence, the logistics of arranging child care to match work shifts have grown increasingly complex". This complexity comes at a significant cost for children; quoting again Carrillo et al. (2017): "Instability and unpredictability at work were reproduced in [...] child-care arrangements at home. This scramble led to inconsistency in children's care and also imposed a heavy psychological burden on parents as they reconciled the difficulty of finding care for their children with the imperative to keep an open availability for work and catch the shifts that became available to them."

From the point of view of logistic operators, excessive shift instability causes higher employee turnover and lower performance, producing a net detrimental effect for the firm. Chung (2022) studies the impact of variable work schedules (VWS) on quick-service restaurant chains and concludes that "despite the common assumption that their [VWS] use helps firms achieve higher performance by matching the supply of labor to demand fluctuations [...] this study demonstrates otherwise", and that "scholars and practitioners should reconsider the general assumption that staffing flexibility helps organisations adapt to uncertain environments". Although the role of schedule volatility on employee turnover has been studied before (see, e.g., Henly & Lambert, 2014; Henly et al., 2006), its impact has increased after the Covid-19 pandemic (see Choper et al., 2022; Bergman et al., 2023; Rhee et al., 2020).

The above considerations clarify that shift flexibility in workforce scheduling in LMD is worth researching and that the literature on this topic can be enriched considering an ethical dimension (Le Menestrel & Van Wassenhove, 2009; Ormerod & Werner, 2013; Bellenguez et al., 2023).

3.3 Problem setting and formulation

In this section, we formalise the problem we are studying and provide several mathematical models to make workforce sizing and scheduling decisions. Section 3.3.1 provides a mathematical description of the considered problem. We present a base mathematical model in Section 3.3.3 and extend it in Section 3.3.4.

3.3.1 Problem description

We consider a logistic operator working in the last mile of the supply chain in an urban environment. The city is divided into a set A of areas, usually corresponding to districts or neighbourhoods, with exactly one satellite in each area. Areas are grouped into regions $\mathcal{R}$, such that $\mathcal{R}$ forms a partition of A.

The daily planning horizon is discretised into a set Θ of periods. The planner chooses the length of the periods in a way that (a) is long enough to ensure that couriers complete their tours and (b) is suitable for accurately estimating the demand based on historical data. In our main application setting, couriers employ sustainable vehicles with limited capacities, such as cargo bikes. Because vehicle capacities limit tour durations, the duration of a period is usually limited to a few hours.

Couriers start their tours at the beginning of each period and return to the starting satellite before the end of the period. If a courier changes his/her assigned satellite between two consecutive periods, we assume the transfer time to be negligible. This assumption is justified because transfers are only possible between satellites in the same region.

Each area has an associated demand distribution, which determines how many deliveries are required during each period. We adopt a scenario-based approach and consider a set S of scenarios. Each scenario $s \in S$ determines, for each area $a \in A$ and period $\theta \in \Theta$, the demand $n^s_{a\theta} \in \mathbb{N}$, i.e., the number of deliveries to perform.

The decision variable is the number of couriers assigned to each area during each period and is denoted with $x_{a\theta} \in \mathbb{N}$ ($a \in A$, $\theta \in \Theta$). This decision is taken at the tactical level; therefore, the assignment persists across all scenarios. Eventually, we will introduce constraints on this assignment, which guarantee, e.g., that couriers work for a minimum number of consecutive periods (a shift). For the moment, we only note that the number of couriers assigned to an area must not necessarily ensure they can deliver all parcels under all scenarios. Indeed, the cost incurred by the planner is the sum of the couriers' labour cost and the expected outsourcing cost. We denote with $c_{a\theta} > 0$ the unit cost of employing a courier in area a for period θ. The labour cost associated with a and θ is thus $c_{a\theta}x_{a\theta}$. We denote with $\omega_{a\theta}(x_{a\theta}) \geq 0$ the random variable representing the outsourcing cost for area a and period θ when employing $x_{a\theta}$ couriers. In our approach, we estimate the expected value of $\omega_{a\theta}$ by computing the average outsourcing cost over all scenarios:

$$\mathbb{E}\left[\omega_{a\theta}(x_{a\theta})\right] \simeq \frac{1}{|S|} \sum_{s \in S} \omega^s_{a\theta}(x_{a\theta}),$$

where $\omega^s_{a\theta}(x_{a\theta})$ is the deterministic outsourcing cost incurred under scenario s. With the above notation, the objective function of our problem is

$$\min_{x_{a\theta} \in \mathbb{N}} \quad \sum_{a \in A} \sum_{\theta \in \Theta} \left(c_{a\theta} x_{a\theta} + \frac{1}{|S|} \sum_{s \in S} \omega^s_{a\theta}(x_{a\theta}) \right). \tag{3.1}$$

Determining the value of $\omega^s_{a\theta}(x_{a\theta})$ is not straightforward. To know how many deliveries can be performed by $x_{a\theta}$ couriers (and, thus, how many must be outsourced), we would have to solve an instance of the $\mathcal{NP}$-complete Capacitated Vehicle Routing Problem (CVRP) for each area, period and scenario. However, knowing the exact value of $\omega^s_{a\theta}$ is unnecessary at the tactical planning level. Therefore, in Section 3.3.2, we devise a method to approximate this value. In the rest of this section, we introduce constraints which, together with the objective function (3.1), will model realistic staff sizing problems faced by LMD operators.

3.3.2 Approximation of the outsourcing costs

We assume that the outsourcing cost depends linearly on the number of outsourced deliveries. Specifically, let $C_{\text{out}} > 0$ be the cost to outsource one delivery and $m^s_{a\theta} \in \mathbb{N}$ the number of couriers needed to fulfil all deliveries in area $a \in A$ during period $\theta \in \Theta$ according to scenario $s \in S$.

Under the assumption that all couriers deliver roughly the same number of parcels, we can write the outsourcing cost function as

$$\omega^s_{a\theta}(x_{a\theta}) = \begin{cases} 0 & \text{if } x_{a\theta} \geq m^s_{a\theta}, \\ (m^s_{a\theta} - x_{a\theta}) \frac{n^s_{a\theta}}{m^s_{a\theta}} C_{\text{out}} & \text{otherwise.} \end{cases} \tag{3.2}$$

Equation (3.2) states that the planner does not incur outsourcing costs if a sufficient number of couriers is hired. Otherwise, a fraction of $1 - x_{a\theta}/m^s_{a\theta}$ of the deliveries must be outsourced at unit cost C_{out}.

The problem of calculating $\omega^s_{a\theta}(x_{a\theta})$ then reduces to the computation of $m^s_{a\theta}$. As mentioned above, its exact value is given by the solution of a CVRP. In the following, we propose to compute an approximation $\hat{m}^s_{a\theta}$. To this end, denote with $\alpha_a > 0$ the surface of area a, with $\bar{r}_a > 0$ the average distance between a point in a and the satellite, with $Q > 0$ and $v > 0$ respectively the capacity and the speed of the courier vehicles, with $\tau > 0$ the service time at the customer's, and with $T > 0$ the duration of a period. We note that capacity Q is expressed in the number of deliveries (thus assuming that parcels are not too dissimilar in size) and that the unit of measure of v is derived from those of $\bar{r}_a$ and T (i.e., units of space over units of time).

Figliozzi (2008) proposed a closed-form approximation of the cost of the optimal solution of a VRP with $n^s_{a\theta}$ customers and m vehicles:

$$k_a \cdot \frac{n^s_{a\theta} - m}{n^s_{a\theta}} \sqrt{\alpha_a \cdot n^s_{a\theta}} + 2\bar{r}_a \cdot m, \tag{3.3}$$

where k_a is a coefficient that depends on the shape of area a and must be learned, e.g., via regression. We extend this formula to use it as an approximation of the average time a courier needs to complete a route, including the service time at the customers:

$$\text{route time} = \frac{1}{m} k_a \frac{n^s_{a\theta} - m}{v \cdot n^s_{a\theta}} \sqrt{\alpha_a \cdot n^s_{a\theta}} + 2\frac{\bar{r}_a}{v} + \frac{n^s_{a\theta}}{m} \cdot \tau. \tag{3.4}$$

The first term approximates the travel time between customers, the second approximates the round trip from the satellite, and the third term accounts for the service time at the customers. Because each courier must respect both the capacity and the route duration constraint, we look for the smallest integer m such that

$$\begin{aligned} & m \geq \frac{n^s_{a\theta}}{Q}, \text{ and} \\ & \frac{1}{m} k_a \frac{n^s_{a\theta} - m}{v \cdot n^s_{a\theta}} \sqrt{\alpha_a \cdot n^s_{a\theta}} + 2\frac{\bar{r}_a}{v} + \frac{n^s_{a\theta}}{m} \cdot \tau \leq T. \end{aligned}$$

Simple algebraic manipulations yield

$$\hat{m}^s_{a\theta} = \left\lceil \max \left\{ \frac{n^s_{a\theta}}{Q}, \frac{\frac{k_a}{v}\sqrt{\alpha_a n^s_{a\theta}} + n^s_{a\theta} \cdot \tau}{T + \frac{k_a}{v \cdot n^s_{a\theta}}\sqrt{\alpha_a n^s_{a\theta}} - \frac{2\bar{r}_a}{v}} \right\} \right\rceil. \tag{3.5}$$

3.3.3 Base model

We introduce a base optimisation model which uses objective function (3.1) and the framework described in Section 3.3.2 to solve a loosely constrained version of our problem. Indeed, the only basic constraints we introduce are: (a) a global upper bound $u \in \mathbb{N}$ on the number of couriers that the logistic operator can employ during any given period and (b) a regional-level upper bound $u_R \in \mathbb{N}$ on the number of couriers that can work in region $R \in \mathcal{R}$ during any given period. These bounds can derive from real-life considerations, such as a staffing budget (for bound u) or the number of available vehicles (for bounds u_R). The model, denoted MBase, reads as follows.

$$
\begin{aligned}
\min \quad & \sum_{a \in A} \sum_{\theta \in \Theta} \left(c_{a\theta} x_{a\theta} + \frac{1}{|S|} \sum_{s \in S} \hat{\omega}^s_{a\theta}(x_{a\theta}) \right) && && \text{(3.6a)} \\
\text{s.t.} \quad & \sum_{a \in R} x_{a\theta} \leq u_R && \forall R \in \mathcal{R},\ \forall \theta \in \Theta && \text{(3.6b)} \\
& \sum_{a \in A} x_{a\theta} \leq u && \forall \theta \in \Theta && \text{(3.6c)} \\
& x_{a\theta} \in \mathbb{N} && \forall a \in A,\ \forall \theta \in \Theta. && \text{(3.6d)}
\end{aligned}
$$

In (3.6b) and (3.6c), the bounds are enforced for all periods $\theta \in \Theta$ to ensure that the maximum workforce size is not exceeded at any period of the planning horizon. Function $\hat{\omega}^s_{a\theta}$ denotes the approximate outsourcing cost $\omega^s_{a\theta}$ in which $m^s_{a\theta}$ is replaced by $\hat{m}^s_{a\theta}$ in eq. (3.2). Indeed, directly using

(3.2), we obtain the following formulation for MBase.

$$\min \quad \sum_{a\in A}\sum_{\theta\in\Theta}\left(c_{a\theta}x_{a\theta} + \frac{1}{|S|}\sum_{s\in S}\Omega^s_{a\theta}\right) \tag{3.7a}$$

$$\text{s.t.} \quad \sum_{a\in R} x_{a\theta} \leq u_R \qquad \forall R\in\mathcal{R},\ \forall\theta\in\Theta \tag{3.7b}$$

$$\sum_{a\in A} x_{a\theta} \leq u \qquad \forall\theta\in\Theta \tag{3.7c}$$

$$\Omega^s_{a\theta} \geq (\hat{m}^s_{a\theta} - x_{a\theta})\frac{n^s_{a\theta}}{\hat{m}^s_{a\theta}}C_{\text{out}} \qquad \forall a\in A,\ \forall\theta\in\Theta,\ \forall s\in S \tag{3.7d}$$

$$x_{a\theta}\in\mathbb{N} \qquad \forall a\in A \tag{3.7e}$$

$$\Omega^s_{a\theta}\geq 0 \qquad \forall a\in A,\ \forall s\in S. \tag{3.7f}$$

In model (3.7a)–(3.7f), we introduced new variables $\Omega^s_{a\theta}$ to hold the value of $\hat{\omega}^s_{a\theta}(x_{a\theta})$. We remark that the above formulation is decomposable by period θ; however, when we add further constraints in Section 3.3.4, this will no longer be the case.

The complete solution of model MBase requires two steps. First, we compute the approximate values $\hat{m}^s_{a\theta}$ using (3.5), for each s, a and θ. Then, we use these values to solve model MBase and to find the optimal values of $x_{a\theta}$ and their corresponding cost.

3.3.4 Shift linking constraints

Model MBase potentially allows employing couriers for just one period or intermittent periods during the day. However, job quality and service level considerations forbid such practices in most real-life situations. To this end, we introduce the concept of shifts: a set of consecutive periods such that if a courier works during one of them, they must work during all of them.

While the concept of a work shift is almost universally employed, its implementation changes from company to company. In the following, we propose three types of shifts with different levels of flexibility. Each will correspond to new variables and constraints extending model MBase; their impact will be evaluated in Section 3.4.

The first type is fixed shifts: partitioning the set of periods Θ into contiguous non-overlapping sets. For example, if the working day is from 9 AM to 9 PM and each period spans two hours, we would have $\Theta = \{1, \ldots, 6\}$. Two fixed shifts could be 9 AM to 3 PM (periods 1 to 3) and 3 PM to 9 PM (periods 4 to 6). The start period and the duration of each shift are given in advance by labor regulations or local uses and are not decision variables. Each courier is assigned to one of these preset shifts.

The second type is flexible shifts. Each courier has an associated shift, i.e., a set of contiguous periods of fixed total duration. However, the start time of each courier's shift is not given in advance and is a decision variable: different couriers can have shifts starting at different times. Unlike fixed shifts, flexible shifts do not need to partition the set of periods and can overlap.

The third type is partially flexible shifts, which provide intermediate flexibility between fixed and flexible shifts. Although they are still decision variables, we limit the number of possible distinct shift start times. For example, we might aim to create four possible shifts (i.e., selecting four possible start times) and then assign one shift to each courier. If the number of possible start times equals the number of periods, then we are in the special case of flexible shifts. On the other hand, limiting the number of shift start times to only a few possibilities decreases the system's flexibility and allows the creation of stable rosters for the couriers.

Figure 3.2 shows three examples of shifts which can be devised for the same demand pattern displayed at the bottom. The blue shifts at the top are fixed with 9 AM and 3 PM start times. The red shifts in the middle are flexible, and the yellow ones at the bottom are partially flexible.

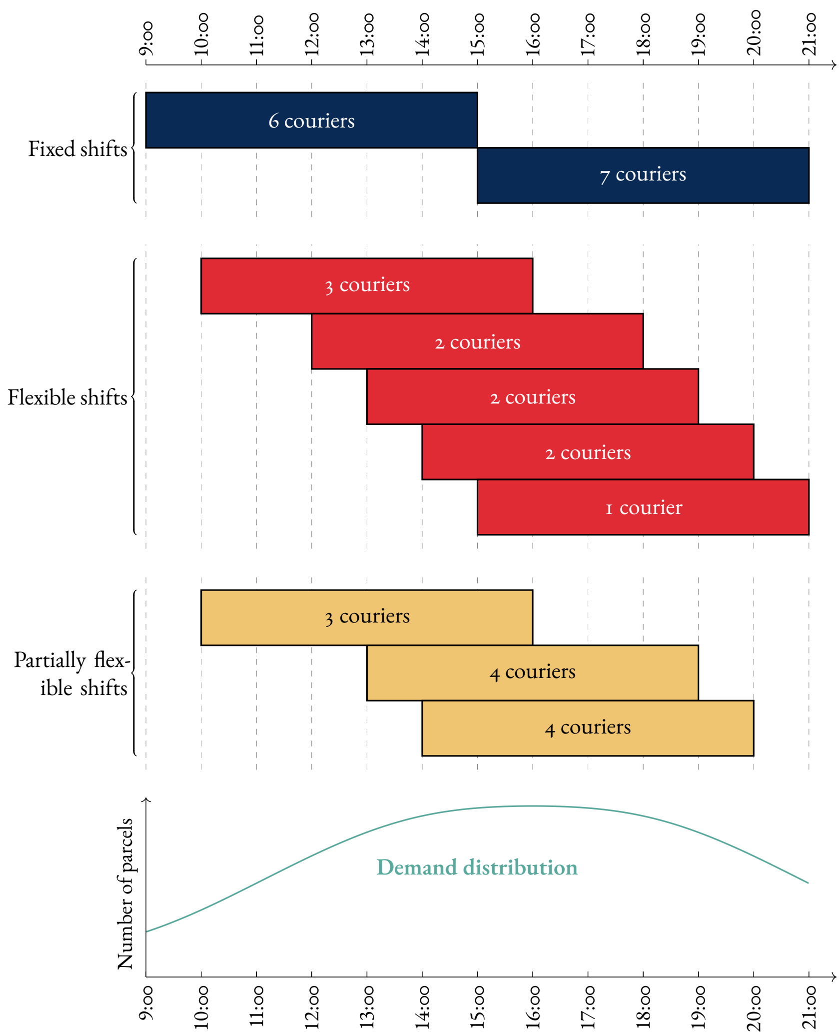

Figure 3.2: Example of fixed (blue), flexible (red), and partially flexible (yellow) shifts for a 12-hour working day. The demand distribution at the bottom shows that the afternoon is busier than the morning.

In the remainder of this section, we introduce the necessary notation, shift-type-specific variables, and constraints that we add to model MBase.

Fixed shifts

Let $\mathcal{P}$ be the set of shifts, i.e., a partition of Θ such that each shift $P \in \mathcal{P}$ is a contiguous set of periods. We denote with θ_P^s and θ_P^e the first and last periods of shift P.

We introduce new variables $y_{a_1 a_2 \theta} \in \mathbb{N}$ denoting the number of couriers moving from area a_1 to area a_2 between periods $\theta - 1$ and θ ($a_1 \neq a_2$, a_1 and a_2 belong to the same region, θ is not the first period of the day).

We add the following constraints to formulation (3.7a)–(3.7f) to model fixed shifts:

$$\sum_{a_2 \in R} y_{a_1 a_2 \theta} \leq x_{a_1 \theta} \qquad \forall R \in \mathcal{R},\ \forall a_1 \in R,\ \forall \theta \in \Theta \tag{3.8a}$$

$$\sum_{a \in R} x_{a\theta} = \sum_{a \in R} x_{a\theta_P^s} \qquad \forall R \in \mathcal{R},\ \forall P \in \mathcal{P},\ \forall \theta \in P \setminus \{\theta_P^s\} \tag{3.8b}$$

$$x_{a_1\theta} = x_{a_1,\theta-1} + \sum_{a_2 \in R \setminus \{a_1\}} y_{a_2 a_1 \theta} - \sum_{a_2 \in R \setminus \{a_1\}} y_{a_1 a_2 \theta}$$
$$\forall R \in \mathcal{R},\ \forall a_1 \in R,\ \forall P \in \mathcal{P},\ \forall \theta \in P \setminus \{\theta_P^s\}. \tag{3.8c}$$

Constraint (3.8a) ensures that no more couriers move away from each area a_1 than there are working in a_1. Constraint (3.8b) ensures that the number of employed couriers stays constant within each region for the duration of each shift, thus forbidding hiring or dismissing couriers in the middle of a shift. Constraint (3.8c) states that the number of couriers working in area a_1 during period θ is given by the number of couriers working in a_1 during the previous period, plus couriers who move into a_1, minus couriers who move out of a_1. We denote with Fixed the model obtained adding (3.8b)–(3.8c) to MBase.

Flexible shifts

To model flexible shift, we add to the already introduced x and y new variables $z^-_{a\theta} \in \mathbb{N}$, denoting the number of couriers starting their shift in area a at the beginning of period θ, and $z^+_{a\theta} \in \mathbb{N}$, denoting the number of couriers ending their shift in area a at the end of period θ.

Denoting with $\ell \in \mathbb{N}$ the shift length, we observe that variables $z^-_{a\theta}$ must be set to zero for all areas $a \in \mathcal{A}$ and for periods $\theta \in \Theta$ such that $\theta > |\Theta| - \ell$. Indeed, a shift has to start before $|\Theta| - \ell$ in order to satisfy shift duration ℓ. Analogously, variables $z^+_{a\theta}$ are set to zero for all areas $a \in \mathcal{A}$ and for periods $\theta \in \Theta$ such that $\theta < \ell$.

To obtain a model for the flexible shifts, we add constraint (3.8a) and the following constraints to formulation (3.7a)–(3.7f):

$$\sum_{a \in R} z^-_{a\theta} = \sum_{a \in R} z^+_{a,\theta+\ell-1} \qquad \forall R \in \mathcal{R},\ \forall \theta \in \Theta,\ \theta \leq |\Theta| - \ell + 1 \tag{3.9a}$$

$$\begin{aligned} x_{a_1\theta} = x_{a_1,\theta-1} &\\ + \sum_{a_2 \in R \setminus \{a_1\}} & y_{a_2 a_1 \theta} \\ - \sum_{a_2 \in R \setminus \{a_1\}} & y_{a_1 a_2 \theta} \\ + z^-_{a_1\theta} - z^+_{a_1,\theta-1} & \end{aligned} \qquad \forall R \in \mathcal{R},\ \forall a_1 \in R,\ \forall \theta \in \Theta,\ \theta > 1 \tag{3.9b}$$

$$x_{a1} = z^-_{a1} \qquad \forall a \in \mathcal{A}. \tag{3.9c}$$

Constraint (3.9a) makes sure that all couriers starting a shift at the beginning of period θ complete it at the end of period $\theta + \ell - 1$. Constraint (3.9b) extends (3.8c) by considering couriers who start or end their shift. Because (3.9b) is defined for $\theta > 1$, constraint (3.9c) addresses the special case of the beginning of the planning horizon, stating that all workers who start a shift during the first period are working in the respective areas. We denote with FLEX the model obtained by adding (3.9a)–(3.9c) to MBASE.

Partially flexible shifts

To model partially flexible shifts, we introduce variables $w_\theta \in \{0,1\}$ ($\theta \in \Theta, \theta \leq |\Theta| - \ell + 1$) taking value 1 iff a shift starts at the beginning of period θ. Let $\mu \in \mathbb{N}^+$ be the maximum number of shifts to create. A model for partially flexible shift uses constraints (3.9a)–(3.9c) together with the following inequalities:

$$\sum_{a \in R} z^-_{a\theta} \leq u_R \cdot w_\theta \qquad \forall R \in \mathcal{R},\ \forall \theta \in \Theta,\ \theta \leq |\Theta| - \ell + 1 \tag{3.10a}$$

$$\sum_{\theta=1}^{|\Theta|-\ell+1} w_\theta \leq \mu. \tag{3.10b}$$

Constraint (3.10a) links the z and w variables, allowing couriers to start their shift only when such a shift is created (value u_R acts as a "big-M" constant). Constraint (3.10b) limits the number of created shifts. We denote with PARTFLEX the model obtained by adding (3.9a)–(3.9c) and (3.10a)–(3.10b) to MBASE.

Dealing with symmetry

Models using variables $y_{a_1 a_2 \theta}$ suffer from symmetry. For example, increasing by one the value of both $y_{a_1 a_2 \theta}$ and $y_{a_2 a_1 \theta}$ yields a new solution with the same cost and corresponding to an unrealistic scenario (two couriers swapping areas without reason). To break this symmetry, we add to the objective function (3.7a) the following term:

$$\varepsilon \cdot \sum_{R\in\mathcal{R}} \sum_{a_1\in R} \sum_{a_2\in R\setminus\{a_1\}} \sum_{\theta\in\Theta} y_{a_1 a_2 \theta}, \tag{3.11}$$

where $\varepsilon > 0$ is a small constant. The term (3.11) penalizes unnecessarily large values of variables $y_{a_1 a_2 \theta}$ and prevents situations such as the one described above. In the above example, increasing by one the value of $y_{a_1 a_2 \theta}$ and $y_{a_2 a_1 \theta}$ would cause the objective function to increase by $2\varepsilon > 0$ making the resulting solution sub-optimal.

3.4 Results

In this section, we present the results of our computational experiments. First, we describe how we generated our instances based on realistic data from four large European cities. Second, we show that the optimization problems presented in Section 3.3 are fast to solve on commonly available computers, making them particularly suitable as decision support tools. Third, exploiting this computational efficiency, we perform a large experimental campaign aimed at deriving managerial insights and assessing the role of shift flexibility on the company's bottom line.

3.4.1 Instances

We generate instances based on Paris, Lyon (France), Berlin and Frankfurt (Germany). There are three main components to instance generation: the geographical subdivision of each city into regions and areas, the demand distribution, and the parameters related to couriers (costs, bounds on workforce size, shift lengths, etc). All parameters are summarised in Table 3.1.

Notation	Value(s)	Description
—	Berlin, Frankfurt, Lyon, Paris	City.
DB	0.5, 1, 2, 4	Number of parcels per 1000 inhabitants and day.
DT	Uniform, Peak, DoublePeak, AtEnd	Demand type.
OC	1.2, 1.5, 1.8, 2	Per-delivery outsourcing cost multiplier.
RM	0.75, 1, 1.5, 3, 5	Multiplier to determine the regional courier upper bound u_R.
GM	0.6, 0.7, 0.8, 0.9, 1	Multiplier to determine the global courier upper bound u.
μ	2, 3, 4	Maximum number of shifts for PartFlex.
—	16	Daily planning horizon in hours.
—	2	Period duration in hours.
k_a	0.77	Regression coefficient for VRP cost estimation.
Q	5	Courier capacity in number of parcels.
v	21	Courier speed in km/h.
τ	5	Courier service time in min.
$c_{a\theta}$	1	Courier labour cost per period.

Table 3.1: Instance generation parameters.

City geography

Each area in the cities corresponds to a postcode. We obtained the corresponding data under the Open Database License from OpenStreetMap (2023). Cities were subdivided into four regions, grouping areas to form compact groups of roughly equal population. We obtained population data from the EU's Global Human Settlement dataset (Schiavina et al., 2023). Figure 3.3 depicts the four cities and how they are divided into areas and regions. Paris has 20 areas, Lyon has 16, Berlin 59 and Frankfurt 32. Satellites are located around the centroids of the areas, ensuring that each satellite falls inside the area. The regression coefficient k_a of the cost approximation used in (3.5) is set to $0.77\ \forall a \in A$, as suggested by Figliozzi (2008) for areas with a central depot.

Demand distribution

Demand is proportional to area population via a Demand Baseline (DB) parameter expressed in the number of parcels per thousand inhabitants and day. When we generate an instance, the daily demand of each area is chosen uniformly at random in the interval $[0.75\text{DB}, 1.25\text{DB}]$. Once the total daily demand is determined, we distribute it among the periods making up the time horizon. Our instances use eight periods of two hours each for a daily planning horizon of 16 hours (6 AM to 10 PM). We consider four ways of assigning demand to each period based on a demand type parameter (DT). We describe them below and visualize them in Figure 3.4.

- For Uniform demand, we distribute the total number of parcels uniformly throughout the planning horizon. Although home deliveries rarely occur steadily throughout the day, we use this demand type as a baseline.
- Peak demand resembles the histogram of a truncated normal distribution with mean $|\Theta|/2$, standard deviation $|\Theta|/6$, left extreme 0 and right extreme $|\Theta|$. It corresponds to a peak in

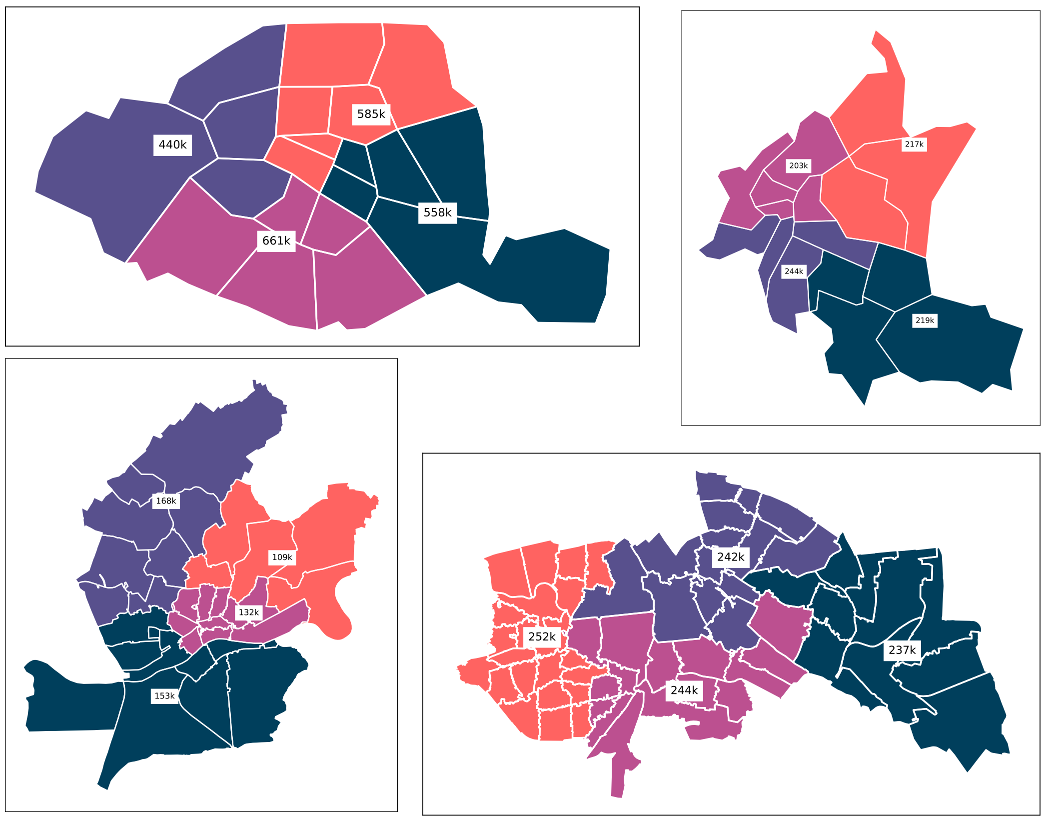

Figure 3.3: The four considered cities and their subdivision into areas (white boundaries) and regions (colored). The numbers indicate the number of people living in each region. Top left: Paris, top right: Lyon, bottom right: Frankfurt, bottom left: Berlin.

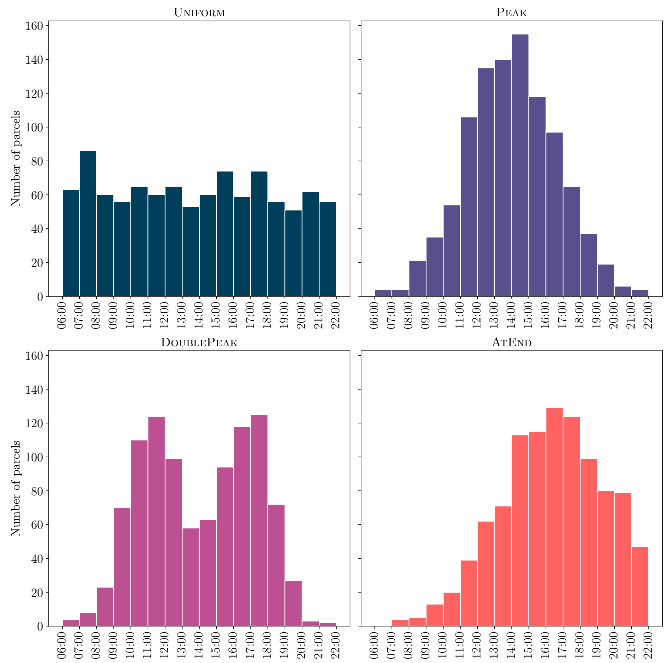

Figure 3.4: Example of hourly parcel demand according to each of the four demand types (DT) used in instance generation. The daily demand in the given area is 1000.

deliveries in the central hours of the day.

- DoublePeak demand follows the histogram of a mixture of two truncated normal distributions. They are similar to the distribution used for Peak demand, but their means are at $|\Theta|/3$ and $2|\Theta|/3$, and their standard deviation is $|\Theta|/10$. It simulates two peak hours: a morning one (around 11 AM) for workplace deliveries and an evening one (around 5 PM) for home deliveries.

- AtEnd is similar to Peak demand, but the mean of the truncated normal distribution is at $2|\Theta|/3$. This corresponds to a situation where most deliveries are made at people's homes at the end of the workday (around 5 PM).

Courier parameters

We consider a uniform fleet of bike couriers with capacity $Q = 5$ parcels and speed $v = 21$ km/h (Romanillos & Gutiérrez, 2020). We normalise the labour costs to $c_{a\theta} = 1\ \forall a \in \mathcal{A},\ \forall\theta \in \Theta$. If couriers travel at full capacity, i.e., carrying five parcels, the courier per-delivery cost is then 0.2. We obtain the per-delivery outsourcing cost C_{out} by multiplying this figure by a multiplier $\texttt{OC}$. For example, when $\texttt{OC} = 1.2$, we set $C_{\text{out}} = 0.2 \cdot 1.2 = 0.24$.

Recall that $\hat{m}^s_{a\theta}$, defined in Section 3.3.2, is the approximate number of couriers required to deliver all parcels in area a during period θ according to scenario s. Then, the average number of couriers required to deliver all parcels in a during θ across all scenarios is $\frac{1}{|S|}\sum_{s\in S}\hat{m}^s_{a\theta}$. Averaging over all periods, we obtain values $\hat{m}_a = \frac{1}{|\Theta|}\sum_{\theta\in\Theta}\hat{m}^s_{a\theta}$ and $\hat{m}_R = \sum_{a\in R}\hat{m}_a$ (for $R \in \mathcal{R}$). This is a rough approximation of the number of couriers per period required in each region to serve the entire demand. Especially for non-Uniform demand types, this average will not be a good approximation, and more couriers will be required during peak periods and fewer during valley periods. Indeed, we only use $\hat{m}_R$ as a baseline to choose parameters u_R and u, i.e., the per-region and global upper bounds on the number of couriers we can employ. We set the regional upper bounds as $u_R = \texttt{RM} \cdot \hat{m}_R$ and the global upper bound $u = \texttt{GM} \cdot \sum_{R\in\mathcal{R}} u_R$, where $\texttt{RM}$ and $\texttt{GM}$ are parameters. When $\texttt{GM}$ takes value 1, global bound u is moot, and only the regional bounds can be tight.

Instance availability

Varying the parameters introduced in this Section (city, DB, DT, OC, RM, GM), the model (MBase, Flex, PartFlex, Fixed) and, for model PartFlex, the value of μ, we obtain a large set of 8 000 instances and 48 000 experiments. We generate 90 scenarios per instance by repeatedly drawing from the relevant random distributions. Preliminary experiments, however, determined that reducing the number of scenarios to 30 does not significantly affect the quality of the cost approximation and, perhaps more

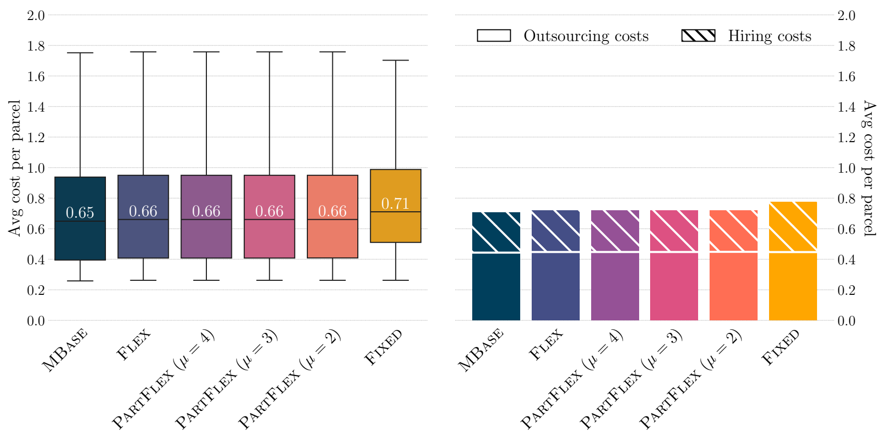

Figure 3.5: Cost per parcel vs. model. The left box plot summarises the cost distribution over all instances. The bar plot on the right shows the average over all instances and splits the cost into its hiring and outsourcing components.

importantly, the overall solution. We provide in repository (Mandal et al., 2024) the instances that we use in this study. The repository also includes the scripts used to generate the instances, the solver, and the scripts used to produce tables and figures.

3.4.2 Insights

We implemented the models in Python using Gurobi 9 as the MIP solver. Gurobi solves each instance in a fraction of a second, ranging from an average of 0.06s for model MBase to 0.13s for PartFlex with $\mu = 2$. This allowed us to run an extensive computational campaign on our large instance set and to draw the managerial insights described in the rest of this section. The main research question is to understand the impact of shift stability on the logistic provider in terms of costs and operational complexity.

High-level impact of flexibility on costs

The main high-level result about costs is depicted in Figure 3.5. The left figure shows the cost per parcel when using the different models. This cost is defined as the objective value of the optimal solution divided by the total number of parcels to deliver over all areas and periods. Each box represents the cost distribution over all the instances and, therefore, refers to 8000 observations. The central line in the box is the median; its value is also written inside the box. The top and bottom borders are the third and first quartiles, respectively. Whiskers extend to the rest of the distribution except for outliers, i.e., observations more extreme than twice the interquartile range. Because our hiring costs are normalized and both hiring and outsourcing costs can vary considerably in different markets, the reader should consider their relative differences rather than their absolute values.

The figure shows two important effects. On the one hand, using fixed shifts results in noticeably higher costs, justifying the assumption that some degree of flexibility is required in an industry with unsteady demand. On the other hand, the difference between the base model (workers can be hired and dismissed at each period), the flexible model (shifts can start at any period), and the partially flexible model (shifts can only start in μ different periods) is small. In particular, moving away from MBase causes a marginal increase in the median cost per parcel (from 0.65 to 0.66, i.e., $+1.54\%$) and the difference between the flexible and the partially flexible models is so small that the costs are identical up to the second decimal digit. Indeed, in the vast majority of the instances, the solutions obtained by Flex are identical to those obtained, e.g., by PartFlex ($\mu = 3$). This observation supports the conclusion that limiting shift instability is a viable strategy that can reconcile the company's bottom line with the workers' well-being.

The right plot in Figure 3.5 also refers to the costs per parcel. The height of each bar corresponds to the average cost over all instances, which we split into its hiring and outsourcing components. As we will see in the following, the ratio of each component in the total costs depends on many factors, the main one being the unit outsourcing cost. This is an exogenous market characteristic, and, in our instances, we only assume that outsourcing a delivery is more expensive than performing it in-house. We control the unit outsourcing cost more precisely through parameter `OC`. Because, in this plot, each

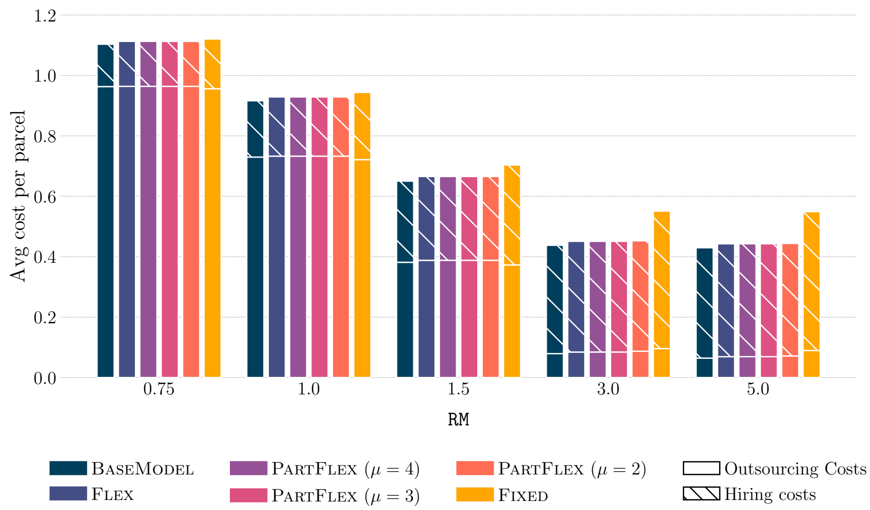

Figure 3.6: Impact of the RM parameter on the cost per parcel.

bar shows the average over all instances, we cannot appreciate the impact of OC. Still, this figure shows that—even in aggregate—using fixed shifts results in sensibly higher hiring costs compared with the other models. When scheduling flexibility is very limited, optimal solutions use a larger workforce and incur higher hiring costs but do not significantly differ in terms of outsourcing costs.

Detailed cost analysis

In the following, we evaluate the effect of the instance parameters that most impact the cost structure of the logistic provider.

Figure 3.6 shows how the costs change with the regional bound parameter RM. Recall that this bound limits the workforce size at a regional level and models external constraints, such as the fleet size, that prevent a decision-maker from hiring too many couriers. As expected, relaxing this bound results in lower costs, and the cost decrease is significant. Therefore, decision-makers who find themselves bound by fleet capacity should look into mid or long-term fleet expansion rather than consistently relying on outsourcing.

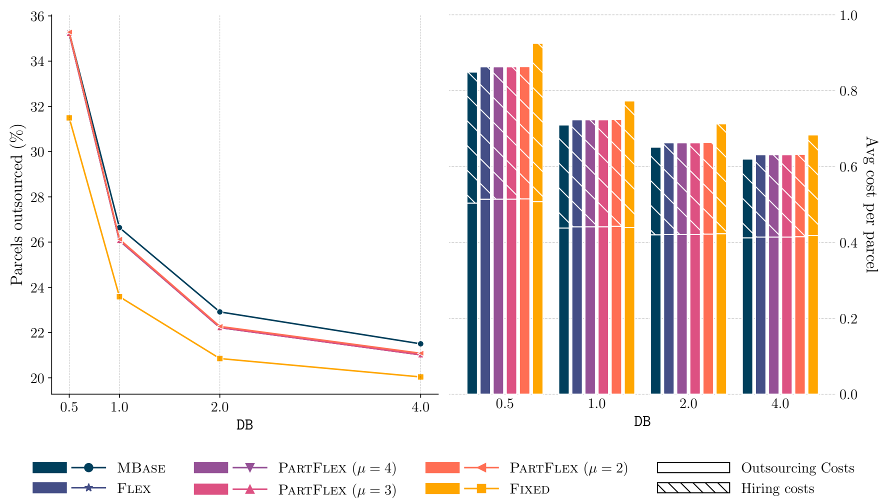

Figure 3.7: Impact of the DB parameter on the number of outsourced parcels and costs.

We also remark that the cost structure also changes when RM changes. When the bound is lax (high RM), Fixed gives relatively larger costs compared to the other models. When the bound is tight (low RM), on the contrary, the cost per parcel is high but similar for all the models. A tight bound means that the operator is subject to structural constraints such as a small fleet or a workforce shortage (i.e., it is understaffed) that are commonly associated with tight or even negative profit margins. Contrary to common intuition, such an operator would not get a large advantage by moving to more flexible schedules; instead, it would compound burnout from understaffing and overwork with decreased job quality due to shift instability. The relationship between overwork, instability, burnout, and mental health has been studied in the medical and social science literature, especially in relation to nurses, doctors, and healthcare workers. These categories have been historically known to be subject to long and intense work hours, demanding both on the physical and emotional levels. Still, the results shown in Figure 3.6 suggest that future studies should not neglect LMD workers and, indeed, some recent research has started to focus on these categories (see, e.g., Pyo et al., 2023; Wei et al., 2023; Couve et al., 2023).

Figure 3.7 shows the impact of the baseline demand parameter DB. The left figure reports the percentage of outsourced parcels, and the right one gives a breakdown of the costs. When demand is low, optimal solutions tend to use outsourcing more (left figure). In this scenario, in fact, a large workforce would be idle for a considerable portion of the time, and outsourcing becomes a more attractive option. This consideration holds for all models, including MBase. When demand grows, the logistic operator outsources fewer deliveries, up to the point when the capacity of the in-house delivery system is reached and the curves in the left figure start flattening. The Fixed model tends to keep a large workforce and, therefore, requires less outsourcing compared to the other models.

The right figure supports three main points. First, as in most other businesses, LMD shows economies of scale, and the cost per parcel decreases when the volume increases. Second, these efficiency gains incur diminishing returns; e.g., doubling DB from 0.5 from 1 produces a larger cost decrease than doubling from 2 to 4. Third, the difference in costs is usually larger between instances with different values of DB than it is between models for a given value of DB. Model Fixed displays higher costs per parcel even for larger volumes (for example, Fixed's costs when $\texttt{DB} = 4$ are higher than MBase's costs when $\texttt{DB} = 2$), but this is the exception rather than the norm. The other models tend to have more similar costs, hinting at the fact that increasing flexibility can only partially mitigate underlying problems such as low demand.

The impact of the outsourcing costs, controlled by parameter OC, is reported in Figure 3.8. The higher the costs, the lower the number of outsourced parcels; the left plot in the figure, however, shows that the relation is not linear. Although the effect is less pronounced than in Figure 3.7, we see that the curves representing the percentage of outsourced parcels tend to flatten when reaching the limit of parcels that in-house couriers can deliver. The right figure shows that increasing the outsourcing costs causes a slight increase in the hiring costs (because it is convenient to employ more in-house couriers) and a large increase in the outsourcing costs.

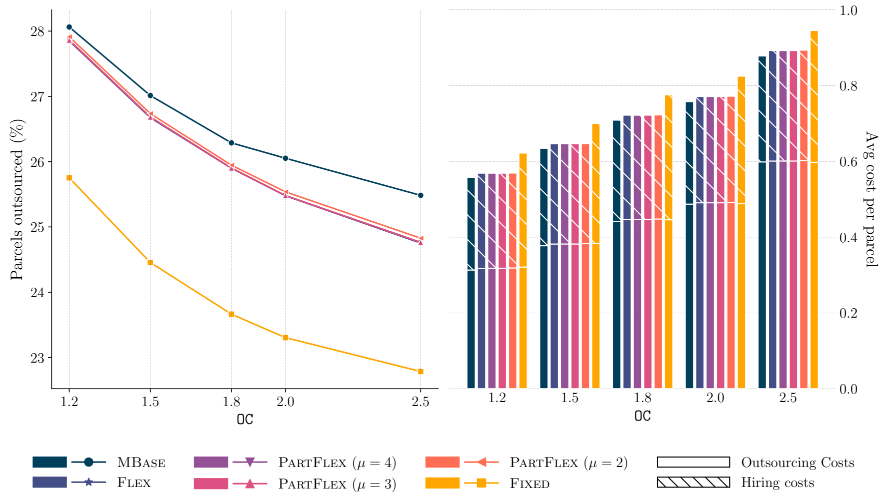

Figure 3.8: Impact of the OC parameter on the number of outsourced parcels and costs.

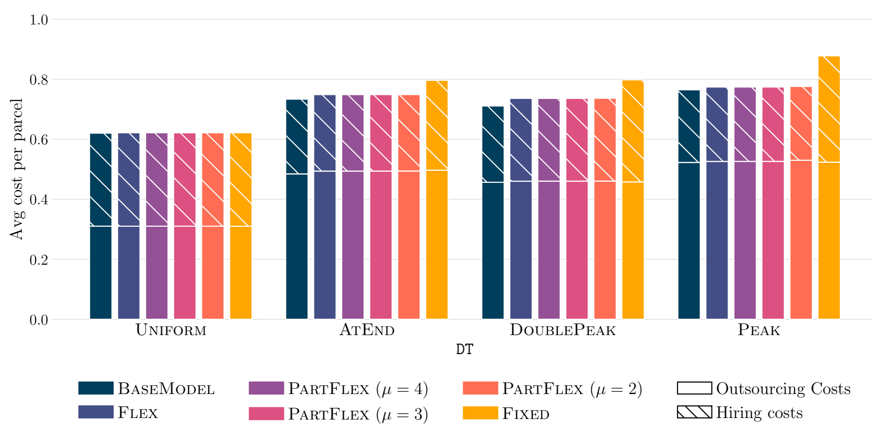

Figure 3.9: Impact of the DT parameter on the costs.

Finally, in Figure 3.9, we focus on the impact of the demand type (parameter DT) on the costs. When the demand is Uniform, costs are low, no flexibility is required, and all models yield roughly the same costs. Furthermore, in a uniform demand scenario, the optimal number of couriers to hire does not change with the period. Therefore, the problem reduces to find *the* best workforce size. This scenario is similar to the classical newsvendor problem: the workforce size is analogous to the order quantity, the number of couriers required to deliver all parcels is the stochastic demand, and the cost difference between outsourcing and in-house delivery is the opportunity cost. Indeed, the cost structure shown in Figure 3.9 also shows a remarkable similarity with the optimal newsvendor solution: optimal solutions are characterised by equal outsourcing and staffing costs, i.e., the solid and the hatched bars have the same height.

The more challenging demand type is Peak, i.e., when the highest parcel volume occurs in the middle of the day. Model Fixed uses two shifts dividing the daily planning horizon into two halves and, as a result, is the least suitable to deal with this demand pattern. Still, we remark that the cost difference between the three types, AtEnd, DoublePeak, and Peak, is small and that the cost structure is similar. These facts suggest that the conclusions that we draw in this analysis are valid for a diverse range of demand types and could be generalized beyond the patterns that we study in this paper.

Impact of flexibility on operations

In this section, we study the impact that the instance generation parameters and the different models have on key indicators of the company's operational practices. The first indicator, which we already presented in Figures 3.7 and 3.8, is the percentage of outsourced parcels. The second is the number of couriers hired as a percentage of the global limit u. The third is the percentage of couriers who change area at the end of each period. This last indicator is used as a proxy of the operational complexity and is related to the geographical stability concept discussed in Section 3.2.3.

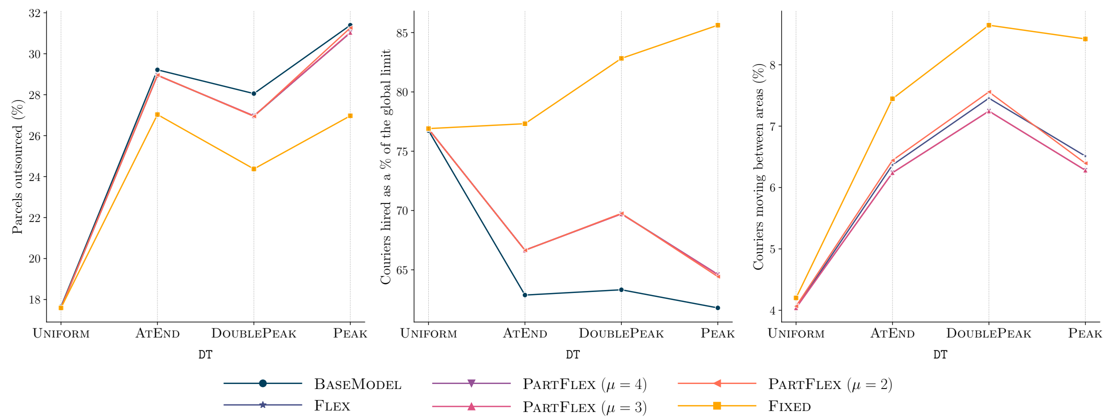

Figure 3.10: Impact of the DT parameter on three company operations metrics.

Figure 3.10 shows the impact of the demand type on the three metrics mentioned above. When the demand is Uniform, as we have seen for the costs, all models show similar characteristics. For the other demand types, however, there are considerable differences. When using Fixed shifts, the percentage of employed couriers increases with non-Uniform demand types. The Flex and PartFlex models, on the other hand, can take advantage of the fact that demand concentrates during some periods of the day (and is much lower during the other periods) and require hiring overall fewer couriers. In particular, the Flex model keeps the number of hired couriers significantly lower compared with the PartFlex models.

In general, all models only require a modest amount of area changes; in this respect, demand type DoublePeak is the most demanding. Still, this metric should be considered with care because, in our instance generation procedure, the number of parcels to deliver in each area is only proportional to its population. Logistic operators might have access to more detailed data, which could exacerbate the demand difference between areas. For example, residential areas might require more deliveries in the late afternoon, while commercial areas could have a higher demand during the mornings.

This figure also shows that the Fixed model is an outlier that not only yields higher costs but

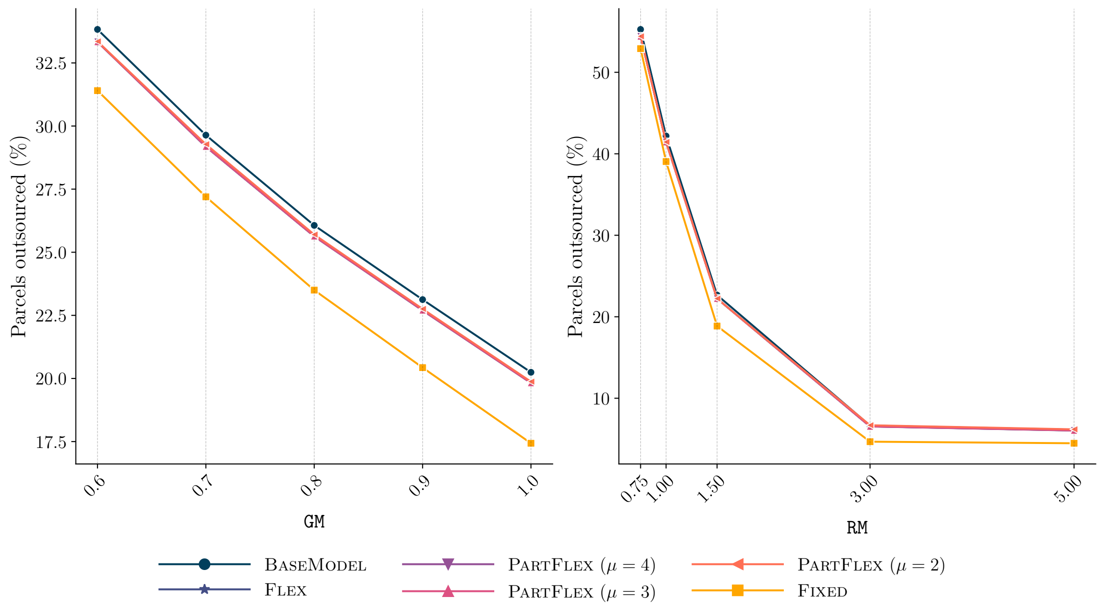

Figure 3.11: Impact of the GM and RM parameters on the number of outsourced parcels.

also requires significantly different operational choices. On the other hand, the Flex and PartFlex models are not too dissimilar, especially when considering the number of parcels outsourced and the area movements required.

Figure 3.11 reports the percentage of outsourced parcels as a function of the global (left) and regional (right) multipliers of the workforce size upper bounds. First, we note that the two multipliers impact this metric differently. The parameter GM decreases the number of outsourced parcels almost linearly, while the relationship between parameter RM and the number of outsourced parcels is non-linear. Furthermore, even when the bounds are large, the optimal amount of outsourcing is strictly positive (around 20% for the highest value of GM and around 7% for the highest value of RM). Indeed, we repeated our computational experiments by completely removing constraints (3.7b) and (3.7c), and we found that the average percentage of outsourced parcels ranged between 4.48% for Fixed and 6.18% for PartFlex ($\mu = 2$). This shows that outsourcing can be economically convenient to bal-

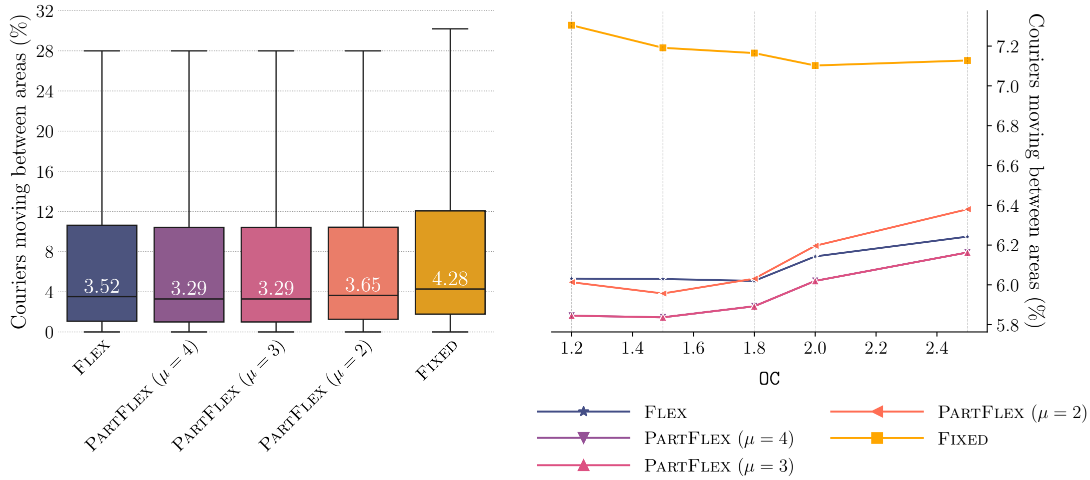

Figure 3.12: Impact of the model and outsourcing costs (OC) on the average number of couriers changing areas at the end of each period. *Note:* the right and the left plot have different y-axis limits.

ance fixed and variable costs, even when there is no tight bound on the workforce size.

Finally, Figure 3.12 shows how the model and the outsourcing costs affect the couriers' mobility between areas at each period. We do not report results relative to model MBase because it does not include the y variables, which are necessary to keep track of courier movements between areas. The distribution of this indicator is skewed and shows large right tails: whereas the medians are all low and similar to each other, the left figure shows that a part of the distribution reaches values of over 25%. The right figure, which is on a different scale compared to the left one, further shows that the means exhibit a larger variation, with model Fixed requiring more courier movement compared to the other models, outlining a trade-off between temporal and geographical stability. Furthermore, when outsourcing is more expensive, in the majority of cases, the company responds by increasing the geographical mobility to better adapt to the demand and outsource less. The Fixed model is an exception in this respect because when OC is high, this model uses a larger workforce that is sometimes idle and requires less repositioning. On the other hand, models that use the courier workforce more also need more movement between areas.

3.4.3 Robustness to changes in demand types

At the operational level, the demand distribution (identified by the parameter DT in our instances) can change on specific days. For example, different patterns can be observed during weekdays and weekends, or during the holiday season. If these differences are predictable, a decision-maker can solve an instance of our problem per each expected demand pattern. Operational decisions, such as rostering, can help reconcile the different solutions. For example, if the weekday problem requires 20 couriers and the weekend one only requires 10, the couriers' roster can exploit this difference to schedule appropriate weekly rest days.

If the variations in demand patterns are more unpredictable, the logistic operator will sometimes have to use a strategic solution devised for a given demand type with a different realized demand type. In this section, we investigate how robust solutions are to changes of the DT parameter. More precisely, we want to estimate how much efficiency a decision-maker would lose if they sized and scheduled their workforce for a given value of DT, but then a different demand type was realized.

To answer this question, we ran the following experiment. For each combination of parameters, we fix the corresponding solution, and we evaluate its cost on instances with the same parameters—city, DB, OC, RM and GM—but different demand type DT. We do so by fixing variables x_{at} to the value they take in the optimal solution of an instance with a given demand type $\mathtt{DT}_1$, and, keeping these variables fixed, we re-solve the models on instances with different demand types $\mathtt{DT}_2 \neq \mathtt{DT}_1$.

Figure 3.13 reports the results of this experiment. The figure shows a heatmap for each of the six models. The value $\mathtt{DT}_1$ used to fix variables x_{at} is on the x-axis, and the value $\mathtt{DT}_2$ used to evaluate the solution cost is on the y-axis. The values reported in the heatmap are the average percent cost increases over all instances sharing the same values for parameters city, DB, OC, RM, and GM. For example, the value corresponding to Peak on the x-axis and AtEnd on the y-axis reports the average cost in-

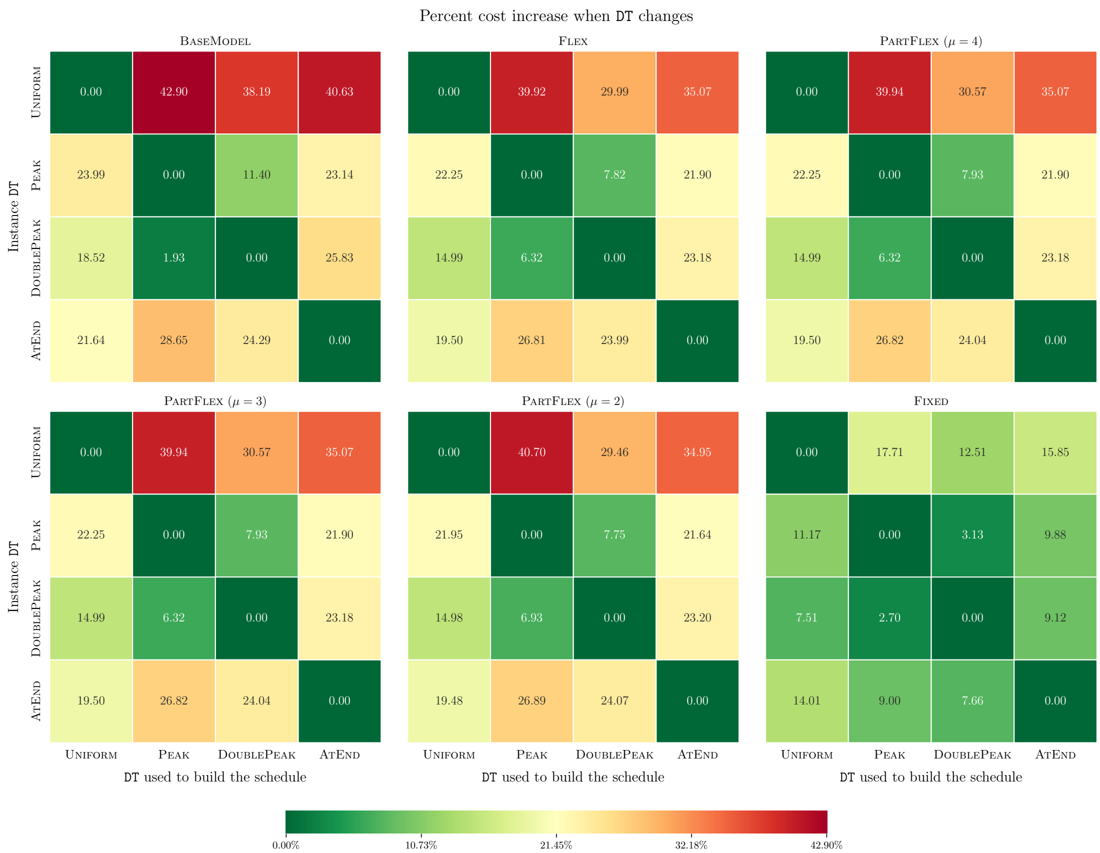

Figure 3.13: Impact of changing the demand type of an instance (parameter DT) on the cost of solutions obtained optimising for a different demand type.

crease incurred when using a solution devised for the Peak demand type, when the actual demand distribution follows the AtEnd pattern and all other instance generation parameters are the same.

Figure 3.13 prompts the following observations. On the one hand, when the realized demand is Uniform, solutions obtained according to other demand types are particularly ineffective (first row of each heatmap). Indeed, for a given area, any solution deploying couriers in a pattern that deviates from a constant value throughout the day is inefficient because demand is constant throughout the day. On the other hand, Peak and DoublePeak cause the smallest cost increases when the realised demand is one of these DTs and the solution was obtained using the other. Furthermore, and most important for our analysis, we remark that the average percent cost increases for the Fixed model are generally the lowest. (The only exception is when using a solution for Peak on a DoublePeak realised demand, in which case the BaseModel shows a smaller cost increase.) In other words, using completely fixed shifts is more expensive but more resilient to changes in demand patterns. The excess courier capacity that is usually present in the solutions of the Fixed model (see the central plot in Figure 3.10) acts as a buffer that helps deal with demand changes.

The above analysis relies on the assumption that the solution devised for a given value of DT must be used without modifications when the realized DT is different. In practical circumstances, the decision-maker might deviate, on the operational level, from the strategic problem solution. For example, by using overtime, they might increase the number of couriers working during some periods. In this case, couriers might be subject to sudden roster variation, a practice that negatively affects their work-life balance. While the impact of deviating from the schedule on workers' well-being is clear, it is less clear whether these deviations help reduce costs. To answer this question, we conducted a small case study based on the demand pattern variation that seems most challenging for all models, i.e., using a solution devised for DT Peak when the realized DT is Uniform. In the case study, we allow the value of variables x_{at} to deviate by at most $\delta \in \{0, \ldots, 3\}$ from the value taken in the optimal solution

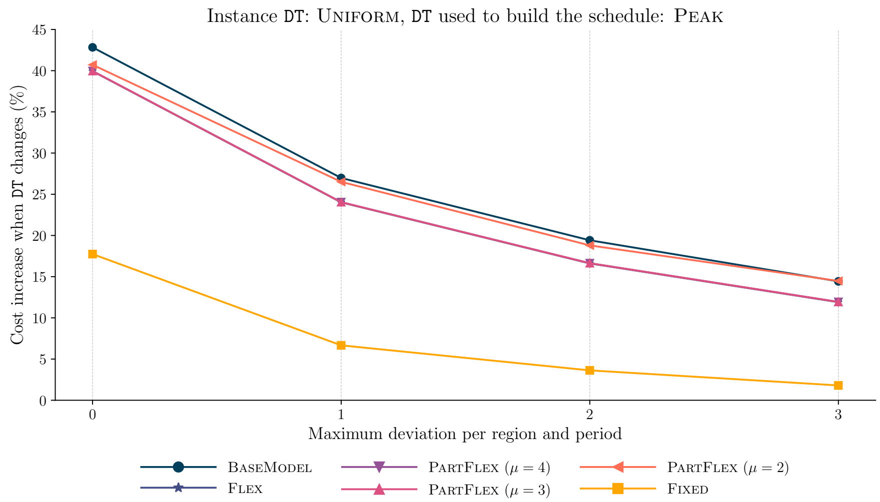

Figure 3.14: Impact of allowing more flexibility to adjust a predetermined solution when the demand type DT changes at the operational level. In this case study, the operational DT is Uniform and the DT used to obtain the solution is Peak.

for DT = PEAK. When $\partial = 0$, the decision maker is not allowed to deviate from the solution, and we recover the case studied in Figure 3.13. For $\partial > 0$, we allow the decision maker to deploy more or fewer couriers in each area and period, up to a difference of $\pm\partial$. Figure 3.14 shows the results of this experiment. Whereas allowing more deviations reduces costs, the FIXED model remains the most competitive in terms of resiliency. Furthermore, the most flexible models (BASEMODEL and FLEX) with an allowed deviation of $\partial = 3$ produce cost increases barely smaller than the FIXED model with $\partial = 0$. And when $\partial = 2$, all other models increase the costs more than the FIXED model with $\partial = 0$.

3.5 Conclusions

In this paper, we have tackled the problem of tactical hiring and scheduling decisions for a company performing parcel deliveries in the last-mile segment of the supply chain. In particular, we have developed mathematical models to determine the correct number of couriers to hire to balance salary costs and outsourcing costs. These latter are paid when the company does not hire enough couriers to deliver all parcels. We have placed particular emphasis on shift stability, i.e., devising shifts with a predictable start time and duration. In doing so, we wanted to explore if flexible shifts, which decrease job satisfaction and disrupt the couriers' work-life balance, are justified by large savings. Our main conclusions are the following:

- Using completely fixed shifts that start at two predetermined times during the day results in significantly higher costs. Overall instances, the average per-parcel cost obtained using fixed shifts is 9.36% higher than the one obtained using extremely flexible schedules, in which couriers can be called into (and out of) at each two-hour period.

- A partially flexible model (PartFlex) that uses two shifts—but allows their start times to be a decision variable—incurs costs that are only 1.89% higher than those obtained with extremely flexible schedules.

- The advantage of flexible schedules compared to fixed ones is more significant when the company can hire a large workforce and has a large fleet. When the company cannot hire many couriers (because it does not have enough vehicles to operate or because market conditions make labor scarce), flexible and fixed schedules yield almost the same costs. The conclusion is that stable shifts are a viable strategy for a company that has trouble finding couriers. Stable shifts do not significantly increase costs, and they provide better working conditions that help attract potential employees.

- As in many industries, we observed economies of scale. When the volume increases, the cost per parcel decreases, although with diminishing returns.

- Predictable demand patterns, such as having one or two daily peak times, do not have a large impact on the total costs, but they significantly change some aspects of the company's operations. For example, instances with two daily peaks require more couriers and more courier movements between geographical areas, compared with instances with a single peak (either in the central or the later part of the day).

- When demand patterns are less predictable, the logistic operator will have to use a schedule optimized for a given pattern in days when the realized pattern is different. Solutions featuring stable shifts are particularly suitable in this case and provide the smallest cost increases. In other words, stable shifts are generally more expensive to implement but are also more resilient to sudden changes in demand patterns.

We conclude by remarking that our work relies on a number of assumptions and that our conclusions are based on computational results over synthetic instances. At the same time, we tested our approach on a variety of instance generation parameters, and we observed significant results consistently over a large number of instances. This suggests that a compromise approach that features limited schedule flexibility deserves further analysis, especially from larger logistic providers using scientific management approaches to optimize their tactical and operational planning decisions.

4

Robust Facility Location in Disaster Preparation for Earthquakes with Aftershocks

joint work with **Laurent Alfandari** and **Ivana Ljubić**

4.1 Introduction

During the early hours of February 6, 2023, regions of Turkey and Syria were struck by a devastating earthquake. The earthquake had a magnitude of 7.8 on the Richter scale, and its epicenter lay near the Turkish region of Kahramanmaras. About 9 hours later, at 13:24 local time, another deadly earthquake of magnitude 7.5 hit the region, around 95 kilometers northeast of the initial earthquake. Moreover, an earthquake of magnitude of 6.4 occurred on February 20 and resulted in the death of 3 people and injured 213. Another 5.6 magnitude earthquake on February 27th caused further destruction when damaged buildings collapsed (CDP, 2024). The series of earthquakes killed over 56,000 people and injured over 100,000 (Ahmed et al., 2023). CDP (2024) also reports damage to more than 230,000 buildings and resulted in economic losses of over $34.2 billion. Not only that, according to the United Nations (UN), Syria was already undergoing a humanitarian crisis, and the earthquakes exacerbated the condition.

The Turkish government and the United Nations (UN), along with its agencies, have provided massive emergency relief support for the affected people (Reliefweb, 2024). The UN deployed disaster assessment experts, coordinated search and rescue, and provided relief materials like food, medical supplies, and blankets, among others (UN, 2023). The World Health Organization (WHO) and World Food Programme (WFP) also extended the support by providing health supplies and food assistance (UN, 2023). An article by Thippa et al. (2023) mentions that several buildings in Turkey were constructed to withstand a single earthquake, but not multiple of them, resulting in losses to human lives and infrastructure. Thus, poor infrastructure and a lack of preparedness aggravated the situation. The earthquakes in Turkey and the devastation that followed highlight the need for improved disaster preparedness, not just in Turkey and Syria but also in other earthquake-prone countries.

A crucial factor to consider in the earthquake preparedness phase is aftershocks. Aftershocks are smaller earthquakes that occur after a larger earthquake and can continue for days, weeks, and sometimes even months after the larger earthquake. They may vary in magnitude as well as frequency. Though they are typically of a smaller scale, aftershocks can cause additional damage to already weakened buildings and infrastructure. They could also trigger tsunamis, avalanches, floods, landslides, fires, and disasters in chemical, industrial, or nuclear firms. Sometimes, the aftershocks themselves are as severe as the main earthquake.

One of the most notable examples of the impact of aftershocks was the 2011 Tohoku earthquake in Japan. The initial earthquake, with a magnitude of 9.0, also triggered a massive tsunami. Following the earthquake, there were over several aftershocks, including a magnitude 7.1 aftershock. The tsunami resulted in a meltdown of three nuclear reactors in the Fukushima Daiichi Nuclear Power Plant, displacing thousands due to the release of radioactive materials (Ishigaki et al., 2013). Nepal was also struck by a devastating earthquake in 2015, with a magnitude of 7.8, and the epicenter lay in the Gorkha district of Nepal. The earthquake was followed by two large aftershocks of magnitudes 6.6 and 6.7 within 24 hours of the main earthquake and was succeeded by several other aftershocks of smaller magnitudes. Another aftershock of magnitude 7.3 hit the country on May 12, causing further damage. The earthquakes also triggered landslides and avalanches (Rafferty, 2023). The earthquakes caused the deaths of approximately 9000 people, injured over 22,000, and about 8 million people were affected (Rafferty, 2023; Reid, 2018). Over 600,000 homes were destroyed and over 288,000 damaged (Reid, 2018). Thus, it is critical to take aftershocks into consideration in the preparedness phase for earthquakes.

In our study, we focus on the preparedness phase of a disaster management system and primarily focus on earthquakes. We consider a robust facility location problem for pre-positioning relief materials near a region prone to earthquakes. Robust optimization is key to studying problems in disaster management because of the lack of availability of data, the unpredictability of the disasters, and the importance of solutions to remain valid in a variety of scenarios (Starr & Van Wassenhove, 2014). In this paper, we study a two-stage problem. In the first stage, the area is affected by the first earthquake whose location is naturally unknown. Most earthquakes are followed by several aftershocks, which we consider the second stage of the problem. The aftershocks can either be earthquakes of magnitude comparable to the first earthquake or earthquakes of smaller magnitudes. This results in deaths, injuries, and thousands of displaced people, who have limited to no access to basic human amenities like food, water, medicines, blankets, etc., for several days. The decision-maker wants to set up facilities to store relief materials that can be used to help these people in need and serve the entire demand caused by such emergencies. Our objective is to determine the location for these facilities so that the worst-case allocation cost for the major earthquake and the aftershocks (proportional to the travel time and demand) is minimized in the event of such a disaster.

The contributions of the paper are the following.

- We propose a robust facility location model for relief material prepositioning for earthquakes and aftershocks. To this end, we propose a novel uncertainty set where the locations of the aftershocks are unknown, with at most Δ aftershocks. This gives rise to a discrete uncertainty set, where Δ aftershocks are selected (from a larger discrete set of possible aftershock realizations), which gives rise to the worst-case demand realization.

- We use mixed-integer programming (MIP) to model the problem. Since the complete model is computationally challenging, we provide three different exact approaches to solve them, two of which are based on branch-and-cut.

- We implement our models on simulated instances and provide a case study on the eastern region of Turkey that was affected by the earthquakes in 2023.

- We find that including aftershocks in our study indeed has an impact on the location decisions with reduced travel times between the facilities and the demand nodes. We also identify four districts in Turkey to set up relief warehouses in the event of such disasters.

The rest of the paper is structured as follows. In the following section, we briefly review the literature pertaining to our study. Section 4.3 describes the problem in detail, and Sections 4.4, 4.5, and 4.6 provide different formulations and solution methods for the same. In Section 4.7, we implement our models on synthetically generated instances as well as provide a case study on the country of Turkey focusing on the 2023 earthquakes. Finally, we conclude our paper in Section 4.9 and provide some directions for future research work.

4.2 Literature review

In this section, we briefly review the literature related to facility location for disaster management and robust optimization. While the literature is quite extensive, we restrict ourselves for the sake of conciseness and scope. Nevertheless, we point the readers to several extensive literature reviews on the topic. For example, see Dönmez et al. (2021) for a review on humanitarian facility location under uncertainty, Amideo et al. (2019) for the location of shelters and evacuation planning, Kaveh et al. (2020) for emergency management systems for earthquakes using optimization methods, Alturki & Lee (2023) for multicriteria models in humanitarian logistics, Adsanver et al. (2023) for approaches for improving coordination, cooperation, and collaboration for humanitarian supply chains using conceptual, empirical, and analytical methods, Gabrel et al. (2014) for a review on robust optimization.

4.2.1 Facility location and disaster management

A quick survey of the literature shows locating various kinds of facilities, both in the pre- and post-disaster phases. Examples include warehouses (Chen et al., 2016; Stienen et al., 2021), distribution centers (DCs) (Paul & MacDonald, 2016; Paul & Wang, 2019; Haghi et al., 2017; Zokaee et al., 2016), shelter sites or evacuation points (EPs) (Chang et al., 2024b; Aghaie & Karimi, 2022), casualty collection points (CCPs) (Alizadeh et al., 2019), mobile facilities like hospitals (Acar & Kaya, 2019) or medical relief centers (Gu et al., 2018; Haghi et al., 2017) or temporary care centers (Sheikholeslami & Zarrinpoor, 2023; Aydin & Cetinkale, 2023), among others. Several works consider more than one kind of facility to be located. For example, Haghi et al. (2017) consider locating DCs and health centers simultaneously to increase the quality of service. Some studies also look at multi-level facility location. For example, Tofighi et al. (2016) study a two-echelon network design model with central warehouses in the first echelon and local DCs (LDCs) in the second. Vahdani et al. (2018) also look at multi-level facility location with warehouses and DCs. Chang et al. (2024a) also consider two levels of facilities, viz., DCs and local relief centers. Khalili-Fard et al. (2024) incorporate a core warehouse (CW) along with local warehouses (LWs) and provisional warehouses. Prepositioned inventory is transported from the CW to the affected areas via LWs, while relief from non-governmental organizations (NGOs) is transported to the affected areas via PWs.

Location decisions are often accompanied by capacity decisions of the facilities, for example, see Paul & MacDonald (2016). Balcik & Beamon (2008) study facility location along with prepositioning of relief materials. Since location and allocation decisions go hand in hand, most papers incorporate allocation decisions along with location decisions (Paul & MacDonald, 2016; Dönmez et al., 2021; Ghasemi & Khalili-Damghani, 2021; Chang et al., 2024b). Ghasemi & Khalili-Damghani (2021) study optimal inventory levels in the warehouses along with location-allocation decisions of suppliers and DCs. Some studies also study routing along with location decisions. Aghaie & Karimi (2022) study the location of temporary shelters, allocating people to them, and routing people from the affected areas to the shelters. Vahdani et al. (2018) study location, inventory stocking, and routing decisions in a two-stage problem. In the first stage, strategic decisions like warehouses and DC locations, their capacities, and inventory levels are made. The second stage incorporates operational decision-making with routing and distribution of critical items to the affected areas, taking into account time windows. Rezaei-Malek et al. (2016) design relief network with optimal location-allocation and distribution decisions as well as inventory stocking and renewing decisions related to perishable commodities. The authors consider aspects like pre-positioning amount, purchase and sale costs, and removal and movement costs for the perishable commodities. Chang et al. (2024a) study a two-stage model with the location of DCs and allocation of vehicles to the DCs for relief distribution in the first stage and vehicle and inventory routing decisions in the second stage. Monroy & Díaz (2021) study multi-level facility locations, including regional rescue centers (RRC) and local rescue centers (LRC), with inventories in the RRC, along with routing decisions between RRCs and LRCs, and between LRCs and affected areas. Khalili-Fard et al. (2024) provide a comprehensive model incorporating decisions like location-allocation, inventory prepositioning and procurement (they consider perishable, non-perishable, and shelf-stable commodities simultaneously), supplier selection, fleet-sizing, supply contract, distribution, and transportation. Their study collaboration between non-governmental organizations and governmental organizations for their relief network. Additionally, their model incorporates contracts with backup suppliers to prevent a potential shortage of relief items in the post-disaster phase. Stienen et al. (2021) study not only the optimal location and number of facilities (or depots) but also potential locations if the number of facilities is expanded. Finally, several studies also incorporate repositioning decisions coupled with location. For example, Acar & Kaya (2019) study locating mobile hospitals, where there is a provision for relocating the above hospitals in the post-disaster phase.

More often than not, social objectives exceed financial objectives in humanitarian logistic problems because the cost of saving lives far outweighs the financial cost minimization. Paul & MacDonald (2016) use an objective function incorporating fatality costs, supply costs, and DC location costs.

Zokaee et al. (2016)'s objective function includes the cost of locating DCs, the cost of transferring relief materials from the supplier to the DCs, and from the DCs to the affected areas, along with the cost of shortages. Ghasemi & Khalili-Damghani (2021) also uses a similar objective function, which minimizes the cost of establishing suppliers and DCs, the cost of storing inventory, and the cost of shortage in the distribution centers.

Due to the multi-faceted goal of designing humanitarian logistics networks, several studies incorporate multi-objective models. For example, Chang et al. (2024b) consider four different kinds of costs in their objective function: the cost of opening shelters, a deprivation cost component, the cost of trapped evacuees, and the cost of exceeding shelter capacities. Haghi et al. (2017) study a multi-objective model that maximizes the response level for the medical needs of the casualties while minimizing the total cost of the preparedness and response phases. Tofighi et al. (2016) study a two-stage model where the operating costs and inventory costs of the warehouses and the LDCs are minimized in the first stage, whereas the second stage is a multi-objective model minimizing the total distribution times, the maximum weighted travel time between the warehouses and LDCs, the total cost of unused inventories, and the weighted shortage cost of unmet demands. The multi-objective model presented in Vahdani et al. (2018) is also similar in the sense that they minimize the cost of establishing the warehouses and DCs and the cost of storing inventory in them in the first stage, while the second stage objective function incorporates minimizing travel costs between facilities and affected areas and between affected areas, minimizing vehicle travel times, and maximizing the reliability of routes traveled by the vehicles. Sheikholeslami & Zarrinpoor (2023) propose a bi-objective model where the primary objective is targeted towards reducing total network cost (facility location, procurement, holding, transportation, and penalty for storing of surplus commodities and their shortages and penalty cost allocated for the sum of injuries that are not placed in care centers) and the second objective maximizes the total coverage of the network. Rezaei-Malek et al. (2016) also formulate a bi-objective model that minimizes average weighted response times, along with the total operational cost (for the handling of perishable commodities) in the pre-disaster phase and the penalty costs of unmet demand and unused commodities at a post-disaster phase. Khalili-Fard et al. (2024)'s model seeks to minimize the total operational costs and the maximum response time.

Several works also incorporate disruption of either facilities, for example, (Paul & MacDonald, 2016), the relief network, or both, which gives rise to uncertainty. For example, Paul & Wang (2019); Vahdani et al. (2018) consider disruptions in both facilities and the relief networks. Tofighi et al. (2016) also include both facility disruption and relief network disruptions, where facility disruptions are manifested as different levels of usable inventory in the storage facilities, and relief network disruptions are incorporated as different transportation times. In our work, we do not consider facility disruptions because the potential locations for the prepositioning warehouses are chosen in relatively safer areas, or in other words, regions with a lower risk of damage from earthquakes. Moreover, we assume that newer facilities will be built incorporating earthquake-resistant building codes and thus have a lower probability of getting damaged.

A review of the literature on humanitarian facility location under uncertainty by Dönmez et al. (2021) states that uncertainty in humanitarian logistics that has been studied arises either from the demand side, or from the supply side, or related to network connectivity. Stienen et al. (2021) consider uncertainty on the demand side where the number of people affected is modeled using an uncertainty set. Haghi et al. (2017) and Zokaee et al. (2016) consider uncertainties in both the demand and the supply side, along with uncertainty in the cost parameters. In Zokaee et al. (2016), the authors study uncertainty in the demand and supply of relief commodities, where they can lie within an uncertainty set with a particular nominal value. Chang et al. (2024a) considers uncertainties in the relief network arising due to unknown parameters for earthquakes. Vahdani et al. (2018) consider uncertainty on the supply side and the relief networks. Tofighi et al. (2016) includes uncertainty in the demand side, supply side, and relief networks together. We handle uncertainty related to the location and magnitudes of earthquakes and aftershocks, which, in turn, is manifested as the uncertainty in demand based on the demand nodes that are affected.

4.2.2 Dealing with uncertainty

The uncertainties in facility location and disaster management is usually handled using either robust optimization (Paul & Wang, 2019; Haghi et al., 2017; Stienen et al., 2021; Zokaee et al., 2016; Vahdani et al., 2018), or stochastic programming (Paul & MacDonald, 2016; Acar & Kaya, 2019; Chang et al., 2024b,a), or a combination of both (Alizadeh et al., 2019; Rezaei-Malek et al., 2016). However, other avenues have been explored as well. For example, Tofighi et al. (2016) incorporates a credibility-measure based possibilistic programming into a scenario-based stochastic programming framework. Sheikholeslami & Zarrinpoor (2023) handles uncertainty using a fuzzy chance-constrained programming method originated in *Me* measure, which prevents extreme attitudes of the decision-makers. Ghasemi & Khalili-Damghani (2021) incorporates a robust simulation-optimization approach where they use simulation to investigate the damage of urban infrastructures and their impact on the demand for relief commodities. Then, they use robust optimization to consider the location decisions of suppliers and DCs, their inventory levels, and finally, the flow of relief commodities between DCs. Rezaei-Malek et al. (2016) utilizes a scenario-based robust stochastic approach for designing the relief network with perishable commodities. Khalili-Fard et al. (2024) tackle uncertainty using both stochastic and fuzzy programming. Stochastic parameters are those that can be estimated from available data, while probabilistic programming is employed for parameters that lack data and information. Taouktsis & Zikopoulos (2024) develop a decision-making tool for installing DCs using a combination of a heuristic algorithm and predictive models based on a binary classification problem with the support of a supervised deep neural network.

We use robust optimization in this work, motivated by the fact that the locations of epicenter and aftershocks are uncertain in nature. Moreover, as stated by Starr & Van Wassenhove (2014), robust solutions are key in humanitarian logistics and disaster preparedness.

Soyster (1973) was the first to study a robust linear programming problem, where the solution remains feasible for all realizations of parameters within a given convex set. However, the solutions obtained are too conservative in nature (Bertsimas & Sim, 2004), because they take into account the worst-case values of the parameters, possibly all of them varying simultaneously. Ben-Tal & Nemirovski (1998, 2000) introduced a less conservative way to model the uncertainty set where, based on statistical estimates, the values taken by the uncertain parameters are considered based on their probability (Gregory et al., 2011). This class of uncertainty sets is ellipsoidal in nature, and the robust counterparts of the linear programming problems give rise to conic quadratic problems (Bertsimas & Sim, 2004). A similar kind of study was also undertaken independently by El Ghaoui & Lebret (1997) and El Ghaoui et al. (1998) around the same period. However, these models, being non-linear, are computationally more challenging than the linear models defined by Soyster (1973) (Bertsimas & Sim, 2004). Bertsimas & Sim (2004) proposed a robust linear programming model based on the idea that not all parameters would take their worst-case values at the same time. They used a parameter 'Γ_i', for each constraint i, to represent the number of parameters in the constraint that can actually deviate to their worst-case value, and thus the solution remains feasible if less than Γ_i of the uncertain parameters change for each constraint. This provides more flexibility to the user who has control over the "degree of conservatism". Our work draws inspiration from Bertsimas & Sim's Γ-robustness approach to generate our uncertainty set for the locations of the earthquakes.

The literature combining facility location and robust optimization is as rich as it is vast, so in the following subsection, we focus on papers specifically dealing with preparedness for multiple disasters, which is the case of our work.

4.2.3 Compound disasters

Most of the studies mentioned above deal with one kind of disaster. However, in reality, different types of humanitarian emergencies may occur together, or one emergency often leads to another. Simultaneous disasters result when more than one kind of humanitarian emergency occurs together. Compound disasters, on the other hand, are those where one disaster leads to another either by directly causing it, or by hindering the resilience and response for the second emergency (Liu & Huang, 2014).

Aydin & Cetinkale (2023) study multiple disasters simultaneously, viz. large-scale earthquakes along with pandemics. They study the location and number of temporary medical facilities for large-scale disasters occurring in a region that has already been hit by a pandemic. In the first stage, they consider locating emergency healthcare facilities to increase the effectiveness of response operations to the disaster, accommodating rotation of medical teams between facilities, and incorporating uncertainty based on demand stochasticity and road network disruptions. In the second stage, they forecast the number of infected individuals along with the severity of infection in the aftermath of the earthquake. Additionally, the authors provide a mathematical model to find the optimal number and location of COVID-19 hospitals and isolation centers. Ozbay et al. (2019) study shelter site location problem for the multi-hazard phenomenon, i.e., a primary disaster followed by a secondary disaster, and they focus their study on earthquakes followed by an aftershock using a multi-stage stochastic MIP model. The shelter sites are located after an earthquake happens and before the aftershock. The location decisions are finalized (along with new locations) after the demands from the first earthquake, and the aftershock is observed in the second and third stages, respectively. The third stage also includes utilization of the shelter sites and employing the conditional value-at-risk (cVaR) risk measure to manage the risk of a shelter site exceeding its capacities. The allocation decisions are based on the nearest assignment to model the real-life behavior of people. The shelter sites have weights on them based on their performance, and they wish to minimize the expected weighted number of established shelter sites while aiming to open shelter sites with higher weights. Mohammadi et al. (2020) design a humanitarian relief network with several decisions– facility location-allocation, fair distribution of relief items, assignment of victims, and routing decisions, including aftershock concerns. They adopt a combination of robust optimization and neutrosophic fuzzy-based approach to handle uncertainty. Bera et al. (2023) also investigates shelter location-allocation planning for multiple disasters, specifically floods and landslides. First, they develop susceptibility maps for floods and landslides using the Random Forest algorithm and Google Earth engine. Second, the shelter location (particularly schools as evacuation centers) and allocation decisions are made using a p-median problem and a maximal covering location problem. They implemented their study in a mountainous village in the Western Ghats region of India in the context of a rainstorm disaster that occurred in 2005 and found that existing shelters were not enough to provide services to everyone within 30 minutes and 60 minutes. Greer et al. (2024) explore dual hazards in Texas and Louisiana, specifically Hurricane Laura, which occurred in August 2020 amidst the COVID-19 crisis. The authors perform a qualitative analysis with emergency management stakeholders and find evidence of improvisation for the response- evacuation and sheltering- to hurricanes. To the best of our knowledge, there exists no paper in the literature that provides a comprehensive model focusing on the case of multiple aftershocks following a main earthquake for relief facility location.

4.3 Problem setting

Let $\mathcal{S}$ be the set of first-stage scenarios for the main earthquake. Each scenario $s \in \mathcal{S}$ is defined by the location of the major earthquake epicenter that can be affected in the first stage, and we assume we have only one earthquake in the first stage.

A major earthquake is usually followed by a series of aftershocks. Let $\mathcal{K}$ denote the set of all possible aftershock locations. The aftershocks that follow depend on the location of the epicenter of the first earthquake, typically lying on and around the fault lines triggered by the main earthquake. Let $\mathcal{K}_s$ denote the second-stage scenario set that can follow the first-stage scenario s.

We consider that in any scenario $s \in \mathcal{S}$, there can be at most Δ aftershocks. In other words, we wish to prepare for the demand arising from one major earthquake followed by Δ aftershocks. We define by $\mathcal{K}_s^{\Delta}$ the uncertainty set that denotes the possible subset of aftershocks in each scenario s, given by

$$\mathcal{K}_s^{\Delta} = \{K \subset \mathcal{K}_s : |K| \leq \Delta\}, \ s \in \mathcal{S}. \tag{4.1}$$

In our setting, we assume that the decision-maker aims to prepare for earthquakes of fixed magnitude, both in the first stage and the second stage. For example, they might want to prepare for scenarios of a major earthquake of a maximum magnitude 8, followed by Δ= 5 earthquakes of a maximum magnitude 6.5 in the second stage. These magnitudes are estimated beforehand, in a sufficiently conservative way such that the demand of the entire affected area can be satisfied.

Let $\mathcal{D}$ be the set of demand nodes that can potentially be affected by the earthquake or aftershocks. Let $\mathcal{F}$ be the set of all locations where a facility (warehouse with relief material) can be set up. Let t_{ij} be the distance (or equivalently time and cost) of traveling between demand node $i \in \mathcal{D}$ and facility node $j \in \mathcal{F}$. In the following subsection, we describe how we estimate the demands at each demand node.

Demand estimation

Each demand node can have demands from the main earthquake, or any of the following aftershocks, or both. We note the demand in terms of the number of people requiring support and relief materials. The demand depends on several factors. It increases with the population of a node and decreases in the distance from the epicenter of the earthquakes. The closer a demand node is to the epicenter, the more damage it incurs. The demand also depends on the magnitude of the earthquakes– the higher the magnitude, the stronger the impact and the more damaging it is.

Some works in the literature have proposed methods for casualty or damage estimation in earthquakes. For example, Urrutia et al. (2014) employ regression analysis using matrices where earthquake parameters like magnitude, intensity, depth of focus, location of the epicenter, and duration are taken into account to estimate damages in terms of the number of deaths, injured, families that are affected, and the cost of damage. Another study by Aleskerov et al. (2005) proposes a cluster-based model to estimate human losses and injuries during earthquakes and, as a result, the shelter needs for people. Clusters could be a single building, a small group of buildings, schools, etc, in a sub-district area. The buildings' characteristics, like construction type, number of stories, year of construction, etc., and the intensity of earthquakes are used to estimate losses and capacities for shelters in each location. Xing et al. (2015) proposes a robust wavelet ν-SVM model for casualty prediction in earthquakes. They use predictors like earthquake magnitude, epicentral intensity, fortification intensity, population density, pre-warning level, in-building probability, location of occurrence, emergency supply support, and building collapse ratio to predict the death rate and injury rate. Gul & Guneri (2016) utilize artificial neural networks (ANN) for casualty estimation based on historical data of various earthquake parameters like occurrence time (day or night), magnitude, and population density to predict the number of injured people.

Since our work focuses more on facility location models than casualty prediction models, we draw inspiration from the literature and use a regression technique for our casualty estimation model, restricted to a smaller set of relevant features for which we had available data. Since no detailed data was available on the specific impact of individual earthquakes on the surrounding areas, we only use magnitude, population, and distance from the epicenter to estimate the demand.

The demand d^1_{si} at each demand node i in the first stage for scenario s is calculated as:

$$d^1_{si} = \Phi_1 \left(P_i, D_{si}, M_1\right)$$

where Φ_1 is a function of the population P_i at node i, the distance D_{si} of the demand node from the earthquake epicenter that is affected in scenario s, and the magnitude M_1 of the first earthquake.

Similarly, in the second stage, the demand at each node i due to an aftershock at node $k \in \mathcal{K}_s$ is given by

$$d^2_{ik} = \Phi_2 \left(P_{i2}, D_{ik}, M_2\right)$$

where, D_{ik} is the distance between the demand node i, and the aftershock location k, P_{i2} is the residual population of node i where people affected by the main earthquake and rescued at the first stage have been subtracted, and M_2 is the typical magnitude of aftershocks.

In the second stage, if a demand node is affected by more than one aftershock, then the demand at that node is taken to be the maximum of the demands caused by each aftershock that affects the demand node, $\max_{k \in K_s} d^2_{ik}$, i.e., the demand induced by the closest aftershock in the subset K_s of aftershocks.

In Appendix B.2, we use the 2023 Turkey earthquake and immediately available data on building damage and affected lives to calibrate a regression model for estimating our demands.

Problem definition

We wish to select a subset F of $\mathcal{F}$ with at most N facilities such that, in any major earthquake scenario $s \in \mathcal{S}$ and a corresponding aftershock scenario $\mathcal{K}^{\Delta}_s$, we are able to satisfy the entire demand by making the closest allocation of the demand nodes to the facilities. This is equivalent to preparing for the worst possible demand over all possible epicenter scenarios $s \in \mathcal{S}$ for the first stage, and all possible subsets of aftershocks $K \subset \mathcal{K}_s^\Delta$ for the second stage. The goal is to find a subset F of facilities to open and to allocate the demand nodes in the first and the second stage, so that the worst-case allocation cost is minimized. Our problem is then given by:

$$\min_{\substack{F \subset \mathcal{F} \\ |F| \leq N}} \left\{ \max_{s \in \mathcal{S}} \left\{ T_s^1(F) + \max_{K \in \mathcal{K}_s^\Delta} T_s^2(F, K) \right\} \right\}, \tag{\textbf{P}}$$

where $T_s^1(F)$ denotes the cost of allocating the affected demand nodes in scenario s to the set F of open facilities in the first stage, each allocation (i, j) incurring a cost of $d_{is}^1 t_{ij}$. Similarly, $T_s^2(F, K)$ denotes the allocation cost of assigning the demand nodes to the open facilities in the aftershock scenario $K \in \mathcal{K}_s^\Delta$. In the second stage, each assignment (i, j) incurs a cost of $t_{ij} \max_{k \in K} d_{ik}^2$ for a given subset K of aftershocks since the demand in the second stage is the maximum demand (associated with the closest aftershock, see above). A summary of notations is provided in Appendix B.3. We will see in Section 4.4 that due to the uncapacitated version of the problem, for a given set F of selected facilities, the optimal assignments of customers to a facility in F will be the same at stage 1 and stage 2, i.e., they will be assigned to the closest facility in F in both stages.

In the following sections, we present different formulations and solution approaches for the problem.

4.4 Formulation with full enumeration of scenarios ($\mathbf{F_{xy}}$)

Let y_j be a binary variable equal 1 if a facility is constructed at location $j \in \mathcal{F}$, and 0 otherwise. We also define binary assignment variables x_{ij} equal to 1 if demand node i is assigned to facility j, and 0 otherwise.

To write the model, we aggregate the first and the second stage scenarios, or, in other words, we fully enumerate all the earthquake-aftershocks scenarios. Each aggregated scenario $\omega \equiv (s, K)$ consists of a major earthquake s in the first stage, followed by a set $K \subseteq \mathcal{K}_s^{\Delta}$ of aftershocks in the second stage. Each aggregated scenario ω can also be equivalently written as (s, K), where $s \in \mathcal{S}$ and $K \subset \mathcal{K}_s^{\Delta}$. Let Ω be the set of all aggregated scenarios described above. We assume that at most one scenario will occur, and we want to make location and allocation decisions in the worst case.

Let $d_{\omega i}^1$ and $d_{\omega i}^2$ be the demands at node i in scenario ω in stages 1 and 2, respectively. While $d_{\omega i}^1$ is simply given by the demand at node i in earthquake scenario s, $d_{\omega i}^2$ is the maximum possible demand at node i in the second stage given that scenario s has occurred in the first stage, and aftershock scenario $K \in \mathcal{K}_s^{\Delta}$ has occurred in the second stage, i.e.,

$$d_{\omega i}^2 = \max_{k \in K} d_{ik}^2.$$

The model with the full enumeration of scenarios is written as

$$\begin{aligned}
\mathbf{F_{xy}}: \quad \min \quad & \theta && && (4.2a)\\
\text{subject to} \quad & \theta \geq \sum_{i \in \mathcal{D}} \sum_{j \in \mathcal{F}} t_{ij}(d_{\omega i}^1 + d_{\omega i}^2) x_{ij} && \omega \in \Omega && (4.2b)\\
& \sum_{j \in \mathcal{F}} x_{ij} = 1 && i \in \mathcal{D} && (4.2c)\\
& y_j \geq x_{ij} && i \in \mathcal{D},\ j \in \mathcal{F} && (4.2d)\\
& 1 \leq \sum_{j \in \mathcal{F}} y_j \leq N && && (4.2e)\\
& \theta \geq 0 && && (4.2f)\\
& x_{ij}, y_j \in \{0, 1\} && i \in \mathcal{D},\ j \in \mathcal{F}. && (4.2g)
\end{aligned}$$

Constraints (4.2b) are used to minimize the allocation costs of stage 1 and stage 2 in the worst-case aggregated scenario. Constraints (4.2c) says that each demand node is allocated to at least one facility node in stage 1, and constraints (4.2d) ensures that if a demand node is allocated to a facility node, then the facility is opened. Finally, constraints (4.2e) ensure that at least one facility is opened and no more than N facilities are opened. We denote by $\mathbf{F_{xy}}$, the formulation of the facility location problem where each aggregated scenario (with a main earthquake followed by Δ aftershocks) is explicitly enumerated, and the objective is to find the location of the warehouses such that the total allocation cost of the demand nodes to the facilities is minimized.

Note that since we study an uncapacitated facility location problem, the variables x_{ij} have the 0-1 property. In other words, each demand node is always allocated to the closest open facility that serves its entire demand.

Proposition 1. *The formulation* (4.2) *is a valid formulation of* (**P**).

Proof. Problem (**P**) is a two-stage problem. In stage 1, after the first earthquake, we make the first-stage allocation decisions. Let us refer to them by x_{ij}^1, which denotes if demand node i is assigned to facility node j. The second-stage decisions also include allocation decisions that are made after the aftershocks are realized. Let them be denoted by x_{ij}^2, which indicates the assignment of demand node i to facility j in stage 2. These (allocation) subproblems are denoted by T^1 and T^2, respectively. Since we do not have capacities on facilities, once they have been established by pre-disaster variables y_j, each potential demand node is assigned to the closest open facility regardless of the location of the earthquake and aftershocks, and the demands at the nodes. Hence, variables x_{ij}^1 and x_{ij}^2 can be replaced equivalently by a unique assignment variable x_{ij}. $\square$

$\mathbf{F_{xy}}$ has $O(|\mathcal{D}| \cdot |\mathcal{F}|)$ variables and an exponential number of constraints. We refer to the solution approach, where we directly use this formulation, as $\mathbf{P_{xy}^{full}}$. However, it cannot be solved easily if the aftershocks are too many in number, as shown in Section 4.7. When $|\Omega|$ is too large, we use cutting planes to separate constraints (4.2b). This method is explained in the following subsection.

4.4.1 Solution approach with separation of scenarios ($\mathbf{P}^{\mathbf{sep}}_{\mathbf{xy}}$)

In this subsection, we explain the solution approach where we separate constraints (4.2b) using lazy cuts. We start with the Relaxed Master Problem (RMP), which at the first iteration is written as:

$$\min \quad \theta \tag{4.3a}$$

$$\text{subject to} \quad \sum_{j\in\mathcal{F}} x_{ij} = 1 \qquad i \in \mathcal{D} \tag{4.3b}$$

$$y_j \geq x_{ij} \qquad i \in \mathcal{D}, j \in \mathcal{F} \tag{4.3c}$$

$$1 \leq \sum_{j\in\mathcal{F}} y_j \leq N \tag{4.3d}$$

$$\theta \geq 0 \tag{4.3e}$$

$$x_{ij},\ y_j \in \{0,1\} \qquad i \in \mathcal{D},\ j \in \mathcal{F}. \tag{4.3f}$$

The model (4.3) is a simple location-allocation problem. The general idea is the following. For any solution (x^*, y^*, θ^*) of (4.3), we check if

$$\theta^* \geq \max_{\omega\in\Omega} \sum_{i\in\mathcal{D}} \sum_{j\in\mathcal{F}} t_{ij}(d^1_{\omega i} + d^2_{\omega i})x^*_{ij},$$

i.e., if θ^* is greater than the largest possible allocation cost over all possible demand vectors. If not, and there exists an aggregated scenario with a worse allocation cost, we add it to the RMP and resolve it.

In each scenario ω, the allocation cost in the first stage τ^1_s is induced by the demand generated by the main earthquake, i.e.,

$$\tau_s^1(x^*) = \sum_{i\in\mathcal{D}} \sum_{j\in\mathcal{F}} t_{ij} d_{si}^1 x_{ij}^* \tag{4.4}$$

where, s denotes the main earthquake in the aggregated scenario ω, with $d_{\omega i}^1 = d_{si}^1$. The allocation cost in the second stage is the maximum cost over all possible demand profiles generated by the Δ aftershocks in scenario ω. This demand can be computed using the following subproblem and can be written as:

$$\tau_s^2(x^*) = \max \sum_{i\in\mathcal{D}} \left(\sum_{j\in\mathcal{F}} t_{ij} x_{ij}^* \right) \max_{k\in\mathcal{K}_s} \left\{ d_{ik}^2 u_k \right\} \tag{4.5a}$$

$$\sum_{k\in\mathcal{K}_s} u_k \leq \Delta \tag{4.5b}$$

$$u_k \in \{0,1\} \qquad k \in \mathcal{K}_s. \tag{4.5c}$$

where binary variables u_k define the subset $K \subseteq \mathcal{K}_s^\Delta$ of aftershocks.

The subproblem τ_s^2 cannot be solved in the above non-linear form. To solve it, we linearize it using variables z_{ik} for $i \in \mathcal{D}$ and $k \in \mathcal{K}_s$, which determines the aftershock k that causes the highest demand for node i. We obtain the following Mixed-Integer Linear Program:

$$
\begin{aligned}
\tau_s^2(x^*) \;=\; \max \;& \sum_{i \in \mathcal{D}} \sum_{k \in \mathcal{K}_s} C_{ik} z_{ik} && && \text{(4.6a)}\\
& \sum_{k \in \mathcal{K}_s} z_{ik} = 1 && i \in \mathcal{D} && \text{(4.6b)}\\
& z_{ik} \leq u_k && i \in \mathcal{D}, k \in \mathcal{K}_s && \text{(4.6c)}\\
& \sum_{k \in \mathcal{K}_s} u_k \leq \Delta && && \text{(4.6d)}\\
& u_k \in \{0,1\} && k \in \mathcal{K}_s && \text{(4.6e)}\\
& z_{ik} \geq 0 && i \in \mathcal{D}, k \in \mathcal{K}_s && \text{(4.6f)}
\end{aligned}
$$

where $C_{ik} = \left(\sum_{j \in \mathcal{F}} t_{ij} x_{ij}^*\right) d_{ik}^2$.

Proposition 2. *Formulation (4.6) is valid for subproblem τ_s^2.*

Proof. The non-linear subproblem (4.5) can be reformulated as:

$$
\begin{aligned}
\tau_s^2(x^*) = \; \max \;& \sum_{i \in \mathcal{D}} V_i \\
& V_i = \max_{k \in \mathcal{K}_s} C_{ik} u_k \qquad i \in \mathcal{D} \\
& \sum_{k \in \mathcal{K}_s} u_k \leq \Delta \\
& u_k \in \{0,1\} \qquad k \in \mathcal{K}_s.
\end{aligned}
$$

The above variable V_i can be defined as the following minimization linear program:

$$
\min V_i \quad \texttt{s.t.}\, V_i \geq C_{ik} u_k, \; k \in \mathcal{K}_s
$$

Its dual (with dual variable z_{ik} associated with constraint k) is:

$$\max \sum_{k\in\mathcal{K}_s} C_{ik}u_k z_{ik}$$
$$\sum_{k\in\mathcal{K}_s} z_{ik} \leq 1$$
$$z_{ik} \geq 0$$

where the inequality constraint can be replaced by an equality $\sum_{k\in\mathcal{K}_s} z_{ik} = 1$ by maximization of the objective. The above dual is quadratic in z and u variables, but since variables u_k are binary it can be equivalently reformulated as:

$$\max \sum_{k\in\mathcal{K}_s} C_{ik} z_{ik}$$
$$\sum_{k\in\mathcal{K}_s} z_{ik} = 1$$
$$z_{ik} \leq u_k \qquad k \in \mathcal{K}_s$$
$$z_{ik} \geq 0$$

Replacing V_i by the above linear program with variables z_{ik} in the first formulation of the proof, we exactly get formulation (4.6). $\square$

For any solution (x^*, y^*, θ^*) of the RMP, we must have

$$\theta^* \geq \tau_s^1(x^*) + \tau_s^2(x^*) \tag{4.10}$$

for each aggregated scenario $\omega = (s, K) \in \Omega$. If $\exists\, \bar{s} \in \mathcal{S}$, such that

$$\theta^* < \tau^1_{\bar{s}}(x^*) + \tau^2_{\bar{s}}(x^*),$$

then we find an aggregated scenario $\bar{\omega} = (\bar{s}, \bar{K})$ that does not satisfy (4.10), and we add the corresponding cut to the RMP for $\bar{\omega}$ in the following way

$$\theta \geq \sum_{i \in \mathcal{D}} \sum_{j \in \mathcal{F}} t_{ij}(d^1_{i\bar{\omega}} + d^2_{i\bar{\omega}})x_{ij} \tag{4.11}$$

and resolve the RMP. $d^2_{i\bar{\omega}}$ is given by $\max\{d^2_{ik}u^*_k,\ k \in \mathcal{K}_s\}$, where u^* is the optimal solution of (4.6) and represents the maximum demand at node i following scenario ω. We denote the whole separation algorithm by $\mathbf{P^{sep}_{xy}}$. Note that the subproblem (4.6) is equivalent to its linear relaxation where binary variables u_k are just set to be continuous. This enables to fasten its solving time.

4.5 Extended formulation ($\mathbf{F^{ext}_{xy}}$)

In this subsection, we discuss a reformulation of $\mathbf{F_{xy}}$. We provide an extended formulation of (4.2). The extended model is similar to $\mathbf{F_{xy}}$, except for constraints (4.2b). Using the value function τ^2_s, we can reformulate the model as:

$$\min \quad \theta \tag{4.12a}$$

$$\text{subject to} \quad \theta \geq \sum_{i \in \mathcal{D}} \sum_{j \in \mathcal{F}} t_{ij} d^1_{si} x_{ij} + \tau^2_s(x) \qquad s \in \mathcal{S} \tag{4.12b}$$

$$\sum_{j \in \mathcal{F}} x_{ij} = 1 \qquad i \in \mathcal{D} \tag{4.12c}$$

$$y_j \geq x_{ij} \qquad i \in \mathcal{D},\ j \in \mathcal{F} \tag{4.12d}$$

$$1 \leq \sum_{j \in \mathcal{F}} y_j \leq N \tag{4.12e}$$

$$\theta \geq 0 \tag{4.12f}$$

$$x_{ij}, y_j \in \{0,1\} \qquad i \in \mathcal{D},\ j \in \mathcal{F} \tag{4.12g}$$

where, for each scenario $s \in \mathcal{S}$, τ_s^2 is given by the reformulated subproblem (4.6).

In model (4.12), constraints (4.12b) are broken down into two parts. In the RHS of the constraints, the first part gives the allocation cost in stage 1 in scenario s, and the second part gives the corresponding second stage allocation cost. The remaining constraints of (4.12) are the same as $\mathbf{F_{xy}}$.

We replace τ_s^2 by its linear relaxation, so that it may be dualized. While the linear programs are not equivalent, the problem has the property that, in almost all cases, the solution of the relaxed problem is the same as the one with binary constraints. Thus it is a heuristic solution approach.

We replace constraints (4.6e) by

$$0 \leq u_k \leq 1 \qquad k \in \mathcal{K}_s \tag{4.13}$$

in problem (4.6). Similar to the approach of Bertsimas & Sim (2004), we dualize (4.6) to obtain a minimization problem and substitute it into the original problem to derive the extended version of problem (4.12).

Let p_{si}, q_{sik}, φ_s, and r_{sk} be the dual variables corresponding to constraints (4.6b), (4.6c), (4.6d), and (4.13), respectively, for each scenario s. Then, the dual problem is given by:

$$\tau_s^2(x^*) = \min \sum_{i \in \mathcal{D}} p_{si} + \Delta\varphi_s + \sum_{k \in \mathcal{K}_s} r_{sk} \tag{4.14a}$$

$$p_{si} + q_{sik} \geq \sum_{j \in \mathcal{F}} t_{ij} d^2_{ik} x^*_{ij} \qquad i \in \mathcal{D}, k \in \mathcal{K}_s \tag{4.14b}$$

$$-\sum_{i \in \mathcal{D}} q_{sik} + \varphi_s + r_{sk} \geq 0 \qquad k \in \mathcal{K}_s \tag{4.14c}$$

$$q_{sik}, r_{sk}, \varphi_s \geq 0, p_{si} \in \mathbb{R} \qquad i \in \mathcal{D}, k \in \mathcal{K}_s, s \in \mathcal{S}. \tag{4.14d}$$

Substituting τ_s^2 by its above dual program in the initial model (4.12a)-(4.12g), we obtain the following extended formulation:

$$\mathbf{F}^{\mathbf{ext}}_{\mathbf{xy}}: \quad \min \ \theta \tag{4.15a}$$

$$\text{subject to} \quad \theta \geq \sum_{i \in \mathcal{D}} \sum_{j \in \mathcal{F}} t_{ij} d^1_{si} x_{ij} + \sum_{i \in \mathcal{D}} p_{si} + \Delta \varphi_s + \sum_{k \in \mathcal{K}_s} r_{sk} \qquad s \in \mathcal{S} \tag{4.15b}$$

$$p_{si} + q_{sik} \geq \sum_{j \in \mathcal{F}} t_{ij} d^2_{ik} x_{ij} \qquad i \in \mathcal{D}, k \in \mathcal{K}_s \tag{4.15c}$$

$$-\sum_{i \in \mathcal{D}} q_{sik} + \varphi_s + r_{sk} \geq 0 \qquad k \in \mathcal{K}_s \tag{4.15d}$$

$$\sum_{j \in \mathcal{F}} x_{ij} \geq 1 \qquad i \in \mathcal{D} \tag{4.15e}$$

$$y_j \geq x_{ij} \qquad i \in \mathcal{D}, \ j \in \mathcal{F} \tag{4.15f}$$

$$1 \leq \sum_{j \in \mathcal{F}} y_j \leq N \tag{4.15g}$$

$$\theta \geq 0 \tag{4.15h}$$

$$x_{ij}, y_j \in \{0, 1\} \qquad i \in \mathcal{D}, \ j \in \mathcal{F} \tag{4.15i}$$

$$q_{sik}, r_{sk}, \varphi_s \geq 0, p_{si} \in \mathbb{R} \qquad i \in \mathcal{D}, j \in \mathcal{F}, k \in \mathcal{K}_s, s \in \mathcal{S}. \tag{4.15j}$$

Model $\mathbf{F}^{\mathbf{ext}}_{\mathbf{xy}}$ has $O(|\mathcal{D}| \cdot |\mathcal{S}| \cdot |\mathcal{K}| + |\mathcal{D}| \cdot |\mathcal{F}|)$ variables, and $O(|\mathcal{S}| + |\mathcal{D}| \cdot |\mathcal{K}| + |\mathcal{D}| \cdot |\mathcal{F}|)$ constraints. It is a compact formulation, so it can be directly solved by a MILP solver. To solve this model, we use the automatic Benders decomposition of CPLEX and refer to this solution approach as $\mathbf{P}^{\mathbf{ext}}_{\mathbf{xy}}$.

4.6 Formulation in the space of location variables ($\mathbf{F_y}$)

In this subsection, we provide a formulation of problem (**P**), driven by the location variables y, by explicitly writing the subproblems T^1_s and T^2_s in function of location variables y. We will refer to this formulation as $\mathbf{F_y}$.

4.6.1 Subproblem T^1_s

For each scenario $s \in \mathcal{S}$ and a given location vector y^*, the subproblem T^1_s is defined as

$$T^1_s(y^*) \;=\; \min_x \sum_{i \in \mathcal{D}} d^1_{si} \sum_{j \in \mathcal{F}} t_{ij}\, x_{ij} \tag{4.16a}$$

$$\sum_{j \in \mathcal{F}} x_{ij} = 1 \qquad i \in \mathcal{D} \tag{4.16b}$$

$$0 \leq x_{ij} \leq y^*_j \qquad i \in \mathcal{D},\, j \in \mathcal{F} \tag{4.16c}$$

where the allocation variables x_{ij} denote the proportion of the demand of node i that is allocated to facility j. We wish to minimize the overall transportation time of the demand or the allocation cost, as also explained earlier. Constraints (4.16b) state that the entire demand of each node i is fulfilled, and (4.16c) ensure that if a demand node is assigned to a site, then a facility is opened there. Even though variables x_{ij} are continuous, we always have an optimal solution where the variables take binary values due to the uncapacitated nature of our problem.

We proceed by writing the dual of T^1_s first. To do so, we write constraint (4.16c) as

$$-x_{ij} \geq -y^*_j \qquad i \in \mathcal{D},\, j \in \mathcal{F} \tag{4.17}$$

Let λ_i and μ_{ij} be the dual variables corresponding to constraints (4.16b) and (4.17), respectively. Then the dual of the (4.16a)-(4.16b), and (4.17), is given by

$$\max_{\lambda,\mu} \sum_{i\in\mathcal{D}} \lambda_i - \sum_{i\in\mathcal{D}} \sum_{j\in\mathcal{F}} y_j^* \, \mu_{ij} \tag{4.18a}$$

$$\lambda_i - \mu_{ij} \leq t_{ij} \, d_{si}^1 \qquad i \in \mathcal{D},\ j \in \mathcal{F} \tag{4.18b}$$

$$\lambda_i \in \mathbb{R},\ \mu_{ij} \geq 0 \qquad i \in \mathcal{D},\ j \in \mathcal{F}. \tag{4.18c}$$

Proposition 3. *The optimal primal and dual solutions of problem $T_s^1(y^*)$ are given by*

$$x_{ij} = \begin{cases} y_j^*, & j < p_i \\ 1 - \sum_{j=1}^{p_i-1} y_j^*, & j = p_i\,, \\ 0, & j > p_i \end{cases} \qquad j \in \mathcal{F} \tag{4.19a}$$

$$\lambda_i = t_{ip_i} d_{si}^1 \tag{4.19b}$$

$$\mu_{ij} = \begin{cases} (t_{ip_i} - t_{ij}) d_{si}^1, & j < p_i \\ 0, & j \geq p_i \end{cases}, \qquad i \in \mathcal{D},\ j \in \mathcal{F} \tag{4.19c}$$

where, for each $i \in \mathcal{D}$, the coefficients t_{ij} are sorted in non-decreasing order as $t_{i1} \leq \ldots \leq t_{im}$, and $p_i = p(i, y^*)$ denotes the index of the critical *facility for i such that:*

$$\sum_{j=1}^{p_i-1} y_j^* < 1 \leq \sum_{j=1}^{p_i} y_j^*.$$

Proof. Proof is similar to Fischetti et al. (2016) and is given in Appendix B.1. □

4.6.2 Subproblem T_s^2

We define subproblem T_s^2 similarly. For each $s \in \mathcal{S}$, for a given y^* and an aftershock scenario $u_s^* \in \mathcal{K}_s^{\Delta}$, we formulate it in the following way:

$$T_s^2(y^*, u_s^*) \;=\; \min_{z_s} \sum_{i\in\mathcal{D}} \sum_{j\in\mathcal{F}} t_{ij}\, z_{sij} \tag{4.20a}$$

$$\sum_{j\in\mathcal{F}} z_{sij} \geq u_{sk}^*\, d_{ik}^2 \qquad i \in \mathcal{D},\ k \in \mathcal{K}_s \tag{4.20b}$$

$$z_{sij} \leq \widehat{D}_i y_j^* \qquad i \in \mathcal{D}, j \in \mathcal{F} \tag{4.20c}$$

$$z_{sij} \geq 0 \qquad i \in \mathcal{D},\ j \in \mathcal{F}. \tag{4.20d}$$

This formulation uses variables z_{sij} which represent the exact demand of node i allocated to facility j, the entirety of which will be allocated to the closest open facility. Constraints (4.20b) ensure that the maximum possible demand of each node i, due to a set of aftershocks described by u_{sk}, is satisfied. Constraints (4.20c) make sure that the allocations are done only to the open facilities. $\widehat{D}_i$ is an upper bound on the demand, and we define $\widehat{D}_i = \max_{k\in\mathcal{K}} d_{ik}^2$.

For the dual of the second subproblem, we reformulate constraints (4.20c) as

$$-z_{sij} \geq -\widehat{D}_i y_j^* \qquad i \in \mathcal{D},\ j \in \mathcal{F}. \tag{4.21}$$

Let α_{sik} and β_{sij}, be the dual variables corresponding to constraints (4.20b) and (4.21), respectively.

Then the dual of $T_s^2(y^*, u_s^*)$ is written as:

$$\max_{\alpha_s,\beta_s} \sum_{i\in\mathcal{D}}\sum_{k\in\mathcal{K}_s} u_{sk}^* d_{ik}^2\, \alpha_{sik} \;-\; \sum_{i\in\mathcal{D}}\sum_{j\in\mathcal{F}} \widehat{D}_i y_j^*\, \beta_{sij} \tag{4.22a}$$

$$\sum_{k\in\mathcal{K}_s} \alpha_{sik} - \beta_{sij} \le t_{ij} \qquad i\in\mathcal{D},\ j\in\mathcal{F} \tag{4.22b}$$

$$\alpha_{sik}, \beta_{sij} \ge 0 \qquad i\in\mathcal{D},\ j\in\mathcal{F},\ k\in\mathcal{K}_s. \tag{4.22c}$$

The objective function contains the product term $u_{sk}\alpha_{sik}$. However, note that $u_{sk}\alpha_{sik} = \alpha_{sik}$, when $u_{sk} = 1$ and 0 when $u_{ks} = 0$. Thus, we can reformulate it in the following way:

$$\max_{u_s\in\mathcal{K}_s^\Delta} T_s^2(y^*, u_s) \;=\; \max_{\alpha_s,\beta_s,u_s} \sum_{i\in\mathcal{D}}\sum_{k\in\mathcal{K}_s} d_{ik}^2\, \alpha_{sik} \;-\; \sum_{i\in\mathcal{D}}\sum_{j\in\mathcal{F}} \widehat{D}_i y_j^*\, \beta_{sij} \tag{4.23a}$$

$$\text{subject to: } \sum_{k\in\mathcal{K}_s} \alpha_{sik} - \beta_{sij} \le t_{ij}, \quad i\in\mathcal{D},\ j\in\mathcal{F} \tag{4.23b}$$

$$\sum_{k\in\mathcal{K}_s} u_{sk} \le \Delta \tag{4.23c}$$

$$\alpha_{sik} \le M u_{sk}, \quad i\in\mathcal{D},\ k\in\mathcal{K}_s \tag{4.23d}$$

$$\alpha_{sik},\ \beta_{sij},\ \ge 0,\ u_{sk}\in\{0,1\}, \quad i\in\mathcal{D},\ j\in\mathcal{F},\ k\in\mathcal{K}_s, \tag{4.23e}$$

where M is an upper bound on α_{sik}. Hence, the problem (**P**) can be stated as:

$$\min_{\substack{y\in Y\\ 1\le\sum_{j\in\mathcal{F}} y_j\le N}} \left\{ \max_{s\in\mathcal{S}} \left\{ \max_{\substack{(\lambda,\mu)\in\mathcal{L}_s^1\\ (\alpha,\beta,u)\in\mathcal{L}_s^2}} \sum_{i\in\mathcal{D}} \lambda_i \;-\; \sum_{i\in\mathcal{D}}\sum_{j\in\mathcal{F}} y_j^*\, \mu_{ij} \;+\; \sum_{i\in\mathcal{D}}\sum_{k\in\mathcal{K}_s} d_{ik}^2\, \alpha_{sik} \;-\; \sum_{i\in\mathcal{D}}\sum_{j\in\mathcal{F}} \widehat{D}_i\, y_j^*\, \beta_{sij} \right\} \right\}, \tag{4.24}$$

where $\mathcal{L}_s^1$ and $\mathcal{L}_s^2$ are the sets of extreme points of the problems (4.18) and (4.23), respectively. We have the following result.

Proposition 4. *The valid model in the space of y variables is given as*

$$\mathbf{F_y}: \quad \min \quad \theta \tag{4.25a}$$

$$\theta \geq \sum_{i\in\mathcal{D}} d^1_{si}\left[t_{ip_i} - \sum_{j\in\mathcal{F}}(t_{ip_i} - t_{ij})^+ y_j\right] + \sum_{i\in\mathcal{D}}\sum_{k\in\mathcal{K}_s} d^2_{ik}\,\alpha^*_{sik} - \sum_{i\in\mathcal{D}}\sum_{j\in\mathcal{F}} \widehat{D}_i y_j \beta^*_{sij}, \tag{4.25b}$$

$$(p_1, \ldots, p_{|\mathcal{D}|}) \in \mathcal{F}^{|\mathcal{D}|}, (\alpha^*, \beta^*, u^*) \in \mathcal{L}^2_s, s \in \mathcal{S}$$

$$1 \leq \sum_{j\in\mathcal{F}} y_j \leq N, \qquad j \in \mathcal{F} \tag{4.25c}$$

$$\theta \geq 0, y_j \in \{0,1\} \qquad j \in \mathcal{F}. \tag{4.25d}$$

Proof. Proof is given in Appendix B.1 □

4.6.3 Solution approach $\mathbf{P_y}$

To solve the above formulation $\mathbf{F_y}$, we separate constraints (4.25b) using lazy cuts. The Master Problem is given by the objective function (4.25a) and constraints (4.25c) and (4.25d).

For any solution, $(\bar{y}, \bar{\theta})$ of the master problem, for each $i \in \mathcal{D}$ we determine $\bar{p}_i$ as its closest open facility. We also find an optimal solution (α^*, β^*, u^*) of the subproblem $T^2_s(\bar{y})$. If we have

$$\bar{\theta} < \sum_{i\in\mathcal{D}} d^1_{i\tilde{s}}\left[t_{i\bar{p}_i} - \sum_{j\in\mathcal{F}}(t_{i\bar{p}_i} - t_{ij})^+ \bar{y}_j\right] + \sum_{i\in\mathcal{D}}\sum_{k\in\mathcal{K}_{\tilde{s}}} d^2_{ik}\,\alpha^*_{\tilde{s}k} \; - \sum_{i\in\mathcal{D}}\sum_{j\in\mathcal{F}} \widehat{D}_i \bar{y}_j \beta^*_{ij\tilde{s}},$$

for some scenario $\tilde{s} \in \mathcal{S}$, then we must add the cut (4.25b), corresponding to scenario $\tilde{s}$, to the master problem, and resolve the master problem. We refer to this branch-and-cut solution approach as $\mathbf{P_y}$.

4.7 Computational study

In this section, we analyze the tractability of the various models and solving methods on a large dataset of simulated instances inspired by real-life earthquake situations, before the real case study of the Turkey 2023 earthquake in Section 4.8. We solve our models on these instances, and provide computational results and analyses. We implemented the models on the Spyder IDE of Python 3.9 and solved them using the CPLEX 22.1.1.0 standard solver. The tests were conducted on an Intel(R) Xeon(R) W-2255 CPU with a clock speed of 3.70 GHz and 96 GB RAM.

4.7.1 Instance generation

The outermost layer of the earth is comprised of tectonic plates, which are rocky and brittle (NOAA, 2023). Several major and minor plates fit together to make up the layer. These plates are in constant motion, and can move together, collide, slide past one another, or move away from each other. The boundaries where the plates meet are fault lines. Additionally, fault lines may be formed on the interior of the plates by built-up stress occurring due to the movement of plates against one another. When the pressure on the fault line surpasses the strength of the rocks, the rocks abruptly break and shift, causing an earthquake. This sudden movement generates seismic waves that travel through the Earth's surface, causing the ground to shake and resulting in an earthquake.

In order to simulate our instances, we mimic fault line behaviour. We generate a set of four fault lines for our instances. The main earthquake and aftershock epicenters are then generated randomly on or around these lines. We assume that any of the aftershocks on a fault line may be triggered in the second stage if one of the primary earthquakes occurs on same fault line in the first stage.

We generate population centers that represent demand nodes within the region. These demand nodes are affected if they are in the vicinity of the main earthquake or aftershock epicenters. We also generate several potential locations for setting up the facilities. The locations are generated such that they are sufficiently far away from the fault lines and, hence, have minimal chances of getting damaged in the event of an earthquake.

The number of main earthquake locations (first-stage scenarios) ranges from 10 to 100 in our instances. The number of aftershocks is fixed to twice the number of scenarios, so they range from 20 to 200. The instances were generated so that the larger instances were inclusive of the smaller ones. In other words, we started with an instance having 10 scenarios and 20 aftershocks. For the instance with 20 scenarios and 40 aftershocks, we generated 10 additional scenarios and 20 additional aftershocks to the first instance. We continued this till we had 100 scenarios and 200 aftershocks.

We classify our instances into *Small (S)*, *Medium (M)*, and *Large (L)*, based on the number of demand nodes. The *Small* instances consist of 100 demand nodes, the *Medium* instances contains 200 demand nodes, and we have 400 demand nodes in the *Large*instances. The demand nodes are also generated in an inclusive manner. The number of potential facility locations is kept fixed at 10 for all the instances.

In Figure 4.1, we present an example to illustrate our simulated instances. The figure displays the major earthquake and aftershock epicenters represented by the red and blue circles, respectively. If any of the main earthquake epicenters are affected, we assume Δ of the blue points lying near the red points, i.e., on the same fault line as the major earthquake, may also be affected. The number of main earthquakes, the total number of aftershocks, and the average number of aftershocks per scenario in each of the instances are given in Table 4.1. In all tables, the character # means "number of". The potential locations for the facilities is denoted by pink crosses, and the demand nodes are represented by the green squares.

As discussed in Section 4.3, the demand caused at any of the nodes due to an earthquake depends

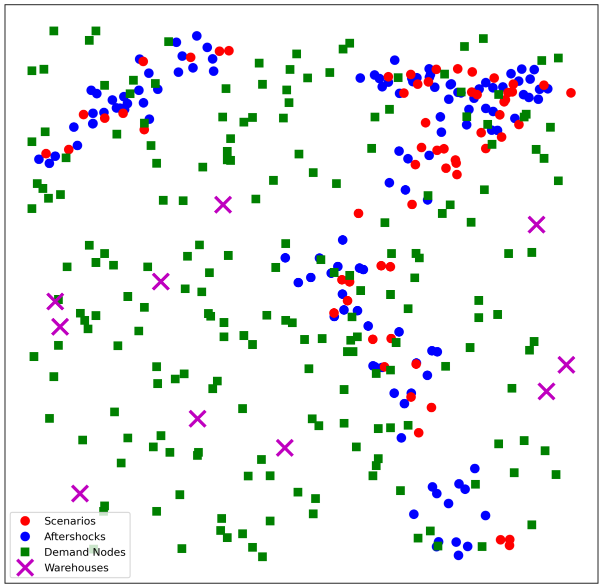

Figure 4.1: An example of an instance with $|\mathcal{S}|$=60, $|\mathcal{K}|$=120, $|\mathcal{D}|$=200, # possible locations for facilities=10

Table 4.1: Summary of instances

Instance Number	1	2	3	4	5	6	7	8	9	10
# possible main earthquakes	10	20	30	40	50	60	70	80	90	100
Total # possible aftershocks	20	40	60	80	100	120	140	160	180	200
Average # aftershocks per scenario	5.5	9.7	14.43	18.7	23.66	29.4	34.34	39.73	44.58	49.74

on three factors– it is increases with the population at the node and the magnitude of the earthquake, and decreases with the distance between the demand node and the earthquake location. With this in mind, we use the following demand function:

$$\text{Demand} = k \cdot \frac{\text{Population} \cdot \text{Magnitude}^{\alpha}}{\text{Distance}^{\beta}} \tag{4.26}$$

where k, α, and β are constants.

Additionally, we introduce a parameter called the *Radius of Impact (RoI)* that indicates if any demand is generated on a node due to an earthquake. If a demand node lies outside the RoI, we set the demand to be zero, otherwise, if it lies inside, the demand is given by the equation (4.26). While there is no fixed radius beyond which an earthquake is not felt, after a certain distance, the severity of the damage is less, and hence, people there do not need additional support. The idea of RoI was inspired by earthquake hazard maps, where areas around fault lines that are at risk of severe, moderate, and low impact are shown by concentric regions. Similar figures are also often observed in maps released after earthquakes. For example, Figure 4.2 shows the earthquake of Gaziantep that occurred on February 6, followed by the aftershock that occurred 9 hours later (source: (Robles et al., 2023)). It shows concentric regions around the earthquake epicenters, representing their intensity. We try to mimic this phenomenon using concentric circles around the earthquakes and aftershocks.

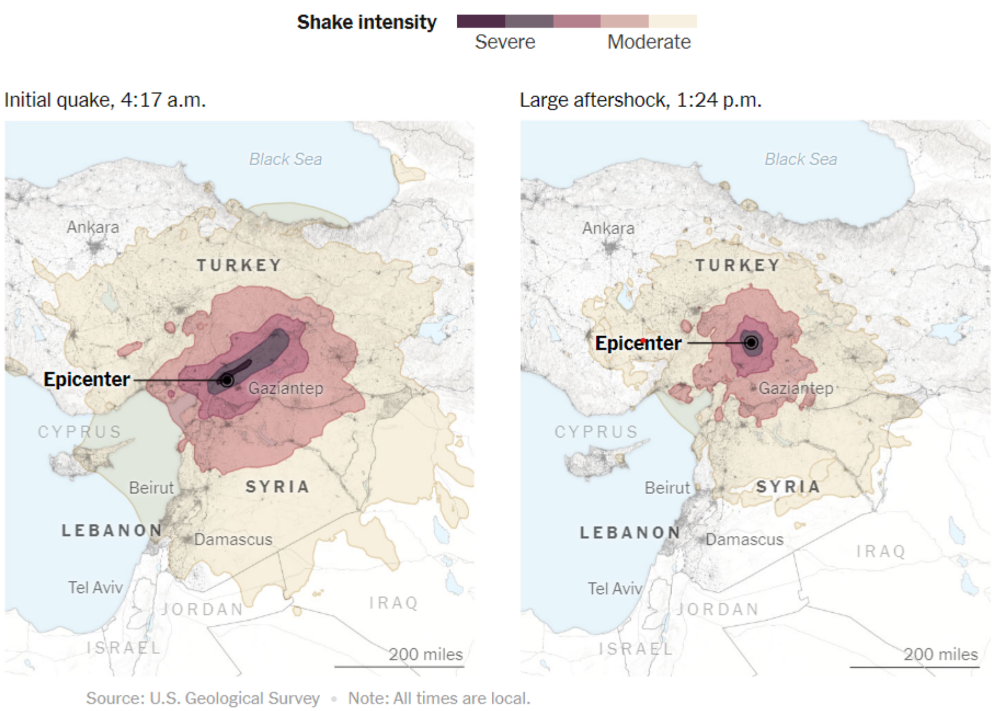

Figure 4.2: The Turkey earthquake of February 2023 and one of its major aftershocks, *Source:* The New York Times

The values of k, α, and β used in our experiments are 0.25, 0.75, and 0.5, respectively. These values were calibrated based on data from the Turkey-Syria earthquake. For more details, refer to the

Appendix B.2. We also chose the values of RoI as 200 for the main earthquake and 100 for the aftershocks. The magnitudes of the main earthquakes were generated between 7.5 and 8.5, while that of the aftershocks lay between 6 and 7.5.

The population at each demand node was randomly generated between 10 and 100 (in thousands of people), and the demand was calculated using (4.26). For the numerical experiments, the values of Δ used are 3, 5, 7, and 10. The number of facilities to be located (N) are 3, 5, and 8.

We allotted a time limit of one hour to CPLEX for solving the models.

4.7.2 Numerical results

We tested our four solution approaches presented in the earlier sections, namely, $\mathbf{P}_{\mathbf{xy}}^{\mathbf{full}}$, $\mathbf{P}_{\mathbf{xy}}^{\mathbf{sep}}$, $\mathbf{P}_{\mathbf{xy}}^{\mathbf{ext}}$, and $\mathbf{P}_{\mathbf{y}}$ on the above instances. Figure 4.3 shows a solution of an instance. The pink crosses represent the locations selected for establishing the facilities.

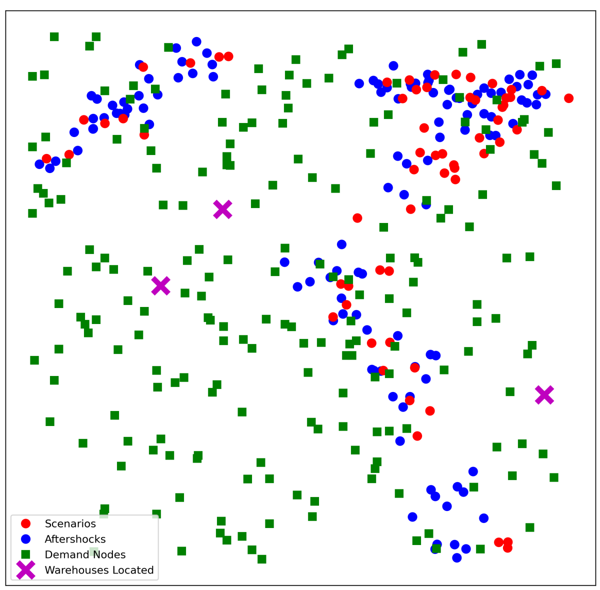

Figure 4.3: An example of the solution of an instance showing the selected facilities, with $|\mathcal{S}|$=60, $|\mathcal{K}|$=120, $|\mathcal{D}|$=200, Δ=3, N=3

In Table 4.2, $\mathbf{P}_{\mathbf{xy}}^{\mathbf{full}}$, which fully enumerates all scenarios, is shown to be largely intractable from some instance sizes. We were able to solve instances of small size only with this model– up to 30 scenarios and 60 aftershocks with a Δ value of 5, and 40 scenarios and 80 aftershocks with a Δ value of 3. We have a large combinatorial problem, where we enumerate $|\mathcal{S}| \times \binom{|K_S|}{\Delta}, S \in \mathcal{S}$ scenarios and build the model. However, we found that once the model was built, it ran fairly quickly. For example, for an instance with 30 scenarios and Δ=5, it took 6520 seconds to build the model, whereas 212 seconds to solve it. For each instance, we report the objective function value, the CPLEX time taken to solve the instance, and the total solution time. We are able to solve for all combinations of Δ and N for instances with only up to 20 epicenters and 40 aftershocks. For instance 3, as soon as Δ exceeds 3, the time taken blows up, as mentioned earlier, and we are unable to find feasible solutions within the time limit. For larger instances, e.g., instance 4 with Δ=5 and N=8, we run into memory errors due to the extensive enumeration of the scenarios and aftershocks. Thus, we refrained from using $\mathbf{P}_{\mathbf{xy}}^{\mathbf{full}}$ for the rest of our analyses.

In Figure 4.4, we solved our three remaining models on *Small* instances first. The solution approach $\mathbf{P}_{\mathbf{xy}}^{\mathbf{sep}}$ is a separation problem. It performs quite well on the *Small* instances. It solved all the instances up to optimality. $\mathbf{P}_{\mathbf{xy}}^{\mathbf{ext}}$ solves the extended formulation of the problem. We used CPLEX autobenders along with our formulation. While this formulation of our problem performs the fastest and solves all the *Small* instances to optimality, CPLEX takes a long time to build the instances, particularly for instances with a higher number of scenarios. For example, for the *Small* instances, the model building time reaches almost 5000 seconds as the number of scenarios goes up to 100. For the *Medium* instances (200 demand nodes), the model building time goes up to 30000 seconds. In approach $\mathbf{P}_{\mathbf{y}}$, we solve the two stages of the problem separately. $\mathbf{P}_{\mathbf{y}}$ took the highest CPLEX time to solve the instances.

While the CPLEX solution time and the total time taken to solve the models are not the same for

Table 4.2: Numerical results using $\mathbf{P}_{\mathbf{xy}}^{\mathbf{full}}$ (NS = No Solution)

Instance Number	# main earthquakes $\lvert\mathcal{S}\rvert$	# aftershocks $\lvert\mathcal{K}\rvert$	Max # warehouses (N)	Delta (Δ)	Objective Function Value	Solve Time CPLEX	Total Solution Time
1	10	20	3	3	20446	0.218	0.971
				5	21172	0.125	0.476
				7	21172	0.204	0.355
				10	21172	0.094	0.249
			5	3	20446	0.797	1.504
				5	21172	0.359	0.652
				7	21172	0.031	0.162
				10	21172	0.047	0.176
			8	3	20446	0.25	0.809
				5	21172	0.125	0.346
				7	21172	0.047	0.147
				10	21172	0.031	0.164
2	20	40	3	3	26914	10.594	21.802
				5	29713	12.656	67.535
				7	29961	20.812	93.442
				10	29961	8.078	17.477
			5	3	24787	5.235	17.243
				5	25157	8.797	61.725
				7	25405	7.734	76.019
				10	25405	3.156	11.349
			8	3	24787	1.015	8.935
				5	25157	3.687	39.406
				7	25405	4.359	51.192
				10	25405	0.718	6.211
3	30	60	3	3	28611	16.188	119.325
				5	29713	211.797	6519.589
				7	NS	NS	NS
				10	NS	NS	NS
			5	3	24787	8.375	88.505
				5	25619	126.766	6365.179
				7	NS	NS	NS
				10	NS	NS	NS
			8	3	24787	7.047	115.555
				5	25157	87.453	6231.710
				7	NS	NS	NS
				10	NS	NS	NS
4	40	80	3	3	28611	89.203	527.525
				5	NS	NS	NS
				7	NS	NS	NS
				10	NS	NS	NS
			5	3	24787	15.797	386.497
				5	NS	NS	NS
				7	NS	NS	NS
				10	NS	NS	NS
			8	3	24787	12.469	359.266
				5	NS	NS	NS
				7	NS	NS	NS
				10	NS	NS	NS

$\mathbf{P_{xy}^{full}}$ and $\mathbf{P_{xy}^{ext}}$, due to the time taken by CPLEX to build the problem, they are almost the same for the other two models, $\mathbf{P_{xy}^{sep}}$ and $\mathbf{P_y}$ as they are branch-and-cut formulations. Figure 4.4 shows the time taken to solve the models on the *Small* instances. It clearly shows the difference in the solution time and the total time taken by $\mathbf{P_{xy}^{ext}}$.

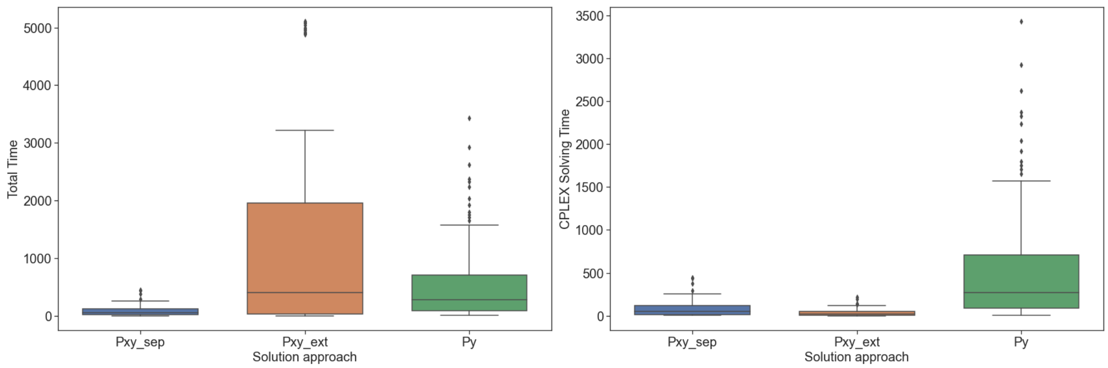

(a) Total Time taken to solve the Small instances **(b)** Time taken by CPLEX to solve the Small instances

Figure 4.4: Comparison of the different solution approaches w.r.t computational time

In Figures 4.5, 4.6, and 4.7, we compare only the two approaches $\mathbf{P_{xy}^{ext}}$ and $\mathbf{P_y}$, and report the CPLEX solution times as the number of scenarios, Δ, and N increases. We observe an exponential increase in the CPLEX solution time as the number of scenarios, and correspondingly the aftershocks, increase for both models, as demonstrated in Figure 4.5. The exponential increase in time is even more prominent for the total time taken by CPLEX for $\mathbf{P_y}$. In Figure 4.6, we report the computational times for different values of Δ. As Δ increases, we observe the solution times to be consistently decreasing for $\mathbf{P_{xy}^{ext}}$, with the median remaining approximately the same, as can be seen from the figure. For $\mathbf{P_y}$, As Δ increases, the median solving time remains the same, particularly for $\Delta = 5, 7, 10$. As we increase the value of N, we notice the computational times to be decreasing for both the approaches $\mathbf{P_{xy}^{ext}}$ and $\mathbf{P_y}$. We predict that this change would be more pronounced as the instance size increases (particularly, the number of demand nodes), but we refrain from doing further experiments with the above two models because of the fact that $\mathbf{P_{xy}^{sep}}$ clearly outperforms the other two computationally. Thus, we focus further analyses on the separation model $\mathbf{P}_{\mathbf{xy}}^{\mathbf{sep}}$.

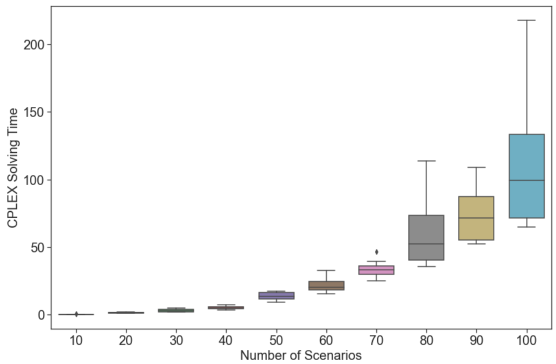

(a) $\mathbf{P}_{\mathbf{xy}}^{\mathbf{ext}}$

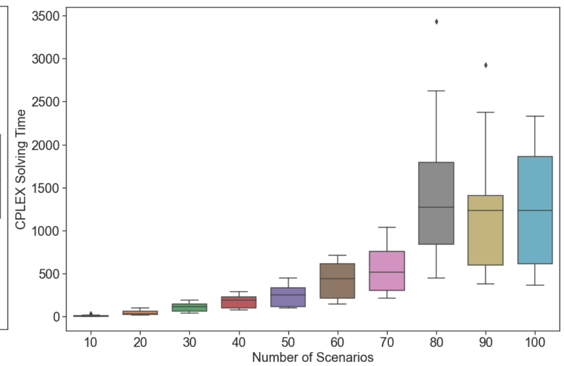

(b) $\mathbf{P}_{\mathbf{y}}$

Figure 4.5: Comparison of CPLEX solution time for the solution approaches $\mathbf{P}_{\mathbf{xy}}^{\mathbf{ext}}$ and $\mathbf{P}_{\mathbf{y}}$ to solve the *Small* instances as the number of scenarios increases

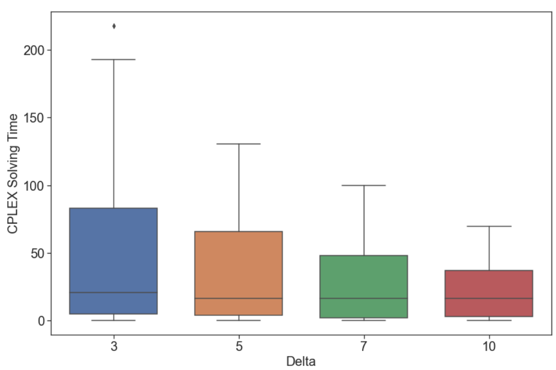

(a) $\mathbf{P}_{\mathbf{xy}}^{\mathbf{ext}}$

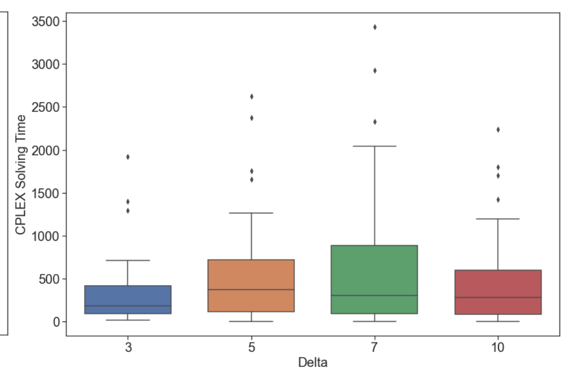

(b) $\mathbf{P}_{\mathbf{y}}$

Figure 4.6: Comparison of CPLEX solution time for the solution approaches $\mathbf{P}_{\mathbf{xy}}^{\mathbf{ext}}$ and $\mathbf{P}_{\mathbf{y}}$ to solve the *Small* instances for different values of Δ

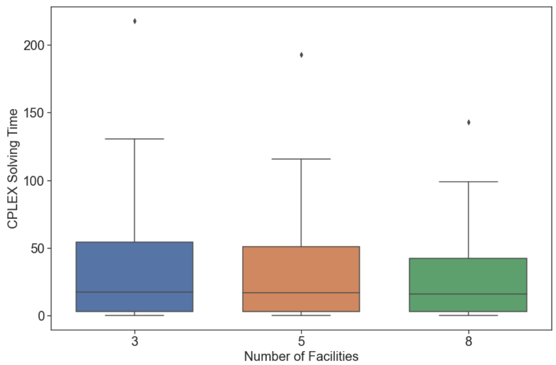

(a) $\mathbf{P_{xy}^{ext}}$

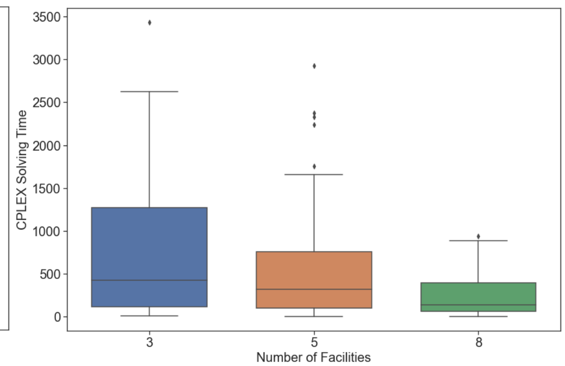

(b) $\mathbf{P_y}$

Figure 4.7: Comparison of CPLEX solution times for the solution approaches $\mathbf{P_{xy}^{ext}}$ and $\mathbf{P_y}$ to solve the *Small* instances for different values of N

We found model $\mathbf{P_{xy}^{sep}}$ to be the best performing one, both in terms of computational time and finding optimal solutions. Thus, we implement this on the *Medium* and the *Large* instances to generate additional insights on the performance of the robust model. Further in the paper, when we refer to the robust model, we refer to the separation model $\mathbf{P_{xy}^{sep}}$ unless otherwise mentioned.

Out of the 360 instances, we were able to find the optimal solution for 356 of them. The four instances for which time ran out before we found the optimal solution each had 100 scenarios, 200 aftershocks, and 400 demand nodes.

Figure 4.8 shows the variation in the objective value and the solving time for $\mathbf{P_{xy}^{sep}}$ as the number of scenarios increases for the *Small*, *Medium*, and *Large* instances. First of all, it is easy to see that the time increases exponentially once again as the number of demand nodes increases. As the number of scenarios increases, we observe the objective values to increase initially, and thereafter, there is only a slight increase in the objective for a higher number of scenarios. The variations in the objective value for instances with the same number of scenarios are also consistent. Thus, for practical applications, it would be enough to consider a small number of scenarios, for example, 50. This would also result in a low solving time of the models.

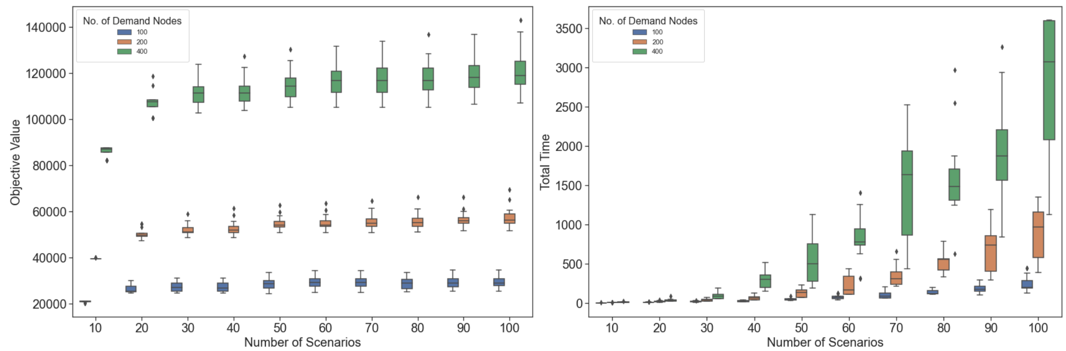

(a) Objective Value

(b) Total solution time

Figure 4.8: Comparison of the objective value and the total time as the number of scenarios increases for the solution approach $\mathbf{P}_{\mathbf{xy}}^{\mathbf{sep}}$

Next, in Figure 4.9, we evaluate the robust model as Δ increases. The objective value increases slightly as Δ increases for each set of sizes. We also show in Figure 4.10 how the locations of selected facilities change as Δ changes. We observe from our experiments that, for higher values of Δ, with everything else remaining constant, the locations of selected facilities stabilize. This can also be seen in Figure 4.10.

We also notice that as Δ increases, the CPLEX computational time decreases. This was counter-intuitive to us, as we expected the time to first increase with an increase in Δ. This expectation is based on the fact that the number of combinations of second-stage scenarios is the highest when Δ is around half the average number of aftershocks per scenario. This fact consistently explained that the computation time of the method $\mathbf{P}_{\mathbf{xy}}^{\mathbf{full}}$ (where all combinations of aftershocks are enumerated) goes up first and then possibly down when Δ increases, see Table 4.2, for example, instance 2. However, for $\mathbf{P}_{\mathbf{xy}}^{\mathbf{sep}}$, we observe that this was not the case since, as mentioned, the computation time decreases with Δ, which is rather good news for realistic applications with many aftershocks.

Finally, we study the impact of the maximum number of facilities to be established, N, on the objective value and the total time. As expected, the objective value, and the variation in the objective value,

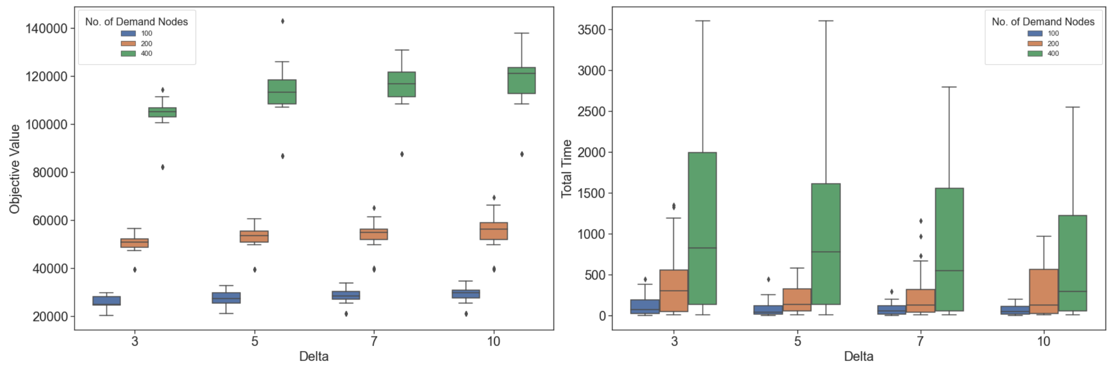

(a) Objective Value as Δ increases

(b) Total time as Δ increases

Figure 4.9: Comparison of the objective value and the total computational time as Δ increases

both decrease as the number of facilities to be established increases. We do not observe a significant impact on the running time as N varies.

In Figures 4.12 and 4.13 we show the worst-case realizations of an earthquake and aftershocks on two small instances. Figure 4.12 shows the variation in aftershock realizations as Δ increases. The value of N was set to 3. We see that even though the worst-case changes, the locations of the facilities remain the same.

Figure 4.13 shows two different worst-cases for the same instance with the same parameter values. This leads us to conclude that we can have multiple worst-case realizations. We hypothesize that this would be more evident for larger instances. However, we could only visualize the worst case for $\mathbf{P}_{\mathbf{xy}}^{\mathbf{full}}$, and since we could not solve the larger instances for $\mathbf{P}_{\mathbf{xy}}^{\mathbf{full}}$, we are unable to report them.

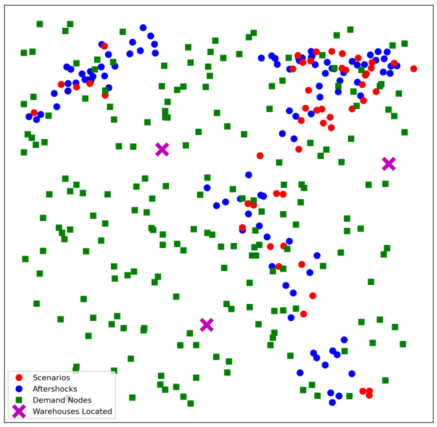

(a) $\Delta = 3$

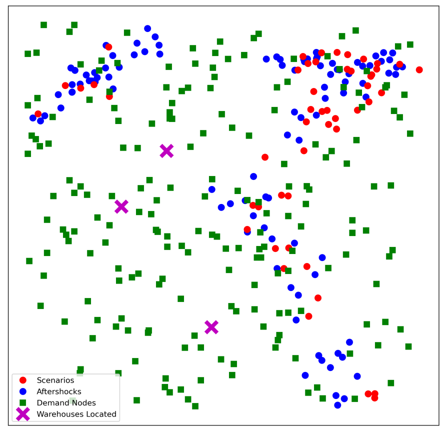

(b) $\Delta = 5$

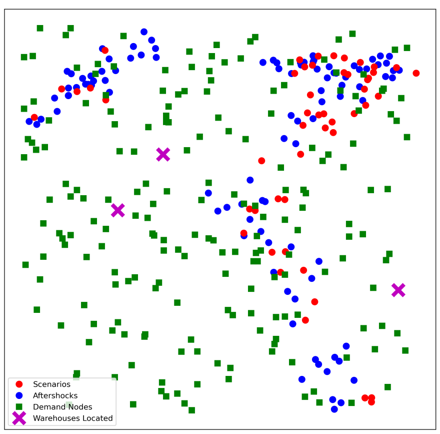

(c) $\Delta = 7$

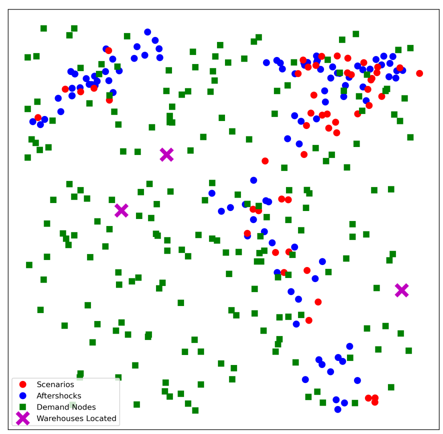

(d) $\Delta = 10$

Figure 4.10: The change in solutions as Δ changes

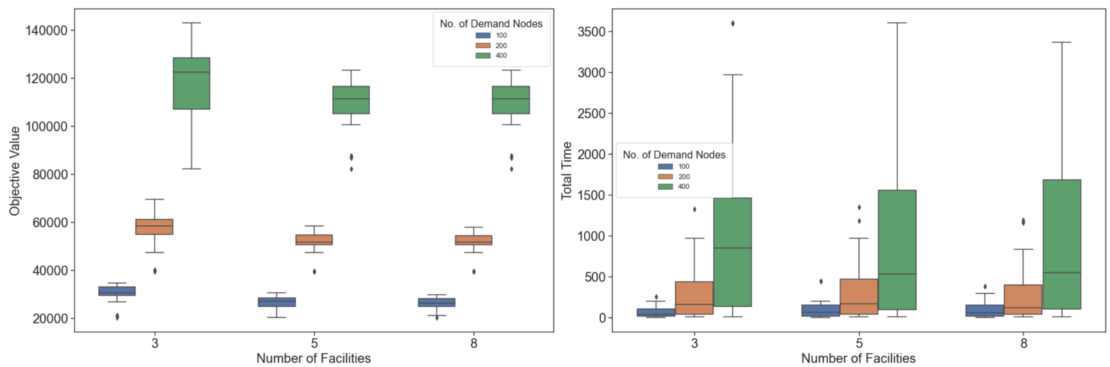

(a) Objective Value as N increases

(b) Total time as N increases

Figure 4.11: Comparison of the objective value and the total time as N increases

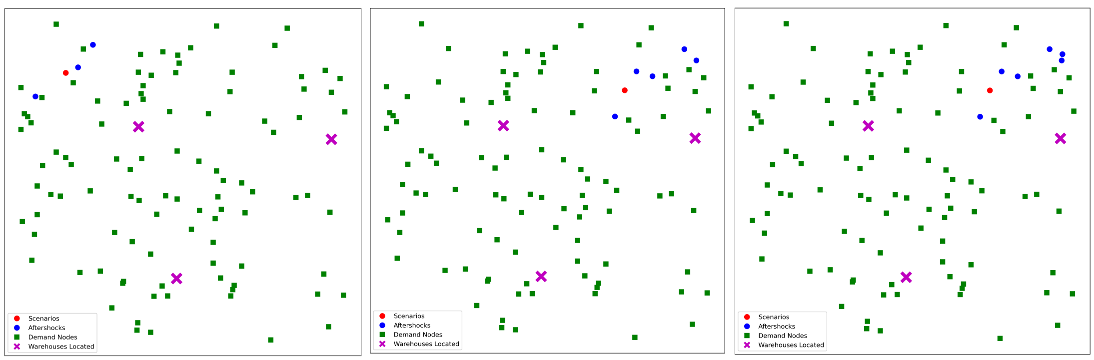

(a) Δ= 3

(b) Δ= 5

(c) Δ= 7

Figure 4.12: The worst-case realizations of the aftershocks as Δ increases

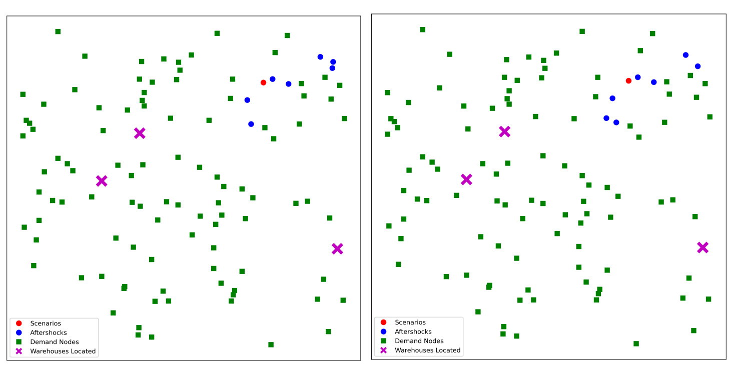

(a)

(b)

Figure 4.13: Two different worst-case realizations of an instance with the same parameter values

4.8 Case study on Turkey-Syria 2023 earthquake

In this section, we provide a case study on Turkey, based on data from the Turkey-Syria earthquake of 2023. We focus our analyses only on Turkey, firstly, because we found detailed earthquake damage data corresponding to Turkey, and secondly, our models are designed for decision-makers at the regional or national level.

Turkey lies at the intersection of three tectonic plates: the Anatolian, the Arabian, and the African, and has been affected by several earthquakes due to the interaction between these plates. Between 1900 and 2023, Turkey has experienced 269 earthquakes that caused loss of lives and property, including 20 earthquakes of magnitude over 7 (Government of Türkiye, 2023). Thus, earthquake preparedness is crucial in Turkey as effective and efficient planning and response to earthquakes is key to saving lives and combatting economic losses.

In February of 2023, Turkey was affected by a series of devastating earthquakes. The first earthquake of magnitude 7.7 hit on February 6 in the Pazarcık district in the Kahramanmaraş province at 4:17 local time. It was followed by another earthquake of magnitude 7.6 approximately nine hours later in the Elbistan district of the same province. Several aftershocks of varying magnitudes followed, including at least 14 more earthquakes of magnitudes 5.4 and above within two days of the main earthquake (Kawoosa, 2023). On February 20, a major aftershock of magnitude 6.3 occurred in the Yayladaği district of the Hatay province. Another aftershock of magnitude 5.6 hit the Malatya province on February 27th. According to Turkey's Disaster and Emergency Management Authority (AFAD), more than 11,000 aftershocks had occurred by March 1st. 11 provinces in Turkey were were majorly affected– Adana, Adıyaman, Diyarbakır, Gaziantep, Hatay, Elazig, Kahramanmaraş, Kilis, Malatya, Osmaniye, Sanliurfa (Government of Türkiye, 2023). Later, six other provinces were also identified as affected because of damages observed (OCHA, 2023a). The list of earthquakes and aftershocks over magnitude 5.4 (inclusive) is provided in the Table B.5.

Not only that, the region continued to face dire circumstances in the months that followed. The provinces of Adıyaman and Şanlıurfa were affected by heavy rainfall in March that caused floods, resulting in casualties and damages to buildings, bridges, and highways (ECHO, 2023). Heavy rain also affected the provinces of Adıyaman, Kahramanmaraş, Malatya, Şanlıurfa, and Hatay on 10 and 11 April and caused floods in tents in the earthquake-hit areas (OCHA, 2023b). A major storm occurred in Pazarcık, affecting 300 households, injuring around 45 people, and damaging the already devastated region (OCHA, 2023c). These additional disasters have made the response and recovery more difficult.

Over 50,000 people lost their lives, 3.3 million people were displaced, almost 2 million people were sheltered in tent camps and container settlements, and buildings and villages were ruined across 110,000 square km (Government of Türkiye, 2023). Table 4.3 provides the data of damages to life in terms of deaths and injured (Göçümlü, 2023), and the number of buildings that were damaged (Hürriyet, 2023). The damages to life were reported as of February 10, 2023, while the damages to property were reported as of February 16, 2023. Heavily damaged buildings are defined as those that have been demolished or need to be demolished urgently as they pose a threat of collapse injuring more people.

Table 4.3: Report of Damages to Life and Property

Province	Damage to Life (As of February 10, 2023)		Damages to Independent Units and Buildings (As of February 16, 2023)							
			Heavy Damages		Moderate Damages		Slight Damages		Undamaged	
	Deaths	Injured	Independent Units	Buildings	Independent Units	Buildings	Independent Units	Buildings	Independent Units	Buildings
Adana	408	7,450	1,274	59	7,270	304	38,261	1,688	78,040	5,313
Adıyaman	3,105	11,778	29,703	6,990	11,179	2,613	38,823	11,694	21,365	9,310
Diyarbakır	212	899	6,932	643	10,095	718	86,925	6,725	178,216	18,039
Gaziantep	2,141	11,563	31,522	12,964	17,050	4,361	179,149	29,471	309,389	89,092
Hatay	5,111	15,613	71,735	15,248	18,146	2,827	62,034	17,212	74,851	29,188
Elazig	5	379	4,043	664	801	138	15,532	1,460	9,503	723
Kahramanmaraş	4,879	9,243	60,051	12,980	7,671	1,058	99,481	20,556	61,932	25,420
Kilis	74	754	1,224	812	1,033	137	16,296	2,208	12,228	2,849
Malatya	289	7,300	44,996	8,365	6,617	945	59,825	8,960	31,894	7,463
Osmaniye	878	2,224	9,595	2,531	2,104	266	40,929	8,034	51,409	22,041
Sanliurfa	304	4,663	2,725	466	4,707	550	112,399	13,507	86,896	19,585

The earthquake of February 2023 is just one of many that have continued to hit the country in the past century. Lying in a region prone to earthquakes makes it extremely essential to be prepared for such calamitous events. In this section, we study the abovementioned earthquake to generate insights on the location of facilities in the region for storing relief materials. We first discuss the generation of instances in the following subsection.

4.8.1 Instance generation for Turkey

We generate the Turkish instances based on the publicly available damage data reported in Table 4.3 following the earthquake of February 2023, and the seismic hazard map provided by AFAD, shown in Figure 4.14. The map shows the regions of Turkey and a visual representation of their risk of being hit by an earthquake. The regions in red are the ones that are at the greatest risk, as they lie along the fault lines, and historically, the majority of the earthquakes have been recorded here. As we move toward the orange and yellow regions, the risk of earthquakes decreases.

We focus our study on the eastern region of Turkey. We include the following provinces in our analyses: Adana, Adiyaman, Agri, Amasya, Ardahan, Artvin, Batman, Bayburt, Bingol, Bitlis, Diyarbakir, Elazig, Erzincan, Erzurum, Gaziantep, Giresun, Gumushane, Hakkari, Hatay, Igdir, Kahramanmaras, Kars, Kayseri, Kilis, Malatya, Mardin, Mus, Ordu, Osmaniye, Rize, Samsun, Sanliurfa, Siirt, Sirnak, Sivas, Tokat, Trabzon, Tunceli, Van, and Yozgat. The demand nodes are considered to be the centers of each district in each of the provinces. We have a total of 420 districts in the provinces in our study, and correspondingly 420 demand nodes.

Guided by the seismic hazard map and the geographical data of Turkey, we construct the map shown in Figure 4.15 for our study. We classify each district of each province in the eastern part of the country into *High-Risk*, *Moderate-Risk*, and *Low-Risk* zones, based on the hazard map. The districts in red are the ones that are at the highest risk of experiencing an earthquake, while the orange districts are the ones with moderate risks of earthquakes. The districts in the yellow region are considered low-

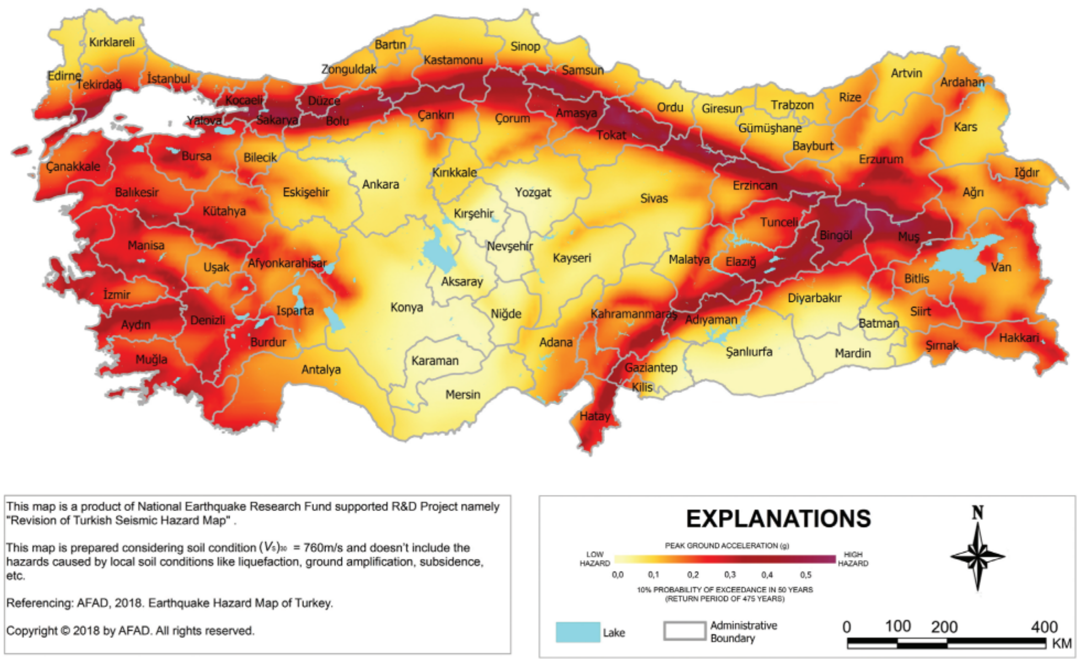

Figure 4.14: The Earthquake Hazard Map of Turkey, *Source:* AFAD

risk zones, and hence, these are the districts chosen for establishing the facilities. Tables B.1, B.2, and B.3 in the Appendix B.2 gives the list of districts in each category. We consider 70% of the earthquakes (including aftershocks) to occur in the red region and 30% in the orange region in our instances.

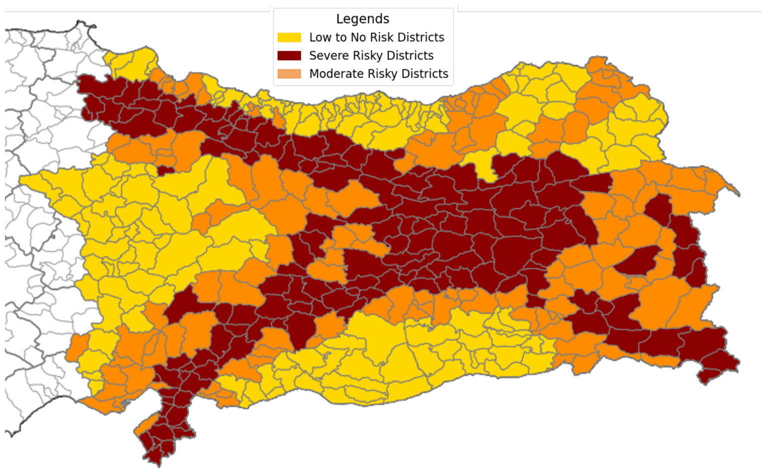

Figure 4.15: Earthquake hazard map used in the paper, classified into High, Moderate, and Low risk areas

We do the following to determine the aftershocks that can follow a major earthquake. We divide the area under study into three regions or risk zones, each region consisting of a collection of Turkish provinces. A major earthquake in one of the risk zones may trigger any Δ number of aftershocks in the same risk zone in the second stage. Table 4.4 lists the provinces in each risk zone. This classification is also based on the idea of fault lines.

Table 4.4: Classification of Turkish provinces into Risk Zones

Risk Zone	Provinces
Zone 1	Adana, Adiyaman, Batman, Diyarbakir, Elazig, Gaziantep, Hatay, Kahramanmaras, Kilis, Malatya, Osmaniye
Zone 2	Agri, Ardahan, Bayburt, Bingol, Bitlis, Erzurum, Hakkari, Igdir, Mus, Rize, Siirt, Sirnak, Van
Zone 3	Amasya,Erzincan, Giresun, Gumushane, Ordu, Samsun, Sivas, Tokat, Tunceli

For Turkey, we generate the number of main earthquakes (or scenarios) ranging from 10 to 100 and aftershocks ranging from 20 to 200. Once again, the number of aftershocks in each instance is twice the number of major earthquakes, and the earthquake locations are generated in an inclusive manner. For the locations of the facilities, we randomly choose 30 of the 69 districts in the low-risk zone. We assume that these facilities will be unaffected by the earthquakes, either because they are in the low-risk zones, and so they will be far off from the epicenters, or they will be earthquake proof buildings. We set the value of Δ to 3, 5, 7, and 10, and the maximum number of facilities to be located to 2, 4, 6, and 8. In total, we had 160 instances for Turkey. The calibration of parameters k, α, β in demand functions is the same as for Section 4.7, which was already based on the Turkish earthquake data (see Appendix B.2 for more details).

4.8.2 Computational results

We use formulation $\mathbf{P}_{\mathbf{xy}}^{\mathbf{sep}}$ to implement our robust model on Turkey. We were able to solve 145 out of the 160 instances to optimality within an hour. Figure 4.16 shows the solution of an instance. Once again, the red and the blue circles represent the scenarios and the aftershocks, respectively. The pink crosses show the locations selected for establishing the facilities. The green squares show the district centers. Figure 4.17 shows the objective function value with respect to the values of Δ and N.

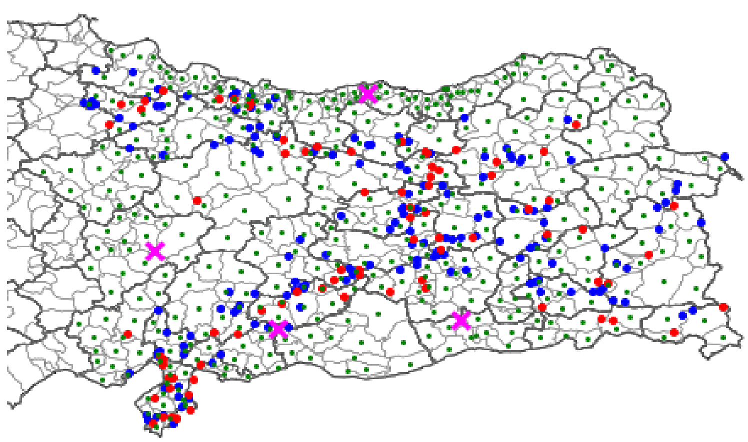

Figure 4.16: The solution of an instance of Turkey showing four locations for the facilities

As expected, the objective value increases with an increase in Δ. From Figure 4.17(b), we infer that it is enough for us to consider locating four facilities in the eastern region. When going from 2 facilities to 4, we see a significant drop in the objective value, whereas, thereafter, the decrease in the objective value as the number of facilities increases is lower.

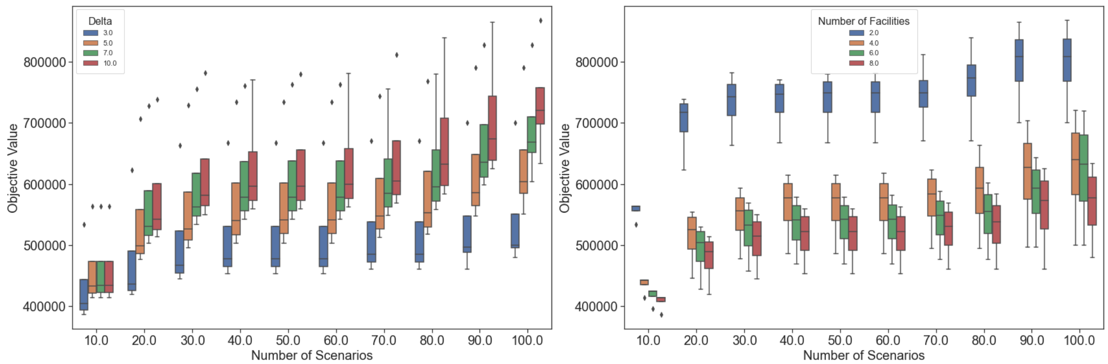

(a) Objective value vs Δ

(b) Objective value vs N

Figure 4.17: The value of the objective function wrt Δ and N as the number of scenarios and aftershocks increases

As we implemented our robust model on the instances, we noticed that some of the locations were selected more often than others, even as the distribution of the main earthquakes and the aftershocks changed. Figure 4.18 shows the percentage of times each location was selected for establishing facilities. For example, district Halfeti was selected 98% of the times, followed by district Mazidagi, which was selected in 91% of the instances. Districts Yesilhisar and Sarikaya were both selected over 60% of the time. Thus, this gives an insight for the decision makers regarding the preferable areas or districts to set up the facilities.

While we estimated our demand using publicly available data from the Turkey 2023 earthquake, we do not use it here to make recommendations about the capacities of the facilities to be built. This is because the data was reported in the early days following the earthquake. As time passed by, the number of affected people was revealed to be much larger. Moreover, there were other local emergencies in the region as well. However, our results related to the locations of the facilities remain valid, as the demand distribution remained similar, with an increase in the proportion of demand.

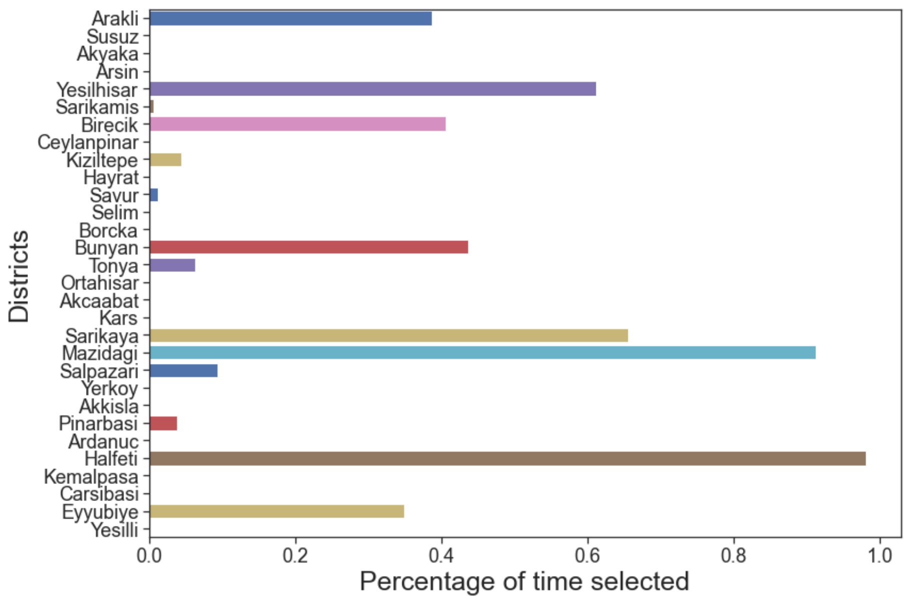

Figure 4.18: Graph showing the percentage of times the location in each district was selected for setting up the facilities

4.8.3 Comparison with a "first-stage only" model without aftershocks

To study the importance of including aftershocks in locating facilities, we remove the aftershocks. We compare our two-stage robust model with a model that uses only the first stage or the main earthquake to select facilities. The first-stage model without aftershocks is given as:

$$\mathbf{P}_{\mathbf{xy}}^{\mathbf{StageI}} : \quad \min \ \theta \tag{4.27a}$$

$$\text{subject to} \quad \theta \geq \sum_{i \in \mathcal{D}} \sum_{j \in \mathcal{F}} t_{ij} d_{si}^{1} x_{ij} \qquad s \in \mathcal{S} \tag{4.27b}$$

$$\sum_{j \in \mathcal{F}} x_{ij} = 1 \qquad i \in \mathcal{D} \tag{4.27c}$$

$$y_j \geq x_{ij} \qquad i \in \mathcal{D},\ j \in \mathcal{F} \tag{4.27d}$$

$$1 \leq \sum_{j \in \mathcal{F}} y_j \leq N \tag{4.27e}$$

$$\theta \geq 0, \quad x_{ij}, y_j \in \{0,1\} \qquad i \in \mathcal{D},\ j \in \mathcal{F} \tag{4.27f}$$

This is the same as model 4.2, with constraint (4.2b) replaced by (4.27b), where the second-stage demand due to the aftershocks have been omitted.

We evaluate the two-stage robust model and $\mathbf{P_{xy}^{StageI}}$ on the instances. Once we have the solution (the locations of the facilities to be established) from $\mathbf{P_{xy}^{StageI}}$, we fix them and evaluate this solution in the second stage, i.e., in the presence of aftershocks. This is done to study the gap between the two-stage robust solution and the first-stage solution when aftershocks occur. In other words, what if we established the facilities without taking aftershocks into account, and later, the region was hit by an earthquake followed by a series aftershocks. Firstly, we notice that the location of the facilities obtained from the robust solution and the stage 1 solution never completely match.

In Figure 4.19, we show the gap between the two-stage robust solution and the stage 1 solution with respect to the number of scenarios, the number of demand nodes, Δ, and N. The gap is calculated via the following formula

$$\text{Gap} = \frac{\text{ROV}_1 - \text{ROV}_2}{\text{ROV}_2} \tag{4.28}$$

where, ROV_1 is the stage 1 solution evaluated when the second stage or the aftershocks occur, and ROV_2 is the two-stage robust solution.

For the instances with 100 scenarios, we see slight negative gaps in the solution. This is because we were not able to solve the instances to optimality using the robust model. The gap between the two solutions goes over 12.5%. On average, up to 90 scenarios, we observe a gap of 4.43%.

As we expected, we observe an increase in the percentage gap as Δ increases, and it becomes more important to consider aftershocks into the decision-making process. As N increases, there is a decrease in the gap. This is because with a higher number of facilities, most of the locations selected overlap. Varying the number of scenarios does not have a significant impact on the median gap.

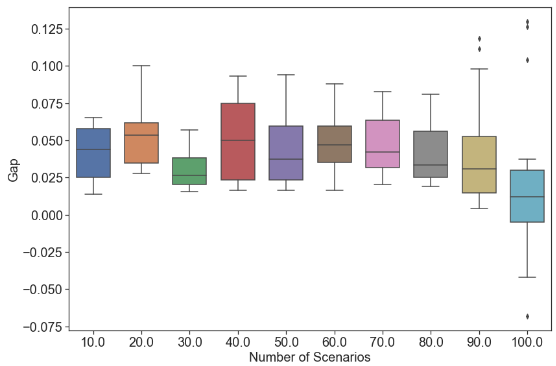

(a) Percentage Gap vs Number of Scenarios

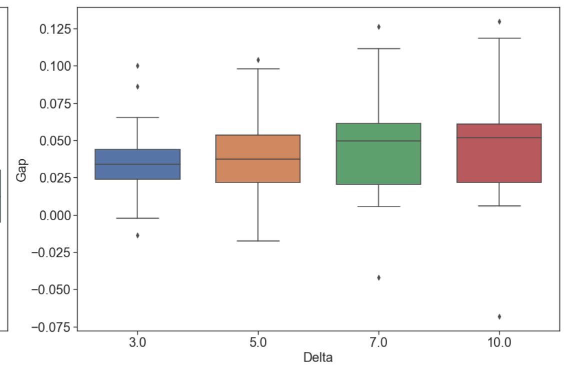

(b) Percentage Gap vs Δ

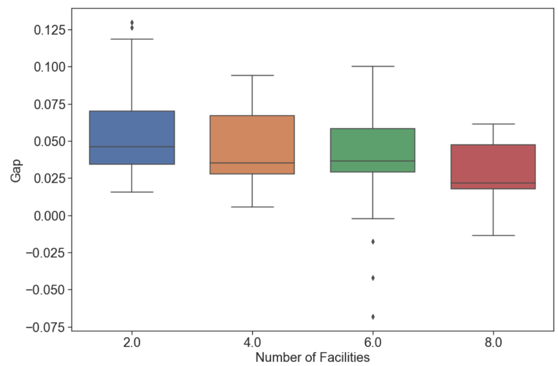

(c) Percentage Gap vs N

Figure 4.19: The percentage gap between the robust solution and the stage 1 solution in the presence of aftershocks

4.9 Conclusion

In this study, we study an uncapacitated facility location problem for earthquake management taking into account aftershocks. We wish to prepare for a situation where a region is hit by a major earthquake followed by at most Δ aftershocks. We adapt a robust modeling approach with our uncertainty set defined as a combination of aftershocks that can potentially follow a major earthquake. To this end, we propose four robust mixed-integer linear programming models. The first is where we fully enumerate all combinations of earthquakes and aftershocks ($\mathbf{P^{full}_{xy}}$). While it is a simple formulation, the number of combinations of scenarios and aftershocks increases exponentially, and we are unable to solve it beyond a few scenarios. We then propose a branch-and-cut solution approach for the above formulation ($\mathbf{P^{sep}_{xy}}$) by separating the constraints related to the demand allocation. Thirdly, we propose an extended formulation for the above problem ($\mathbf{P^{ext}_{xy}}$). Finally, we formulate the problem in two stages ($\mathbf{P_y}$)– the first determining the worst-case demand following the major earthquake, and the second related to the worst-case demand because of Δ aftershocks.

Out of the four models, we find $\mathbf{P^{sep}_{xy}}$ to be the one that performs the best computationally. $\mathbf{P^{ext}_{xy}}$, although is solved the fastest once the model is built, CPLEX takes a prohibitive time to build the MILP initially, so it does not compete with $\mathbf{P^{sep}_{xy}}$ at all for the total computation time. $\mathbf{P_y}$'s performance lies in between the two. We observe that the models become more challenging to solve as the number of major earthquakes and aftershocks increase. Counterintuitively, we observe that as Δ increases for the best method $\mathbf{P^{ext}_{xy}}$, it results in a decrease in the computational time, contrary to the $\mathbf{P^{full}_{xy}}$ approach.

We also provide a case-study on the eastern region of Turkey with recommendations for locations where facilities can be set up. We use publicly available demand data following the Turkey-Syria earthquakes of February 2023 to calibrate our demands. We find four locations in the districts of Halfeti, Mazidagi, Yesilhisar, and Sarikaya, where the facilities can be set up. We also observe gaps of up to 12.5% in the solution if aftershocks are not taken into account. These insights can guide the facility location decisions not just in Turkey, but in other regions as well.

Though our models are based on earthquakes and aftershocks, they are not limited to aftershocks only. They can also be applied to any kind of simultaneous or compound disasters. The aftershocks in the second stage can be replaced by other disasters like floods, tsunamis, landslides, fires, which occur around the same time in a neighboring region of the primary disaster or the earthquake, either as a result of the earthquake or independently. As long as we are able to estimate or forecast the demands due to any of the emergencies, our model can serve as a viable decision support tool.

While we provide an initial study taking into account the impact of aftershocks, there are several avenues for future research. Firstly, it would be interesting to study the models and the solution structures under capacity constraints and consider inventory prepositioning. We have also assumed that the facilities would not be damaged by the earthquakes. However, there might be facility disruptions or network disruptions between the facilities and the demand nodes, which would be worth looking further into. Another interesting direction would be to study multi-level facility location, with relief-storing warehouses at the higher level and local distribution centers at the city level, which can serve as both shelter sites for evacuees and relief distribution points.

B

Appendix Chapter 4

B.1 Proof of Propositions

Proof of Proposition 3

First, we check the primal and dual feasibility of the proposed solution.

For a given $i \in \mathcal{D}$, the first constraint of the primal subproblem is:

$$\sum_{j \in \mathcal{F}} x_{ij} = \sum_{j=1}^{p_i - 1} y_j^* + 1 - \sum_{j=1}^{p_i - 1} y_j^* + 0 \; = \; 1$$

For the second primal constraint, we have $x_{ij} \geq 0$ from its definition. For each $i \in \mathcal{D}$

$$x_{ij} = \begin{cases} y_j^*, & j < p_i \\ 1 - \sum\limits_{j=1}^{p_i - 1} y_j^*, & j = p_i \\ 0, & j > p_i \end{cases} \quad \leq \quad y_j^*.$$

The first and the third cases are trivial. For $j = p_i$, we have $1 - \sum_{j=1}^{p_i-1} y_j^* - y_{p_i}^* = 1 - \sum_{j=1}^{p_i} y_j^* \leq 0$, which follows from the choice of p_i. Thus, x_{ij} is a feasible solution of the primal subproblem (4.16).

For verifying the dual feasibility, for each $i \in \mathcal{D}$ and $j \in \mathcal{F}$, when $j < p_i$,

$$\lambda_i - \mu_{ij} \; = \; t_{ip_i} d_{si}^1 \; - \; t_{ip_i} d_{si}^1 + t_{ij} d_{si}^1 = t_{ij} d_{si}^1,$$

and when $j \geq p_i$,

$$\lambda_i - \mu_{ij} = t_{ip_i} d_{si}^1 \leq t_{ij} d_{si}^1$$

follows from the choice of p_i. Since p_i is the closest open facility to i, $t_{ip_i} \leq t_{ij}, \;\; \forall j \in \mathcal{F}$.

Next, we evaluate the objective functions of the primal and the dual. The objective of the primal is:

$$\sum_{i\in\mathcal{D}} d_{si}^1 \sum_{j\in\mathcal{F}} t_{ij}x_{ij} = \sum_{i\in\mathcal{D}} \left(\sum_{j=1}^{p_i-1} d_{si}^1 t_{ij} y_j^* + d_{si}^1 t_{ip_i} - \sum_{j=1}^{p_i-1} d_{si}^1 t_{ip_i} y_j^* \right).$$

The value of the dual objective is:

$$\sum_{i\in\mathcal{D}} \lambda_i - \sum_{i\in\mathcal{D}} \sum_{j\in\mathcal{F}} y_j^* \mu_{ij} = \sum_{i\in\mathcal{D}} t_{ip_i} d_{si}^1 - \sum_{i\in\mathcal{D}} \sum_{j=1}^{p_i-1} t_{ip_i} d_{si}^1 y_j^* + \sum_{i\in\mathcal{D}} \sum_{j=1}^{p_i-1} t_{ij} d_{si}^1 y_j^*.$$

Since the solution described in Proposition 3 is feasible for the primal subproblem (4.16) and the dual subproblem (4.18), and give the same objective values for both, it is also an optimal solution for the subproblems.

Proof of Proposition 4

The formulation in the space of the y variables, denoted by $\mathbf{F_y}$ is

$$\min_{\substack{y\in Y \\ 1\le \sum_{j\in\mathcal{F}} y_j \le N}} \left\{ \max_{s\in\mathcal{S}} \left\{ \max_{\substack{(\lambda,\mu)\in\mathcal{L}_s^1 \\ (\alpha,\beta,u)\in\mathcal{L}_s^2}} \sum_{i\in\mathcal{D}} \lambda_i - \sum_{i\in\mathcal{D}} \sum_{j\in\mathcal{F}} y_j^* \mu_{ij} + \sum_{i\in\mathcal{D}} \sum_{k\in\mathcal{K}_s} d_{ik}^2 \alpha_{sik} - \sum_{i\in\mathcal{D}} \sum_{j\in\mathcal{F}} \widehat{D}_i y_j^* \beta_{sij} \right\} \right\}. \tag{B.1}$$

Writing the above model in the extended form, we have,

$$\min \;\; \theta \tag{B.2a}$$

$$\theta \geq \sum_{i\in\mathcal{D}} \lambda_i^* \; - \sum_{i\in\mathcal{D}}\sum_{j\in\mathcal{F}} \mu_{ij}^* y_j \; + \sum_{i\in\mathcal{D}}\sum_{k\in\mathcal{K}_s} d_{ik}^2 \, \alpha_{sik}^* \; - \sum_{i\in\mathcal{D}}\sum_{j\in\mathcal{F}} \widehat{D}_i y_j \beta_{sij}^* \tag{B.2b}$$

$$(\lambda,\mu) \in \mathcal{L}_s^1, \;\; (\alpha,\beta,u) \in \mathcal{L}_s^2 \;\; s \in \mathcal{S}$$

$$1 \leq \sum_{j\in\mathcal{F}} y_j \leq N \qquad j \in \mathcal{F} \tag{B.2c}$$

$$y_j \in \{0,1\} \qquad j \in \mathcal{F}. \tag{B.2d}$$

Using Proposition 3, for any choice of y^*, we have a closed-loop formula that gives us an extreme point of the dual of the problem $T^1_{s,i}(y^*)$. We notice that different values of y^* correspond to different "critical items". Since each critical item corresponds to a different facility, there are $|\mathcal{F}|$ of them, one for each $p \in \mathcal{F}$, and so

$$\begin{aligned} T^1_{s,i}(y^*) &= \max_{\lambda\in\mathbb{R}^{|\mathcal{F}|},\mu\geq 0} \;\; \{\lambda_i \; - \sum_{j\in\mathcal{F}} y_j^* \, \mu_{ij} : \lambda_i - \mu_{ij} \leq t_{ij} d^1_{si}, j \in \mathcal{F}\} \\ &= \max_{p_i\in\mathcal{F}} \{t_{ip_i} - \sum_{j\in\mathcal{F}} (t_{ip_i} - t_{ij})^+ y_j^*\}. \end{aligned}$$

Hence, since $T^1_s(y^*) = \sum_{i\in\mathcal{D}} T^1_{s,i}(y^*)$ we have

$$T^1_s(y^*) = \max_{(p_1,\ldots,p_{|\mathcal{D}|})\in\mathcal{F}^{|\mathcal{D}|}} \sum_{i\in\mathcal{D}} d^1_{si} \left[t_{ip_i} - \sum_{j\in\mathcal{F}} (t_{ip_i} - t_{ij})^+ y_j^* \right].$$

Therefore, the equation (B.2b) can be restated as:

$$\theta \geq \sum_{i \in \mathcal{D}} d^1_{si} \left[t_{ip_i} - \sum_{j \in \mathcal{F}} (t_{ip_i} - t_{ij})^+ y_j \right] + \sum_{i \in \mathcal{D}} \sum_{k \in \mathcal{K}_s} d^2_{ik}\, \alpha^*_{sik} - \sum_{i \in \mathcal{D}} \sum_{j \in \mathcal{F}} \widehat{D}_i y_j \beta^*_{sij}, \tag{B.3}$$

$$(\alpha^*, \beta^*, u^*) \in \mathcal{L}^2_s, s \in \mathcal{S}, (p_1, \ldots, p_{|\mathcal{D}|}) \in \mathcal{F}^{|\mathcal{D}|}.$$

Replacing (B.2b) by (B.3), we get the formulation $\mathbf{F_y}$.

B.2 Turkey Earthquake

Table B.1: Eastern Turkish districts that lie in the Severe Risk category for Turkish instances

	Provinces and Districts
	Adiyaman: Celikhan, Gerger, Golbasi, Adiyaman, Sincik, Tut
	Agri: Diyadin, Eleskirt
	Amasya: Gumushacikoy, Hamamozu, Amasya, Merzifon, Suluova, Tasova
	Batman: Sason
	Bingol: Adakli, Genc, Karliova, Kigi, Bingol, Solhan, Yayladere, Yedisu
	Bitlis: Hizan, Mutki
	Diyarbakir: Cungus, Dicle, Hani, Kulp, Lice
	Elazig: Alacakaya, Aricak, Karakocan, Kovancilar, Maden, Elazig, Palu, Sivrice
	Erzincan: Cayirli, Kemaliye, Erzincan, Otlukbeli, Refahiye, Tercan, Uzumlu
	Erzurum: Askale, Cat, Hinis, Horasan, Karacoban, Karayazi, Koprukoy, Palandoken, Pasinler, Tekman, Yakutiye
	Gaziantep: Islahiye, Nurdagi
	Giresun: Alucra, Camoluk, Sebinkarahisar
Severe-Risk	**Gumushane:** Kelkit, Kose, Siran
	Hakkari: Derecik, Hakkari, Semdinli, Yuksekova
	Hatay: Altinozu, Antakya, Belen, Defne, Dortyol, Hassa, Iskenderun, Kirikhan, Kumlu, Payas, Reyhanli, Samandag, Yayladagi
	Kahramanmaras: Caglayancerit, Dulkadiroglu, Ekinozu, Goksun, Nurhak, Pazarcik, Turkoglu
	Malatya: Akcadag, Arapgir, Arguvan, Battalgazi, Dogansehir, Doganyol, Kale, Puturge, Yazihan, Yesilyurt
	Mus: Bulanik, Haskoy, Korkut, Malazgirt, Mus, Varto
	Ordu: Akkus, Aybasti, Golkoy, Kabatas, Korgan, Kumru, Mesudiye
	Osmaniye: Bahce, Duzici, Hasanbeyli, Osmaniye, Toprakkale
	Samsun: Asarcik, Ayvacik, Havza, Kavak, Ladik, Vezirkopru
	Siirt: Baykan, Pervari
	Sirnak: Beytussebap
	Sivas: Akincilar, Dogansar, Golova, Koyulhisar, Susehri
	Tokat Almus, Basciftlik, Erbaa, Niksar, Resadiye
	Tunceli: Mazgirt, Tunceli, Nazimiye, Ovacik, Pulumur
	Van: Bahcesaray, Caldiran, Catak, Ozalp, Saray, Tusba

Table B.2: Eastern Turkish districts that lie in the Moderate Risk category for Turkish instances

	Provinces and Districts
Moderate-Risk	**Adana:** Ceyhan, Imamoglu, Karatas, Kozan, Pozanti, Saimbeyli, Saricam, Yumurtalik, Yuregir **Adiyaman:** Besni, Kahta, Samsat **Agri:** Dogubayazit, Hamur, Agri, Patnos, Taslicay, Tutak **Amasya:** Goynucek **Ardahan:** Cildir, Damal, Gole, Hanak, Ardahan, Posof **Batman:** Kozluk **Bayburt:** Aydintepe, Demirozu, Bayburt **Bitlis:** Adilcevaz, Ahlat, Guroymak, Bitlis, Tatvan **Diyarbakir:** Cermik, Egil, Ergani, Hazro, Kayapinar, Kocakoy, Silvan, Sur, Yenisehir **Elazig:** Agin, Baskil, Keban **Erzincan:** Ilic, Kemah **Erzurum:** Ispir, Narman, Oltu, Pazaryolu, Senkaya **Gaziantep:** Araban, Sehitkamil, Yavuzeli **Hakkari:** Cukurca **Hatay:** Arsuz, Erzin **Igdir:** Aralik, Igdir, Karakoyunlu, Tuzluca **Kahramanmaras:** Afsin, Andirin, Elbistan, Onikisubat **Kilis:** Kilis, Musabeyli, Polateli **Malatya:** Darende, Hekimhan **Ordu:** Camas, Gurgentepe, Kabaduz **Osmaniye:** Kadirli, Sumbas **Rize:** Ardesen, Camlihemsin, Cayeli, Derepazari, Findikli, Guneysu, Hemsin, Ikizdere, Iyidere, Kalkandere, Rize, Pazar **Samsun:** Atakum, Canik, Carsamba, Ilkadim, Salipazari, Tekkekoy **Siirt:** Eruh, Kurtalan, Siirt, Sirvan, Tillo **Sirnak:** Cizre, Sirnak, Silopi, Uludere **Sivas:** Altinyayla, Divrigi, Hafik, Imranli, Ulas, Zara **Tokat:** Artova, Tokat, Pazar, Turhal, Zile **Tunceli:** Cemisgezek, Hozat, Pertek **Van:** Baskale, Edremit, Ercis, Gevas, Gurpinar, Ipekyolu, Muradiye

Calibration of the demand function

To estimate the values of k, α, and β in formula (4.26) with a regression technique, we proceed in the following way. Table 4.3 gives the damages to human life (deaths and injuries) and property (independent units (IU) and buildings). Using this data, for each province, we calculate the demand using the

Table B.3: Eastern Turkish districts that lie in the Low Risk category for Turkish instances

	Provinces and Districts
Low-Risk	**Artvin:** Ardanuc, Arhavi, Borcka, Hopa, Kemalpasa, Artvin, Murgul, Savsat, Yusufeli **Kars:** Akyaka, Arpacay, Digor, Kagizman, Kars, Sarikamis, Selim, Susuz **Kayseri:** Akkisla, Bunyan, Hacilar, Melikgazi, Pinarbasi, Talas, Yesilhisar **Mardin:** Artuklu, Dargecit, Derik, Kiziltepe, Mazidagi, Midyat, Nusaybin, Omerli, Savur, Yesilli **Sanliurfa:** Akcakale, Birecik, Ceylanpinar, Eyyubiye, Halfeti, Haliliye, Harran, Suruc, Viransehir **Trabzon:** Akcaabat, Arakli, Arsin, Besikduzu, Carsibasi, Caykara, Dernekpazari, Duzkoy, Hayrat, Koprubasi, Macka, Of, Ortahisar, Salpazari, Surmene, Tonya, Vakfikebir, Yomra **Yozgat:** Bogazliyan, Candir, Yozgat, Sarikaya, Sefaatli, Sorgun, Yenifakili, Yerkoy

following formula:

$$\begin{aligned}\text{Observed Demand Data} = {} & (\text{Heavily Damaged IU} + 0.3 * \text{Moderately Damaged IU}) \\ & * \text{Percentage Residential Units} * \text{Unit Size}. \end{aligned} \tag{B.4}$$

All the people living in units that have been completely damaged would need shelter and basic amenities. Among the moderately damaged buildings, we assume that 30% of the people would need relief materials, and finally, the people whose houses have been moderately damaged are assumed to not require any external support. We also have some other parameters in the equation. The *Percentage Residential Units* refers to the percentage of residential buildings among all possible buildings. We take the value to be 0.6, excluding buildings like shopping areas, offices, schools, and other public places. *Unit Size* refers to the average number of people living in each unit or average family size, and we use the value 3.17 according to available public data (TSI, 2023). Thus, using the above formula, we estimate the demands in each of the affected province.

Next, we proceed toward calibrating the values of parameters k, α, and β in the demand equation (4.26). For each of the provinces and each earthquake, we create a distance matrix (created using the Haversine formula), which is shown in Table B.4. Then, for each province, we select the "most damaging earthquake", based on the distance between the province and the earthquake epicenter, and

Table B.4: Distance (in kilometers) between the provinces and the earthquake epicenters

Earthquake Index	***S0***	***A1***	***A2***	***A3***	***A4***	***A5***	***A6***	***A7***	***A8***	***A9***	***A10***	***A11***	***A12***	***A13***	***A14***
Magnitude	*7.8*	*5.7*	*6.7*	*5.6*	*7.5*	*6.0*	*5.4*	*5.8*	*5.7*	*6.0*	*5.4*	*5.4*	*5.5*	*5.4*	*5.5*
Province															
Adana	**152.08**	148.32	140.52	120.20	201.35	270.80	199.99	246.91	270.02	158.53	234.49	284.35	229.21	316.98	231.41
Adıyaman	126.47	129.67	137.89	164.97	**98.15**	32.92	97.77	50.82	42.15	158.38	49.40	48.22	48.07	48.79	57.49
Diyarbakır	294.08	297.69	305.74	330.12	**266.26**	187.65	266.41	214.07	192.92	327.17	219.87	183.42	220.93	141.74	226.25
Gaziantep	**36.00**	39.67	44.98	62.05	106.66	124.62	104.57	113.07	129.28	134.11	95.78	143.47	83.71	159.84	100.05
Hatay	**136.50**	134.75	127.64	99.42	221.89	266.00	219.86	249.41	269.13	208.87	232.83	283.93	222.58	304.18	234.23
Elazig	251.03	253.70	261.76	290.12	**189.74**	120.32	190.78	142.49	119.66	245.37	156.25	105.04	164.09	80.87	158.18
Kahramanmaraş	**41.11**	40.11	43.96	69.37	53.68	114.07	51.68	90.77	113.62	64.51	77.75	128.20	73.01	160.37	75.05
Kilis	**56.63**	57.81	56.19	49.25	144.64	169.79	142.48	157.58	174.37	158.47	140.31	188.61	128.52	204.10	143.95
Malatya	167.76	170.01	177.79	206.51	**101.62**	39.03	102.62	55.57	34.54	158.64	71.09	19.98	81.12	41.23	71.37
Osmaniye	**70.03**	66.35	58.39	39.54	134.29	194.72	132.51	172.86	195.26	111.73	158.59	210.05	151.56	239.28	157.06
Sanliurfa	**157.18**	161.09	168.26	187.96	169.16	113.94	168.14	129.94	123.18	224.40	122.93	126.88	115.32	105.24	132.04

the magnitude of the earthquake. This is a heuristic assignment because multiple earthquakes were in the vicinity of a demand node with different distances and magnitudes, but no available public data ever reported the damages caused by each individual earthquake and aftershock in each province. For each province, the distance that is reported in bold corresponds to the most impactful earthquake for that province.

Thus, once we have the estimated demand at each province using the distance from and the magnitude of the most damaging earthquake, and the population of the province from equation (4.26), and the actual demand using the formula (B.4), we calibrate the values of k, α, and β using least square estimation from the scipy package in python. The values we obtain are 0.25, 0.75, and 0.5, respectively.

Now. once we have generated our instances by randomly locating the earthquakes and aftershocks, we can use equation (4.26) to calculate the demand at each of the district centers due to each earthquake. Next, we implement our models on the Turkey instances.

Table B.5: Summary of Earthquakes and Aftershocks in Turkey of magnitude 5.4 or more between 6^{th} and 10^{th} February, 2023, (Source: USGS)

Earthquake Index	Date	Time	Latitude	Longitude	Magnitude	Place
S0	6^{th} Feb	01:17:34	37.2199	37.0189	7.8	Pazarcik, Kahramanmaras
A1	6^{th} Feb	01:26:50	37.2241	36.9749	5.7	22 km ENE of Nurdagi
A2	6^{th} Feb	01:28:15	37.1893	36.8929	6.7	14 km E of Nurdagi
A3	6^{th} Feb	01:36:27	36.9921	36.6832	5.6	Turkey-Syria border region
A4	6^{th} Feb	10:24:50	38.0155	37.2056	7.5	Elbistan, Kahramanmaras
A5	6^{th} Feb	10:26:46	38.0264	38.1044	6	11 km W of Çelikhan, Turkey
A6	6^{th} Feb	10:32:08	37.9962	37.2033	5.4	7 km S of Ekinözü, Turkey
A7	6^{th} Feb	10:35:58	38.0249	37.8023	5.8	9 km SW of Dogansehir, Turkey
A8	6^{th} Feb	10:51:30	38.0981	38.0511	5.7	15 km E of Dogansehir, Turkey
A9	6^{th} Feb	12:02:11	38.0582	36.5114	6	4 km NNE of Göksun, Turkey
A10	6^{th} Feb	15:14:34	37.8789	37.7345	5.4	13 km NE of Gölbasi, Turkey
A11	6^{th} Feb	15:33:32	38.19	38.1756	5.4	13 km SSW of Yesilyurt, Turkey
A12	7^{th} Feb	03:13:12	37.7639	37.7309	5.5	Central Turkey
A13	7^{th} Feb	07:11:15	38.0971	38.6398	5.4	7 km NNE of Sincik, Turkey
A14	8^{th} Feb	11:11:52	37.9368	37.6607	5.4	Central Turkey

B.3 Summary of Notations

Table B.6: List of sets and indices for the problem

Notations	
$\mathcal{S}$	set of all first-stage scenarios of the major earthquake (indexed by s)
$\mathcal{K}$	set of all aftershock nodes (indexed by k)
$\mathcal{K}_s$	set of all aftershocks in scenario s (indexed by k)
$\mathcal{D}$	set of all demand nodes (indexed by i)
$\mathcal{F}$	set of all facility nodes (indexed by j)

Table B.7: List of parameters

Parameters	
d^1_{si}	The demand at node i in stage 1 in scenario s
d^2_{ik}	The demand at node i due to an aftershock at node k in stage 2 in scenario s
t_{ij}	The travel time between demand node i and facility node j
Δ	The number of aftershocks to be protected against in the second stage
N	The maximum number of warehouses that can be constructed

5

Conclusion

In this thesis, we study two essays on last mile logistics. The first focuses on using public transportation systems for last mile deliveries. The second essay deals with workforce sizing and scheduling their shifts. Finally, in the third essay, we study a novel facility location problem in preparing for earthquakes, considering aftershocks and other emergencies that may follow.

In Chapter 2, we study an innovative last-mile logistics strategy that employs public transit networks to transport packages into urban areas. This restricts traditional delivery trucks inside the living area, reducing emissions and congestion on roads. To this end, we define the 3T-DPPT, and propose a comprehensive MILP formulation. We use a decomposition matheuristic solution approach, the decomposition based on the natural three tiers of the problem and the order of solving them. We provide numerical experiments to demonstrate the efficiency and effectiveness of the system using instances that are generated to mimic real cities. Our approach successfully handles instances with up to 80 customers. We find that the decomposition technique focused on solving the second tier of the problem first performs the best, striking a good balance between the objective values and solution time. We also investigate the impact of service costs related to the public transportation network, the frequency of public vehicles, and their available capacities, on the solutions obtained. Our results demonstrate that this system can reduce the length of trips performed by traditional delivery trucks (86 %) and dedicated delivery vehicles (51% for the trucks and freighters). Our concluding hypothesis is that the reduction in emissions and congestion would be significantly higher when we implement the system in large cities with an extensive public transportation network.

The above delivery strategy provides ample avenues for future research. First, the inherent uncertainties in the system require further investigation. On the one hand, customer orders may be unknown or dynamically arriving, while on the other hand, public vehicles may be subject to delays or have unreliable capacities. Thus, there are uncertainties in the demand as well as in the service network, and they can be handled using stochastic or robust optimization. The problem needs to be studied at a strategic level to include decisions like using one or multiple CDCs in the city, selecting lines and stops, and collaboration between multiple service providers and stakeholders (for example, different last mile logistics companies, public transit providers, and the administrative board of the city). One could also look into the problem at the tactical level and investigate fleet-sizing decisions for the trucks, freighters, and personnel, decisions related to the schedule of the public vehicles for transporting the packages, and decisions related to whether or not it would be beneficial to set up locker services at the stops, among others. Owing to the computational complexity of the problem, we need to develop efficient solution strategies that can solve large instances.

In Chapter 3, we continue with our study on last-mile logistics but focus on the tactical planning problem of workforce hiring and shift scheduling decisions. We develop models that seek to balance a delivery company's hiring and outsourcing costs. We study three different kinds of shift schedules for the freighters hired– fixed schedules (two determined starting times during the day), flexible schedules (having the possibility of starting the shifts at any time of the day), partially flexible schedules (two fixed shifts whose starting time is a decision variable). We tested our models on instances generated based on four European cities– Paris, Lyon, Berlin, and Frankfurt with a variety of instance generation parameters. We find the average per-parcel cost using fixed shifts is 9% higher than that of completely flexible shifts. On the other hand, partially flexible shifts incur only 2% higher costs than the flexible shift schedule model. Thus, it is an economical solution for the delivery company and a sustainable solution for the freighters, providing them with better working conditions.

One of the most interesting extensions to this study would be to investigate districting decisions coupled with workforce sizing, instead of considering the existing districts of the city. Determining a heterogeneous fleet for transport, like drones, robots, and outsourced deliveries, along with hiring decisions may also prove beneficial to the delivery company. Finally, studying rostering decisions from the worker's point of view, taking into account their preferences and familiarity, would help improve their working conditions further.

In Chapter 4, we shift our attention to disaster preparedness and study an uncapacitated facility location problem for earthquakes and aftershocks. We develop a two-stage robust model, where a region can be hit by a major earthquake in the first stage, followed by at most Δ aftershocks in the second stage. We first propose a MILP formulation that fully enumerates all possible earthquake and aftershock combinations. This becomes computationally challenging, leading us to employ two branch-and-cut formulations and an extended formulation approach to redesign the problem. We implement our models on synthetic instances designed to mimic fault line behaviors. Of all the models, we find Model $\mathbf{P}_{\mathbf{xy}}^{\mathbf{sep}}$ to perform the best computationally. We also use our approach to study the Turkey-Syria earthquake of 2023, with a focus on setting up facilities in the eastern region of Turkey. We find that including aftershocks can improve the location-allocation decisions by up to 12.5%.

Disaster management is an extensive process with an unlimited scope for improvement. Our model can be extended to include capacity limitations and inventory prepositioning decisions. Moreover, uncertainties in all facets of the problem– the demand side (uncertain volume of demands), the supply side (facility disruptions), and the service network (network disruptions and travel time uncertainties)– need to be carefully investigated. Our goal should be working toward a detailed disaster mitigation, preparedness, response, and recovery plan, to minimize the lives affected by humanitarian emergencies.

There are a plethora of problems that we, as a society, need to look into, and find sustainable solutions that balance social, environmental, and economic costs successfully.

References

Acar, M. & Kaya, O. (2019). A healthcare network design model with mobile hospitals for disaster preparedness: A case study for Istanbul earthquake. *Transportation Research Part E: Logistics and Transportation Review*, 130, 273–292.

Adsanver, B., Balcik, B., Bélanger, V., & Rancourt, M.-È. (2023). Operations research approaches for improving coordination, cooperation, and collaboration in humanitarian relief chains: A framework and literature review. *European Journal of Operational Research*.

Aghaie, S. & Karimi, B. (2022). Location-allocation-routing for emergency shelters based on geographical information system (ArcGIS) by NSGA-II (Case study: Earthquake occurrence in Tehran (District-1)). *Socio-Economic Planning Sciences*, 84, 101420.

Ahmed, S. K., Chandran, D., Hussein, S., Sv, P., Chakraborty, S., Islam, M. R., & Dhama, K. (2023). Environmental health risks after the 2023 Turkey-Syria earthquake and salient mitigating strategies: a critical appraisal. *Environmental Health Insights*, 17, 11786302231200865.

Aleskerov, F., Say, A. I., Toker, A., Akin, H. L., & Altay, G. (2005). A cluster-based decision support system for estimating earthquake damage and casualties. *Disasters*, 29(3), 255–276.

Alfonso, V., Boar, C., Frost, J., Gambacorta, L., & Liu, J. (2021). *E-commerce in the pandemic and beyond*. Bulletin 36, Bank for International Settlements.

Alizadeh, M., Amiri-Aref, M., Mustafee, N., & Matilal, S. (2019). A robust stochastic casualty collection points location problem. *European Journal of Operational Research*, 279(3), 965–983.

Altay, N. & Green III, W. G. (2006). OR/MS research in disaster operations management. *European journal of operational research*, 175(1), 475–493.

Alturki, I. & Lee, S. (2023). A systematic survey of multicriteria models in humanitarian logistics. *International Journal of Disaster Risk Reduction*, (pp. 104209).

Amideo, A. E., Scaparra, M. P., & Kotiadis, K. (2019). Optimising shelter location and evacuation routing operations: The critical issues. *European Journal of Operational Research*, 279(2), 279–295.

Ananat, E. & Gassman-Pines, A. (2021). Work schedule unpredictability: Daily occurrence and effects on working parents' well-being. *Journal of Marriage and Family*, 83, 10–26.

Arrieta-Prieto, M., Ismael, A., Rivera-Gonzalez, C., & Mitchell, J. (2022). Location of urban micro-consolidation centers to reduce the social cost of last-mile deliveries of cargo: A heuristic approach. *Networks*, 79(3), 292–313.

Aydin, N. & Cetinkale, Z. (2023). Simultaneous response to multiple disasters: Integrated planning for pandemics and large-scale earthquakes. *International journal of disaster risk reduction*, 86, 103538.

Azcuy, I., Agatz, N., & Giesen, R. (2021). Designing integrated urban delivery systems using public transport. *Transportation Research Part E: Logistics and Transportation Review*, 156, 102525.

Bacher, P., Klopp, J. M., Ortbauer, M., & Lackner, M. (2024). The potential of combining passenger rail with freight: A New York city case study. *Journal of Public Transportation*, 26, 100093.

Balcik, B. & Beamon, B. M. (2008). Facility location in humanitarian relief. *International Journal of Logistics*, 11(2), 101–121.

Banerjee, D., Erera, A. L., & Toriello, A. (2022). Fleet sizing and service region partitioning for same-day delivery systems. *Transportation Science*, 56, 1327–1347.

Baron, E. (2019). Amazon looks to turn public buses into mobile delivery stations. Accessed 01.10.2021.

Behiri, W., Belmokhtar-Berraf, S., & Chu, C. (2018). Urban freight transport using passenger rail network: Scientific issues and quantitative analysis. *Transportation Research Part E: Logistics and Transportation Review*, 115, 227–245.

Behrendt, A., Savelsbergh, M., & Wang, H. (2023). A prescriptive machine learning method for courier scheduling on crowdsourced delivery platforms. *Transportation Science*, 57(4), 889–907.

Bellenguez, O., Brauner, N., & Tsoukiàs, A. (2023). Is there an ethical operational research practice? And what this implies for our research? *EURO Journal on Decision Processes*, 11.

Ben-Tal, A. & Nemirovski, A. (1998). Robust convex optimization. *Mathematics of operations research*, 23(4), 769–805.

Ben-Tal, A. & Nemirovski, A. (2000). Robust solutions of linear programming problems contaminated with uncertain data. *Mathematical programming*, 88(3), 411–424.

Bera, S., Gnyawali, K., Dahal, K., Melo, R., Li-Juan, M., Guru, B., & Ramana, G. (2023). Assessment of shelter location-allocation for multi-hazard emergency evacuation. *International Journal of Disaster Risk Reduction*, 84, 103435.

Bergman, A., David, G., & Song, H. (2023). "I quit"': Schedule volatility as a driver of voluntary employee turnover. *Manufacturing & Service Operations Management*, 25(4), 1416–1435.

Bertsimas, D. & Sim, M. (2004). The price of robustness. *Operations Research*, 52(1), 35–53.

Boysen, N., Fedtke, S., & Schwerdfeger, S. (2021). Last-mile delivery concepts: a survey from an operational research perspective. *OR Spectrum*, 43, 1–58.

Carlsson, J. G., Liu, S., Salari, N., & Yu, H. (2024). Provably good region partitioning for on-time last-mile delivery. *Operations Research*, 72, 91–109.

Carrillo, D., Harknett, K., Logan, A., Luhr, S., & Schneider, D. (2017). Instability of work and care: How work schedules shape child-care arrangements for parents working in the service sector. *Social Service Review*, 91(3), 422–455.

Caspersen, E. & Navrud, S. (2021). The sharing economy and consumer preferences for environmentally sustainable last mile deliveries. *Transportation Research Part D: Transport and Environment*, 95, 102863.

Castillo, V., Bell, J., Mollenkopf, D., & Stank, T. (2022). Hybrid last-mile delivery fleets with crowdsourcing: A systems view of managing the cost-service trade-off. *Journal of Business Logistics*, 43, 36–61.

Cavallaro, F., Eboli, L., Mazzulla, G., & Nocera, S. (2023). Design of integrated passenger-freight transport: A multi-stakeholder perspective. *Journal of Public Transportation*, 25, 100069.

CDP (2024). 2023 Turkey-Syria earthquake. Accessed 23.08.2024.

Chang, K.-H., Chiang, Y.-C., & Chang, T.-Y. (2024a). Simultaneous location and vehicle fleet sizing of relief goods distribution centers and vehicle routing for post-disaster logistics. *Computers & Operations Research*, 161, 106404.

Chang, K.-H., Pan, Y.-J., & Chen, H. (2024b). Shelter location–allocation problem for disaster evacuation planning: A simulation optimization approach. *Computers & Operations Research*, 171, 106784.

Chen, Y., Zhao, Q., Wang, L., & Dessouky, M. (2016). The regional cooperation-based warehouse location problem for relief supplies. *Computers & Industrial Engineering*, 102, 259–267.

Cheng, G., Guo, D., Shi, J., & Qin, Y. (2018a). Planning city-wide package distribution schemes using crowdsourced public transportation systems. *IEEE Access*, 7, 1234–1246.

Cheng, G., Guo, D., Shi, J., & Qin, Y. (2018b). When packages ride a bus: Towards efficient city-wide package distribution. In *2018 IEEE 24th International Conference on Parallel and Distributed Systems (ICPADS)* (pp. 259–266).: IEEE.

Choper, J., Schneider, D., & Harknett, K. (2022). Uncertain time: Precarious schedules and job turnover in the US service sector. *ILR Review*, 75(5), 1099–1132.

Chung, H. (2022). Variable work schedules, unit-level turnover, and performance before and during the COVID-19 pandemic. *Journal of Applied Psychology*, 107, 515–532.

Cleophas, C., Cottrill, C., Ehmke, J. F., & Tierney, K. (2019). Collaborative urban transportation: Recent advances in theory and practice. *European Journal of Operational Research*, 273(3), 801–816.

Contrive Datum Insights (2023). *First and Last Mile Delivery Market Size, Share & Trends Estimation Report*. Technical Report 44470, Contrive Datum Insights.

Couve, C., Lam, T., & Verlinghieri, E. (2023). *Delivering Good Work: Labour, employment and wellbeing in London's cargo bike sector*. Technical report, University of Westminster.

Crainic, T. G., Gonzalez-Feliu, J., Ricciardi, N., Semet, F., & Van Woensel, T. (2021). *Operations research for planning and managing city logistics systems*. Technical Report 45, CIRRELT.

Crainic, T. G., Ricciardi, N., & Storchi, G. (2009). Models for evaluating and planning city logistics systems. *Transportation Science*, 43(4), 432–454.

Dai, H. & Liu, P. (2020a). Workforce planning for o2o delivery systems with crowdsourced drivers. *Annals of Operations Research*, 291, 219–245.

Dai, H. & Liu, P. (2020b). Workforce planning for O2O delivery systems with crowdsourced drivers. *Annals of Operations Research*, 291, 219–245.

Delle Donne, D., Alfandari, L., Archetti, C., & Ljubić, I. (2023a). Freight-on-transit for urban last-mile deliveries: A strategic planning approach. *Transportation Research Part B: Methodological*, 169, 53–81.

Delle Donne, D., Alfandari, L., Archetti, C., & Ljubić, I. (2023b). Freight-on-transit for urban last-mile deliveries: A strategic planning approach. *Transportation Research Part B: Methodological*, 169, 53–81.

Delle Donne, D., Santini, A., & Archetti, C. (2024). Integrating public transport in sustainable last-mile delivery: Column generation approaches. *Optimization Online*.

Deloison, T., Hannon, E., Huber, A., Heid, B., Klink, C., Sahay, R., & Wolff, C. (2020). *The Future of the Last-Mile Ecosystem*. Technical report, World Economic Forum.

Dickson, A., Golden, L., & Bruno, R. (2018). *Scheduling Stability: The Landscape of Work Schedules and Potential Gains From Fairer Workweeks in Illinois and Chicago*. Technical Report 3172354, Social Science Research Network.

Dönmez, Z., Kara, B. Y., Karsu, Ö., & Saldanha-da Gama, F. (2021). Humanitarian facility location under uncertainty: Critical review and future prospects. *Omega*, 102, 102393.

ECHO (2023). Türkiye - floods (MGM, AFAD, media) (ECHO daily flash of 16 March 2023). Accessed 10.05.2023.

El Ghaoui, L. & Lebret, H. (1997). Robust solutions to least-squares problems with uncertain data. *SIAM Journal on matrix analysis and applications*, 18(4), 1035–1064.

El Ghaoui, L., Oustry, F., & Lebret, H. (1998). Robust solutions to uncertain semidefinite programs. *SIAM Journal on Optimization*, 9(1), 33–52.

Elbert, R. & Rentschler, J. (2021). Freight on urban public transportation: A systematic literature review. *Research in Transportation Business & Management*, (pp. 100679).

Ertogral, K., Akbalik, A., & González, S. (2017). Modelling and analysis of a strategic fleet sizing problem for a furniture distributor. *European Journal of Industrial Engineering*, 11(1), 49–77.

Fatehi, S. & Wagner, M. (2022). Crowdsourcing last-mile deliveries. *Manufacturing & Service Operations Management*, 24, 791–809.

Fatnassi, E., Chaouachi, J., & Klibi, W. (2015). Planning and operating a shared goods and passengers on-demand rapid transit system for sustainable city-logistics. *Transportation Research Part B: Methodological*, 81, 440–460.

Figliozzi, M. A. (2008). Planning approximations to the average length of vehicle routing problems with varying customer demands and routing constraints. *Transportation Research Record*, 2089(1), 1–8.

Fischetti, M., Ljubi'c, I., & Sinnl, M. (2016). Redesigning benders decomposition for large-scale facility location. *Management Science*, 63(7), 2146–2167.

Franceschetti, A., Honhon, D., Laporte, G., Van Woensel, T., & Fransoo, J. C. (2017). Strategic fleet planning for city logistics. *Transportation Research Part B: Methodological*, 95, 19–40.

Gabrel, V., Murat, C., & Thiele, A. (2014). Recent advances in robust optimization: An overview. *European journal of operational research*, 235(3), 471–483.

Galkina, A., Schlosserb, T., Galkinaa, O., Hodákováb, D., & Cápayovább, S. (2019). Investigating using urban public transport for freight deliveries. *Transportation Research Procedia*, 39, 64–73.

Gatta, V., Marcucci, E., Nigro, M., Patella, S. M., & Serafini, S. (2019a). Public transport-based crowdshipping for sustainable city logistics: Assessing economic and environmental impacts. *Sustainability*, 11(1), 145.

Gatta, V., Marcucci, E., Nigro, M., & Serafini, S. (2019b). Sustainable urban freight transport adopting public transport-based crowdshipping for b2c deliveries. *European Transport Research Review*, 11(1), 1–14.

Ghasemi, P. & Khalili-Damghani, K. (2021). A robust simulation-optimization approach for pre-disaster multi-period location–allocation–inventory planning. *Mathematics and computers in simulation*, 179, 69–95.

Ghilas, V., Cordeau, J.-F., Demir, E., & Woensel, T. V. (2018). Branch-and-price for the pickup and delivery problem with time windows and scheduled lines. *Transportation Science*, 52(5), 1191–1210.

Ghilas, V., Demir, E., & Van Woensel, T. (2013). Integrating passenger and freight transportation: Model formulation and insights. *Proceedings of the 2013 Beta Working Papers; Technische Universiteit Eindhoven: Eindhoven, The Netherlands*, 441, 1–23.

Ghilas, V., Demir, E., & Van Woensel, T. (2016a). An adaptive large neighborhood search heuristic for the pickup and delivery problem with time windows and scheduled lines. *Computers & Operations Research*, 72, 12–30.

Ghilas, V., Demir, E., & Van Woensel, T. (2016b). The pickup and delivery problem with time windows and scheduled lines. *INFOR: Information Systems and Operational Research*, 54(2), 147–167.

Ghilas, V., Demir, E., & Van Woensel, T. (2016c). A scenario-based planning for the pickup and delivery problem with time windows, scheduled lines and stochastic demands. *Transportation Research Part B: Methodological*, 91, 34–51.

Goeke, D., Roberti, R., & Schneider, M. (2019). Exact and heuristic solution of the consistent vehicle-routing problem. *Transportation Science*, 53(4), 1023–1042.

Gonzalez-Feliu, J. (2012). Freight distribution systems with cross docking: A multidisciplinary analysis. *Journal of the Transportation Research Forum*, 51(1).

Goulart, P., Longaray Andrade, A., Munhoz da Silva, P. R., & Amaral Adamoli, T. (2021). Programação linear para dimensionamento de frota de un operador logístic (linear programming for fleet sizing of a logistic operator). *Revista Eletrônica de Estratégia e Negócios*, 14, 60–84.

Government of Türkiye (2023). Türkiye earthquakes recovery and reconstruction assessment. Accessed 09.05.2023.

Greer, A., Murphy, H., Wu, T., & Clay, L. (2024). Navigating dual hazards: Managing hurricane evacuation and sheltering operations amidst covid-19. *International Journal of Disaster Risk Reduction*, (pp. 104773).

Gregory, C., Darby-Dowman, K., & Mitra, G. (2011). Robust optimization and portfolio selection: The cost of robustness. *European Journal of Operational Research*, 212(2), 417–428.

Groër, C., Golden, B., & Wasil, E. (2009). The consistent vehicle routing problem. *Manufacturing & Service Operations Management*, 11(4), 630–643.

Gu, J., Zhou, Y., Das, A., Moon, I., & Lee, G. M. (2018). Medical relief shelter location problem with patient severity under a limited relief budget. *Computers & Industrial Engineering*, 125, 720–728.

Gul, M. & Guneri, A. F. (2016). An artificial neural network-based earthquake casualty estimation model for istanbul city. *Natural hazards*, 84, 2163–2178.

Göçümlü, B. C. (2023). Sağlık Bakanı Koca: 10 ilde 17 bin 929'u hekim olmak üzere 143 bin 829 personelimiz hizmet veriyor. Accessed 21.03.2023.

Haghi, M., Ghomi, S. M. T. F., & Jolai, F. (2017). Developing a robust multi-objective model for pre/post disaster times under uncertainty in demand and resource. *Journal of Cleaner Production*, 154, 188–202.

Harknett, K., Schneider, D., & Luhr, S. (2022). Who cares if parents have unpredictable work schedules?: Just-in-time work schedules and child care arrangements. *Social Problems*, 69, 164–183.

Henly, J. & Lambert, S. (2014). Unpredictable work timing in retail jobs: Implications for employee work–life conflict. *ILR Review*, 67(3), 986–1016.

Henly, J., Shaefer, L., & Waxman, E. (2006). Nonstandard work schedules: Employer- and employee-driven flexibility in retail jobs. *Social Service Review*, 80(4), 609–634.

Huang, H., Savkin, A. V., & Huang, C. (2020a). A new parcel delivery system with drones and a public train. *Journal of Intelligent & Robotic Systems*, 100(3), 1341–1354.

Huang, H., Savkin, A. V., & Huang, C. (2020b). Scheduling of a parcel delivery system consisting of an aerial drone interacting with public transportation vehicles. *Sensors*, 20(7), 2045.

Hürriyet (2023). In provinces affected by earthquakes, 61,722 buildings must be demolished urgently. Accessed 21.03.2023.

Ishigaki, A., Higashi, H., Sakamoto, T., & Shibahara, S. (2013). The Great East-Japan Earthquake and devastating tsunami: an update and lessons from the past Great Earthquakes in Japan since 1923. *The Tohoku journal of experimental medicine*, 229(4), 287–299.

Jayawardene, V., Huggins, T. J., Prasanna, R., & Fakhruddin, B. (2021). The role of data and information quality during disaster response decision-making. *Progress in disaster science*, 12, 100202.

Kaveh, A., Javadi, S., & Moghanni, R. M. (2020). Emergency management systems after disastrous earthquakes using optimization methods: A comprehensive review. *Advances in Engineering Software*, 149, 102885.

Kawoosa, V. M. (2023). 10,000 tremors: How Turkey has been rattled by aftershocks since the feb. 6 earthquake. Accessed 10.05.2023.

Khalili-Fard, A., Hashemi, M., Bakhshi, A., Yazdani, M., Jolai, F., & Aghsami, A. (2024). Integrated relief pre-positioning and procurement planning considering non-governmental organizations support and perishable relief items in a humanitarian supply chain network. *Omega*, 127, 103111.

Kiba-Janiak, M., Marcinkowski, J., Jagoda, A., & Skowrońska, A. (2021). Sustainable last mile delivery on e-commerce market in cities from the perspective of various stakeholders. literature review. *Sustainable Cities and Society*, (pp. 102984).

Kleywegt, A., Shapiro, A., & Homem-de Mello, T. (2002). The sample average approximation method for stochastic discrete optimization. *SIAM Journal on Optimization*, 12(2), 479–502.

Kovacs, A., Golden, B., Hartl, R., & Parragh, S. (2014). Vehicle routing problems in which consistency considerations are important: A survey. *Networks*, 64, 192–213.

Kunz, N. & Van Wassenhove, L. (2019). Fleet sizing for UNHCR country offices. *Journal of Operations Management*, 65, 282–307.

Laporte, G. & Louveaux, F. (1993). The integer l-shaped method for stochastic integer programs with complete recourse. *Operations Research Letters*, 13(3), 133–142.

Le Menestrel, M. & Van Wassenhove, L. (2009). Ethics in operations research and management sciences: A never-ending effort to combine rigor and passion. *Omega*, 37(6), 1039–1043.

Liu, M. & Huang, M. C. (2014). Compound disasters and compounding processes: Implications for disaster risk management. *The United Nations Office for Disaster Risk Reduction*.

Liu, S., He, L., & Zuo-Jun, M. S. (2021). On-time last-mile delivery: Order assignment with travel-time predictors. *Management Science*, 67(7), 4095–4119.

Lopez, E. (2017). Last mile distances shrink as logistics infrastructure grows. Accessed 03.10.2023.

Loxton, R. & Lin, Q. (2011). Optimal fleet composition via dynamic programming and golden section search. *Journal of Industrial and Management Optimization*, 7, 875–890.

Mandal, M. P., Santini, A., & Archetti, C. (2024). Instance generator for the Tactical LMD Staffing Problem.

Marinov, M., Giubilei, F., Gerhardt, M., Özkan, T., Stergiou, E., Papadopol, M., & Cabecinha, L. (2013). Urban freight movement by rail. *Journal of Transport Literature*, 7, 87–116.

Masson, R., Trentini, A., Lehuédé, F., Malhéné, N., Péton, O., & Tlahig, H. (2017). Optimization of a city logistics transportation system with mixed passengers and goods. *EURO Journal on Transportation and Logistics*, 6(1), 81–109.

Mohammadi, S., Darestani, S. A., Vahdani, B., & Alinezhad, A. (2020). A robust neutrosophic fuzzy-based approach to integrate reliable facility location and routing decisions for disaster relief under fairness and aftershocks concerns. *Computers & Industrial Engineering*, 148, 106734.

Mohan, S. (2008). Scheduling part-time personnel with availability restrictions and preferences to maximize employee satisfaction. *Mathematical and Computer Modelling*, 48(11), 1806–1813.

Monroy, A. G. A. & Díaz, H. L. (2021). A parallel programming approach to the solution of the location-inventory and multi-echelon routing problem in the humanitarian supply chain. *Transportation Research Procedia*, 58, 495–502.

Monteiro Ferraz, A., Cappart, Q., & Vidal, T. (2022). Deep learning for data-driven districting and routing. In *Proceedings of the 11th Triennial Symposium on Transportation Analysis* (pp. 1–4).

Mourad, A., Puchinger, J., & Van Woensel, T. (2021). Integrating autonomous delivery service into a passenger transportation system. *International Journal of Production Research*, 59(7), 2116–2139.

Mucowska, M. (2021). Trends of environmentally sustainable solutions of urban last-mile deliveries on the e-commerce market—a literature review. *Sustainability*, 13(11), 5894.

NOAA (2023). Jetstream max: Plate tectonics and earthquakes. Accessed 22.06.2024.

Nogueira, G. P. M., de Assis Rangel, J. J., & Shimoda, E. (2021). Sustainable last-mile distribution in b2c e-commerce: Do consumers really care? *Cleaner and Responsible Consumption*, 3, 100021.

OCHA (2023a). Türkiye - 2023 earthquakes situation report no. 13, as of 6 April 2023 [EN/TR]. Accessed 10.05.2023.

OCHA (2023b). Türkiye - 2023 earthquakes situation report no. 14, as of 13 April 2023 [EN/TR]. Accessed 10.05.2023.

OCHA (2023c). Türkiye - 2023 earthquakes situation report no. 16, as of 27 April 2023 [EN/TR]. Accessed 10.05.2023.

Onur, O. (2019). Freight on transit as a new concept for city logistics. Accessed 17.01.2023.

OpenStreetMap (2023). Copyright and license.

Ormerod, R. & Werner, U. (2013). Operational research and ethics: A literature review. *European Journal of Operational Research*, 228(2), 291–307.

Ozbay, E., Çavuş, Ö., & Kara, B. Y. (2019). Shelter site location under multi-hazard scenarios. *Computers & operations research*, 106, 102–118.

Ozturk, O. & Patrick, J. (2018). An optimization model for freight transport using urban rail transit. *European Journal of Operational Research*, 267(3), 1110–1121.

Pandey, P., Gajjar, H., & Shah, B. (2021). Determining optimal workforce size and schedule at the retail store considering overstaffing and understaffing costs. *Computers & Industrial Engineering*, 161. Article ID 107656.

Paul, J. A. & MacDonald, L. (2016). Location and capacity allocations decisions to mitigate the impacts of unexpected disasters. *European Journal of Operational Research*, 251(1), 252–263.

Paul, J. A. & Wang, X. J. (2019). Robust location-allocation network design for earthquake preparedness. *Transportation research part B: Methodological*, 119, 139–155.

Pyo, J., Park, E. J., Ock, M., Lee, W., Lee, H. J., & Choi, S. (2023). How has COVID-19 affected the work environment of delivery workers?: An interpretative phenomenological analysis. *Plos One*, 18.

Rafferty, J. P. (2023). Nepal earthquake of 2015. Accessed 03.04.2023.

Rahimi-Vahed, A., Crainic, T. G., Gendreau, M., & Rei, W. (2015). Fleet-sizing for multi-depot and periodic vehicle routing problems using a modular heuristic algorithm. *Computers & Operations Research*, 53, 9–23.

Rai, H. B., Van Lier, T., Meers, D., & Macharis, C. (2017a). Improving urban freight transport sustainability: Policy assessment framework and case study. *Research in Transportation Economics*, 64, 26–35.

Rai, H. B., Verlinde, S., Merckx, J., & Macharis, C. (2017b). Crowd logistics: an opportunity for more sustainable urban freight transport? *European Transport Research Review*, 9(3), 1–13.

RailwayTechnology (2020). GB Railfreight trials use of commuter trains to deliver parcels. Accessed 01.10.2021.

Ranieri, L., Digiesi, S., Silvestri, B., & Roccotelli, M. (2018). A review of last mile logistics innovations in an externalities cost reduction vision. *Sustainability*, 10(3), 782.

Reid, K. (2018). 2015 Nepal earthquake: Facts, FAQs, and how to help. Accessed 03.04.2023.

Reliefweb (2024). Türkiye/syria: Earthquakes- feb 2023. Accessed 23.08.2024.

Restrepo, M., Semet, F., & Pocreau, T. (2019). Integrated shift scheduling and load assignment optimization for attended home delivery. *Transportation Science*, 53, 917–1212.

Reul, M. (2019). Amazon to use public transport as parcel carrier. Accessed 01.10.2021.

Rezaei-Malek, M., Tavakkoli-Moghaddam, R., Zahiri, B., & Bozorgi-Amiri, A. (2016). An interactive approach for designing a robust disaster relief logistics network with perishable commodities. *Computers & Industrial Engineering*, 94, 201–215.

Rhee, M.-K., Park, S. K., & Lee, C.-K. (2020). Pathways from workplace flexibility to turnover intention: Role of work–family conflict, family–work conflict, and job satisfaction. *International Journal of Social Welfare*, 29(1), 51–61.

Ritchie, H. & Rosado, P. (2022). Natural disasters. *Our World in Data*. https://ourworldindata.org/natural-disasters.

Robles, P., Chang, A., Holder, J., Leatherby, L., Reinhard, S., & Wu, A. (2023). Mapping the damage from the earthquake in Turkey and Syria. Accessed 22.06.2024.

Rodríguez-Martín, I., Salazar-González, J.-J., & Yaman, H. (2019). The periodic vehicle routing problem with driver consistency. *European Journal of Operational Research*, 273(2), 575–584.

Romanillos, G. & Gutiérrez, J. (2020). Cyclists do better. analyzing urban cycling operating speeds and accessibility. *International Journal of Sustainable Transportation*, 14, 448–464.

Ruiz-Torres, A., Alomoto, N., Paletta, G., & Pérez, E. (2015). Scheduling to maximise worker satisfaction and on-time orders. *International Journal of Production Research*, 53(9), 2836–2852.

Saito, S. (2021). Next stop, package delivery: Bus and courier link up to serve rural area. Accessed 28.09.2021.

Santini, A., Viana, A., Klimentova, X., & Pedroso, J. P. (2022). The probabilistic Travelling Salesman Problem with crowdsourcing. *Computers & Operations Research*, 142. Article ID 105722.

Schiavina, M., Freire, S., Carioli, A., & MacManus, K. (2023). GHS-POP R2023A - GHS population grid multitemporal (1975-2030).

Schmidt, J., Tilk, C., & Irnich, S. (2022). Using public transport in a 2-echelon last-mile delivery network. *European Journal of Operational Research*.

Schneider, M. (2016). The vehicle-routing problem with time windows and driver-specific times. *European Journal of Operational Research*, 250, 101–119.

Shehadeh, K., Wang, H., & Zhang, P. (2021). Fleet sizing and allocation for on-demand last-mile transportation systems. *Transportation Research Part C: Emerging Technologies*, 132.

Sheikholeslami, M. & Zarrinpoor, N. (2023). Designing an integrated humanitarian logistics network for the preparedness and response phases under uncertainty. *Socio-Economic Planning Sciences*, 86, 101496.

Smilowitz, K., Nowak, M., & Jiang, T. (2013). Workforce management in periodic delivery operations. *Transportation Science*, 47(2), 214–230.

Soyster, A. L. (1973). Convex programming with set-inclusive constraints and applications to inexact linear programming. *Operations research*, 21(5), 1154–1157.

Starr, M. K. & Van Wassenhove, L. N. (2014). Introduction to the special issue on humanitarian operations and crisis management. *Production and Operations Management*, 23(6), 925–937.

Stienen, V., Wagenaar, J., Den Hertog, D., & Fleuren, H. (2021). Optimal depot locations for humanitarian logistics service providers using robust optimization. *Omega*, 104, 102494.

Taniguchi, E., Thompson, R. G., & Yamada, T. (2016). New opportunities and challenges for city logistics. *Transportation Research Procedia*, 12, 5–13.

Taouktsis, X. & Zikopoulos, C. (2024). A decision-making tool for the determination of the distribution center location in a humanitarian logistics network. *Expert Systems with Applications*, 238, 122010.

Thippa, P. K., Tripathi, R., & Bhat, G. (2023). A case study on performance of structures during turkey-syria multiple earthquakes occurred on february 6, 2023. In *IOP Conference Series: Earth and Environmental Science*, volume 1280 (pp. 012023).: IOP Publishing.

Tofighi, S., Torabi, S. A., & Mansouri, S. A. (2016). Humanitarian logistics network design under mixed uncertainty. *European Journal of Operational Research*, 250(1), 239–250.

Trentini, A. & Mahléné, N. (2010). Toward a shared urban transport system ensuring passengers & goods cohabitation. *TeMA-Journal of Land Use, Mobility and Environment*, 3(2).

Trentini, A. & Malhene, N. (2012). Flow management of passengers and goods coexisting in the urban environment: Conceptual and operational points of view. *Procedia-Social and Behavioral Sciences*, 39, 807–817.

TSI (2023). Statistics on family, 2022. Accessed 13.08.2024.

Turan, H. H., Jalalvand, F., Elsawah, S., & Ryan, M. (2022). A joint problem of strategic workforce planning and fleet renewal: With an application in defense. *European Journal of Operational Research*, 296, 615–634.

Ulmer, M. & Savelsbergh, M. (2020). Workforce scheduling in the era of crowdsourced delivery. *Transportaion Science*, 54, 1113–1133.

UN (2023). Türkiye-syria earthquake response. Accessed 23.08.2024.

Urrutia, J., Bautista, L., & Baccay, E. (2014). Mathematical models for estimating earthquake casualties and damage cost through regression analysis using matrices. In *Journal of Physics: Conference Series*, volume 495 (pp. 012024).: IOP Publishing.

Vahdani, B., Veysmoradi, D., Noori, F., & Mansour, F. (2018). Two-stage multi-objective location-routing-inventory model for humanitarian logistics network design under uncertainty. *International journal of disaster risk reduction*, 27, 290–306.

Van den Bergh, J., Beliën, J., De Bruecker, P., Demeulemeester, E., & De Boeck, L. (2013). Personnel scheduling: A literature review. *European Journal of Operational Research*, 226(3), 367–385.

Verlinde, S. (2015). *Promising but challenging urban freight transport solutions: freight flow consolidation and off-hour deliveries*. PhD thesis, Ghent University.

Villa, R. & Monzón, A. (2021). A metro-based system as sustainable alternative for urban logistics in the era of e-commerce. *Sustainability*, 13(8), 4479.

Viu-Roig, M. & Alvarez-Palau, E. J. (2020). The impact of e-commerce-related last-mile logistics on cities: A systematic literature review. *Sustainability*, 12(16), 6492.

Wang, Y., Zhao, L., Savelsbergh, M., & Wu, S. (2022). Multi-period workload balancing in last-mile urban delivery. *Transportation Science*, 56, 1348–1368.

Wei, H., Shi, H., Kou, Y., Yu, M., Wang, Y., Li, S., Li, S., Armitage, C., Chandola, T., Whelan, P., Zhang, Y., Xu, Y., & van Tongeren, M. (2023). Understanding technostress in the gig economy — a job demands-resources analysis of chinese couriers.

Werneck, R. (2022). Last mile deliveries at Amazon. Keynote at the 12^{th} DIMACS Implementation Challenge Workshop.

Xing, H., Zhonglin, Z., & Shaoyu, W. (2015). The prediction model of earthquake casuailty based on robust wavelet v-svm. *Natural Hazards*, 77, 717–732.

Yildiz, B. & Savelsbergh, M. (2019). Provably high-quality solutions for the meal delivery routing problem. *Transportation Science*, 53, 1372–1388.

Yura, K. (1994). Production scheduling to satisfy worker's preferences for days off and overtime under due-date constraints. *International Journal of Production Economics*, 33(1), 265–270.

Yurchisin, M. & Jaeger, A. (2021). The sustainable last mile. Faster. Greener. Cheaper. *Our World in Data*. https://www.accenture.com/ie-en/insights/consulting/sustainable-last-mile-delivery.

Zeitler, M. (2019). Deliveries by tram- a viable solution for sustainable urban logistics? Accessed 16.01.2023.

Zhou, X., Zhao, C., & Fengjie, X. (2024). Research on collaborative delivery route planning for rural public buses and express delivery vehicles based on passenger and freight integration.

Zokaee, S., Bozorgi-Amiri, A., & Sadjadi, S. J. (2016). A robust optimization model for humanitarian relief chain design under uncertainty. *Applied Mathematical Modelling*, 40(17-18), 7996–8016.